STRUCTURE AND PETROLOGY OF THE SAN GABRIEL ANORTHOSITE-SYENITE BODY, LOS ANGELES COUNTY, CALIFORNIA

Thesis by

Bruce Alan Carter

In Partial Fulfillment of the Requirements

for the Degree of

Doctor of Philosophy

California Institute of Technology

Pasadena, California

1980

(Submitted May 5, 1980)

ACKNOWLEDGEMENTS

The insight and broad knowledge of Professor Leon Silver have greatly contributed to the quality and breadth of this research project.

During the tenure of this study, I have benefited from numerous stimulating discussions with Caltech faculty and graduate students. Jan Mayne provided invaluable suggestions and assistance with the drafting of maps and other illustrations.

I would also like to express my deep gratitude to all the friends and family members who aided me in so many tangible and intangible ways during the course of this work.

Financial support was provided by National Science Foundation Grants No. GA-15989 and No. EAR-76-23153, and by Project Agreement #7 under Atomic Energy Commission Contract No. AT(04-3)-767, CALT-767P7-72.

ABSTRACT

The San Gabriel anorthosite-syenite body is part of large layered intrusive, part of which underlies about 250 square kilometers in the western San Gabriel Mountains between the San Gabriel and San Andreas fault zones 30 kilometers north of Los Angeles. Although not subjected to post-emplacement regional metamorphism, the Precambrian anorthosite is intruded by the early Triassic Mt. Lowe granodiorite and the late Cretaceous Mt. Josephine granodiorite, and is deformed by broad folds of at least two ages (Triassic(?) and mid-Cenozoic), which have produced several kilometers of structural relief within the body.

Several sets of faults in the area were active in Teritiary time, but none of them show evidence of Holocene activity. From oldest to youngest, these faults include: (1) several more or less east-west faults with major apparent right-lateral or left-lateral and dip-slip displacements; (2) a NE-trending fault set with important left-lateral displacements; and (3) younger NW-trending faults with small dip-slip and right-lateral displacements. The San Gabriel fault, which lies 1-4 kilometers southwest of its margin, must cut the anorthosite-syenite body at depth and may offset anorthositic rocks at least 28-46 kilometers in a right-lateral sense.

The San Gabriel anorthosite-syenite body is part of a large allochthonous sheet which is floored by a zone of unusual cataclastic gneisses, exposed in the northeastern part of the area in and near to Mill Canyon. Slickensides, lineations and minor folds within this zone suggest latest movement parallel to a N-S or NE-SW direction. Strongly deformed and mylonitized gneisses below the anorthosite include lineated granodioritic gneiss possibly equivalent to the late-Cretaceous Mt. Josephine granodiorite, gabbroic to

anorthositic gneisses, and layered amphibolitic gneisses unlike any others seen in the western San Gabriel Mountains. Large thrust displacements probably occurred within this zone as well as along the Vincent thrust 45 kilometers to the east, which resembles this zone and may be related to it.

The anorthosite-syenite body was intruded into previously metamorphosed, granulite-grade Mendenhall gneiss about 1200 million years ago. The body is a large, layered intrusive in which bottom crystal accumulation produced the observed anorthosite-gabbro-syenite differentiation suite. The part of this body now exposed was at least 10 kilometers in thickness and about 15 kilometers in diameter. It probably had the form of an inverted cone, with a sub-horizontal, concordant uppper contact. Primary quartz is rare in rocks of this suite; the following lithologies have been distinguished on the basis of the percentage and composition of their constituent feldspars: anorthosite, leucogabbro, gabbro, ferrogabbro (all with calcic andesine), ultramafite (olivine, augite, ilmenite and apatite), jotunite (predominantly antiperthitic sodic andesine), mangerite (antiperthite and mesoperthite) and syenite (predominantly mesoperthite).

The San Gabriel anorthosite-syenite body has been subdivided into three main stratigraphic units (from oldest to youngest): (1) The lowest, largest unit consists of thick sequences of massive anorthosite alternating with layered leucogabbro. This unit is at least 7 kilometers in thickness and becomes more mafic near its top. (2) The overlying syenite unit locally attains thickness of at least 3-5 kilometers, but is commonly much thinner or absent. In some areas, the basal 100-1000 meters of this unit is extremely mafic, but otherwise it is farily homogeneous and massive, with no cyclic or cryptic layering. (3) The uppermost jotunite unit is a highly compositionally variable unit which intruded overlying granulite gneiss

and has been subdivided into 5 subunits. This unit is at least 3-4 kilometers in maximum thickness. It is apparently younger than the syenite, and in places grades downward into syenite. Several masses of hornblende-bytownite gabbro within anorthosite are probably not directly related to the anorthosite-syenite body.

Primary cumulate structures and textures in these rocks have greatly aided the structural interpretation of this body and provide strong evidence of its origin by bottom crystal accumulation. Large, 6 to 25-centimeter hypersthene crystals, which ophitically enclose numerous well-oriented 1 to 3-centimeter plagioclase tablets, indicate a cumulate origin of the leucogabbro. Occasional crescumulate layers in leucogabbro, especially near the margin of the body, formed when first plagioclase and then hypersthene grew from the floor upward into the magma. Slump structures are poorly defined in leucogabbro, but are excellently developed in the mafic lower part of the syenite unit and in some parts of the jotunite unit, and include 1 to 20-meter slump blocks and deformed compositional layers. Many 3-centimeter to 3-meter layers in the mafic lower part of the syenite unit and in the jotunite unit are both size- and density-graded, with coarser, ferromagnesian-mineral-enriched bases, and are extremely useful structural indicators.

Large angular blocks of anorthosite (to 20 meters) are abundant in layered mafic rocks at the base of the syenite unit and in some parts of the jotunite unit. These are slump blocks, which indicate that parts of the syenite and jotunite units accumulated at the base of major tectonic scarps which developed in rocks of the anorthosite-leucogabbro unit which formed the floor of the chambers of the later magmas.

All of the 20 chemical analyses of rocks from this body are iron-rich; the lowest $FeO+Fe_2O_3/FeO+Fe_2O_3+MgO$ ratio (wt. %) is 0.61 and most are between 0.70 and 0.95, which suggest that the original magma was probably similarly iron-rich.

Chemical analyses of these rocks define general trends with substantial scatter on variation diagrams, and in detail those from each of the three units define individual fields with little or no overlap. Thus a common line of descent for all rocks of the body seems somewhat unlikely The estimated makeup of the entire body is about 46% anorthosite, 23% leucogabbro, 4% gabbro, 12% syenite, 11% jotunite and 4% ultramafite, giving the following suggested average composition: SiO_2, 53.73%, TiO_2, 1.17%, Al_2O_3, 22.33%, Fe_2O_3, 1.66%, FeO, 4.54%, MgO, 1.72%, CaO, 8.08%, Na_2O, 5.05%, K_2O, 1.18%, P_2O_5, 0.42%.

Limited mineral composition data show that: (1) Plagioclase in anorthosite and leucogabbro ranges between about An_{35} and An_{55} with most between An_{40} and An_{50}. Plagioclase in not concentrically zoned, but is inhomogeneous with a range of about 3-4% anorthite in individual crystals. (2) There are cyclic compositional variations of plagioclase in the anorthosite-leucogabbro unit, with more albite-rich and more anorthite-rich compositons alternating over hundreds of meters of the stratigraphic section. (3) There is no apparent consistent cryptic variation of proxene and olivine compositions within the syenite and jotunite units.

Postcumulous recrystallization has drastically altered the fabric of most anorthositic and leucogabbroic rocks and has produced extremely coarse grained textures. Pervasive deuteric uralitic alteration of the primary ferromagnesian minerals in all but a few rocks of the syenite and jotunite units suggests that the magma probably had a relatively high water content.

It is possible that all of the rocks of the San Gabriel anorthosite-syenite body could have been produced by differentiation by fractional crystallization of a trachyandesitic parent magma, successive fractions of which were intruded into the magma chamber. However, the detailed sequence of lithologies, mineral compositions and the compositions of the three units suggest that at least two independently generated magmas may have combined to produce the San Gabriel anorthosite-syenite body.

Some important contributions of this study are: (1) the detailed geologic map of the anorthosite-syenite body and determination of its post-emplacement structural history; (2) the description of the complete suite of lithologies and their contact relationships; (3) the description of the mineralogical compositions of each lithology and the recognition of cryptic variation of plagioclase in the anorthosite-leucogabbro unit; (4) the description of the sequence of post-accumulation processes including recrystallization and the hydration of most primary ferromagnesian minerals; (5) the recognition of uninverted pigeonite in rocks of the jotunite and syenite units; and (6) recognition that this andesine anorthosite massif is actually a large deformed stratiform pluton.

TABLE OF CONTENTS

	Page
CHAPTER 1: INTRODUCTION	1
GENERAL	2
FIELD SETTING	5
CHAPTER 2: FIELD MAP UNITS	11
INTRODUCTION	12
MENDENHALL GNEISS	14
INTRODUCTION	14
LITHOLOGY AND FIELD RELATIONSHIPS	15
PRE-METAMORPHIC LITHOLOGY	21
ANORTHOSITE-SYENITE BODY	21
INTRODUCTION	21
Lithologies, Lithologic Map Units, and Primary Stratigraphic Units	22
Rock Nomenclature	23
Contacts and Attitudes	27
ANORTHOSITE LEUCOGABBRO UNIT	30
Anorthosite	31
Leucogabbro	35
Gabbro	37
SYENITE UNIT	39
Ultramafic Syenite Subunit	41
Normal Syenite Subunit	42
JOTUNITE UNIT	43
Anorthosite Block Subunit	47

Lower Jotunite Subunit 47

Layered Jotunite Subunit 48

Ultramafic Jotunite Subunit 51

Upper Jotunite Subunit 52

JOTUNITIC GABBRO PEGMATITE 56

GABBROIC DIKE ROCKS 57

HORNBLENDE-BYTOWNITE GABBRO 58

MICROPEGMATITE AND PEGMATITE DIKES 61

MT. LOWE GRANDIORITE 62

LAMPROPHYRE DIKES 64

MT. JOSEPHINE GRANDIORITE 65

APLITE 66

ROCKS OF THE MILL CANYON STRUCTURE 67

LINEATED GRANODIORITIC GNEISS 67

GABBROIC TO ANORTHOSITIC GNEISS 68

MILL CANYON LAYERED AMPHIBOLITIC GNEISS 68

CENOZOIC SEDIMENTARY AND VOLCANIC ROCKS 70

VASQUEZ FORMATION 70

MINT CANYON FORMATION 72

PACOIMA FORMATION 73

QUATERNARY TERRACE GRAVELS 73

QUATERNARY LANDSLIDE DEPOSITS 74

QUATERNARY ALLUVIUM 75

CHAPTER 3: STRUCTURE 76

INTRODUCTION 77

PRE-ANORTHOSITE STRUCTURE 77

STRUCTURES RELATED TO THE EMPLACEMENT AND CRYSTALLIZATION OF THE ANORTHOSITE-SYENITE BODY 79

INTRODUCTION 79

EXTERNAL FORM 80

INTERNAL STRUCTURES 88

Major Units 88

Compositional Layering 93

Slump Structures and Block Accumulation 102

Other Structures 113

SYNPLUTONIC TECTONISM 119

Introduction 119

Buck Canyon Synform 124

Origin of the Buck Canyon Synform 131

Other Synplutonic Tectonism 133

POST-ANORTHOSITE STRUCTURE 134

MT. LOWE GRANODIORITE EMPLACEMENT 134

FOLDS 136

North-Northeast Folds 137

East-West Folds 141

Reactivation of North-Northwest Folds 145

Warping on East-West Axis 145

CENOZOIC FAULTS 146

Older, Generally East-West Faults 147

Soledad Fault 147

Lonetree Fault 151

Slaughter Canyon Fault 153

Younger, Northeast-Trending Faults 154

Pole Canyon Fault 158

Oak Spring Canyon Fault 158

Magic Mountain Fault 159

Transmission Line Fault 160

Mt. Gleason Fault 164

Fox Creek Fault 164

Mill Creek Fault 165

MILL CANYON STRUCTURE 165

CHAPTER 4: FIELD PETROLOGY AND PETROGRAPHY 176

INTRODUCTION 177

ANORTHOSITE-LEUCOGABBRO UNIT 177

GENERAL 177

ANORTHOSITE 179

LEUCOGABBRO 183

GABBRO 199

POSTCUMULOUS RECRYSTALLIZATION OF ANORTHOSITE AND LEUCOGABBRO 202

SYENITE UNIT 209

ULTRAMAFIC SYENITE SUBUNIT 209

NORMAL SYENITE SUBUNIT 211

JOTUNITE UNIT 222

ANORTHOSITE BLOCK SUBUNIT 222

LOWER JOTUNITE SUBUNIT 225

LAYERED JOTUNITE SUBUNIT 226

ULTRAMAFIC JOTUNITE SUBUNIT 229

UPPER JOTUNITE SUBUNIT 235

CHAPTER 5: ROCK AND MINERAL CHEMISTRY 238

INTRODUCTION 239

ROCK COMPOSITIONS 239

DATA 239

ANALYZED ROCKS 245

DISCUSSION 251

AVERAGE COMPOSITION 265

MINERAL COMPOSITIONS 267

FERROMAGNESIAN MINERALS 269

General 269

Composition of Pyroxene and Olivine 273

Pyroxene Exsolution and Inversion 279

Inclusions 288

Uralitic Alteration of Pyroxene and Olivine 288

FELDSPARS 297

General 297

Composition 298

Recrystallization 310

Exsolution 312

CHAPTER 6: PETROGENESIS AND STRUCTURAL EVOLUTION 320

INTRODUCTION 321

PRE-INTRUSION CONDITIONS 321

THE PLUTON 322

STRUCTURAL EVOLUTION DURING AND IMMEDIATELY FOLLOWING CRYSTALLIZATION 323

SLUMPING 323

SCARPS 327

CATACLASIS 329

FAULTING 330

ORIGIN OF THE UNITS 331

THE ANORTHOSITE-LEUCOGABBRO UNIT 331

THE SYENITE UNIT 338

THE JOTUNITE UNIT 340

MAGMA 343

CRYSTALLIZATION AND MAGMATIC TRENDS 349

THE SINGLE MAGMA HYPOTHESIS 352

THE INDEPENDENT MAGMAS HYPOTHESIS 356

POST-CRYSTALLIZATION PROCESSES 358

POSTCUMULOUS RECYRSTALLIZATION 359

URALITIZATION 360

CHAPTER 7: MASSIF-TYPE ANORTHOSITE AND THE SAN GABRIEL BODY 362

INTRODUCTION 363

OTHER ANORTHOSITE BODIES 363

THE SAN GABRIEL BODY 369

REFERENCES 376

APPENDIX A. MODES OF ROCKS OF THE SAN GABRIEL ANORTHOSITE-SYENITE BODY 388

ILLUSTRATIONS

FIGURES		Page
1.	INDEX MAPS	6
2.	IMPORTANT PHYSIOGRAPHIC FEATURES	8
3.	SIMPLIFIED GEOLOGIC MAP	13
4.	MENDENHALL GNEISS OUTCROP	17
5.	MENDENHALL GNEISS OUTCROP	18
6.	ROCK NOMENCLATURE: QUARTZ-FELDSPAR	25
7.	ROCK NOMENCLATURE: FELDSPAR-COLOR INDEX	26
8.	ANORTHOSITE OUTCROP	32
9	ANORTHOSITE OUTCROP	33
10.	LEUCOGABBRO OUTCROP	36
11.	LAYERED JOTUNITE OUTCROP	50
12.	UPPER JOTUNITE OUTCROP	54
13.	UPPER JOTUNITE OUTCROP	55
14.	HORNBLENDE BYTOWNITE	60
15.	MILL CANYON LAYERED AMPHIBOLTIC GNEISS OUTCROP	69
16.	PRECAMBRIAN SYNPLUTONIC STRUCTURAL FEATURES	81, 82, 83
17.	SLUMPING OF THE MARGIN OF THE ANORTHOSITE-SYENITE BODY	86, 87
18.	SHEARED GABBRO	89
19.	SIMPLIFIED RECONSTRUCTION OF THE BODY	94
20.	FINE-SCALE LAYERING IN GABBRO	95
21.	GRADED LAYERS IN JOTUNITE	96
22.	SLUMPED GRADED LAYERS IN JOTUNITE	97
23.	GRADED LAYERS IN JOTUNITE	99

24.	CRESCUMULATE LAYER IN LEUCOGABBRO	100
25.	WILLOW-LAKE-TYPE CRYSTALS IN GABBRO	103
26.	ANORTHOSITE BRECCIA	104
27.	ANORTHOSITE BRECCIA	105
28.	ANORTHOSITE BLOCKS IN ULTRAMAFITE	106
29.	ANORTHOSITE SLUMP BLOCK	107
30.	GRADED LAYERS IN JOTUNITE	109
31.	ANORTHOSITE XENOLITH IN JOTUNITE	110
32.	ANORTHOSITE WEDGE CUTTING LEUCOGABBRO	114
33.	ANORTHOSITE WEDGE CUTTING LEUCOGABBRO	115
34.	ANORTHOSITE WEDGE CUTTING LEUCOGABBRO	116
35.	FORMATION OF ANORTHOSITE WEDGES IN LEUCOGABBRO	117, 118
36.	CHANNEL STRUCTURE IN JOTUNITE	120
37.	SUMMARY OF STRUCTURAL ORIENTATION INDICATORS	121, 122, 123
38.	DIAGRAMMATIC CROSS SECTION OF THE BUCK CANYON SYNFORM	126
39.	STRUCTURES PRODUCED BY EMPLACEMENT OF THE MT. LOWE GRANODIORITE	138, 139, 140
40.	CENOZOIC EAST-WEST FOLDS	142, 143, 144
41.	OLDER, EAST-WEST FAULTS	148, 149, 150
42.	YOUNGER, NORTHEAST-TRENDING FAULTS	155, 156, 157
43.	AUGEN GNEISS FROM MILL CANYON, PHOTOMICROGRAPH	168
44.	GNEISS FROM MILL CANYON, PHOTOMICROGRAPH	169
45.	CROSS SECTIONS OF THE MILL CANYON STRUCTURE	172
46.	ANORTHOSITE OUTCROP	181
47.	OPHITIC LEUCOGABBRO	184
48.	PYROXENE (URALITE) IN OPHITIC LEUCOGABBRO	185
49.	PYROXENE (URALITE) IN OPHITIC LEUCOGABBRO	186

50.	NON-OPHITIC LEUCOGABBRO	188
51.	OPHITIC AND NON-OPHITIC LEUCOGABBRO (1055A and B)	189
52.	OPHITIC LEUCOGABBRO PHOTOMICROGRAPH	191
53.	URALITE PSEUDOMORPH PHOTOMICROGRAPH	192
54.	URALITE PSEUDOMORPH PHOTOMICROGRAPH	194
55.	PLAGIOCLASE-URALITE REACTION RIM PHOTOMICROGRAPH	196
56.	PLAGIOCLASE-URALITE REACTION RIM PHOTOMICROGRAPH	197
57.	SEQUENCE OF TEXTURAL DEVELOPMENT DURING POSTCUMULOUS RECRYSTALLIZATION OF ANORTHOSITE AND LEUCOGABBRO	204, 205
58.	PARTIALLY RECRYSTALLIZED CUMULATE PLAGIOCLASE PHOTOMICROGRAPH	208
59.	MESOPERTHITE WITH SWAPPED BORDERS, PHOTOMICROGRAPH	213
60.	MESOPERTHITE WITH SWAPPED BORDERS, PHOTOMICROGRAPH	214
61.	FERROMAGNESIAN AGGREGATE IN SYENITE, PHOTOMICROGRAPH	215
62.	FERROMAGNESIAN AGGREGATE IN SYENITE, PHOTOMICROGRAPH	216
63.	FERROMAGNESIAN AGGREGATE IN SYENITE, PHOTOMICROGRAPH	218
64.	FERROMAGNESIAN AGGREGATE IN SYENITE, PHOTOMICROGRAPH	219
65.	FERROMAGNESIAN AGGREGATE IN SYENITE, PHOTOMICROGRAPH	220
66.	LEUCOSYENITE PHOTOMICROGRAPH	223
67.	LEUCOSYENITE PHOTOMICROGRAPH	224
68.	ANDESINE TABLETS IN JOTUNITE, PHOTOMICROGRAPH	228
69.	GRADED LAYER OF JOTUNITE	230
70.	GRADED LAYERS IN JOTUNITE	231
71.	FERROGABBRO PHOTOMICROGRAPH	233
72.	ULTRAMAFITE PHOTOMICROGRAPH	234
73.	FERROGABBRO PHOTOMICROGRAPH	236
74.	GRADED LAYERS IN JOTUNITE	237

75.	A-F-M DIAGRAM	253
76.	An-Ab-Or DIAGRAM	254
77.	Al_2O_3 vs. An/An+Ab DIAGRAM	256
78.	K_2O vs. SiO_2 DIAGRAM	257
79.	MgO vs. FeO DIAGRAM	259
80.	P_2O_5 vs. DIFFERENTIATION INDEX DIAGRAM	260
81.	TiO_2 vs. CaO+MgO DIAGRAM	262
82.	NORMATIVE APATITE VS. ILMENITE+MAGNETITE DIAGRAM	264
83.	COMPARISON OF THE THREE UNITS ON VARIATION DIAGRAMS	266
84.	DISTRIBUTION OF UNURALITIZED ROCKS	271
85.	UNURALITIZED SYENITE, PHOTOMICROGRAPH	272
86.	PARTIALLY URALITIZED SYENITE, PHOTOMICROGRAPH	274
87.	COMPOSITION OF PYROXENE AND OLIVINE	276
88.	COMPOSITION OF AUGITE VS. VERTICAL POSITION	277
89.	CLINOPYROXENE LAMELLAE IN HYPERSTHENE, PHOTOMICROGRAPH	280
90.	CLINOPYROXENE LAMELLAE IN HYPERSTHENE, PHOTOMICROGRAPH	281
91.	CLINOPYROXENE LAMELLAE IN HYPERSTHENE, PHOTOMICROGRAPH	282
92.	CLINOPYROXENE LAMELLAE IN HYPERSTHENE, PHOTOMICROGRAPH	283
93.	UNINVERTED PIGEONITE, PHOTOMICROGRAPH	285
94.	UNINVERTED PIGEONITE, PHOTOMICROGRAPH	286
95.	PIGEONITE COMPOSITIONS	287
96.	OPAQUE OXIDE-HYPERSTHENE INTERGROWTH, PHOTOMICROGRAPH	289
97.	OPAQUE OXIDE LAMELLAE IN AUGITE, PHOTOMICROGRAPH	290
98.	OPAQUE OXIDE LAMELLAE IN AUGITE, PHOTOMICROGRAPH	291
99.	URALITE PSEUDOMORPH, PHOTOMICROGRAPH	292

100.	URALITE PSEUDOMORPH, PHOTOMICROGRAPH	294
101.	COMPOSITIONS OF AMPHIBOLES IN URALITE	296
102.	COMPOSITIONS OF PLAGIOCLASE IN LEUCOGABBRO (1055A, B)	300
103.	PLAGIOCLASE COMPOSITIONS IN TRAVERSE ONE	301
104.	PLAGIOCLASE COMPOSITIONS IN TRAVERSE TWO	303
105.	HISTOGRAMS OF PLAGIOCLASE COMPOSITIONS	304
106.	ORTHOCLASE CONTENT OF ANALYZED PLAGIOCLASE	309
107.	ANTIPERTHITE EXSOLUTION, PHOTOMICROGRAPH	314
108.	ANTIPERTHITE EXSOLUTION, PHOTOMICROGRAPH	315
109.	ANTIPERTHITE EXSOLUTION, PHOTOMICROGRAPH	316
110.	ANTIPERTHITE EXSOLUTION, PHOTOMICROGRAPH	317
111.	ANTIPERTHITE EXSOLUTION, PHOTOMICROGRAPH	318
112.	STRUCTURAL EVOLUTION DURING AND IMMEDIATELY FOLLOWING CRYSTALLIZATION OF THE ANORTHOSITE-SYENITE BODY	324, 325, 326
113.	MODEL FOR THE CRYSTALLIZATION OF THE MAGMA WHICH FORMED THE ANORTHOSITE-SYENITE BODY	350, 351

ILLUSTRATIONS

FIGURES		Page
1.	INDEX MAPS	6
2.	IMPORTANT PHYSIOGRAPHIC FEATURES	8
3.	SIMPLIFIED GEOLOGIC MAP	13
4.	MENDENHALL GNEISS OUTCROP	17
5.	MENDENHALL GNEISS OUTCROP	18
6.	ROCK NOMENCLATURE: QUARTZ-FELDSPAR	25
7.	ROCK NOMENCLATURE: FELDSPAR-COLOR INDEX	26
8.	ANORTHOSITE OUTCROP	32
9	ANORTHOSITE OUTCROP	33
10.	LEUCOGABBRO OUTCROP	36
11.	LAYERED JOTUNITE OUTCROP	50
12.	UPPER JOTUNITE OUTCROP	54
13.	UPPER JOTUNITE OUTCROP	55
14.	HORNBLENDE BYTOWNITE	60
15.	MILL CANYON LAYERED AMPHIBOLTIC GNEISS OUTCROP	69
16.	PRECAMBRIAN SYNPLUTONIC STRUCTURAL FEATURES	81, 82, 83
17.	SLUMPING OF THE MARGIN OF THE ANORTHOSITE-SYENITE BODY	86, 87
18.	SHEARED GABBRO	89
19.	SIMPLIFIED RECONSTRUCTION OF THE BODY	94
20.	FINE-SCALE LAYERING IN GABBRO	95
21.	GRADED LAYERS IN JOTUNITE	96
22.	SLUMPED GRADED LAYERS IN JOTUNITE	97
23.	GRADED LAYERS IN JOTUNITE	99

24.	CRESCUMULATE LAYER IN LEUCOGABBRO	100
25.	WILLOW-LAKE-TYPE CRYSTALS IN GABBRO	103
26.	ANORTHOSITE BRECCIA	104
27.	ANORTHOSITE BRECCIA	105
28.	ANORTHOSITE BLOCKS IN ULTRAMAFITE	106
29.	ANORTHOSITE SLUMP BLOCK	107
30.	GRADED LAYERS IN JOTUNITE	109
31.	ANORTHOSITE XENOLITH IN JOTUNITE	110
32.	ANORTHOSITE WEDGE CUTTING LEUCOGABBRO	114
33.	ANORTHOSITE WEDGE CUTTING LEUCOGABBRO	115
34.	ANORTHOSITE WEDGE CUTTING LEUCOGABBRO	116
35.	FORMATION OF ANORTHOSITE WEDGES IN LEUCOGABBRO	117, 118
36.	CHANNEL STRUCTURE IN JOTUNITE	120
37.	SUMMARY OF STRUCTURAL ORIENTATION INDICATORS	121, 122, 123
38.	DIAGRAMMATIC CROSS SECTION OF THE BUCK CANYON SYNFORM	126
39.	STRUCTURES PRODUCED BY EMPLACEMENT OF THE MT. LOWE GRANODIORITE	138, 139, 140
40.	CENOZOIC EAST-WEST FOLDS	142, 143, 144
41.	OLDER, EAST-WEST FAULTS	148, 149, 150
42.	YOUNGER, NORTHEAST-TRENDING FAULTS	155, 156, 157
43.	AUGEN GNEISS FROM MILL CANYON, PHOTOMICROGRAPH	168
44.	GNEISS FROM MILL CANYON, PHOTOMICROGRAPH	169
45.	CROSS SECTIONS OF THE MILL CANYON STRUCTURE	172
46.	ANORTHOSITE OUTCROP	181
47.	OPHITIC LEUCOGABBRO	184
48.	PYROXENE (URALITE) IN OPHITIC LEUCOGABBRO	185
49.	PYROXENE (URALITE) IN OPHITIC LEUCOGABBRO	186

50.	NON-OPHITIC LEUCOGABBRO	188
51.	OPHITIC AND NON-OPHITIC LEUCOGABBRO (1055A and B)	189
52.	OPHITIC LEUCOGABBRO PHOTOMICROGRAPH	191
53.	URALITE PSEUDOMORPH PHOTOMICROGRAPH	192
54.	URALITE PSEUDOMORPH PHOTOMICROGRAPH	194
55.	PLAGIOCLASE-URALITE REACTION RIM PHOTOMICROGRAPH	196
56.	PLAGIOCLASE-URALITE REACTION RIM PHOTOMICROGRAPH	197
57.	SEQUENCE OF TEXTURAL DEVELOPMENT DURING POSTCUMULOUS RECRYSTALLIZATION OF ANORTHOSITE AND LEUCOGABBRO	204, 205
58.	PARTIALLY RECRYSTALLIZED CUMULATE PLAGIOCLASE PHOTOMICROGRAPH	208
59.	MESOPERTHITE WITH SWAPPED BORDERS, PHOTOMICROGRAPH	213
60.	MESOPERTHITE WITH SWAPPED BORDERS, PHOTOMICROGRAPH	214
61.	FERROMAGNESIAN AGGREGATE IN SYENITE, PHOTOMICROGRAPH	215
62.	FERROMAGNESIAN AGGREGATE IN SYENITE, PHOTOMICROGRAPH	216
63.	FERROMAGNESIAN AGGREGATE IN SYENITE, PHOTOMICROGRAPH	218
64.	FERROMAGNESIAN AGGREGATE IN SYENITE, PHOTOMICROGRAPH	219
65.	FERROMAGNESIAN AGGREGATE IN SYENITE, PHOTOMICROGRAPH	220
66.	LEUCOSYENITE PHOTOMICROGRAPH	223
67.	LEUCOSYENITE PHOTOMICROGRAPH	224
68.	ANDESINE TABLETS IN JOTUNITE, PHOTOMICROGRAPH	228
69.	GRADED LAYER OF JOTUNITE	230
70.	GRADED LAYERS IN JOTUNITE	231
71.	FERROGABBRO PHOTOMICROGRAPH	233
72.	ULTRAMAFITE PHOTOMICROGRAPH	234
73.	FERROGABBRO PHOTOMICROGRAPH	236
74.	GRADED LAYERS IN JOTUNITE	237

75.	A-F-M DIAGRAM	253
76.	An-Ab-Or DIAGRAM	254
77.	Al_2O_3 vs. An/An+Ab DIAGRAM	256
78.	K_2O vs. SiO_2 DIAGRAM	257
79.	MgO vs. FeO DIAGRAM	259
80.	P_2O_5 vs. DIFFERENTIATION INDEX DIAGRAM	260
81.	TiO_2 vs. CaO+MgO DIAGRAM	262
82.	NORMATIVE APATITE VS. ILMENITE+MAGNETITE DIAGRAM	264
83.	COMPARISON OF THE THREE UNITS ON VARIATION DIAGRAMS	266
84.	DISTRIBUTION OF UNURALITIZED ROCKS	271
85.	UNURALITIZED SYENITE, PHOTOMICROGRAPH	272
86.	PARTIALLY URALITIZED SYENITE, PHOTOMICROGRAPH	274
87.	COMPOSITION OF PYROXENE AND OLIVINE	276
88.	COMPOSITION OF AUGITE VS. VERTICAL POSITION	277
89.	CLINOPYROXENE LAMELLAE IN HYPERSTHENE, PHOTOMICROGRAPH	280
90.	CLINOPYROXENE LAMELLAE IN HYPERSTHENE, PHOTOMICROGRAPH	281
91.	CLINOPYROXENE LAMELLAE IN HYPERSTHENE, PHOTOMICROGRAPH	282
92.	CLINOPYROXENE LAMELLAE IN HYPERSTHENE, PHOTOMICROGRAPH	283
93.	UNINVERTED PIGEONITE, PHOTOMICROGRAPH	285
94.	UNINVERTED PIGEONITE, PHOTOMICROGRAPH	286
95.	PIGEONITE COMPOSITIONS	287
96.	OPAQUE OXIDE-HYPERSTHENE INTERGROWTH, PHOTOMICROGRAPH	289
97.	OPAQUE OXIDE LAMELLAE IN AUGITE, PHOTOMICROGRAPH	290
98.	OPAQUE OXIDE LAMELLAE IN AUGITE, PHOTOMICROGRAPH	291
99.	URALITE PSEUDOMORPH, PHOTOMICROGRAPH	292

100.	URALITE PSEUDOMORPH, PHOTOMICROGRAPH	294
101.	COMPOSITIONS OF AMPHIBOLES IN URALITE	296
102.	COMPOSITIONS OF PLAGIOCLASE IN LEUCOGABBRO (1055A, B)	300
103.	PLAGIOCLASE COMPOSITIONS IN TRAVERSE ONE	301
104.	PLAGIOCLASE COMPOSITIONS IN TRAVERSE TWO	303
105.	HISTOGRAMS OF PLAGIOCLASE COMPOSITIONS	304
106.	ORTHOCLASE CONTENT OF ANALYZED PLAGIOCLASE	309
107.	ANTIPERTHITE EXSOLUTION, PHOTOMICROGRAPH	314
108.	ANTIPERTHITE EXSOLUTION, PHOTOMICROGRAPH	315
109.	ANTIPERTHITE EXSOLUTION, PHOTOMICROGRAPH	316
110.	ANTIPERTHITE EXSOLUTION, PHOTOMICROGRAPH	317
111.	ANTIPERTHITE EXSOLUTION, PHOTOMICROGRAPH	318
112.	STRUCTURAL EVOLUTION DURING AND IMMEDIATELY FOLLOWING CRYSTALLIZATION OF THE ANORTHOSITE-SYENITE BODY	324, 325, 326
113.	MODEL FOR THE CRYSTALLIZATION OF THE MAGMA WHICH FORMED THE ANORTHOSITE-SYENITE BODY	350, 351

TABLES: Page:

I. CHEMICAL ANALYSES OF ROCKS OF THE SAN GABRIEL ANORTHOSITE-SYENITE BODY 240-3

II. CHEMICAL ANALYSES OF ANORTHOSITE FROM OAKESHOTT. 244

III. ESTIMATED AVERAGE COMPOSITION OF THE LITHOLOGIES AND THE ENTIRE ANORTHOSITE-SYENITE BODY 268

IV. AVERAGE COMPOSITIONS OF URALITIC AMPHIBOLES 295

V. AVERAGE COMPOSITION LESS VARIOUS PERCENTS OF PLAGIOCLASE 345

VI. AVERAGE COMPOSITION LESS VARIOUS PERCENTS OF ANDESINE ANTIPERTHITE 346

PLATES IN POCKET

I. GEOLOGIC MAP OF THE SAN GABRIEL ANORTHOSITE-SYENITE BODY

II. GEOLOGIC CROSS SECTIONS

III. MAP AND DIAGRAMMATIC CROSS SECTION OF THE JOTUNITE SUBUNITS

IV. THE ANORTHOSITE-SYENITE BODY AFTER RESTORATION OF CENOZOIC FAULT DISPLACEMENTS

V. GEOLOGIC MAP OF THE MILL CANYON WINDOW

CHAPTER 1

INTRODUCTION

GENERAL

The San Gabriel anorthosite-syenite terrain underlies about 250 square kilometers in the western San Gabriel Mountains and constitutes a well-defined massif-type pluton.

Anorthosite is a rock consisting almost entirely of plagioclase. Anorthosite occurs abundantly both as thick layers in stratified gabbroic plutons, and as large Precambrian massif-type plutons in areas of high-grade (mostly granulite facies) metamorphic rocks (Anderson, 1969). Typical massif-type plutons are thick sheets or lenses with domed roofs. Typically, the core of coarse massive anorthosite is surrounded by marginal gabbroic rocks generally containing 10 to 35 percent pryoxene (less commonly including olivine). Often only minor amounts of more mafic rocks (gabbro, periodotite) are present. Primary minerals are plagioclase (andesine to labradorite), hypersthene, augite, olivine, ilmenite and apatite. Mineral stratification and cumulate structures are present at least locally, and may be pervasive through thick sections in some massif-type anorthosite plutons. Closely associated with anorthosite are a varied suite of pyroxene-bearing rocks of very different composition--granitic, granodioritic, quartz syenitic, charnockitic and other similar rocks.

Important questions regarding massif-type anorthosite plutons include: (1) What is the relationship between anorthosite massifs and the stratified gabbroic plutons which frequently include thick sequences of anorthosite? (2) What are the detailed relationships between the various lithologies? (3) Are anorthosites and related gabbroic rocks cogeneric with the associated charnockitic rocks, or have they formed from independently generated primary magmas? (4) What is the nature

and origin of the parent magma of the anorthosite suite? (5) What is the nature of the mechanism whereby plagioclase is concentrated in extremely large masses? (6) What is the geological setting and tectonic environment of emplacement of massif-type plutons? These and other questions must be addressed in any study of massif-type anorthosite plutons (DeWaard, 1969).

Rocks of the San Gabriel suite include andesine anorthosite, leucogabbro, gabbro, jotunite, mangerite, syenite and quartz syenite. The San Gabriel rocks are exposed in an area of steep slopes and generally poor exposures. Pervasive fracturing and deep weathering of outcrops are common but this terrain has not been affected by post-plutonic high-grade regional metamorphism. Therefore, primary texture, structure and mineralogy are preserved in many rocks of this suite. In contrast to most other massif-type anorthosite plutons, the primary ferromagnesian minerals in rocks of the San Gabriel suite have been pervasively altered (commonly to uralite) at a late (deuteric) stage of magmatic activity.

Rocks of this suite have been affected by major post-plutonic deformation, including major episodes of folding and high-angle faulting. This terrain is tectonically floored by a thick zone of cataclastic rocks which were produced by important thrust movement.

Rocks of the anorthosite-syenite suite are present outside of the San Gabriel Mountains, but constitute considerably smaller, scattered exposures separated by major faults or by widespread younger plutonic or sedimentary and volcanic rocks. Rocks of this suite are present along the north margin of the Soledad Basin, several kilometers north of the San Gabriel Mountains. They are also present east of the San Andreas

fault in the Orocopia, Little Chuckawalla and Eagle Mountains, more than 150 kilometers to the southeast (Crowell and Walker, 1962; Silver, 1971; Powell and Silver, 1980).

Hershey (1902) briefly referred to anorthosite from Soledad Canyon, but the first comprehensive description was by Miller (1928, 1929, 1930, 1931), who published a reconnaissance geologic map of the body in 1934. Miller described the "anorthosite series" as comprised of four facies: anorthosite proper, dioritic and gabbroic facies, white and femic facies of anorthosite, and magnetite-rich facies. A series of studies by Oakeshott (1936, 1937, 1938, 1948, 1949) culminated in a more detailed geologic map and petrographic description of the rocks of the western half of the body in 1958. Oakeshott described the series as: anorthosite, gabbroic rocks, titanomagnetite rocks and gabbro pegmatite. He concluded that a parent magma of anorthositic gabbro composition differentiated from early anorthosite and marginal gabbro-norite through late residual ilmenite-magnetite-apatite-pyroxenite and pegmatites. In a study of the western half of the body, Higgs (1954) mapped and described the major units of the "norite-anorthosite complex" as norite, norite-anorthosite transition rock, anorthosite and apatite-ilmenite rock. He described the sequence of crystallization of the magmatic minerals (olivine(?), hypersthene, then andesine), described the uniform protoclastic shattering, and the subsequent development of a variety of deuteric minerals.

Crowell (1962) and Crowell and Walker (1962) described gabbro, diorite, anorthosite, syenite and related rocks of the San Gabriel body and correlated them, based on similarities in field relations and petrography, with a similar suite in the Orocopia Mountains, near the Salton

Sea. Silver, et al. (1963) reported on uranium-thorium-lead isotopic studies of rocks of the San Gabriel body and concluded that they have an age of about 1200 million years. Preliminary results of this study have been reported in Silver and Carter (1965), Carter (1970), Carter and Silver (1971, 1972). Cummings and Regan (1976) report the results of an aeromagnetic survey of the western San Gabriel Mountains.

The present work has emphasized field and petrographic study of the rocks of the anorthosite-syenite body. The mapping is of a detailed reconnaissance nature--thick brush, difficult terrain and deeply weathered rocks made it unfeasible to walk very many contacts. Gradational contacts and a diversity of lithologies, some difficult to differentiate in hand specimen, required that the distribution of lithologies be generalized in some places (Plate I). The petrography of the lithologies is reported, and numerous photomicrographs are used to convey the essential character of this rock suite. Limited chemistry and mineralogic studies are also reported and serve to outline the general chemical trends. Field work was started in 1966 and continued intermittently until 1970, most of it being done during the springs and summers of 1968 and 1969. In all, about 300 days were spent on field work for this study.

FIELD SETTING

The San Gabriel anorthosite-syenite terrain lies in the western San Gabriel Mountains about 30 kilometers northeast of Los Angeles, California (Figure 1). This east-west trending range is about 95 kilometers long by 40 kilometers wide and is one of the Transverse Ranges of Southern California. The area studied ranges in elevation from about 580

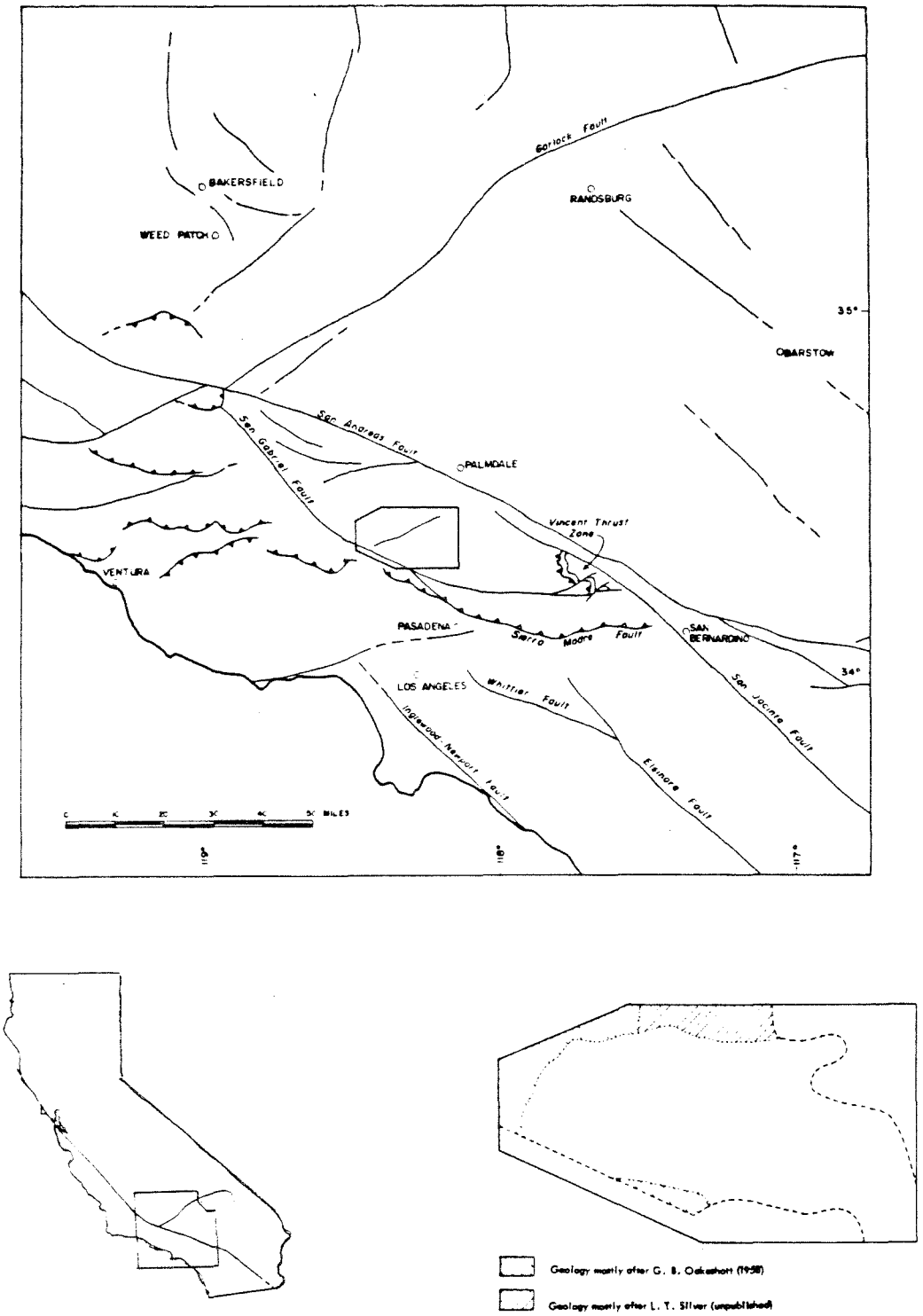

Figure 1. Index maps of the area covered by this study.

meters on the northwestern margin of the range, to about 2000 meters in the eastern part of the area. The Santa Clara River, bounding the northwestern edge of the San Gabriel Mountains, approximately defines the north edge of the study area. South from the Santa Clara River, this area includes the Magic Mountain-Mt. Gleason ridge, Pacoima Canyon, much of the Mendenhall Peak-Iron Mountain ridge, and southeast of Mt. Gleason, parts of the Fox Creek, Mill Creek, and upper Big Tujunga drainages.

The Little Tujunga Canyon Road is a paved highway which crosses the westernmost edge of the study area, the Santa Clara Road skirts the northernmost edge of the area along the Santa Clara River, and the Angeles Forest highway (U.S. highway N3) crosses the eastern part of the area. Narrow paved roads run to Magic Mountain from the west and to Mt. Gleason from the east, but the principal access to the central part of the area is by means of unsurfaced mountain roads, built and maintained by the U.S. Forest Service, especially those on Mendenhall ridge, in Pacoima Canyon, and along the Magic Mountain-Mt. Gleason ridge (Figure 2). These are good mountain roads, but may become impassable in wet weather, and some of them may be closed during periods of high fire danger. Only a few of the trails which formerly criss-crossed the area are presently maintained, although some of them are still passable. The Forest Service has constructed firebreaks along the crests of many of the ridges in this area and these brush-free ridges greatly facilitate access.

The western San Gabriel Mountains are covered predominantly by chaparral brushland, typical species of which include chamise, scrub oak, ceanothus, manzanita, mountain mahogany, and chaparral yucca. Access in much of the area is severely restricted by this dense, often nearly impenetrable brush, particularly at elevations below about 1700 meters.

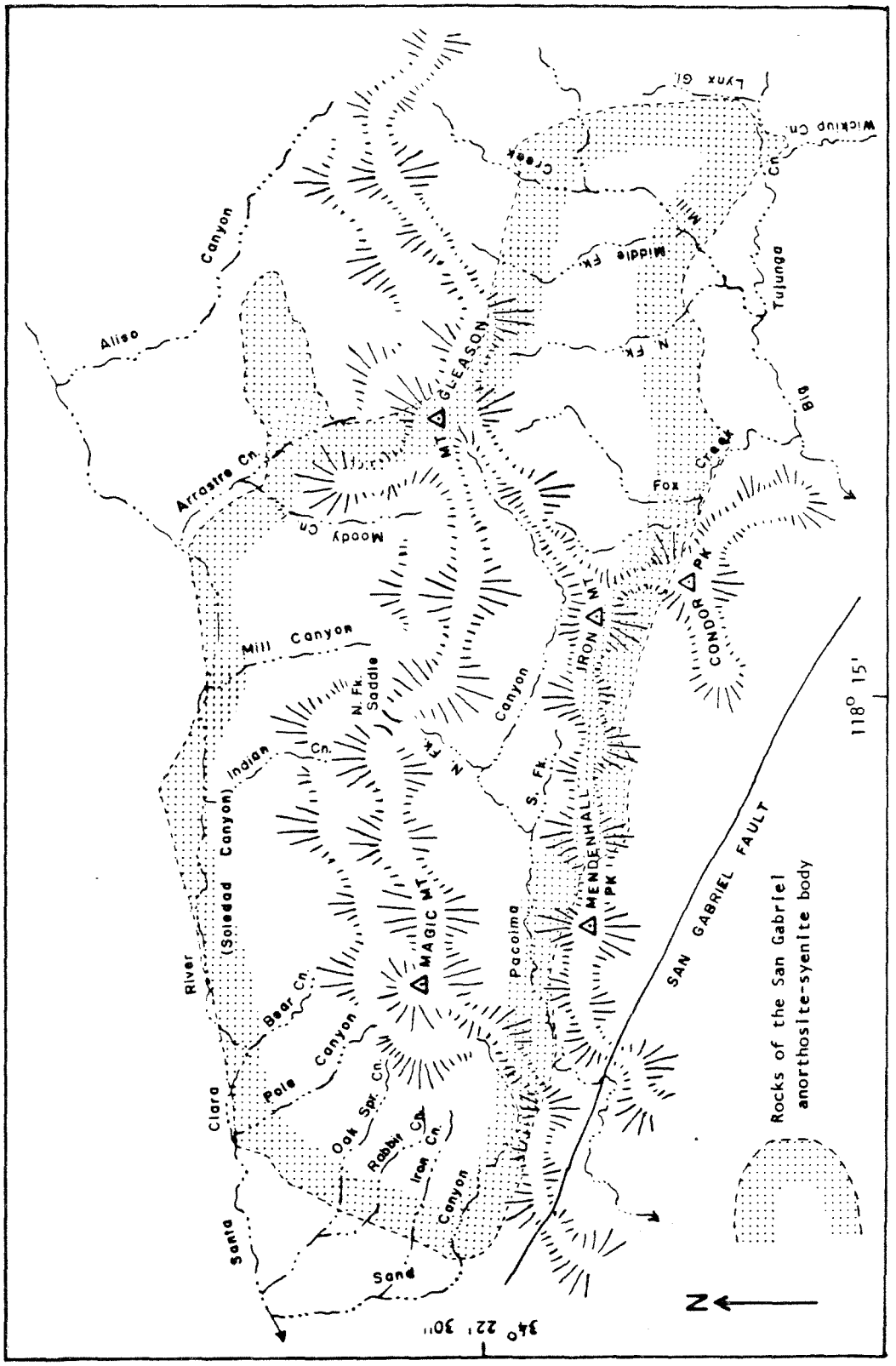

Figure 2. Important Physiographic Features of the Western San Gabriel Mountains.

Vegetation in the canyon bottoms includes white alder, cottonwood, California sycamore and willows, sometimes mixed with coast live oak. Canyon live oak occurs on steep rocky slopes and in canyons at higher elevations, and bigcone spruce is common on north-facing slopes and in canyons between elevations of about 750 meters and 1800 meters. Yellow pine forest occurs above about 1800 meters in the vicinity of Mt. Gleason and is composed predominantly of western yellow pine and coulter pine, with a little incense cedar.

This is an area of rugged topography where local relief is typically 500 to 1000 meters, and more than half of the slopes exceed the angle of repose (Sinclair, 1954). The steep topography and thin soil cover result in abundant exposures, but extensive fracturing and alteration of the rocks, deep weathering, and displacements due to mass movement, and dense brush make geologic mapping difficult. Generally, the best exposures are in canyon bottoms, in roadcuts and along the tops of some ridges.

Mapping at the scale of 1:24,000 was done on the 7-1/2 minute series of topographic quadrangle maps published by the United States Geological Survey between 1953 and 1960. Two of these quadrangles have a contour interval of 25 feet (Sunland and San Fernando) and the other six have a 40-foot contour interval (Mint Canyon, Agua Dulce, Action, Condor Peak, Pacifico Mountain and Chilao Flat).

The geologic map (Plate 1) consists of a synthesis of the field data drafted on a base constructed from the 15-minute Tujunga Quadrangle and the topographic base of the 15-minute San Fernando Quadrangle used by Oakeshott (1958, Plates 1, 2). Two-hundred-foot contours from these maps were used to make the topographic base for Plate 1.

The San Gabriel anorthosite-syenite body is intrusive into granulite gneisses, mostly of quartzo-feldspathic composition. It has, in turn, been intruded mostly just along its margins, by earliest granodioritic rocks (the Mt. Lowe granodiorite) and again by late Mesozoic granodioritic rocks (the Mt. Josephine granodiorite). Oligocene(?) and younger sedimentary and volcanic rocks border the anorthosite-syenite body, mostly along its north and northeast margins.

The body has been divided into three major stratigraphic units, each comprised of a distinctive group of lithologies and each in a distinctive stratigraphic position within the body. Most of the body consists of anorthosite and interlayered leucogabbro. These two lithologies, together with smaller amounts of gabbro, constitute the anorthosite-leucogabbro unit. Syenite and associated mafic rocks constitute the syenite unit. A diverse series of layered gabbroic rocks, many of them potassium-rich, constitute the jotunite unit.

The San Gabriel anorthosite-syenite body has been affected by younger deformation which includes the following major episodes: (1) Strong shearing and recrystallization along the northeast margin occurred during emplacement of the Mt. Lowe granodiorite, which also produced a series of open folds with northwest trends within the body. (2) Middle Tertiary compression produced east-west folds which developed several kilometers of structural relief. (3) Several more or less east-west faults have major apparent right-lateral or left-lateral and dip-slip displacements. (4) A set of northeast-trending faults have major left-lateral displacements. (5) The entire body may be part of an allochthonous sheet which is floored by a zone of strongly sheared gneiss, exposed in the Mill Canyon window.

CHAPTER 2

FIELD MAP UNITS

INTRODUCTION

Rocks in this area range from middle Proterozoic to Quaternary in age. Although nearly all the rocks exposed in the mountains themselves are crystalline, they include some Cenozoic clastic sediments and volcanics. This study concerns mainly the metamorphic and plutonic rocks (Figure 3). To the north and northwest, however, the anorthosite-syenite body is bordered by sedimentary and volcanic rocks of several Cenozoic formations. These are briefly described, although no attempt was made to map or even to comprehensively describe these rocks except as they occur in contact with the body. The rock units are described in order from oldest to youngest according to their known relative age sequence. Two relatively minor crystalline units and some dike rocks are described in order of their probable ages within the known sequence.

Besides the anorthosite-syenite body, only the pre-anorthosite Mendenhall gneiss was mapped over any extensive area, primarily in order to determine the aerial extent, pre-intrusive conditions and structural history of the body, and, therefore, even this unit is not discussed in detail. Some of the younger granitic rocks, notably the Mt. Lowe granodiorite and Mt. Josephine grandiorite, have strongly affected the post-emplacement structural development of the anorthosite-syenite body. These younger units were mapped and described only near their contacts with the body. Descriptions of these units are, therefore, brief and do not constitute a comprehensive treatment of their nature and origin but simply a brief outline of their salient features in order to help put the anorthosite-syenite body into its proper geologic context.

The greater part of this section consists of systematic descriptions of the various lithologies constituting the anorthosite-syenite body. It

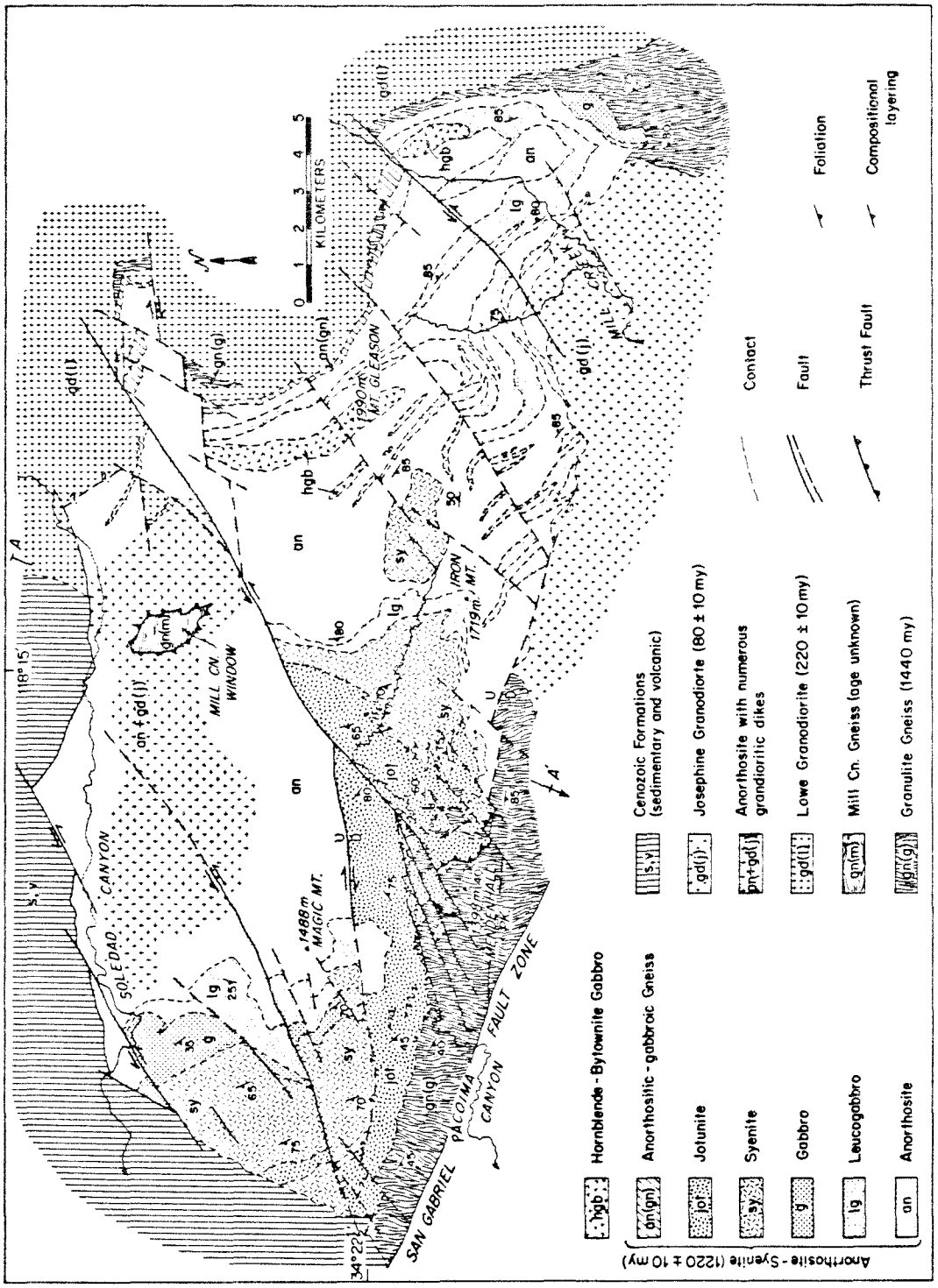

SIMPLIED GEOLOGIC MAP OF THE SAN GABRIEL ANORTHOSITE-SYENITE BODY, LOS ANGELES COUNTY, CALIFORNIA

Figure 3.

is primarily descriptive of the rocks of the anorthosite-syenite body; inferences and conclusions are presented elsewhere. Detailed petrography and mineralogy, the structural and petrologic evolution and the chemistry and petrogenesis of this body are described elsewhere and are included in this chapter only to the extent necessary to present a balanced description of these rocks. Separation of the observed facts from the inferences and conclusions based upon them is necessary because many of the more important and interesting conclusions are based on incomplete and sometimes even contradictory evidence.

MENDENHALL GNEISS

INTRODUCTION

Dark, layered, quartz-bearing gneiss containing variable proportions of ferromagnesian minerals crops out in several parts of the area mapped. This gneiss was included in the igneous and metamorphic rocks of Miller's (1934) San Gabriel Formation, and was named the Mendenhall gneiss by Oakeshott (1958) for exposures on and near Mendenhall Peak. Oakeshott (1937, 1954) first considered it as possibly related to the anorthosite-syenite body, perhaps altered border phase, but Higgs (1954) recognized that it was distinctly different from the anorthositic rocks, and Oakeshott (1958) described it as granulitic gneiss older than, and intruded by, rocks of the anorthosite-syenite body. Silver, et. al. (1963) have reported isptopic age determinations (U-Th-Pb) on zircons from rocks which intrude the Mendenhall gneiss, indicating that it must be older than 1200 million years, and data from zircons from the gneiss itself suggest that it may have been metamorphosed about 1440 million years ago.

The largest exposure of Mendenhall gneiss, about 16 kilometers long and 1-2 kilometers wide, appears in the southwest part of the map area (Plate I) between the anorthosite-syenite body and the San Gabriel fault, and extends from Sand Canyon to Trail Canyon. A second outcrop of Mendenhall gneiss (about 3 x 5 kilometers in area) appears in upper Big Tujunga Canyon, bordering the southeast limit of the anorthosite-syenite body. A relatively thin, discontinuous screen of deformed and recrystallized Mendenhall gneiss separates rocks of the anorthosite-syenite body from the Mt. Lowe granodiorite along the northeast margin of the body. The Mendenhall gneiss is best observed in roadcuts near Mendenhall Peak, but is also well exposed along the Little Tujunga Road in Bear Canyon and in upper Big Tujunga Canyon near the mouth of Wildcat Gulch.

The interior of the Mendenhall gneiss was mapped in the southwestern area and in part of the area south of Big Tujunga Canyon. Structural attitudes of the layering (and foliation), fold axes, and some faults were recorded. It was not possible at the scale used to define any mappable lithologic units, so that detailed internal structures within the gneiss have not been resolved.

LITHOLOGY AND FIELD RELATIONSHIPS

Mendenhall gneiss forms steep, rugged slopes and weathers to a dark brown color in most outcrops, tending to resemble some exposures of layered gabbroic rocks of the anorthosite-syenite body. Its strong compositional layering is usually conspicuous and close examination nearly always reveals the presence of quartz and of a penetrative metamorphic fabric.

The Mendenhall gneiss consists of several characteristic lithologies: blue-grey fine to coarse-grained biotite-hornblende quartzo-feldspathic granulite gneiss, altered greenish brown amphibolite, and biotite schist (Figures 4, 5). The most common lithology is quartzo-feldspathic granulite gneiss which contains irregular seams and aggregates of ferromagenesian minerals. Irregular, often lenticular alternating light and dark layers are typically 1 millimeter to 1 centimeter thick, but are commonly thicker. The presence of abundant blue-grey quartz is characteristic of these rocks.

The texture of the rocks of the Mendenhall gneiss is granoblastic (xenoblastic-granular), the "granulitic fabric" typical of granulites. Quartz, feldspars and pyroxene (not altered to uralite) were the most important primary minerals of the Mendenhall gneiss. Most rocks contain 15% to 40% irregular, anhedral grains or mosaics of blue-grey quartz. Some quartz replaces plagioclase, and is present in fractures cutting across earlier grains. Anhedral to subhedral grains of plagioclase make up 20% to 65% of most rocks. It is mostly oligoclase to andesine (An_{15-35}) in composition and is usually distinctly antiperthitic, containing numerous minute lamellae or blebs of exsolved alkali-feldspar. Plagioclase is saussuritized in some rocks and is commonly replaced by a fine mosaic of biotite, muscovite and quartz. Anhedral microcline, orthoclase and mesoperthite are generally less altered than the plagioclase and constitute 5% to 40% of most rocks. Relict pyroxene, both hypersthene and augite, is present in only a few rocks but pseudomorphs after pyroxene consisting of coronitic aggregates of green hornblende, biotite, chlorite and quartz are present in nearly all rocks. Rims of fibrous blue-green hornblende outline the original crystal forms of

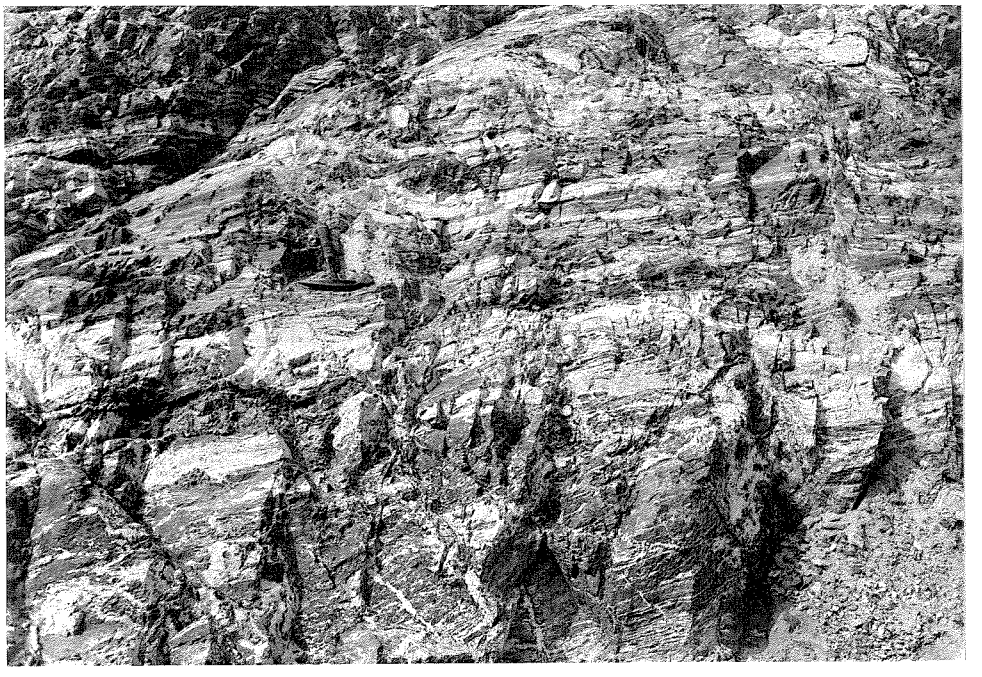

Figure 4. Typical quartzo-feldspathic Mendenhall gneiss from roadcut about 800 meters east of Bear Divide. Quartzo-feldspathic leucocratic layers alternate with layers of similar quartz and feldspars with much higher dark mineral content.

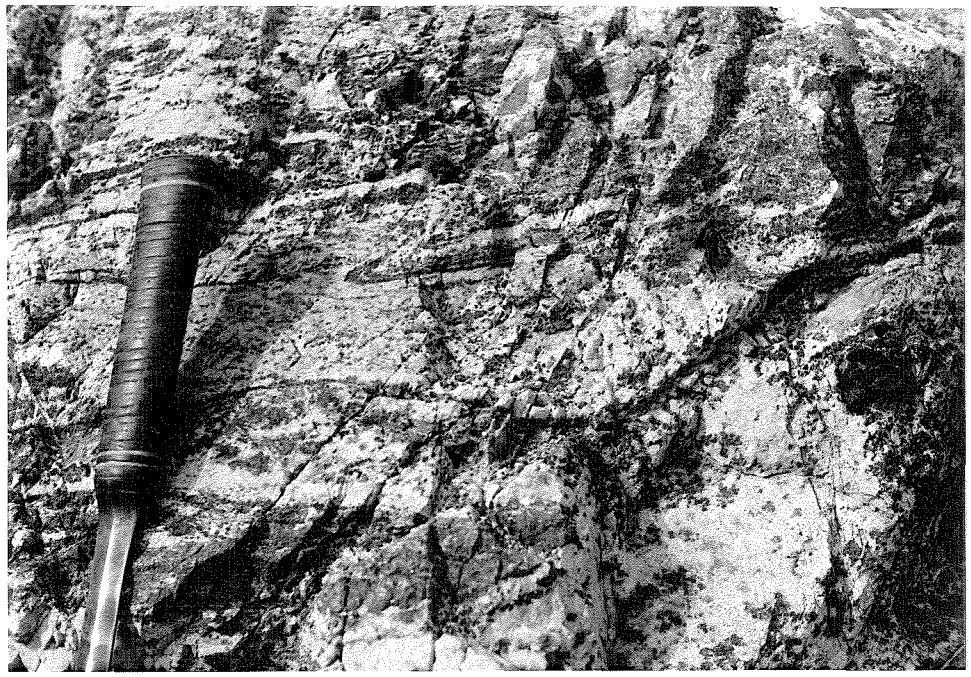

Figure 5. Typical Mendenhall gneiss from roadcut about 800 meters east of Bear Divide. The gneiss displays minor folds and late coarse quartzo-feldspathic mobilizate segregation.

some pseudormorphs. The very common, more irregular clusters of green hornblende, biotite, chlorite, quartz and calcite probably represent complete replacement of original pyroxene.

Green hornblende, biotite and chlorite are later minerals than the original quartz, feldpars and pyroxene and represent a retrograde assemblage developed in these rocks at some time following granulite facies metamorphism. Chlorite commonly partially replaces both hornblende and biotite. Accessory minerals include ilmenite, magnetite, apatite, pyrite and garnet. Very late secondary minerals which occur in fractures or as replacements of earlier minerals include biotite, muscovite, chlorite, epidote, leucoxene, quartz and calcite.

The Mendenhall gneiss can be distinguished from all other rocks in this area by the presence of abundant quartz and by the characteristic metamorphic fabric. The presence of abundant pseudomorphs or coronitic aggregates of retrograde minerals after original pyroxene serves to distinguish Mendenhall gneiss from other metamorphic rocks of the western San Gabriel Mountains.

Many Cenozoic faults cut the gneiss, and it is in fault contact with the adjacent rocks in many places. It is separated from Mesozoic granodioritic rocks by a branch of the San Gabriel fault in lower Pacoima Canyon and for about 8 kilometers northwest of Bear Divide. It is in fault contact with anorthositic rocks over a distance of about 5 kilometers in the Slaughter Canyon area, and also in several places north and east of Mendenhall Peak.

Over a distance of about 11 kilometers, between Mendenhall Peak and Bear Canyon, much of the contact between Mendenhall gneiss and rocks of the anorthosite-syenite body is intrusive. Along this contact,

layered granulite gneiss is in contact with the strongly layered rocks of the jotunite unit and often the two similar-appearing units can be distinguished only by careful hand lens examination. However, in the better exposures gabbroic dikes clearly crosscut gneiss and gneiss xenoliths are present in the jotunitic gabbro. Mapping of this concordant contact can be difficult, and requires closely spaced, detailed traverses; it is only approximately located in some places where exposures are poor. Sill-like intrusive bodies of jotunite in gneiss and tabular xenoliths of gneiss in jotunite near the contact make its exact location more difficult to determine. Northeast of Mendenhall Peak an area of about 5 square kilometers underlain predominantly by jotunite was mapped as gneiss by Oakeshott (1958).

Mt. Lowe granodiorite was concordantly emplaced against Mendenhall gneiss in upper Big Tujunga Canyon and elsewhere along the northeast margin of the anorthosite-syenite body. A high degree of plastic deformation, cataclasis, and recrystallization of the gneiss near the contact occurred during emplacement of the Mt. Lowe grandiorite. Deformed Mendenhall gneiss can be distinguished from other deformed rocks near this contact on the basis of its abundant quartz.

Mendenhall gneiss is intruded by Mesozoic Mt. Josephine granodiorite southeast of Mendenhall Peak and east of Strawberry Peak. No obvious metamorphic effects were seen more than a few centimeters from the contact, and numerous gneiss xenoliths are present in granodiorite hundreds of meters from the contact.

PRE-METAMORPHIC LITHOLOGY

Mendenhall gneiss in the western San Gabriel Mountains consists entirely of quartzo-feldspathic and amphibolitic layers and contains no quartzite, pelitic components or calc-silicate rocks. Pronounced layering on a relatively fine scale might be at least in part inherited from the pre-metamorphic rocks. Field relationships and primary structures in the anorthosite-syenite body suggest that this layering was probably sub-horizontal prior to intrusion of the anorthosite-syenite body. Oakeshott (1958) has suggested that this gneiss represents metamorphosed quartz monzonitic to quartz dioritic rocks. A possible alternative is that it originally consisted of intermediate to acidic volcanics.

ANORTHOSITE-SYENITE BODY

INTRODUCTION

The anorthosite-syenite body is comprised of three main units: 1) the anorthosite leucogabbro unit consists principally of anorthosite but also includes significant proportions of leucogabbro, and lesser amounts of gabbro; 2) the syenite unit consists principally of syenite, but includes a very mafic subunit near its contact with the anorthosite-leucogabbro unit; and 3) the jotunite unit is a compositionally variable mafic unit which has been subdivided into five subunits. Other relatively minor rock types of the anorthosite-syenite body include gabbroic to anorthositic gneiss and a variety of gabbroic dike rocks. The general characteristics of these stratigraphic units are described in this chapter and the petrography is described in Chapter 4.

Lithologies, Lithologic Map Units and Primary Stratigraphic Units

Mapping of the San Gabriel anorthosite-syenite body has allowed the separation of ten main lithologic map units, each made up of one or more fairly distinctive and well-defined lithologies. In addition, twelve other categories could sometimes be mapped, each consisting of a mineralogical, compositional, textural or structural variation of one of the main lithologic map units (Plate I). A few additional lithologies could only be distinguished by thin section study and so were not useful as field units. Some lithologies are very widespread, occurring in rocks in many parts of the body (gabbro, ultramafite) and others are much more restricted in occurrence (leucosyenite, sodic gabbro). Field studies have shown the distribution of field lithologies which were used to define the lithologic map units and their variations (Plate I).

Based on the resulting map patterns, it has been possible to divide the anorthosite-syenite body into primary stratigraphic units and subunits, each consisting of an assemblage of lithologies and lithologic map units, but each distinguishable from the others on the basis of either general lithologic, compositional, textural, or structural characteristics or relative stratigraphic position within the body. A given exposure may be potentially attributable to more than one stratigraphic unit or subunit, but the overall map patterns allow assignment to the appropriate stratigraphic unit or subunit. Stratigraphic units and subunits are not separately indicated on Plate I although they are fairly obvious based on lithologies, as described below, and a schematic diagram of their relative structural positions is shown in Chapter 4, and the distribution of jotunite subunits is shown in Plate III.

The descriptions in this chapter are organized according to the primary stratigraphic units and subunits. The major lithologies are described under the unit or subunit where they are most abundant.

Rock Nomenclature

Comparison of different anorthosite-charnockite suites is made difficult by the fact that different rock terminologies and definitions are used by different investigators. Even anorthosite is defined differently by different investigators, and associated rocks are given little known names such as farsundite and opdalite as well as such common names as syenite and granodiorite. Rock boundaries are commonly transitional so that lithologic boundaries on maps are drawn according to the investigator's interpretation of the rock terms and definitions. Rocks of the anorthosite-charnockite suite are distinctly different from other suites in several ways: (1) rocks of similar mineralogy commonly have extremely different color indices (C.I. = percentage of ferromagnesian minerals), sometimes ranging from 0 to 100 in a single outcrop; (2) "Gabbroic" rocks of this suite (dark, pyroxene-olivine rocks) commonly have more sodic plagioclase (andesire) than in typical gabbros so that "diorite" is sometimes used in naming them; (3) most rocks of this suite, including those of granitic composition, contain orthopyroxene as their dominant ferromagnesian mineral; and (4) feldspars in rocks of this suite commonly show intimate exsolution textures; perthite, antiperthite and mesoperthite are very common in these rocks. For the above reasons, it is appropriate to use a separate terminology to distinguish rocks of this suite from the more common rocks of virtually identical chemical

composition, but it is equally important to define the terminology used before any description of the anorthosite-syenite body is presented. Good discussions of nomenclature of rocks of the anorthosite kindred are given by Kolderup (1904), Goldschmidt (1916), Hodal (1945) and DeWaard (1969).

Figure 6 shows the modal compositions and nomenclature adopted for use in this study. All anorthosite-related rocks in the San Gabriel Mountains contain less than 10% quartz, but anorthosite-related quartz syenite is present elsewhere in southern California and so is included in the nomenclature. It is important to note that feldspar proportions are determined by thin section estimates of the proportions of fine-scale exsolution intergrowths, and thus are subject to substantial error and are not always useable for naming rocks in the field. For this reason, mangerite was not used as a field term. Most mangerite was mapped as syenite, but some may have been mapped as jotunite (monzodiorite). Based on subsequent thin section study, the field distinction between jotunite and syenite was probably fairly consistently applied at about 35% potassium feldspar.

Figure 7 shows the color index and nomenclature used in this study. The nomenclature adopted was based primarily on field occurrence. For example, most jotunite has a C.I. between 25 and 50 and no "leucojotunite" name was necessary, mangerite was not a useful field term and so was not separated into different catagories, and a C.I. exceeding 40 was unusual for syenite so that ferrosyenite is designated at a different C.I. than ferrojotunite or ferrogabbro.

The terms syenite and quartz syenite were used because of their prior use to describe rocks of this suite (Crowell and Walker, 1962).

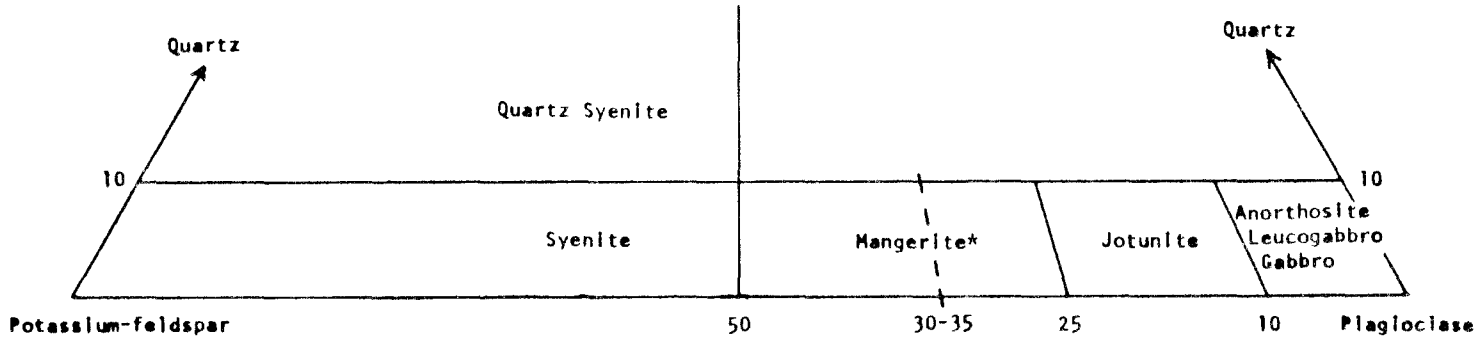

Figure 6. Rock nomenclature, based on feldspar composition vs. quartz. (*mangerite is not a useful field lithology--dashed line indicates approximate field division between syenite and jotunite).

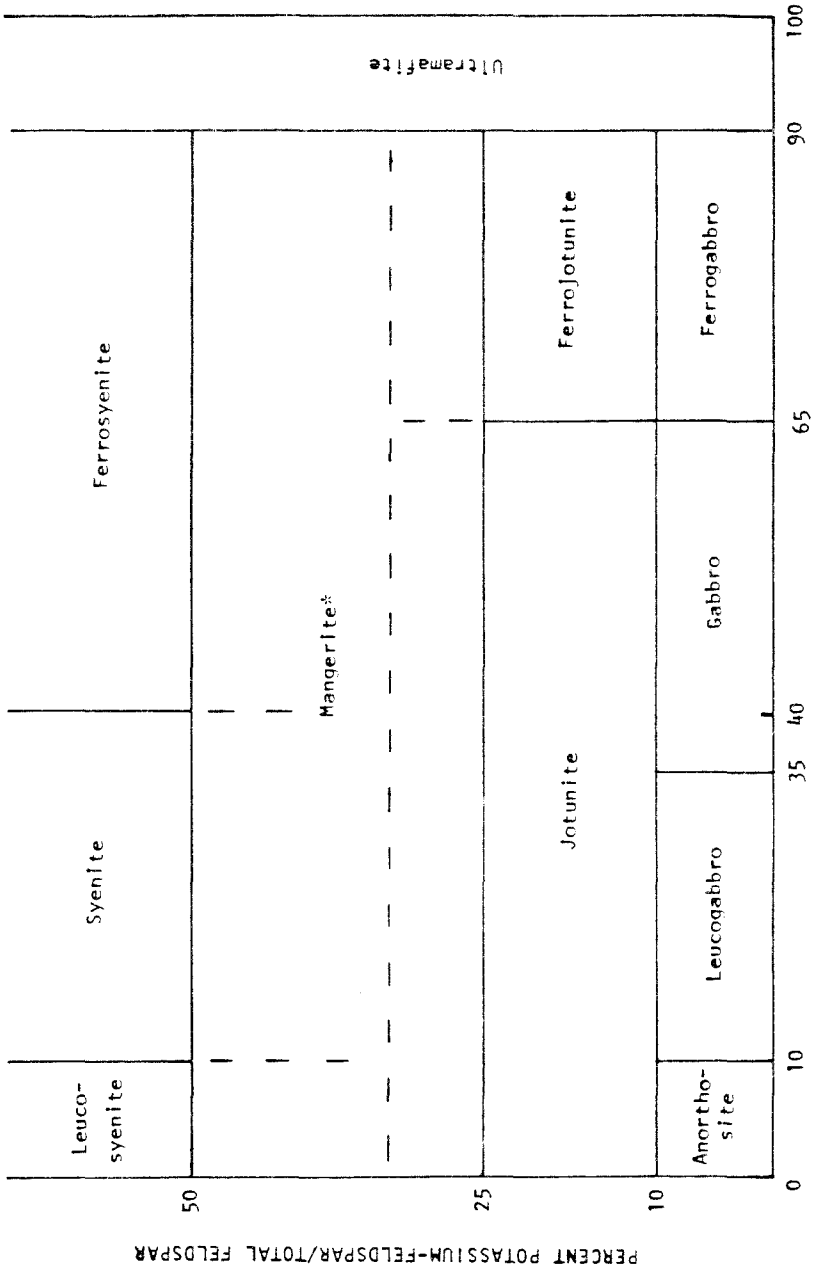

Figure 7. Rock nomenclature, based on feldspar composition vs. color index. (*mangerite is not a useful field lithology--dashed lines indicate approximate field division between syenite and jotunite).

In other anorthosite-charnockite suites, orthopyroxene commonly predominates over clinopyroxine and olivine. Primary ferromagnesians in the San Gabriel suite are almost universally altered, so that the predominance of orthopyroxene cannot be positively confirmed (see Chapter 4). For this reason, the term gabbro has been used rather than norite even though jotunite and mangerite have been retained.

Contacts and Attitudes:

The overall anorthosite-syenite body appears to have been concordantly intruded into Mendenhall gneiss along that part of its upper contact now exposed. Although the approximate original location of part of its base can be inferred, it is nowhere seen. The intrusive complex was at least 10 kilometers in maximum thickness and perhaps about 20 kilometers in diameter, although its original shape and extent can only be inferred. A penetrative edge of the intrusion is only a few hundred meters in local thickness south of Upper Big Tujanga Canyon, but this thickness increases rapidly to the north-west and west, apparently reaching 7 kilometers in the Middle Fork Mill Creek and possibly 12 - 15 kilometers in Soledad Canyon at the northwestern edge of the exposed body. It probably thins toward the south near Slaughter Canyon where the syenite and jotunite units together are only a few hundred meters in thickness, compared to a total of nearly 5 kilometers for the two units about 3 kilometers north in Pacoima Canyon. However, since its base is not exposed, the thickness of the anorthosite is unknown in this area and may not undergo a similar change in thickness.

About 13 kilometers of the upper contact is exposed between Slaughter Canyon and Sand Canyon along the southwest edge of the body;

Particularly good exposures are present in Pacoima Canyon and east of Mendenhall Peak. Gabbroic rocks of the jotunite unit intrude generally sub-horizontal gneisses in this area along a contact which is nearly always sub-parallel to the layering and foliation of the gneiss. The contact is commonly relatively narrowly-defined, especially in the west, but elsewhere is a zone several hundred meters in thickness in which numerous sill-like bodies of gabbro intrude the adjacent gneiss, sometimes isolating bodies of gneiss to produce xenoliths which generally parallel the contact. The gneiss xenoliths reach 30 to 50 meters in thickness and more than a kilometer in length, constituting mappable bodies in some instances. Gabbroic sills in gneiss are usually only a few meters in thickness. About 19 kilometers of the contact is exposed along the northeastern boundary of the body where it was strongly deformed during emplacement of the Mt. Lowe Granodiorite. Tabular screens of partially recrystallized Mendenhall gneiss separate anorthosite from Mt. Lowe granodiorite along parts of this contact. Primary layering in the anorthositic rocks and the probable original foliation of the gneiss both approximately parallel the contact which therefore was probably originally concordant, but because of the deformation, little else can be said of the nature of the original contact in this area.

Between Fall Creek and Wickiup Canyon, the southwest margin of the anorthosite has been intruded by granitic rocks related to the Mt. Josephine granodiorite. The granitic rocks contain xenoliths of Mendenhall gneiss 0.5 to 2 kilometers southwest of the contact, and xenoliths of anorthosite up to 0.5 kilometers southwest of the contact. Layering in the xenoliths is similar in orientation to that in nearby

gneiss and anorthosite. Xenoliths within the contact zone, which is up to 400 meters wide, are very little rotated or displaced; a few contacts within the anorthosite-syenite body can be projected across the contact and traced through several xenoliths within the granitic rocks. These observations suggest that the xenoliths have not been greatly displaced during intrusion of the granitic magma and that they can be used to locate the approximate original position of the basal anorthosite-Mendenhall gneiss contact which appears to have been generally concordant in this area.

The edge of the anorthosite-syenite body is seen only in upper Big Tujunga Canyon where exposures are poor. The upper and lower contacts and internal layering are roughly parallel to the layering and foliation of the adjacent Mendenhall gneiss.

The orientation of compositional layering was measured wherever possible. Only representative attitudes were recorded; some are averages of up to ten separate measurements. Only primary surfaces were measured, usually the orientation of primary compositional layering. The orientation of plagioclase tablets ophitically included within larger pyroxene crystals is normally parallel to the compositional layering where both are present, and was, therefore, measured in a few instances where compositional layering was not seen. A few rocks have a slight preferred orientation of ferromagnesian minerals or groups of minerals which is normally parallel to compositional layering and was measured in a few places where layering was not seen.

Primary layering and mineral orientation may be masked by any of several superimposed features. Deeply weathered rocks and poor exposures obscure attitudes, especially on ridges and on brushy slopes.

Distinct shear zones and pervasive distributed shearing frequently mask primary layering and sometimes produce a foliation. Younger dikes, mostly gabbroic or granitic, are quite common and may rarely be mistaken for primary layering, especially where gabbroic dikes have been modified by shearing. Small faults and joints also can obscure primary attitudes.

ANORTHOSITE-LEUCOGABBRO UNIT

Anorthosite, leucogabbro and gabbro together comprise the largest of the three units which is at least 7 kilometers thick and exposed over about 170 square kilometers. Anorthosite consists of large anhedral crystals of white, gray and lavender calcic andesine with less than 1% to, at most, 10% coarse dark green to black ferromagnesian minerals and aggregates and makes up an estimated 70% of the unit. Leucogabbro is a compositionally layered rock containing an average of 10-35% ferromagnesian minerals in addition to calcic andesine and is especially common in the southeastern part of the body, along Mill Creek, where it forms thick cyclically layered sub-units alternating with anorthosite sub-units and makes up as much as 40% of the total section. Gabbro is a compositionally layered rock consisting of calcic andesine and more than 35% ferromagnesian minerals which occurs as a thick subunit near the top of this unit in Pole Canyon in the western part of the body and as smaller discontinuous bodies along the upper contact along the eastern and northeastern boundaries of the anorthosite-syenite body. An estimated 20% of this unit is leucogabbro and less than 10% is gabbro. These three rock types differ mainly in the percentage of their constituent minerals; mineral compositions and textures are similar in

most of these rocks. These three rock types, in the approximate proportions given, together constitute an estimated minimum of 65-75% of the total body and dominate its overall form and general compositional character.

Anorthosite

Anorthosite crops out over about 125 square kilometers and accounts for about half of the exposed area of the San Gabriel anorthosite-syenite body. It is a massive coarse-grained rock which forms locally resistant outcrops in canyon bottoms but is usually deeply weathered, and often forms even slopes with very little bedrock exposure. Good exposures of anorthosite can be seen in roadcuts along Angeles Forest Highway and along the Magic Mountain-Mt. Gleason ridge. In Soledad Canyon, it has been especially intensely shattered, crushed and altered by post-emplacement intrusive and tectonic activity.

Pure anorthosite consits of anhedral equant plagioclase crystals, 3 to 20 centimeters in diameter which show no significant preferred crystallographic or geometric orientation (Figure 8). In a few outcrops, however, it consists of tabular plagioclase crystals (parallel to(010)) which exhibit a slight preferred orientation parallel to layering in nearby leucogabbro outcrops. Such preferred orientation of plagioclase in anorthosite appears to be the exception rather than the rule. Primary layering is rare or absent in much of the anorthosite, but in many outcrops small quantities of ferromagnesian minerals (often 1-5%) are commonly found in compositional layers. Thick anorthosite containing no ferromagnesian minerals alternates with a few layers (commonly 5-100 centimeters thick) containing as much as 5-20% ferromagnesian minerals (Figure 9).

Figure 8. Typical outcrop of anorthosite about 1.5 kilometers south of Monte Cristo Creek. Crystals of andesine are about 15-25 centimeters in diameter but appear to be much smaller because of the numerous fractures characteristic of nearly all anorthosite in this body.

Figure 9. Anorthosite with a few thin layers of leucogabbro, near the mouth of the Middle Fork of Mill Creek.

Alteration along minute fractures gives the appearance of a foliation or layering in some outcrops, but closer examination shows that this is a superimposed alteration feature. Crushing superimposed on some rocks has produced slightly elongate crystal fragments which can exhibit a slight preferred orientation, but is also a recognizably younger feature. Well-developed joint sets, with or without alteration along them, produce a gross parallel structure in some anorthosite outcrops. Outcrops with small amounts of ferromagnesian minerals which have been smeared out along small faults may exhibit a foliation which is not always easily recognizable as being an entirely superimposed feature. Consanguineous mafic dikes usually intrude anorthosite parallel to the orientation of layering in nearby leucogabbro. When these dikes are strongly sheared by younger deformation, they produce a layering which may be difficult to distinguish from sheared primary layering.

Anorthosite masses are commonly gradational into leucogabbro in many places along Mill Creek in the east, and in upper Pole and Bear Canyons in the west. The transition appears as a gradual increase of ferromagnesian minerals, often grading from 0 to 25% over distances of a few tens of meters to more than 400 meters.

Anorthosite is everywhere separated from the Mt. Lowe granodiorite in the northeast by a narrow zone of gneissic rocks, some of them highly deformed, partially recrystallized anorthosite and related gabbroic rocks, and others similarly deformed Mendenhall gneiss, all of which were deformed by emplacement of the granodiorite. Mt. Josephine granodiorite discordantly intrudes anorthosite with well-preserved primary features along the southern edge of the body. Anorthosite

generally is separated from Mendenhall gneiss by a layer of gabbro or leucogabbro of variable thickness in upper Big Tujunga Canyon.

Leucogabbro

The average light brown to light grey leucogabbro has a color index of about 20 to 25. Typical outcrops have a non-homogeneous layered appearance (figure 10). It is usually more deeply weathered than anorthosite because its ferromagnesian minerals are so susceptible to weathering. It forms low, rounded outcrops along canyon walls, and even in roadcuts as much as 10 meters below the surface and along canyon bottoms, exposures are often of poor quality due to the deep weathering. In a few exposures in deep roadcuts, relatively fresh specimens can be found in the centers of large, spheriodially weathered boulders.

Leucogabbro is always compositionally layered with 1 centimeter to 10 meter layers which differ only in their relative proportions of plagioclase to ferromagnesian minerals. Much leucogabbro consists of a coarse anorthosite matrix surrounding 1-40 centimeter uralitized pyroxene which commonly ophitically encloses 0.5 to 3 centimer tabular plagioclase crystals. Some leucogabbro consists of 2 to 5 centimeter equant subhedral plagioclase subophitically enclosed by uralite aggrigates after original pyroxene of similar 5.20. Occasional much coarser-grained layers occur within normal leucogabbro. These 0.5 to 3 meter layers are sometimes strongly asymmetric, consisting of a course-grained anorthosite layer adjacent to a similarly coarse-grained layer of uralitized pyroxene.

Figure 10. Typical cyclically layered leucogabbro from the North Fork of Mill Creek. Dark spots are individual crystals of pyroxene (now uralite).

Leucogabbro occurs as thick 150-750 meter mappable subunits separated by anorthosite subunits of comparable or greater thickness. Because of the gradational changes between anorthosite and leucogabbro, units were defined by the estimated ferromagnesian mineral content of an area of at least 50 square meters. If possible, the area estimated was taken perpendicular to the compositional layering of the rocks in the outcrop. This was difficult in areas away from roads or major canyons where outcrops are limited; the relative abundance of anorthositic interlayers in a given area was probably sometimes overestimated because of its greater resistance to weathering. Leucogabbro subunits were successfully followed over distances of several kilometers in the southeastern part of the body, but in Fox Creek and near Messenger Flats, where access is more difficult, leucogabbro layers could not readily be mapped, in part because they are thinner and in part because they display less compositional contrast with anorthosite.

Gabbro

Gabbro appears as a dark brown to grey coarse-grained rock with a color index of 35 to 65, which forms rounded outcrops covered by abundant disintegrated granules. Relatively fresh outcrops can be found only in deep stream canyons such as in Pole Canyon. Typical gabbro can also be seen in Big Tujunga Canyon above the mouth of Wickiup Canyon. About 8 square kilometers is underlain by gabbro, most of it in the western part of the body between leucogabbro and syenite.

Pronounced compositional layering is as characteristic of gabbro as it is of leucogabbro. Layers typically range from 1 millimeter to as much as 1 meter in thickness, differing mainly in their color index.

Plagioclase (2-10 millimeters) is typically sub-ophitically enclosed by aggregates of uralite and other alteration minerals after original pyroxene of comparable size, and exhibits a slight degree of preferred orientation parallel to the layering.

Gabbro is gradational with both leucogabbro and syenite. Leucogabbro grades into gabbro over distances of several tens to a few hundreds of meters. Gradation into syenite occurs over distances of a few hundreds of meters in a zone which is parallel to compositional layering in the rocks on either side of the contact. The transition is from medium-grained layered gabbro (color index about 45) into relatively mafic syenite (color index 35-40) of about the same or slightly smaller grain size, containing numerous, more ferromagnesian-rich gabbroic layers 0.2-3 meters thick, which gradually decrease in abundance away from the contact so that the syenite is nearly homogeneous a thousand meters from the contact. The syenite-gabbro contact is best exposed west of Magic Mountain in upper Iron Canyon. Elsewhere, it is poorly exposed and consequently its nature is imperfectly known.

Gabbro forms a series of relatively small discontinuous bodies in contact with deformed Mendenhall gneiss or Mt. Lowe granodiorite along the northeast margin of the body. These rocks were strongly deformed by emplacement of the Mt. Lowe granodiorite. Typical gabbroic gneiss is exposed in road cuts in Mill Creek where Angeles Forest Highway crosses the northeastern margin of the body.

Some gabbroic rocks near the contact with rocks of the syenite unit north and west of Magic Mountain contain very sodic modal and normative plagioclase. Microscopically, these rocks often contain more abundant alteration minerals (biotite, amphibole, epidote, etc.) than other

gabbroic rocks, but megascopically they are indistinguishable from other gabbros of this unit. The location of sodic gabbro is indicated on the geologic map (plate I) only where thin section study has been adequate to confirm its presence; the distribution of sodic gabbro could not be defined on the basis of field study alone.

SYENITE UNIT

Rocks assigned to the syenite unit crop out over about 40 square kilometers in the San Gabriel Mountains, about half of this exposed west and northwest of Magic Mountain, and the remainder exposed in the central part of the Buck Canyon Synform in upper Pacoima Canyon. West of Magic Mountain, this unit is apparently more than 5500 meters in thickness, and in the center of the Buck Canyon synform it is approximately 4500 meters in thickness.

The syenite unit is found in contact with rocks of the anorthosite-leucogabbro unit in the area north and west of Magic Mountain and in the Buck Canyon synform in upper Pacoima Canyon. Syenite is a massive, generally homogeneous rock consisting predominantly of mesoperhite, and is almost entirely lacking in any compositional layering. The syenite unit also contains some ferromagnesian-rich rocks with well-developed compositional layering. Except for these layered rocks, most of the compositional differences within syenite are minor variations in the type and abundance of ferromagnesian minerals, or of the average feldspar composition, or reflect different degrees of alteration. Quartz syenite was not observed except as minor float near North Fork Saddle. However, quartz syenite associated with other anorthositic and gabbroic rocks is exposed north of the Soledad Basin and elsewhere in southern

California east of the San Andreas fault (Silver and Carter, 1965, Crowell and Walker, 1962). In the Buck Canyon synform, both the base and the top of the syenite unit are in un-faulted contact with underlying and overlying rocks of the anorthosite-leucogabbro and jotunite units respectively. The lower contact is approximately concordant with layering in rocks of the adjacent anorthosite-leucogabbro unit and is quite complex in detail (see Chapter 3). In Pacoima Canyon, many tabular bodies of ultramafic rock are present in syenite near this contact; some are probably thick layers in the normal sequence, and others are perhaps intrusive, sill-like bodies. West of Magic Mountain there are fewer ultramafic rocks in syenite near its contact with gabbro.

The upper contact of the syenite unit in Pacoima Canyon is with the strongly compositionally layered rocks of the jotunite unit. This contact is generally concordant but the two rock types interfinger on the limbs of the Buck Canyon synform. In lower Sand Canyon, rocks of the syenite unit are in contact with a thin anorthosite layer which forms the base of an overlying gabbroic subunit. Numerous small xenoliths of Mendenhall gneiss are present in syenite near this contact immediately north of Sand Canyon, but with this exception, rocks of the syenite unit are not in contact with Mendenhall gneiss.

The syenite unit has been divided into two subunits: (1) The ultramafic syenite subunit consists of layered ultramafic to gabbroic rocks (with color indices between 40 and 100) which in some places contain large angular blocks of anorthosite and where present, always occurs adjacent to the contact with the anorthosite-leucogabbro unit; (2) The normal syenite subunit consists of homogeneous syenite (color index about 25) and constitutes the greater part of the syenite unit.

Ultramafic Syenite Subunit

The ultramafic syenite subunit is quite variable in both lithology and structure. Rocks assigned to this subunit include gabbro, ferrogabbro, ferrojotunitic gabbro, ferrosyenite, ultramafite, jotunite and mangerite. Many of these rocks show strong compositional layering; others are massive. All types may contain large, angular xenoliths of anorthosite, particularly near the contact with the anorthosite-leucogabbro unit. Because of the susceptibility to weathering of their ferromagnesian minerals, the best exposed outcrops of this subunit are found in roadcuts and a few canyon bottoms. Most of these rocks are weathered dark brown to rusty brown in color and even the soil produced on rocks of this subunit has a characteristic dark brown color.

Lithologies of the ultramafic syenite subunit occur as thick tabular bodies 10 to 100 meters in thickness which include both normal stratigraphic layers and a few sills. Three to fifty centimeter compositional layering is most common and is primarily the result of differences in the color index of different layers, reflected as differences in weathering resistance. Common mineral grading in individual layers is evidenced by feldspar-enriched tops and feldspar-depleted bases. The mafic rocks of the ultramafic syenite subunit commonly contain numerous large (1 to 15 meter) angular blocks of anorthosite, especially near the contact with rocks of the anorthosite-leucogabbro unit. Compositional layers can be observed to drape over some of the anorthosite blocks. These rocks grade into syenite of the normal syenite subunit by gradual decrease of their color index.

The ultramafic syenite subunit has been distinquished in the Buck Canyon synform in upper Pacoma Canyon but has not been distinquished

as a separate subunit north and west of Magic Mountain where the syenite unit does not contain so many mafic rocks or anorthosite blocks near its contact with rocks of the anorthosite-leucogabbro unit.

Normal Syenite Subunit

Typical syenite is made up of alkali feldspar grains and about 15-35% ferromagnesian minerals, consisting of altered pyroxene and/or olivine. Rare leucosyenite (color index less than 10) and unusual ferrosyenite (color index more than 40) are present. Typical syenite is homogeneous with equant crystals of chatoyant feldspar which gives the rock a distinctive appearance. The original ferromagnesian minerals commonly have been altered to small equant aggregates of micas, amphiboles, epidote and quartz. Black biotite, conspicuous in these aggregates, is sparse in the other rocks of the intrusion. The rock has a light brown color in outcrop but fresh surfaces are slightly green to bluish in color. Syenite is slightly more resistant to weathering than anorthosite and leucogabbro, and forms irregular slopes with few prominant outcrops. Exposures are best observed in stream bottoms, as in lower Iron, Rabbit and Oak Springs Canyons. Excellent syenite exposures can be seen on the Mendenhall Ridge road about 1.5 kilometers northwest of Iron Mountain, and on the Magic Mountain road about 1.5 kilometers southwest of Magic Mountain.

Most syenite shows little or no compositional or textural layering. Lithologic variations can be found over distances of a few hundred meters, but rarely as distinct layers of any consistent orientation. In general, syenite near the base of the subunit is more leucocratic, or at least contains more numerous leucocratic patches than higher in

the section. Syenite near the base displays a greater abundance of fine-grained biotite and quartz in the aggregates formed by alteration of the original ferromagnesian mineral (pyroxenes and/or olivine).

There are scarce ferrosyenite layers 30 to 150 centimeters thick within the normal syenite subunit. They usually contain 40% - 60% ferromagnesian minerals and have extremely gradational contacts with normal syenite. No size or compositional grading has been observed in these layers west of Magic Mountain. Similar mafic layers 8 - 60 centimeters thick occur sporadically throughout the syenite in the Buck Canyon synform, commonly in layered sequences tens to even a few hundred meters thick alternating with normal syenite. These dark layers are often mangeritic or even jotunitic in composition, and commonly show excellent mineral grading. In the center of the Buck Canyon synform, at least 80% of the normal syentie subunit is syenite.

JOTUNITE UNIT

Rocks of the jotunite unit crop out over about 45 square kilometers and show the greatest compositional variability of the units making up the San Gabriel anorthosite-syenite body. The jotunite unit is exposed over an area about 16 kilometers long by 2 - 3 kilometers wide along the southern edge of the body. It is structurally the uppermost unit and, in places, attains thicknesses of 3 to 4 kilometers between the syenite unit and the Mendenhall gneiss which forms the roof of the body. Rock types present include jotunite, ferrojotunite, mangerite, and gabbro with lesser amounts of anorthosite, syenite, ferrosyenite, leucogabbro, ferrogabbro, and ultramafite. Compositional layering is

conspicuous on all scales from a few centimeters to hundreds of meters. Jotunite is probably the most abundant rock type present, and the average composition of this unit is about that of a jotunite (monzodiorite).

Rocks of this unit are generally deeply weathered and form smooth brush-covered slopes which have few outcrops except where very steep. Useful outcrops are found only in the deeply incised canyons and in a few roadcuts. Weathering of the abundant ferromagnesian minerals gives these rocks their characteristic brown to orange-brown color, although less-weathered rocks in stream bottoms are grey in color. Some of the ultramafic rocks are highly resistant and form prominent outcrops in the bottom of Pacoima Canyon. This unit is best seen in Pacoima Canyon, particularly below the mouth of the North Fork; good exposures also occur along the road west of Magic Mountain and along the ridge east of Mendenhall Peak. A good view of the upper intrusive contact is exposed along the road about 4 kilometers southwest of Magic Mountain where massive, almost unlayered gabbro contains large (2-6 meter) xenoliths of gneiss near the contact, and sends several 0.3-1.5 meter dikes out into the gneiss. Other intrusive relationships are visible elsewhere, especially in Pacoima Canyon and along the ridge east of Mendenhall Peak. Large tabular gneiss xenoliths are abundant a few hundred meters or more below the contact in some places, and numerous sill-like gabbroic bodies are common in gneiss above the contact, mostly parallel to the gneissosity.

Layered gabbroic rocks of the jotunite unit closely resemble some of the darker parts of the Mendenhall gneiss they intrude. Distinct preferred orientation of feldspar, quartz and amphibole, although

usually not pronounced, is a nearly ubiquitous fabric element in Mendenhall gneiss, in contrast to the equigranular, unfoliated texture of the gabbroic rocks. Where quartz is not megascopically visible in Mendenhall gneiss, the two rock types can be distinguished only by the presence or absence of this mineral foliation.

The base of the jotunite unit is in contact with rocks of the syenite unit and possibly with rocks of the anorthosite-leucogabbro unit in some places. Most of this contact has been cut out by the Lonetree fault (Chapter 3) and the rest of it is exposed in areas with difficult access and exposure. The location and even the nature of the basal contact is based on much interpretation and inference. Best exposures occur in the Buck Canyon synform in Pacoima Canyon, south of Magic Mountain and in lower Sand Canyon.

Syenite appears to grade upward into rocks of the jotunite unit in the Buck Canyon synform. This gradation also occurs laterally by interfingering; the approximate syenite-jotunite contact appears to be structurally about 1000 meters higher in the axis of the synform than it is on its northern limb (cross sections E-E', F-F', plate II).

South of the Lonetree fault the base of the jotunite unit is faulted everywhere except possibly in Dagger Flat and Dorothy Canyons, south of Magic Mountain. In this area, parts of the jotunite unit are in poorly exposed contact with anorthosite, which is part of the anorthosite-leucogabbro unit. This contact has been mapped as several faults by Higgs (1954) but not by Oakeshott (1958). No persuasive evidence of faulting was observed, for example, in Dorothy Canyon where the contact is abrupt, and several faults of quite different orientations would be required to account for its trend. Anorthosite blocks up to

a few tens of meters in size, are present in ultramafic rocks of the jotunite unit immediately adjacent to this contact which suggests that it is an intrusive rather than a fault contact.

The jotunite unit is subdivided into five subunits which differ significantly in composition, texture, or structure, although they were not recognized as throughgoing map units during the initial mapping, and their detailed outcrop distributions are imperfectly known because of poor exposures and access, their compositional similarities and tectonic complications. However, each subunit can be distinctly characterized and will be described as it occurs in a given type locality. The approximate distribution of each subunit has been recognized from the mapping, and is shown schematically in Plate IIIA. Plate IIIB is a schematic cross-section through the jotunite unit showing the known and inferred relationship of subunits.

The five jotunite subunits are described in order from lowest to highest. (1) The anorthosite block subunit is very ferromagnesian-rich, usually poorly layered, and contains numerous large angular blocks of anorthosite. (2) The lower jotunite subunit usually exhibits relatively poorly developed compositional layering, but does not contain any anorthosite blocks. (3) The layered jotunite subunit exhibits well-developed 5-30 centimeter compositional layering, with individual layers which commonly persist over distances of tens of meters and very often exhibit well-developed mineral grading. (4) The ultramafic jotunite subunit consists mostly of ferrogabbroic rocks which are often massive but sometimes show compositional layering (occasionally graded), and may contain large anorthosite blocks in one area. (5) The upper jotunite subunit is commonly massive, but it locally contains strongly

developed graded layering, shows abundant evidence of extensive slumping, and contains numerous gneiss xenoliths, especially near its upper contact with Mendenhall gneiss.

Anorthosite Block Subunit:

In the upper part of the North Fork Pacoima Canyon, rocks stratigraphically overlying syenite contain numerous large anorthosite blocks. On the average these rocks have a slightly lower color index than those of the ultramafic syenite subunit in the Buck Canyon synform which also contains many anorthosite blocks. The ferromagnesian-rich matrix between the conspicuous anorthosite blocks averages about 50% ferromagnesian minerals, is usually gabbroic, but sometimes jotunitic, and often exhibits little or no compositional layering. However, some of these rocks exhibit pronounced compositional layering which is usually strongly mineral graded. Rocks of this subunit distinctly resemble rocks of the ultramafic subunit of the syenite unit exposed in the nearby Buck Canyon synform, and might be part of that suite. However, these rocks definitely overlie rocks of the syenite unit east of North Fork Saddle, and so are most reasonably included within the jotunite unit. Rocks of this subunit probably reach a maximum thickness of about one kilometer.

Lower Jotunite Subunit

The lower jotunite is obscured by poor exposures and complex contacts. It is best exposed along the lower part of the North Fork of Pacoima Canyon and along Pacoima Canyon for about 1.5 kilometer above the mouth of the North Fork. Rocks of this unit are in contact with the underlying syenite in and south of Pacoima Canyon where the contact

is extremely gradational and consists of extensive interlayering of the two rock types. The contact on plate I is somewhat arbitrary, but was mapped at the place where an estimated 50% of the section is syenite and the remainder is jotunite (recognized on the basis of its more ferromagnesian-rich composition, its more pronounced compositional layering, and the subophitic nature of its ferromagnesian minerals). The syenite and jotunite units appear to interfinger extensively, with relatively thin (less than 30 meter?) lower jotunite south of Pacoima Canyon changing to probably more than 900 meter(?) thickness north of the canyon. The large and abrupt change in thickness of the syenite unit in this area appears to be almost entirely compensated for by complementary changes in thickness of the lower jotunite and anorthosite-block subunits which thicken to the northwest as the underlying syenite thins (plate II).

Layered Jotunite Subunit

The layered jotunite subunit is similar in lithology to the underlying lower jotunite subunit, but is strongly compositionally layered throughout its entire section. It is best exposed in Pacoima Canyon between the mouths of the South and North Forks, although the Transmission Line fault lies only a few hundred meters northwest of the canyon, and other faults could be present a short distance southeast of the canyon. This section of the layered jotunite subunit appears to be thicker (about 700 meters) than it is farther west (about 300 meters) which may be in part due to tectonic repetition of part of the section in Pacoima Canyon. The large fault on at least one side of the canyon, the abundance of minor faults in these rocks, and the seemingly

anomalously large thickness of this subunit in Pacoima Canyon permit this possibility.

This subunit is nearly all of jotunitic composition and is characterized by strongly developed 5 to 30 centimeter compositional layering. Individual layers are persistent and do not pinch out or even change significantly in thickness in most exposures. At least a few mineral graded layers can be found in almost every outcrop, and in some outcrops (Figure 11) almost every layer is graded. A typical graded layer usually has about 35-50% ferromagnesian minerals at the base grading upward to about 10-25%, with relatively sharp upper and lower contacts. The compositional difference between top and bottom of individual layers is not always so pronounced, and the average composition of individual layers also varies, usually in the range of about 20 to 60% ferromagnesian minerals. As will be discussed in the next chapter, the graded layers are interpreted to be the product of density controlled sedimentation of cumulate minerals. However, although the average composition of layers in different parts of this subunit is variable, in a single outcrop individual layers are usually quite similar in average composition (Figure 11). Some relatively homogeneous jotunite is present in this subunit, but its average composition and texture is nearly identical to that of the layered jotunite, and in some places it grades into layered jotunite along the strike.

Both contacts of this subunit appear to be gradational. In Pacoima Canyon, the layering decreases into unlayered or indistinctly layered but otherwise very similar jotunite of the underlying basal jotunite subunit. Near the top of the subunit in Pacoima Canyon a

Figure 11. Conspicuous layering in rocks of the layered jotunite subunit of the jotunite unit in Pacoima Canyon near the mouth of Lonetree Canyon. Exposures are commonly excellent in stream bottoms but are very poor on most slopes due to deep weathering, colluvial cover and thick chaparral vegetation.

distinct but gradual increase in average ferromagnesian content occurs in otherwise similar layered rocks and continues to increase upward over about a hundred meters into rocks of the ultramafic subunit. A similar gradation between the two subunits occurs over a much shorter distance in Rattlesnake Canyon.

Ultramafic Subunit

Very mafic rocks of this subunit are well-exposed in the lower part of Rattlesnake Canyon and near its mouth in Pacoima Canyon. Most of the rocks in this subunit contain between 50% and 100% ferromagnesian minerals. The average color index is about 65, but those with color index of 100 are the most striking. In outcrop, these rocks are broken by joints and fractures along which extensive alteration has occurred, so that they appear as large rusty-orange blocks.

These rocks usually exhibit a distinct fabric of oriented mineral grains. Elongated anhedral feldspar crystals are most conspicuous in hand specimen, but microscopically, all the minerals are seen to share this preferred orientation. Fine-scale, but often indistinct compositional layering is visible only in the better outcrops. Some rocks of this subunit are massive although preferred orientation of mineral grains is still present. Rocks exposed along the road 3 kilometers southwest of Magic Mountain are very poorly layered, but ellipsoidal feldspar aggregates show preferred orientation. A few rocks of this subunit show pronounced rhythmic layering and abundant evidence of slumping. Rocks of this subunit reach a total thickness of at least 500 meters near the mouth of Rattlesnake Canyon.

The lower contact of this subunit with the layered jotunite subunit has been described above. Its upper contact with upper jotunite subunit rocks is exposed in only a few places and is best seen near the mouth of Rattlesnake Canyon where it appears to be gradational. Near the contact, ultramafic subunit rocks alternate with massive jotunite typical of the upper jotunite subunit over a distance of about 100 meters within which 3 to 10 meter irregular bodies of the two rock types occur. The two rock types are not interlayered, but are simply alternating patches with relatively sharp contacts, gradational over a few centimeters to a few tens of centimeters, with little tendency toward elongation of the bodies parallel to layering in the adjacent rocks. In some places however, ultramafic rocks are present in the upper jotunite subunit as irregular, often elongate, 3 to 30 meter bodies with relatively sharp contacts hundreds of meters above the ultramafic-upper jotunite contact.

Upper Jotunite Subunit

Rocks of the upper jotunite subunit are exposed along much of the course of Pacoima Canyon below the mouth of its South Fork, along the lower 3 kilometers of Sand Canyon, and along the ridge east of Mendenhall Peak. However none of these places contain a complete section. Rocks typical of this subunit will be described as they occur in Pacoima Canyon near the mouth of Gooseberry Canyon, along the road 1.5 kilometers east of Mendenhall Peak.

These rocks are commonly deeply weathered. Most rocks of this subunit are coarse, massive jotunite with very little compositional layering, but sometimes they exhibit relatively diffuse compositional layering

which may have more than one orientation, even though obvious cross-cutting relations are not seen. This is probably the most homogeneous of all the subunits of the jotunite unit; the average composition of 100 square meter areas in any of the outcrops would probably be nearly identical,with a color index of 40-50. A few rocks display pronounced compositional layering which most often occurs in 3 to 10 meter thick horizons alternating with thicker sections with little or no discernible layering. Where present, layered rocks of this subunit show abundant evidence of slumping, and extreme density grading of the layers is common (Figures 12, 13). Lenses of ultramafic rocks are common in a few parts of this subunit.

Gneiss xenoliths are much more abundant in this subunit than in any other part of the body. Large tabular xenoliths with little or no contact effects are abundant near the upper contact. In the middle and lower parts of this subunit, blocky xenoliths are less common and often show some evidence of contact metamorphism. These xenoliths can be seen in Sand Canyon 4 kilometers southwest of Magic Mountain and in lower Pacoima Canyon, where they can be recognized by their metamorphic fabric and thin mafic layers, even though quartz is commonly absent and their mineralogy is similar to that of the surrounding jotunite. There is some evidence that most xenoliths in the middle and lower parts of this subunit occur at specific horizons sub-parallel to the contact, which suggests the possibility of multiple intrusive pulses during emplacement and crystallization of the upper jotunite subunit.

The thickness of the upper jotunite subunit is probably about 600-1200 meters in Sand and Pacoima Canyons and may reach 1200-1800 meters east of Mendenhall Peak. In lower Sand Canyon, rocks of this

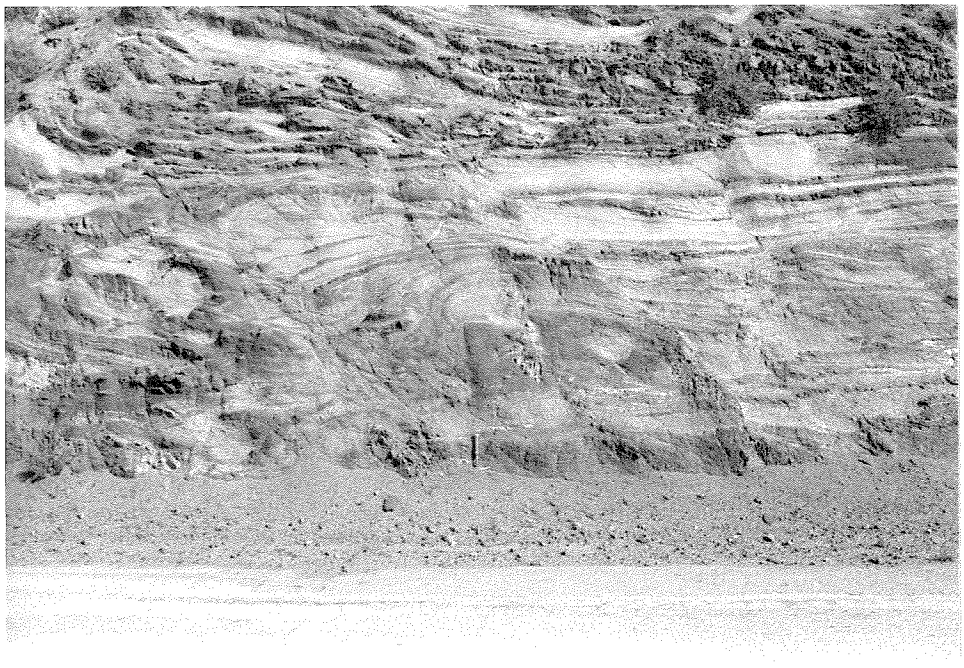

Figure 12. Cyclically layered jotunite from the upper jotunite subunit. Note the large slump block of jotunite in the center. Roadcut about 3 kilometers southwest of Magic Mountain.

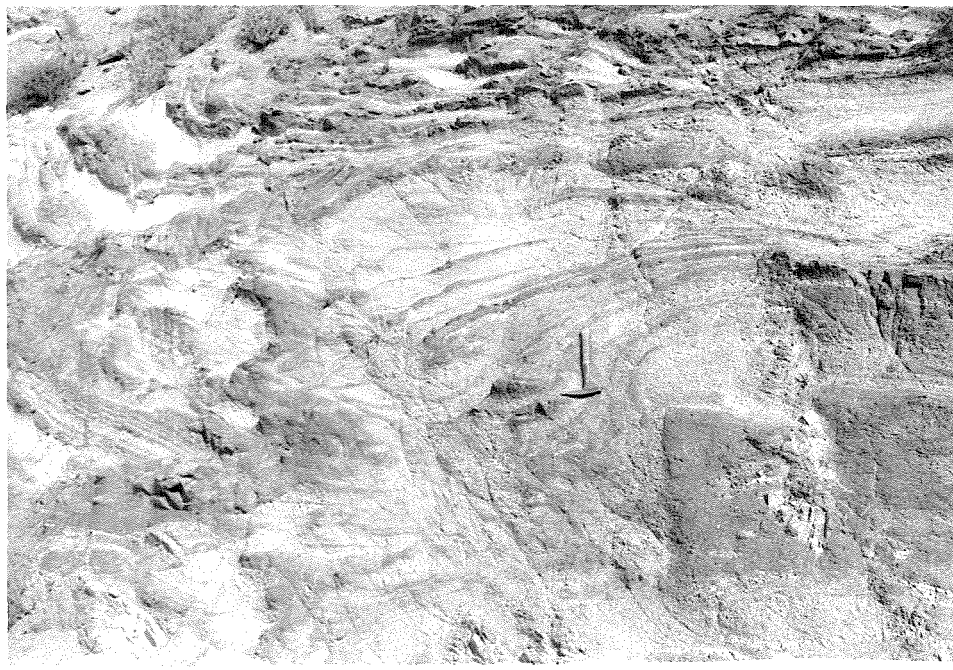

Figure 13. Slump structure in layered jotunite of the upper jotunite subunit (detail of left side of Figure 12). Roadcut about 3 kilometers southwest of Magic Mountain.

subunit are more mafic and homogeneous than those described above, and very few, randomly oriented compositional layers or slump structures are evident. In lower Gooseberry Canyon, rocks of this subunit are slightly more mafic, are almost always compositionally layered, and exhibit fewer slump structures.

Correlation of jotunite subunits between Pacoima Canyon and the ridge east of Mendenhall Peak was not possible. Rocks of the jotunite unit along this ridge lie between anorthosite (and/or syenite) and the overlying gneiss and attain an estimated thickness of about 2500 meters, but cannot be subdivided into the several subunits recognized elsewhere. They have been tentatively correlated with the upper jotunite subunit rocks which they most closely resemble. These rocks (many of which were mapped as "Mendenhall gneiss" by Oakeshott (1958) and Higgs (1954) are uralitized jotunites and gabbros, many of which are nearly homogeneous, with indistinct compositional layering over tens or even hundreds of meters of section. Compositional layering is occasionally well developed, but mineral grading is rare, and slump structures may be completely absent. There is no preferred orientation of minerals in much of this rock.

JOTUNITIC GABBRO PEGMATITE

On the basis of grain size alone, many of the gabbroic rocks of the anorthosite-syenite body could be called pegmatites. However, the rocks described here are clearly late-crystallizing rocks markedly coarser than the surrounding rocks of the same or similar composition. Most of the pegmatites are in the syenite and jotunite units. Only the larger bodies are shown on plate I. Jotunitic gabbro pegmatite is

particularly abundant in rocks near the contact between the syenite and jotunite units in the Buck Canyon synform in Pacoima Canyon above the mouth of the North Fork. Pegmatites in this area have been described by Neuerburg (1954), Jahns (1954) and Silver et. al. (1963).

The jotunitic gabbro pegmatite is a very coarse-grained rock which normally has gradational contacts, but locally crosscuts the surrounding jotunitic gabbro. Concentric zones contain extremely large 25-75 centimeter andesine, pyroxene (now uralite), hornblende, and biotite crystals and vary from outer andesine-pyroxene pegmatite, through andesine-hornblende pegmatite and andesine-oligoclase-biotite pegmatite to a core of quartz-perthite-albite-biotite pegmatite. Apatite is abundant and both zircon and allanite are also present in some pegmatite bodies. The pegmatite bodies are large (up to 200 meters) lenses generally parallel to layering in the surrounding rock. Only the larger pegmatite bodies include all of the mineralogical zones and include massive quartz cores. The gradational nature of most contacts and the mineralogical similarities to the surrounding jotunitic rocks suggest that the pegmatite bodies represent segregation masses developed during the later stages of crystallization of the jotunitic gabbro.

GABBROIC DIKE ROCKS

Dikes of medium to coarse grained, ferromagnesian-rich rocks cut Mendenhall gneiss near the contact with the anorthosite-syenite body as well as the various rocks of the body itself. Most of these rocks have color indices between 40 and 80 and often contain coarse plagioclase, some with a preferred orientation which may be

perpendicular to the dike. These dikes were produced by late-crystallizing mafic magmas of the anorthosite-syenite body and are more abundant in the upper part of the body than in the lower part of the anorthosite-leucogabbro unit. Most of these dike rocks are compositionally and texturally similar to the various gabbroic rocks of the jotunite unit but rarely show distinct compositional layering. Some of the larger of these dikes were mapped in the Mendenhall gneiss but few were mapped in the anorthosite-syenite body because of their abundance and generally small size.

A few dikes are extremely ferromagnesian-rich, with color indices commonly to 100, and contain 1 to 10 meter segregations of almost pure apatite-ilmenite rock. Apatite-ilmenite rock may comprise as much as 50% of a few dikes, which are designated separately on the geologic map (Plate I), but most often comprise no more than 10 to 20% of these dikes.

HORNBLENDE-BYTOWNITE GABBRO

Near the northeast margin of the anorthosite-syenite body, a resistant hornblende-rich rock forms three large bodies elongate in a north-south direction parallel to the nearby anorthosite-Mt. Lowe granodiorite contact. The largest body of this rock underlies Mt. Gleason and is about 5 kilometers long and 0.7 kilometers wide; a second much smaller body lies about 1 kilometer west of Mount Gleason, and a third underlies Rabbit Peak to the east (Plate I). A coarse, prismatic hornblende-rich phase of this unit is highly resistant and weathers to large rounded boulders of striking black and white layered rock which mantle the slopes underlain by this unit.

The characteristic lithology of this unit is a coarse (0.5-6 centimeter), layered black prismatic hornblende, grey plagioclase gabbro which contains small amounts of green chlorite, large skeletal epidote and minor pyrite (Figure 14). The layers (1-20 centimeter) differ in both color index and grain size. Hornblende is commonly perpendicular to the layers, which are often "wrinkled" or folded on a small scale (5-20 centimeter wavelength). Hornblende crystals as long as 20 centimeters are present in some layers.

A second major lithology of this unit is a layered fine-to medium-grained, foliated, chlorite-hornblende-epidote-bytownite gabbro. This rock is somewhat more abundant than the coarser hornblende-rich gabbro. This layered rock (3-100 centimeter layers) occurs in thick sequences which alternate with less common layers of nearly pure anorthosite (which is much more calcic than any other anorthosite in the map area). A few large angular 10 to 200 centimeter xenoliths of calcic anorthosite are present within the chlorite-hornblende gabbro on Mt. Gleason, but most calcic anorthosite occurs as thick layers within either the green chlorite-hornblende gabbro or the coarse hornblende-rich gabbro.

Rocks of this unit do not resemble the anorthosite, leucogabbro or gabbro of the anorthosite-syenite body. These latter rocks do not contain large prismatic primary hornblende, such calcic plagioclase, or abundant chlorite. Rocks of this unit resemble some of the rocks of the anorthosite-leucogabbro unit which have been recrystallized along the contact with the Mt. Lowe granodiorite. The gabbroic to anorthositic gneiss along this contact is not so coarse-grained, but a very common lithology is a coarse hornblende rock, and fine-grained chlorite-hornblende rocks are also present. The contact of the

Figure 14. Coarse layered hornblende-rich lithology of the hornblende-bytownite gabbro near Rabbit Peak.

hornblende-bytownite gabbro with normal anorthosite is gradational over 6-20 meters. At the contact, hornblende-rich layers gradually decrease in abundance and plagioclase increases until pure anorthosite is present.

The hornblende-bytownite gabbro has been considered to be part of the anorthosite-syenite body by previous authors (Oakeshott, 1958) and has been so indicated on the legend of the geologic map (Plate I). However, in spite of its spatial association with the anorthosite-syenite body, and its plagioclase-rich composition, hornblende-bytownite gabbro probably is not part of the primary anorthosite-syenite suite. Hornblende-bytownite gabbro differs from rocks of the anorthosite-syenite suite in that it has plagioclase which is much more calcic and compositionally zoned and primary hornblende rather than secondary amphibole after original pyroxene.

MICROPEGMATITE AND PEGMATITE DIKES

Small micropegmatite dikes are present in rocks near the contact of jotunitic gabbro with Mendenhall gneiss, especially in lower Pacoima Canyon. These dikes were produced during intrusion of the anorthosite-syenite body, probably by limited partial melting of Mendenhall geneiss, and are too small to represent on Plate I.

Small (0.5-3 meter) irregular bodies of coarse granitic pegmatite with gradational contacts occur in the quartzo-feldspathic parts of the Mendenhall gneiss. These pegmatites are granitic segregations which were mobilized during metamorphism of the Mendenhall gneiss and are too small to represent on Plate I.

Dikes of coarse granite pegmatite are common in the northeastern part of the area. These consist of variable proportions of pink or

cream-colored potassium feldspar, quartz (sometimes in graphic intergrowth), sodic plagioclase, muscovite, biotite and accessory minerals. Most pegmatite bodies are too small to show on the geologic map (Plate I), but they can reach as much as 1 kilometer in length. These pegmatites are probably related to the late Mesozoic Mt. Josephine granodiorite.

MT. LOWE GRANODIORITE

More than 250 square kilometers of the San Gabriel Mountains is underlain by a large, northwest-trending granodioritic pluton. This pluton was named the Mt. Lowe granodiorite by Miller (1934). Isotopic ratios in zircons from this body (U-Th-Pb) indicate that it is about 220± 10 million years old, and thus of early Triassic age (Silver, 1971). The Mt. Lowe granodiorite was studied where it borders the anorthosite-syenite body.

The Mt. Lowe granodiorite body consists of several rock types: leucocratic rocks are exposed in the Mount Pacifico-Chilao Flat area to the east and a more mafic border phase is exposed on Parker Mountain near the northern edge of the map area. Foliation is present in all rocks of the body and is particularly strongly developed, and accompanied by conspicuous compositional layering, near its contacts with rocks of the anorthosite-syenite body along its western margin. Its western contact with anorthositic rocks and older gneisses was probably originally straight and was compositionally zoned with hornblende-bearing, dioritic Parker Mountain border phase between the older rocks to the west and the more leucocratic granodioritic phases in the central part of the body to the east. The overall form of this pluton

north of the San Gabriel fault is that of a northwest-trending dome plunging to the northwest beneath the eastern part of the Soledad basin in the north and truncated by the San Gabriel fault zone on the south.

The rocks of the central part of this body consist of about 10% - 60% large (to 10 centimeters) subhedral to euhedral microcline phenocrysts in a 1-2 millimeter groundmass of subhedral to anhedral oligoclase, anhedral orthoclase, usually less than 10% anhedral quartz, and smaller amounts of biotite, epidote, zircon, apatite, and opaques. The more mafic border rocks (Parker Mountain diorite) contain 5-10% of 1-2 centimeter hornblende crystals, more biotite and fewer, smaller phenocrysts than the rocks from the central part of the body. Ferromagnesian minerals have a slight preferred orientation in rocks of the central part of the body, and define a very strong foliation in rocks near its margin. Microcline phenocrysts are oriented parallel to this foliation and become augen in the strongly deformed marginal rocks. Adjacent to the contact the microcline augen may be stretched out into extremely thin layers parallel to the strong foliation, which is parallel to the contact. Compositional layering is conspicuous near the contact and consists of strongly foliated granodiorite alterating with 30-100 centimeter layers of finer-grained, more leucocratic rock which is more weakly foliated and may represent dikes produced during the later stages of crystallization of the Mt. Lowe granodiorite. No good examples of Mt. Lowe granodiorite intruding older rocks were seen, but dikes probably related to the Mt. Lowe granodiorite (on the basis of similar lithology) are present in the older rocks near the contact east of Mt. Gleason.

Along its western contact, Mt. Lowe granodiorite was probably nearly entirely crystallized before final emplacement upwards into its present position. Emplacement of this largely solidified crystal mush was accompanied by strong shearing, especially along its margin, which affected both the crystal mush and the adjacent country rocks. The deformation strongly deformed and partially recrystallized the anorthositic rocks and Mendenhall gneiss near its margin.

LAMPROPHYRE DIKES

Numerous medium to fine grained amphibolitic to lamprophyric dikes occur throughout the area mapped, especially in the eastern part of the area. These dikes usually have low dips and often occur in large swarms. They are most common in the Mt. Lowe granodiorite and in rocks of the anorthosite-syenite body near its contact with the Mt. Lowe granodiorite, and they do not occur in the Mt. Josephine granodiorite. They are too numerous, and usually too small to show on the geologic map (Plate I) although locally they were valuable as markers showing the sense and cumulative magnitude of displacement along closely-spaced faults of small (tens of meters or less) individual displacement. Some of these dikes are sheared and altered so that they resemble dark schists, but normally, even when they occur in anorthosite, their fine grain size and lack of abundant apatite, ilmenite and uralitic pseudomorphs after pyroxene distinguish these dikes from mafic dikes related to the anorthosite.

MT. JOSEPHINE GRANODIORITE

Light to dark grey, medium to coarse-grained granitic rocks crop out over several square kilometers south of the anorthosite-syenite body, form a complex stockwork of dikes in anorthosite south of Soledad Canyon, and crop out over large areas elsewhere in the San Gabriel Mountains and adjoining parts of the Transverse Ranges. This unit is named after Josephine Peak, 5 kilometers south of the anorthosite-syenite body, which is underlain by these rocks. Granodiorite near Josephine Peak has an age of 80± 10 million years, determined from the U-Th-Pb isotopic ratios in zircons (Carter and Silver, 1971). Elsewhere in the area similar rocks are assumed to be of similar, late Mesozoic age on the basis of lithologic and sequential similarity.

The rocks mapped as Mt. Josephine granodiorite include hornblende diorite, hornblende quartz diorite, hornblende-biotite quartz diorite, biotite granodiorite, biotite-(hornblende) quartz monzonite and biotite granite. The most common rock type in the area mapped is medium to coarse grained granodiorite, followed by quartz diorite. The granodiorite typically consists of about 35-45% subhedral to euhedral oligoclase surrounded by about 20-25% anhedral potassium feldspar and 25-35% anhedral quartz with about 10% biotite and locally a little hornblende. Some rocks exhibit slight foliation but most are massive. Xenoliths of diorite in quartz diorite and of quartz diorite in granodiorite are common in some areas and dikes of grandiorite, quartz monzonite and granite are common in the more mafic rocks.

Granodioritic rocks intrude about 10 kilometers of the anorthosite-syenite body's southern margin, and intrude Mendenhall gneiss west of Condor Peak and east of Strawberry Peak. Xenoliths of the older rocks,

especially of gneiss, are abundant as much as 1 kilometer from the contacts, and scattered gneiss xenoliths are present throughout the area between the anorthosite body and the San Gabriel fault zone.

A complex stockwork of dikes and small stocks intrudes anorthosite and leucogabbro between Soledad Canyon and the Transmission Line fault between Bear and Arrastre Canyons. These dikes consist of granodiorite, quartz monzonite, granite, aplite and pegmatite and have no apparent preferred orientation following any throughgoing pre-existing structures in the anorthosite. These rocks are correlated with the Mt. Josephine granodiorite on the basis of their lithologic similarities. Granitic dikes are so common in the area between Mill and Arrastre Canyons that much of the area is shown as granite on earlier geologic maps (Jahns and Meuhlberger, 1954; Oakeshott, 1958; Jennings and Strand, 1969) even though deeply weathered anorthosite is present between the numerous granitic dikes in the few outcrops present.

These dikes were probably intruded by forceful injection along irregular joints or small faults in a relatively stress-free tectonic environment. The two main areas of abundant dikes in anorthosite are located in the basal anorthosite-leucogabbro unit in the cores of the major inferred antiforms. This suggests that intrusion was primarily into the lower part of the anorthosite-syenite body.

APLITE

Many fine-grained granite aplite dikes were noted in the area east of Mill Creek, but most were not mapped. West of Mill Creek mapping of these dikes was about as complete as the limited exposures and brushy slopes permitted. Aplite dikes are abundant in the southeast part of

the body, and seem to be most abundant between the middle of the anorthosite-syenite body and the contact with the Mt. Lowe granodiorite. Aplite dikes are also present in the Mendenhall gneiss south of Big Tujunga Canyon. Many of these dikes are sub-horizontal, and blocky jointing with 1-15 centimeter spacing is prominent in many of them. These dikes may be related to the Mt. Josephine granodiorite.

ROCKS OF THE MILL CANYON STRUCTURE

Unusual gneissic rocks are exposed over an area of about 1 X 2.5 kilometers in Mill Canyon and similar rocks are exposed in smaller areas in upper Bootleggers Canyon to the east and in Mattox Canyon to the west (Plate I). The three lithologies distinguished in the Mill Canyon structure are (a) lineated granodioritic gneiss, (b) gabbroic to anorthositic gneiss and (c) the Mill Canyon layered amphibotitic gneiss. These lithologies constitute map units defined by tectonic boundaries (discussed in more detail in the following chapter).

LINEATED GRANDIORITIC GNEISS

Light brown to pink, massive lineated granodioritic gneiss consists of quartz, plagioclase, potassium feldspar and a few percent biotite and muscovite. This is a cataclastic rock which has a weak to strong lineation. Indistinct compositional layering is present in a few places. Over much of the outcrop area the orientation of the lineation is fairly consistent, plunging gently toward the southeast.

GABBROIC TO ANORTHOSITIC GNEISS

Gabbroic to anorthositic gneiss separates granodiorite gneiss from amphibolitic gneiss in part of the area. Most of this gneiss is gabbroic. This gneiss contains a few 0.5-3 meter layers and lenses of anorthosite which show extreme cataclasis and recrystallization along their margins but sometimes have undeformed cores of coarse unrecrystallized anorthosite. One large anorthosite body approximately 15 meters across consists of only slightly brecciated unrecrystallized anorthosite but shows marginal cataclasis and lies within strongly deformed and recrystallized gabbroic gneiss. It represents a more competent block around which the less competent gabbroic rock was deformed.

MILL CANYON LAYERED AMPHIBOLITIC GNEISS

Dark, strongly layered and folded amphibolitic gneiss consists of 1-10 centimeter layers of amphibolite alterating with less abundant quartzo-feldspathic layers. This layered gneiss is deformed by complex folding, probably of at least two different ages. Most folds are tight, even isoclinal, but open folds are also present. Fold limbs are typically a meter or two apart, often with open curving noses, although much smaller and tighter folds are present in many outcrops (Figure 15). Axial planes of the larger folds may have a general preferred orientation, but in many outcrops they appear to be almost randomly oriented. Boudin are common in some outcrops, usually 1-2 meters long, but sometimes much larger.

Mill Canyon amphibolitic gneiss, particularly in the northern part of the area in Mill Canyon, is cross-cut by granodioritic dikes which

Figure 15. Typical exposure of the Mill Canyon layered amphibolitic gneiss in Mill Canyon. Note the isoclinal folds in some layers and the large augen in others.

exhibit a deformational fabric. They cross-cut some of the tight folds in the amphibolitic gneiss, but have been affected by some of the broader folds. These dikes may be correlative with the adjacent lineated granodioritic gneiss.

CENOZOIC SEDIMENTARY AND VOLCANIC ROCKS

North of the western San Gabriel Mountains and south of the Sierra Pelona,the Soledad structural basin contains several Cenozoic clastic sedimentary and volcanic formations. Some of these terrigenous formations contain clasts derived from the anorthosite-syenite body and were probably deposited near their present positions relative to the body. These formations record a complex middle and late Cenozoic geologic history which must have also affected the adjacent anorthosite-syenite body. A full treatment of this history is outside the scope of this study. Those formations actually bordering on the anorthosite-syenite body are described below in general terms.

VASQUEZ FORMATION

The Vasquez formation consists of about 4,500 meters of coarse nonmarine sandstone and conglomerate interbedded with basalt and andesite which unconformably overlie pre-Tertiary crystalline rocks along the north and east sides of the Soledad basin. This formation was first described, under a different name, by Hershey (1902), and has recently been described by Oakeshott (1958), Muehlberger (1958) and Spittler and Arthur (1973). A comprehensive program of field mapping and paleosource studies in the Vasquez formation is in progress by Leon Silver. The age of this formation is pre-late lower Miocene, and is probably

Oligocene (Oakeshott, 1958) although no diagnostic fossils have been recovered.

The Vasquez formation underlies several square kilometers of the eastern Soledad basin, a faulted structural basin plunging moderately towards the west and southwest. At the northern edge of the basin the Vasquez strata are very steep and even overturned in places. Rocks of this formation are juxtaposed against rocks of the anorthosite-syenite body by several faults of different ages. The eastern edge of this basin, near the San Andreas fault, is probably also very steeply inclined (Leon Silver, personal communication). The Vasquez formation is exposed in several different areas, often fault-bounded, separated by areas of crystalline rocks. The Vasquez formation is unconformably overlain by the middle to lower Miocene nonmarine Tick Canyon formation in Tick Canyon, and by the upper Miocene nonmarine Mint Canyon formation in the southern part of the basin near the San Gabriel Mountains.

The Vasquez sedimentary rocks are light-colored red, yellow and buff sandstone and conglomerate and lesser amounts of mudstone and shale. Most of the coarse clastic sediments were deposited by mud or debris flows from the adjacent high areas, especially along the south and southeast sides of the basin. Prominent conglomerate units containing distinctive clasts of anorthosite, Parker Mountain diorite, Mt. Lowe granodiorite, or combinations of these rock types can be traced for several kilometers from their source area in the southeast (Leon Silver, personal communication).

Pyroxene andesite and basalt flows are present in lower part of the Vasquez formation. These dark reddish-brown to black, fine-grained

flows constitute units sometimes exceeding 300 meters in thickness. They commonly contain a few percent of phenocrysts, mostly plagioclase but usually with some pyroxene, in a fine-grained sometimes vesicular groundmass. A few tuff beds are present in the northern part of the basin and volcanic breccias and agglomerates make up a large part of the formation in the eastern-most part of the basin near the San Andreas fault zone. Crowell (1973) reports a potassium argon age of about 24 m.y. for one of the volcanic flows in the Vasquez formation.

MINT CANYON FORMATION

The upper Miocene to lower Pliocene Mint Canyon formation (Oakeshott, 1958, Durham, Jahns and Savage, 1954) consists of more than 1200 meters of nonmarine clastic sedimentary rocks which unconformably overlie the Vasquez formation. It consists of fine to coarse grained clastic fluviate and lacustrine sediments derived chiefly from the Sierra Pelona and San Gabriel Mountains. Anorthosite boulders and pebbles are abundant in the Mint Canyon formation north and west of the western part of the anorthosite-syenite body where these sediments resemble Quaternary alluvium in the larger river channels. Thick (0.5-2 meter) conglomerate beds alternate with coarse sandstone or pebbly sandstone beds of similar thickness west of the mouth of Pole Canyon. Bedding is indistinct in most outcrops.

A tuff bed near the mouths of Rabbit and Oak Springs Canyons may correlate with the one mapped by Oakeshott (1958) in the upper part of this formation about 3 kilometers to the southwest. If this is the same bed, then the upper part of the Mint Canyon formation uncomformably overlies syenitic rocks north of Iron Canyon and this contact does not

represent the basal unconformity of the Mint Canyon formation.

PACOIMA FORMATION

Middle Pleistocene Fanglomerate exposed as discontinuous remnants around the western margin of the San Gabriel Mountains was named the Pacoima formation by Oakeshott (1952, 1958). Rocks correlated with the Pacoima formation (Oakeshott, 1958) are exposed near the mouth of Sand Canyon where about 10 meters of coarse, poorly-bedded sandstone and conglomerate unconformably overlie the Mint Canyon formation and the westernmost anorthositic rocks. Sub-angular clasts in this unit are derived almost entirely from Mendenhall gneiss and syenitic rocks presently exposed to the south and east. The proportions of the clast lithologies are similar to those in the Quaternary alluvium in Sand Canyon, suggesting that the drainages from which this formation was deposited were similar to present drainages, although generally smaller clasts suggests that topographic relief during deposition was probably less than at present. It is possible that these rocks are equivalent in age to some of the Quaternary terrace gravels, although most terrace gravels show fresher geomorphic form, are less dissected and consist of less consolidated sediment, and this exposure probably does represent a separate unit.

QUATERNARY TERRACE GRAVELS

Small areas of elevated terrace gravels occur along most of the larger streams of the area, many of them only a few meters but others as much as 200-300 meters above present stream courses. These coarse, unbedded to poorly bedded gravels were deposited along active streams

depositing debris similar in lithology, coarseness and rounding to that in present stream channels. Many larger terraces are found along the Santa Clara River on the northern margin of the mountains.

A broad surface of low relief in the northeastern part of the area between Mill Canyon and Aliso Canyon is covered by a thin veneer of gravel. The gravel is coarse, usually poorly bedded, and contains subrounded clasts derived from the area 1 to 6 kilometers to the south and east. The more resistant lithologies are concentrated in these deposits, notably the hornblende-bytownite gabbro and some lithologies of the Mt. Lowe granodiorite. Similar gravels are exposed along several flat ridge crests west of Mill Canyon where the same surface has been more deeply dissected.

QUATERNARY LANDSLIDE DEPOSITS

Landslides are less common in this area than they are in the eastern part of the San Gabriel Mountains, but Morton and Streitz (1969) show several large landslides in this area and others were noted during the course of mapping. Large landslides are present on the west side of Rabbit Peak and on the flanks of Magic Mountain. Landslides consist of broken rubble and blocks which were considerably jumbled during sliding.

Headwall scarps of large block slumps are present on the ridge between the south and main forks of Pacoima Canyon and on the ridge west of Slaughter Canyon, each consisting of a 30 to 60 meter trench with a few meters of closure.

Landslides and slumps were not systematically mapped although their recognition was important because unrecognized landslides or slumps could greatly complicate the interpretation of lithologic distributions and structural attitudes.

QUATERNARY ALLUVIUM

Coarse deposits of boulders, gravel and sand are present along most of the streams in the area. Their widest extent is along the Santa Clara River near Pole Canyon and near Acton where the river crosses wide alluvial floodplains. These deposits consist of locally derived clasts and include ilmenite-magnetite-rich sand and fine gravel concentrated from debris eroded from the anorthosite-syenite body. Oakeshott (1958) reports that pits dug in alluvium in upper Sand Canyon, where alluvium is not over 60 meters wide, extended to 20 meters without reaching bedrock, and similar pits in Pacoima Canyon above Dagger Flat show the alluvium to be more than 13 meters deep.

CHAPTER 3

STRUCTURE

INTRODUCTION

Pre-anorthosite structural features in the western San Gabriel Mountains are seen only in the small exposed area of Mendenhall gneiss (but could include some of those in the Mill Canyon amphibolitic gneiss). Several structural features developed during and soon after intrusion and crystallization of the anorthosite-syenite body play an important part in the development of its form and have important bearing on its petrologic evolution. A long and complex post-anorthosite structural history has obscured older structural features. Some of the younger structural features, such as different fault sets and some folds, may have developed synchronously or with overlapping ages rather than in the strict sequence in which they are described.

PRE-ANORTHOSITE STRUCTURE

Only a fragmentary record of definitely pre-anorthosite structure is preserved in the western San Gabriel Mountains, in the relatively small area underlain by Mendenhall gneiss along the southwestern and southeastern margins of the anorthosite-syenite body. A more complete pre-anorthosite record has been recognized a few kilometers to the north in Soledad Canyon in the crystalline basement forming the bottom and northern edge of the Soledad basin (Silver, 1971). In the north, older strata underwent two periods of metamorphism, the second of granulite grade, separated by an episode of intrusion of porphyritic granodiorite and quartz monzonite, all prior to intrusion of the San Gabriel aanorthosite-syenite body. The present structural grain of these older rocks is generally east-west, but has probably been transposed by Cenozoic structural episodes.

Layered, quartzo-feldspathic granulite Mendenhall gneiss is the only definitely known pre-anorthosite rock preserved in the area mapped. The original form of the anorthosite-syenite body was apparently that of a large concordant stratiform intrusion. Based on primary structures in rocks of the anorthosite-syenite body (see synplutonic structure), the Mendenhall gneiss was probably sub-horizontal in orientation before intrusion of the body and nearly so after its final crystallization. Small tight folds are abundant in many parts of the Mendenhall gneiss (Figure 5), and larger, more open folds are present in some places.

Attitudes of compositional layering and foliation were measured where consistent over several tens of meters; usually one representative attitude out of four or five measured is recorded on the geologic map. These attitudes are variable but have a generally northwest orientation in the western outcrop of Mendenhall gneiss which is elongate in a northwest direction. In the area near Mendenhall Peak the overall structure is that of a broad, east-west trending synform. Gneiss adjacent to the anorthosite-syenite body on the north side of Mendenhall Ridge has moderate to high dips to the south, while gneiss south of Mendenhall Ridge generally has moderate dips to the north. This broad synform is offset by a series of strike-slip faults, however, and can not be followed farther to the northwest in Sand Canyon, or to the east of Slaughter Canyon. Mendenhall gneiss in upper Big Tujunga Canyon has more consistent attitudes, typically about N 75°W, 75 -80° NE, and constitutes a nearly vertical, northwest-trending homoclinal sequence generally concordant with most layering in the adjacent anorthosite-syenite body. Tight isoclinal folds with axial planes parallel to the

foliation usually have similar axial plunges in a given outcrop. Their limbs are usually attenuated and are often disconnected. These folds are present in all parts of the gneiss, but especially in the lower Slaughter Canyon area. Representative folds of this type are shown on the geologic map. In Big Tujunga Canyon, folds of similar appearance were produced by deformation which occurred adjacent to the contact during emplacement of the Mt. Lowe granodiorite.

Larger, open to tight folds with unattenuated limbs typically a meter to several meters apart have variably oriented axial planes which are themselves refolded in some instances. These folds occur in relatively limited zones of complexly deformed gneiss and are not shown on the geologic map because of their usually highly variable attitudes even in a given outcrop. These folds may have developed during or soon after metamorphism, but could be the result of deformation during intrusion and crystallization of the anorthosite-syenite body. Augen are developed in gneiss in at least one of these fold zones; similar augen are found elsewhere near the contact with the anorthosite-syenite body, probably produced by minor contact recrystallization.

Rare bouden are 3 meter or larger lenses of less deformed, slightly layered gneiss surrounded by more highly deformed, more strongly layered gneiss.

STRUCTURES RELATED TO EMPLACEMENT AND CRYSTALLIZATION OF THE ANORTHOSITE-SYENITE BODY

INTRODUCTION

The question of the nature and origin of massif-type anorthosite has generated much discussion (Isachsen, 1969). The relationship of

massif-type anorthosite to anorthosite layers in mineralogically stratified gabbroic intrusions is one of great interest. It is clear that the understanding of large and small scale structural features can contribute greatly to understanding the nature and origin of massif-type anorthosite. Structures produced by crystal accumulation have contributed greatly to the understanding of the origin of stratified gabbroic intrusions (Irvine, 1965), and have also been described in some massif-type anorthosite bodies (Emslie, 1968). Block structures consisting of angular blocks of one rock in another are common features of many massif-type anorthosite bodies (Buddington, 1939, Grout and Schwartz, 1939, Taylor, 1956, Bridgewater and Harry, 1968, Wiebe, 1978). Spectacular medium and small scale structures as well as well-defined overall structural relationships between major stratigraphic units are found in the San Gabriel body. Understanding the various structural features can contribute greatly to understanding the nature and origin of the body. These structures provide important evidence on the tectonic environment during crystallization and on the sequence of magmatic changes, both in composition and in crystallization behavior. Major synplutonic structural features are shown in Figure 16.

EXTERNAL FORM

About 13 kilometers of the upper contact is exposed along the southwest edge of the body where gabbroic rocks of the jotunite unit concordantly intrude generally sub-horizontal gneiss. A low-angle reverse fault cuts the roof of the body east of Mendenhall Peak and can be followed for about 3 kilometers. A thick zone of deformed Mendenhall gneiss occurs along this fault, some of which contains augen

Figure 16 Precambrian structures developed during emplacement and crystallization of the San Gabriel anorthosite-syenite body: (1) Buck Canyon synform.

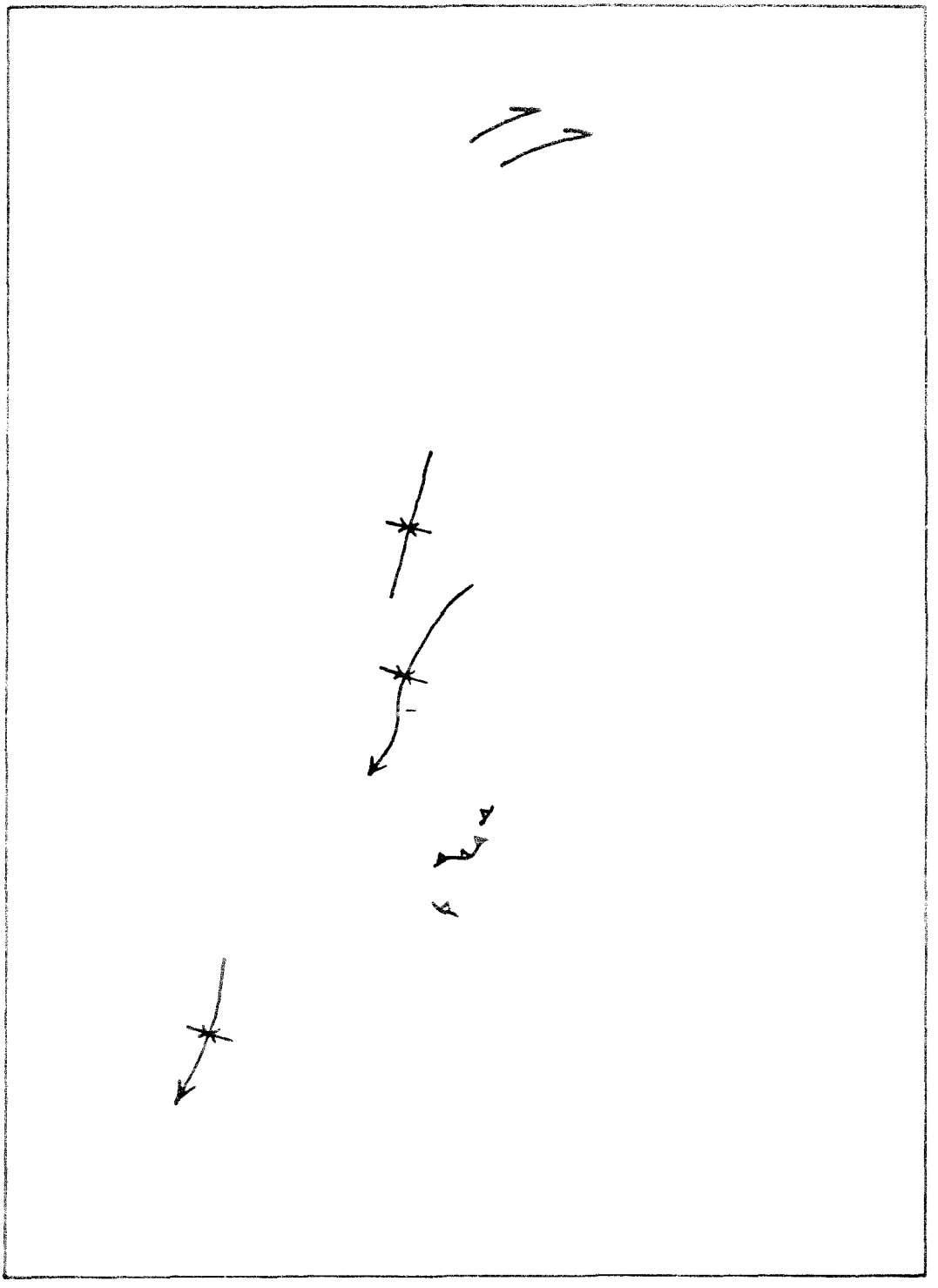

Figure 16.

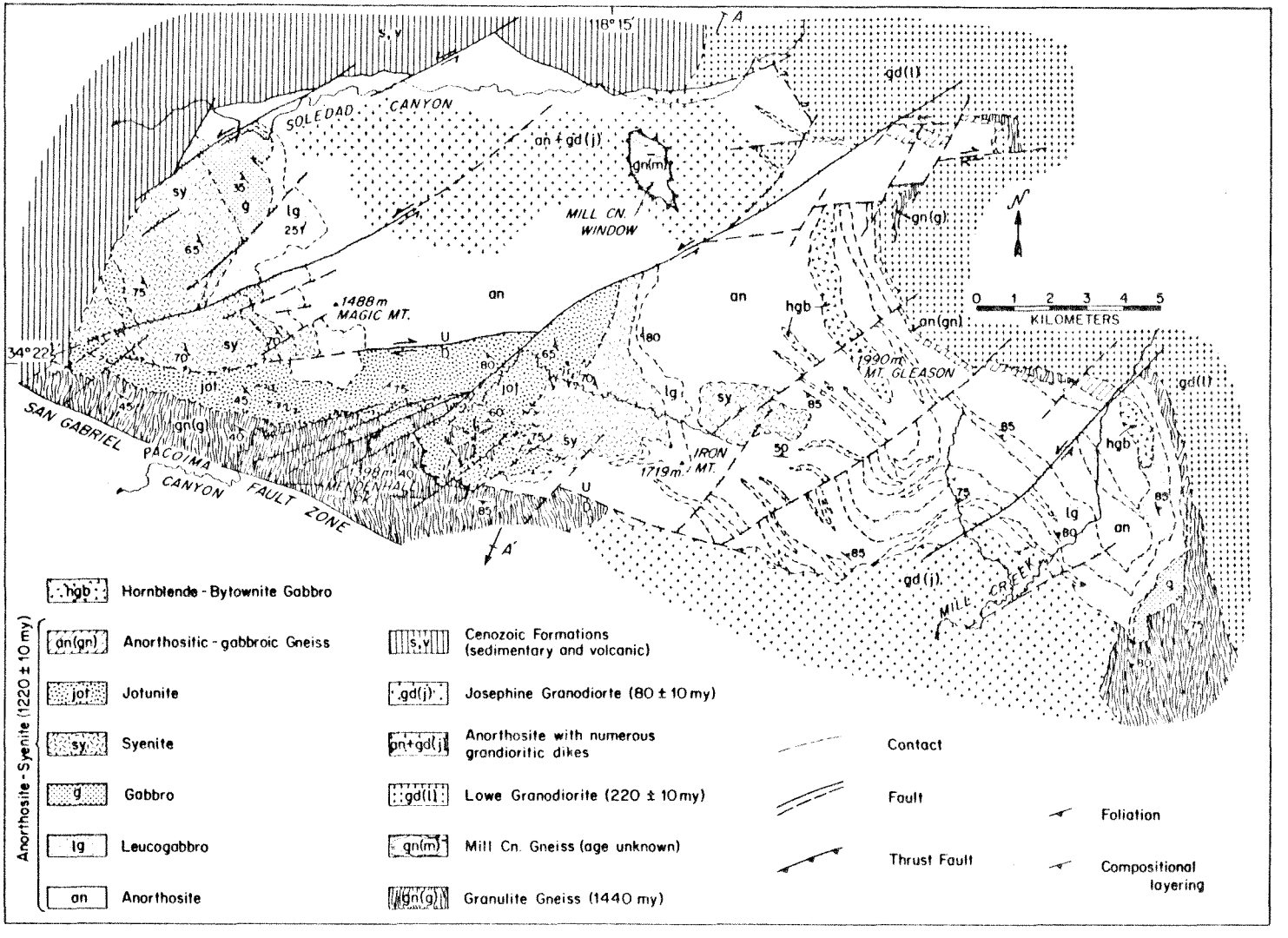

SIMPLIED GEOLOGIC MAP OF THE SAN GABRIEL ANORTHOSITE-SYENITE BODY, LOS ANGELES COUNTY, CALIFORNIA

Figure 16.

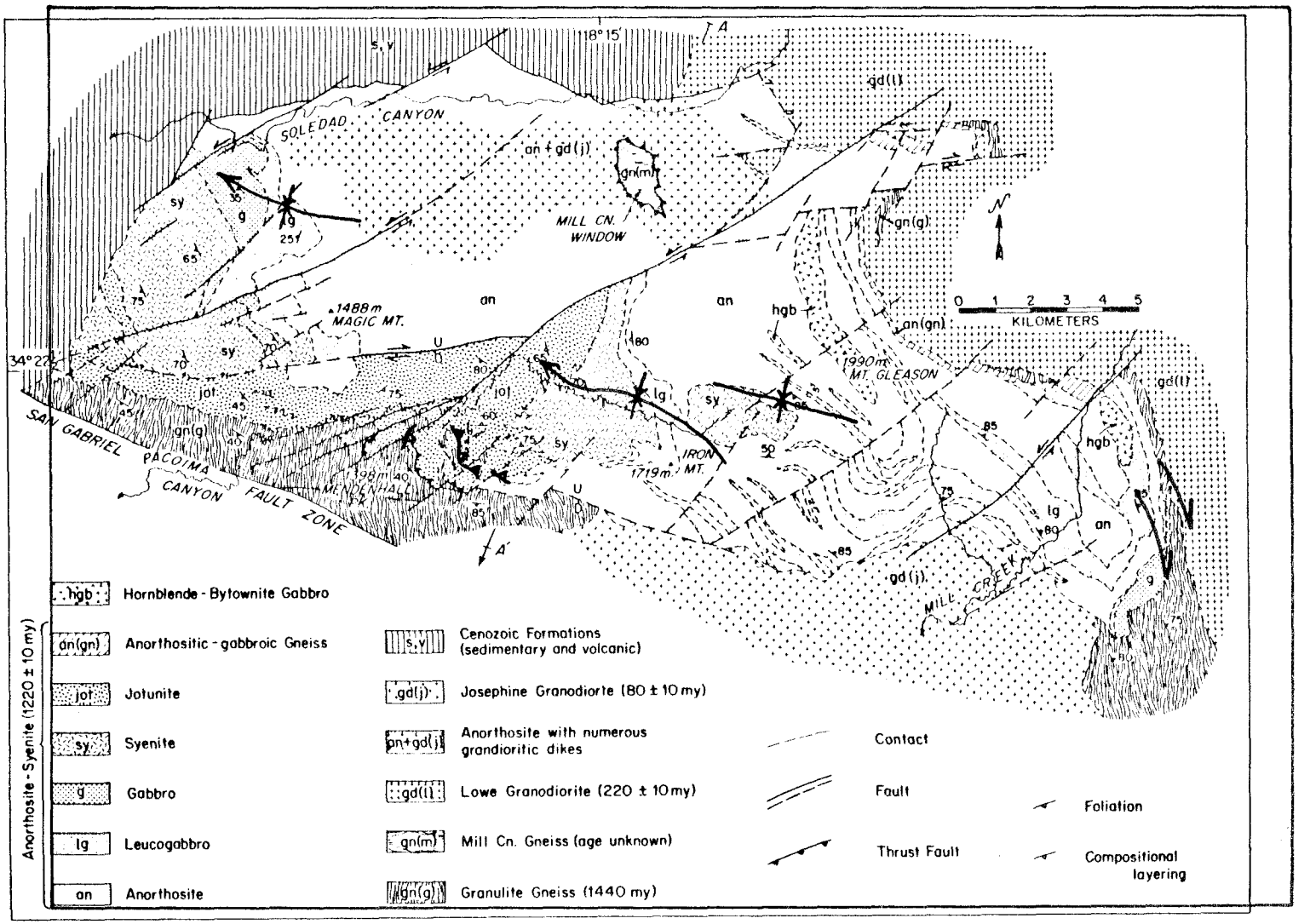

SIMPLIED GEOLOGIC MAP OF THE SAN GABRIEL ANORTHOSITE-SYENITE BODY, LOS ANGELES COUNTY, CALIFORNIA

Figure 16.

Figure 16.

produced by high temperature recrystallization. These augen resemble those present elsewhere in the Mendenhall gneiss immediately adjacent to the contact, suggesting contact metamorphic origin. Along much of its length this fault separates rocks of the jotunite unit in the hanging wall from Mendenhall gneiss in the foot wall. Upward displacement of the jotunitic rocks probably totaled about 300 to 600 meters. This fault is cut by all of the Cenozoic fault sets in this area and represents the oldest fault recognized. High temperature recrystallization of gneiss along the fault suggests that it was active during or soon after emplacement of the anorthosite-syenite body. Restoration of Mesozoic and Cenozoic folding suggests that this was originally a reverse fault which displaced the more central roof of the body upward and outward toward the margin. It is probable that this fault was produced by upward emplacement of the anorthosite-syenite body into the overlying Mendenhall gneiss.

The lower contact is exposed for about 800 meters in lower Wickiup Canyon where coarse anorthosite overlies Mendenhall gneiss. Both rocks are badly brecciated near the contact; no cross-cutting was observed. Elsewhere the approximate original location of the lower contact can only be inferred based on the distribution of xenoliths in younger intrusive rocks.

About 1200 meters of the margin of the body west of Lynx Gulch trends at a high angle (about 70°) to foliation and layering in the adjacent gneiss, and this discordant trend is apparently reflected by layering and contacts within that part of the body. Since the floor diverges from the normally concordant roof, the total increase in thickness of the body across this feature is about 1600 meters.

A post-intrusion origin, such as by Cenozoic faulting, is unlikely since other contacts are undisturbed across the northeast or southwest projection of this feature (Plate I). The southeasternmost edge of the anorthosite-syenite body is about 500 meters thick and seems to terminate abruptly along a contact perpendicular to layering and lithologic contacts within the body and to layering and foliation in the Mendenhall gneiss, and might be similar to the segment of the contact described above.

These discordant segments could represent either normal fault-like displacements or sharp monoclinal flextures in the gneiss produced by upward wedging of the magma, although no obvious structural discontinuity of anomalous attitudes were recognized in the overlying gneiss. It is possible that the edge of this large stratiform intrusion was originally only slightly discordant and had a simple wedge-shaped form as illustrated schematically in Figure 17a. The discordant segments might have been produced by outward movements of the upper parts of the body (Figure 17b) to produce the present configuration of the body (Figure 17c). This outward displacement of some of the cumulate rocks could have occurred during crystallization when the cumulate rocks were still poorly consolidated. Tilting of the margin of the body could have resulted in massive outward slumping of poorly consolidated cumulate rocks which caused upward displacement of the roof near the margin. This tilting and slumping hypothesis is supported by the configuration of the upper contact near the edge of the body,by the configuration of the anorthosite, leucogabbro, and gabbro subunits which have irregularities suggesting something other than simple cumulate origin,by zones of strong shearing of gabbro in Big Tujunga

Figure 17. Proposed development of the lithologic distribution of the southeastern margin of the San Gabriel anorthosite-syenite body. Anorthosite and leucogabbro were formed primarily by bottom crystal accumulation in a chamber mostly concordant with underlying and overlying Mendenhall gneiss. It is proposed that during accumulation, major sliding (or slumping) of poorly-consolidated rocks outward toward the edge of the body occurred, perhaps due in part to accumulation on a sloping floor. (a) Configuration of the edge of the body which would have resulted if no sliding had occurred. (b) Initial sliding (arrows) took place after accumulation of a little more than half of the section. (c) Continued sliding occurred during accumulation of the upper part of the section, resulting in the present distribution of lithologies (this diagram also shows the distribution of younger rocks intruded after the anorthosite and leucogabbro had been steeply tilted).

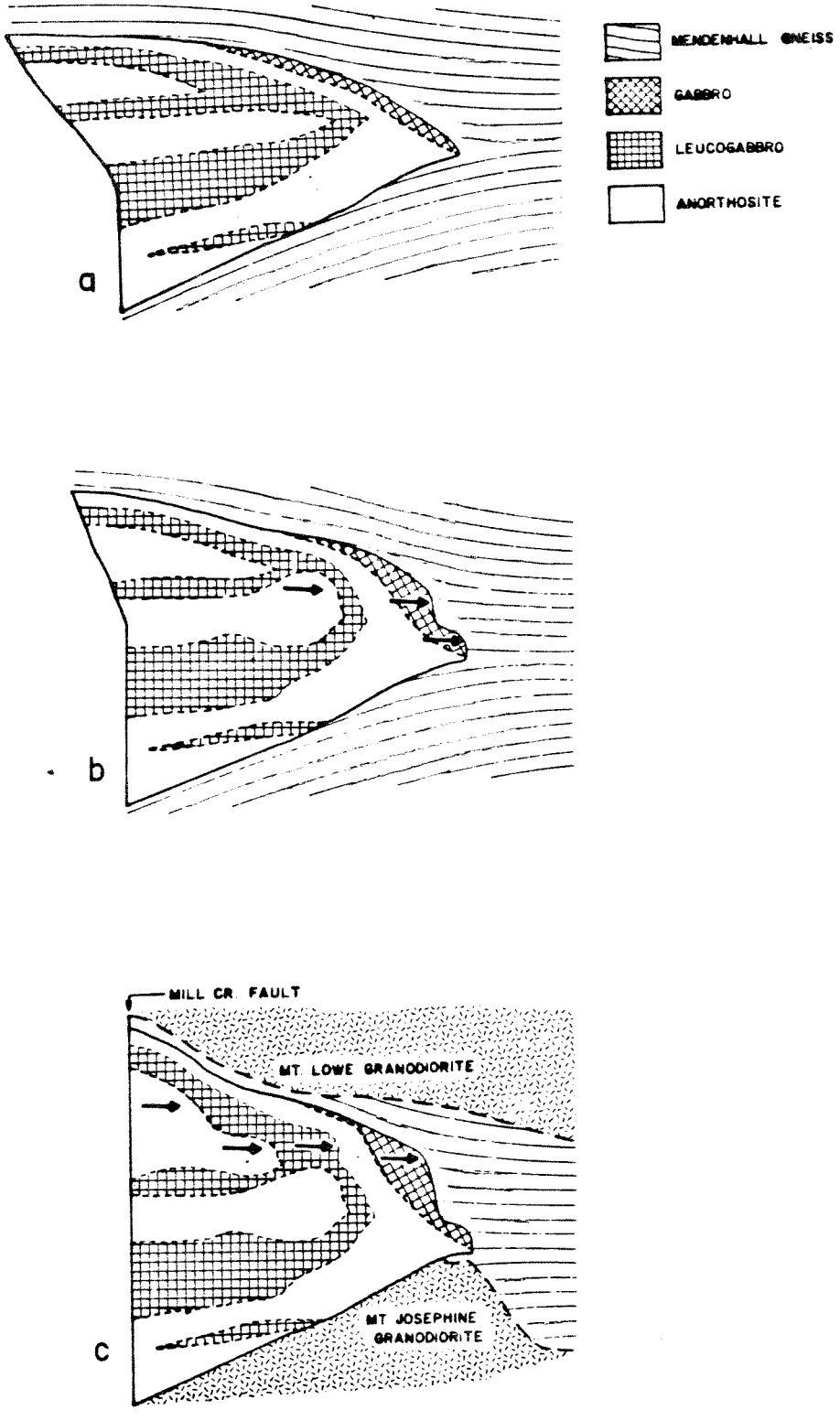
MENDENHALL GNEISS
GABBRO
LEUCOGABBRO
ANORTHOSITE
a
b
MILL CR. FAULT
MT. LOWE GRANODIORITE
MT JOSEPHINE
GRANODIORITE
c

Figure 17.

Canyon (Figure 18), and by the presence of abundant minor slump structures in the anorthosite-leucogabbro unit confined to the upper part of the unit southeast of the Mill Creek fault.

The overall original shape of the anorthosite-syenite body is poorly known, but several observations are pertinent. The body was large, with a diameter of 10 kilometers or more. Much of the original roof of the body is exposed along its southwest and northeast margins. Wherever observed, the roof can be shown or inferred to have been a concordant, sub-horizontal intrusive contact. The original edge of the body in upper Big Tujunga Canyon thickens rapidly to at least about 7 kilometers toward the center of the body. These observations are compatible with an original shape of an inverted cone (Figure 112). However, the above constraints allow other possibilities: a more sheet-like form is possible, and there is the possibility of a more irregular non-symmetric original shape.

INTERNAL STRUCTURES

Major Units

The anorthosite-leucogabbro unit is made up predominantly of anorthosite but contains many thick subunits of layered leucogabbro and some layered gabbro in a few places. Several aspects of the field distribution of these three rock types may have bearing on the origin of the body. Stratigraphic variation occurs, with the lower (and most abundant) anorthosite (with or without leucogabbro) gradually changing upward into leucogabbro and then gabbro which is discontinuous, usually relatively thin, and forms the top of the unit. Gabbro is abundant only west and northwest of Magic Mountain where it attains a thickness of

Figure 18. Strongly sheared gabbro adjacent to the roof near the southwest margin of the anorthosite-syenite body in Big Tujunga Canyon.

1500 meters or more and is overlain by syenite to the west. Gabbro is present just below the roof of the body along the present northeast margin as several discontinuous lensoid masses generally only a few tens of meters thick, most of which exhibit gneissosity produced by deformation accompanying the emplacement of the Mt. Lowe granodiorite. The gabbro in Big Tujunga Canyon is the largest of these masses which accumulated just below the original roof of the body.

Gabbro probably crystallized from mafic magma which pooled beneath the roof in some parts of the body, perhaps in sags in the underlying rocks. The thick gabbro north and west of Magic Mountain might have been produced by magma collected from an originally thin widely-distributed layer, remnants of which were trapped below the roof elsewhere. Evidence of deep sags and pools of gabbroic magma is less persuasive than the evidence of similar sags and pools of syenitic magma higher in the section. Just west of the mouth of Bear Canyon, mafic gabbro with poorly developed compositional layering (with sometimes disorganized orientations) contains large (3-30 meter) angular blocks of anorthosite and leucogabbro, suggesting its proximity to a steep scarp similar to that along the north side of the Buck Canyon synform (see below). In this area the gabbro increases in thickness from about 300 meters to about 1500 meters over a distance of 2-3 kilometers, with reciprocal thinning of the underlying leucogabbro from about 600 meters to 200 meters or less, so that the thickest gabbro is only several tens of meters stratigraphically above anorthosite in Soledad Canyon (Plate I).

Areal variation of anorthosite, leucogabbro and gabbro also occurs within the anorthosite-leucogabbro unit. Gabbro at the top of the anorthosite-leucogabbro unit forms a thick mass in the west, but only

a few relatively small bodies along the northeast margin and in the vicinity of the Buck Canyon synform. This difference in the amount of gabbro present at the top of the unit may be due either to tectonic movements which produced localized pools of late gabbroic magma or else to areal differences in crystallization behavior.

Significant areal variation is seen in the distribution of leucogabbro subunits. In the southeast part of the body, leucogabbro subunits constitute as much as 35-40% of the total unit whereas in the central and northwest parts of the body leucogabbro subunits (which are small and more discontinuous and so could not be mapped) probably make up at the most 10-15% of the total section, excluding the upper leucogabbro and gabbro part of the unit north and west of Magic Mountain. In large areas leucogabbro subunits are virtually absent. A cross section through this unit along Mill Creek in the southeast shows that about 30% of the total is leucogabbro which occurs as thick subunits more or less evenly distributed from top to bottom of the section. A cross section parallel to and about one kilometer south of Soledad Canyon in the northwest shows that about 10% of the section is leucogabbro and 10-15% is gabbro, both of which occur at the top of the unit overlying a very thick section of anorthosite containing almost no leucogabbro. Thus the total ferromagnesian content of the anorthosite-leucogabbro unit is probably similar in each area, but is distributed very differently.

The approximate boundary between these two types of distributions runs northeast through Iron Mountain and Mount Gleason. Northwest of the boundary, slight ferromagnesian-enrichment is seen at the top of the anorthosite-leucogabbro unit along the north flank of the Buck

Canyon synform, more pronounced ferromagnesian-enrichment is seen farther west near Magic Mountain, and a very thick mass of ferromagnesian-enriched leucogabbro and gabbro is present northwest of Magic Mountain. Southeast of the boundary, near Messenger Flats and upper Moody Canyon, numerous small unmapped leucocratic leucogabbro layers are present in anorthosite; farther southeast in Fox Creek leucogabbro subunits are larger, and could be mapped with difficulty. Farther southeast, in the several forks of Mill Creek, prominent leucogabbro subunits are quite distinct and readily mapped. Thus the boundary between these areas of different distribution of ferromagnesians is quite gradational. It affects the entire stratigraphic section and probably reflects different conditions of crystallization. The southeast part of the body, where well-developed leucogabbro subunits are present throughout the section, is near the original margin of the anorthosite-syenite body. The western part of the body where the gabbro is thickest, is also where the overlying syenite unit (and perhaps the jotunite unit as well) is thickest, and may constitute a more central, thicker, part of the body. Thus the variations within the anorthosite-leucogabbro unit may reflect crystallization conditions which differed between the margin and the center of the body.

The syenite unit consists of an underlying ultramafic syenite subunit comprised largely of layered gabbroic to ultramafic rocks, some containing large blocks of anorthosite, and an overlying normal syenite subunit comprised almost entirely of massive syenite. Rocks of the normal syenite subunit are about 2 kilometers thick in the axis of the Buck Canyon synform. Rocks of the ultramafic syenite subunit are absent on the south flank and reach about 1 kilometer thickness in the axis,

as well as on the north flank of the synform where the normal syenite subunit thins and disappears to the north. Ultramafic syenite subunit rocks are less abundant (perhaps absent) north and west of Magic Mountain where the normal syenite subunit reaches an estimated 4 to 5 kilometers thickness, although 500-600 meters of ultramafic syenite subunit rocks are present south of Magic Mountain.

Gabbroic rocks of the jotunite unit reach about 3 kilometers thickness along the southern edge of the body. This unit is divided into five subunits. These subunits vary in thickness and some are present only in local parts of the unit. The approximate distribution and inferred stratigraphic and areal variation of these subunits are shown schematically on Plate III.

The approximate distribution and structural-stratigraphic relationships of the major units and lithologies of the San Gabriel anorthosite-syenite body are shown schematically in Figure 19.

Compositional Layering

Almost all gabroic rocks of the anorthosite-syenite body are rhythmically layered, with alternating 1 centimeter to 5 meter layers of differing color index (Figures 20, 21). Many rhythmic layers have gradational contacts with adjacent layers, but some are mineralogically graded or show other evidence bearing on the origin of the gabbroic rocks.

Mineral grading is present in many of the gabbroic to ultramafite layers which are abundant in the jotunite unit and the ultramafic syenite (Figures 21, 22) and are rare in the normal syenite subunit. Each layer consists of a ferromagnesian-rich part which changes gradually into a

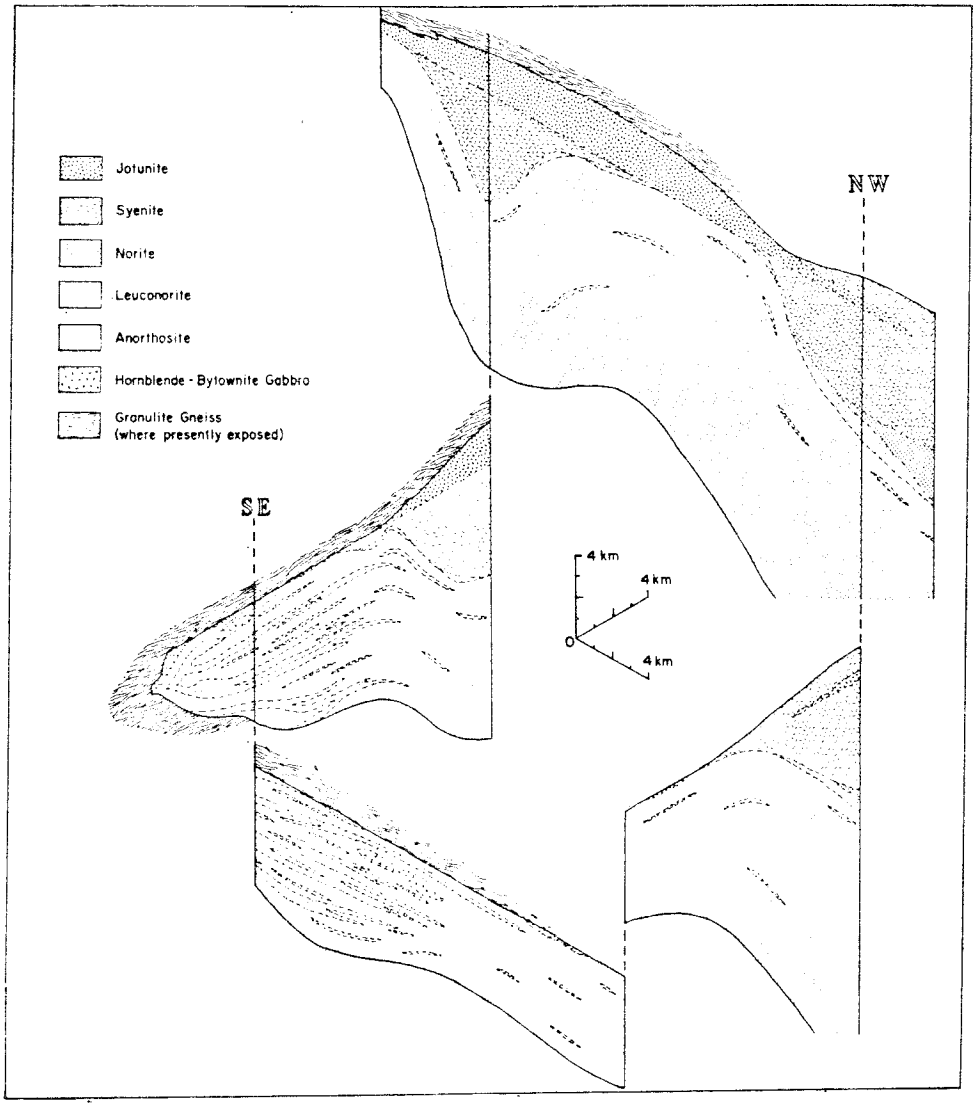

Figure 19. Diagrammatic reconstruction (fence diagram) of the San Gabriel anorthosite-syenite body, showing the approximate distribution and structural-stratigraphic relationships of the major units and lithologies.

Figure 20. Fine scale layering in gabbro of the anorthosite block subunit of the jotunite unit near North Fork Saddle. Note the small gabbroic dike near the right margin.

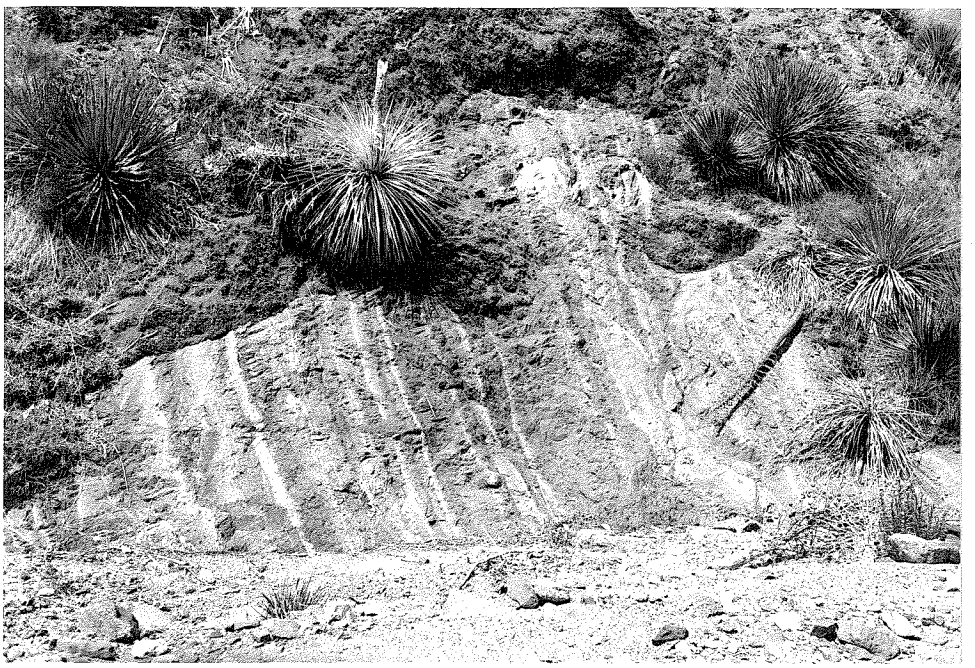

Figure 21. Graded layers in the layered jotunite subunit of the jotunite unit near the mouth of Bad Canyon. The original top of the sequence is interpreted to be to the left.

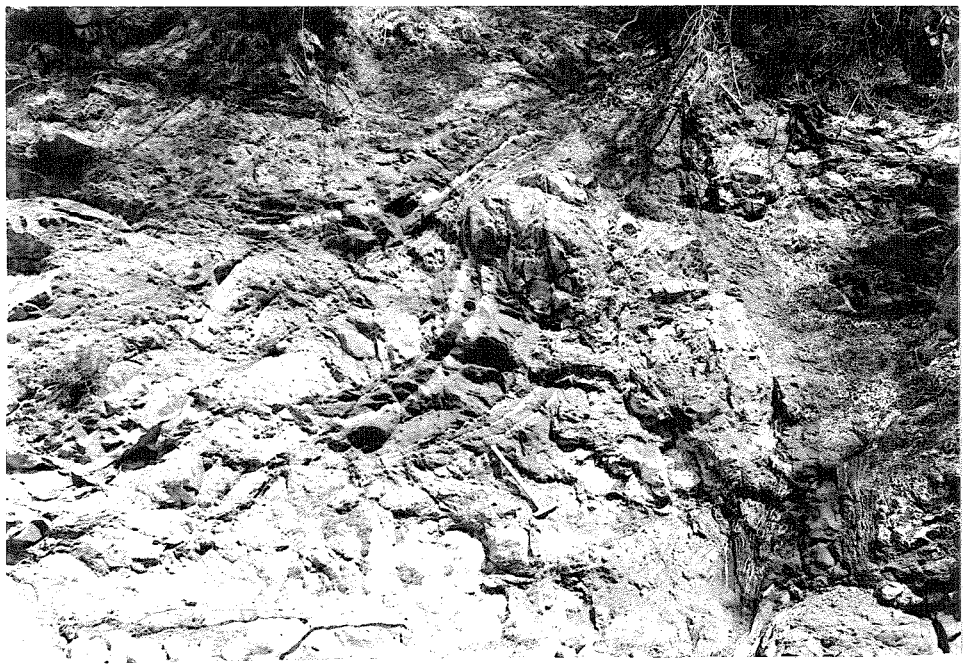

Figure 22. Slumped graded layers in the upper jotunite subunit of the jotunite unit in Pacoima Canyon near the mouth of Spring Canyon. Note the thick bases with color indices of 100 in some layers. The abrupt thickness changes of some layers may be due to slumping while still plastic.

a ferromagnesian-depleated part. Elongate plagioclase crystals in these layers usually show a preferred orientation parallel to layering (Figure 23). In some instances as much as a meter of the layer contains no feldspar but grades into leucocratic rocks (Figure 22). The ferromagnesian minerals in the very mafic parts of some of these layers are size graded, changing gradually to smaller grain size in the part of the layer with greater feldspar abundance. Where both are present, the size grading is always consistent with the mineral grading (the layer grades toward smaller grains in the same direction as it grades toward lower color index). These layers are interpreted as forming from a single episode of crystallization, during and after which the denser minerals (pyroxene, olivine, ilmenite, apatite) settled more rapidly than the less dense minerals (mostly andesine antiperthite). Tabular plagioclase crystals normally settled so as to be sub-parallel to the floor of the chamber and the layering. This interpretation suggests that the layering was formed in an original sub-horizontal oreintation.

In the anorthosite-leucogabbro unit most layers have gradational contacts, and none show the type of gradation described above. A few layers, however, consist of plagioclase and pyroxene (uralite) crystals, some of which are elongate perpendicular to the layering (Figure 24). On one side the plagioclase crystals all terminate along the same plane while on the other side some crystals extend farther than others. Some pyroxene crystals adjacent to the plagioclase are also oriented perpendicularly to layering but most are not. These are interpreted to be crescumulate layers which formed when first plagioclase and then pyroxene grew into the melt from a base of accumulated crystals. In some layers plagioclase crystals display crystal faces on the upper

Figure 23. Graded layers in the layered jotunite subunit of the jotunite unit near the mouth of Bad Canyon. The pen lies in the ferromagnesian-rich part of a layer which grades to the left into more leucocratic rock. The leucocratic part of an adjacent layer lies to the right of the pen. Note the preferred orientation of cumulate plagioclase crystals parallel to the layering.

Figure 24. Asymmetric crescumulate layer in leucogabbro in Mill Creek. Coarse plagioclase crystals grew into magma from the left side of the layer. Different crystals grew to different lengths. Crystallization of plagioclase was followed by crystallization of pyroxene to form the right side of the layer. This layer probably formed in a sub-horizontal orientation

end and none on their bases. The sequence is always plagioclase first, followed by pyroxene (uralite) in these cresumulate layers. Such layers could form on any solid-magma interface of any orientation, but other evidence of bottom crystal accumulation in adjacent rocks (slump structures, graded layers) indicates that these layers formed in sub-horizontal orientations.

Asymmetric patches of coarse plagioclase, pyroxene (uralite) and ilmenite are common in leucogabbro in the eastern part of the anorthosite-leucogabbro unit. They are sometimes irregular but are usually lenticular parallel to other layering in leucogabbro and sometimes form well defined 0.5-3 meter layers. The grain size ranges from 2 to 3 centimeters up to 2 meters. Proportions are variable but average about 25-30% pyroxene (uralite), 65-70% plagioclase, and usually no more than about 5% ilmenite. The asymmetry is sometimes pronounced, with plagioclase on one side of the layer and pyroxene (uralite) and ilmenite on the other. Even the very irregular patches often exhibit this asymmetry, which is visible only where it is surrounded by different, more homogeneous rock, usually finer grained leucogabbro. Few asymmetric layers are observed except in the eastern part of the anorthosite-leucogabbro unit where leucogabbro is common.

The sense of asymmetry of these layers is always consistent with that of obvious crescumulate layers in adjacent rocks. Thus, the plagioclase-rich part of each layer probably formed first on the floor of the chamber and was followed by pyroxene and some ilmenite crystallizing above it. This is the same crystallization sequence seen in the more obvious crescumulate layers. In the anorthosite-syenite body as a whole, most plagioclase crystallized before most pyroxene and this

sequence occurs on a much smaller scale in these layers. These layers may represent perpendicular-plagioclase crescumulate layers which have been recrystallized to form larger, non-oriented crystals.

Branching, 15-30 centimeter, "Willow-Lake-type" plagioclase crystals are present in a few places in gabbro of the anorthosite-leucogabbro unit (Figure 25). These crystals formed by growth from a rock into adjacent magma. Comparison with orientations of other indicators suggests that this growth occurred from an underlying base into overlying magma.

Slump Structures and Block Accumulation

Anorthosite blocks occur in mafic rocks of the ultramafic syenite subunit, in at least two subunits of the jotunite unit, in large sill-like layered gabbroic bodies in syenite near the western edge of the body, and in gabbro near the top of the anorthosite-leucogabbro unit (Plate I). These mostly consist of angular blocks of massive anorthosite 0.5 to 30 meters in diameter, surrounded by a matrix of mafic rock with a color index of 50 and often much higher (Figure 26). Although most blocks are anorthosite, a few consist of leucogabbro. All variations occur, from widely scattered blocks in thick mafic layers to accumulations consisting of more block material than matrix (Figure 27). The mafic rock commonly is compositionally layered and some shows mineral grading in layers which drape across the angular blocks (Figures 28, 29). Anorthosite blocks are often concentrated in distinct horizons within mafic rocks (Plate I).

These blocks appear to have accumulated on the floor of the chamber at a time when abundant ferromagnesian minerals were accumulating on

Figure 25. Willow-Lake-type plagioclase crystals in gabbro near the top of the anorthosite-leucogabbro unit in Lynx Gulch. Crystals branched as they grew into the magma (now to the right in the photograph

Figure 26. Breccia consisting of angular anorthosite slump blocks in an ultramafite matrix. From the anorthosite block subunit of the jotunite unit near North Fork Saddle.

Figure 27. Megabreccia of angular anorthosite blocks in a matrix of mafic to ultramafic rock. From the ultramafic syenite subunit near the contact with anorthosite of the underlying anorthosite-leucogabbro unit on the south flank of Magic Mountain.

Figure 28. Layer of coarse angular anorthosite blocks within a mafic to ultramafic matrix. Some of the overlying graded layers drape across anorthosite blocks. From the ultramafic syenite subunit near its contact with anorthosite of the underlying anorthosite-leucogabbro unit along the road south of Sold. Note the geologic hammer near the left margin of the photograph.

Figure 29. Layered gabbroic rocks draped across a large slump block of anorthosite. Other anorthosite blocks are visible on the right. Anorthosite block subunit of the jotunite unit, about 1.6 kilometers south of North Fork Saddle.

the floor. This must have occurred at a time when plagioclase either sank in the magma or at least did not float at a rate greater than the rate that the mafic rocks accumulated. The high color index of most of the mafic rocks suggests that either very small amounts of plagioclase was crystallizing or else plagioclase crystals did not sink significantly in the magma. Possibly the large anorthosite blocks sank (or at least did not float) in the same magma in which liquidus plagioclase crystals floated (or at least did not sink). This effect could be the result of the greater size of the blocks or the crystallization of less dense plagioclase than that in the blocks. Grain mount observations indicate that in some instances the mafic matrix contains more alkali-enriched feldspar (An 25-35 antiperthite) than that in the enclosed anorthosite blocks (An 35-45). The angular shape and sharp contacts of blocks indicate that anorthosite was well-lithified and brittle prior to accumulation of the rocks in which they occur.

A few small blocks (to 50 centimeters) appear to have been loosely-aggregated clots of tabular crystals at the time of incorporation into the surrounding mafic rocks (Figures 30,31). These may have been clots of initally rafted crystals which were later engulfed by rocks accumulating on the floor of the chamber. However, no evidence of the existence of large accumulations of rafted crystals has been recognized near the roof or elsewhere in the anorthosite-syenite body.

Slump blocks of other lithologies are abundant only in rocks of the upper jotunite subunit which contain angular to rounded, 0.5 to 5 meter blocks of both gabbroic rocks and granulite gneiss (Figures 12, 13). The gabbroic blocks usually have sharp contacts and resemble the gabbro they occur in. Gneiss blocks commonly have diffuse contacts several

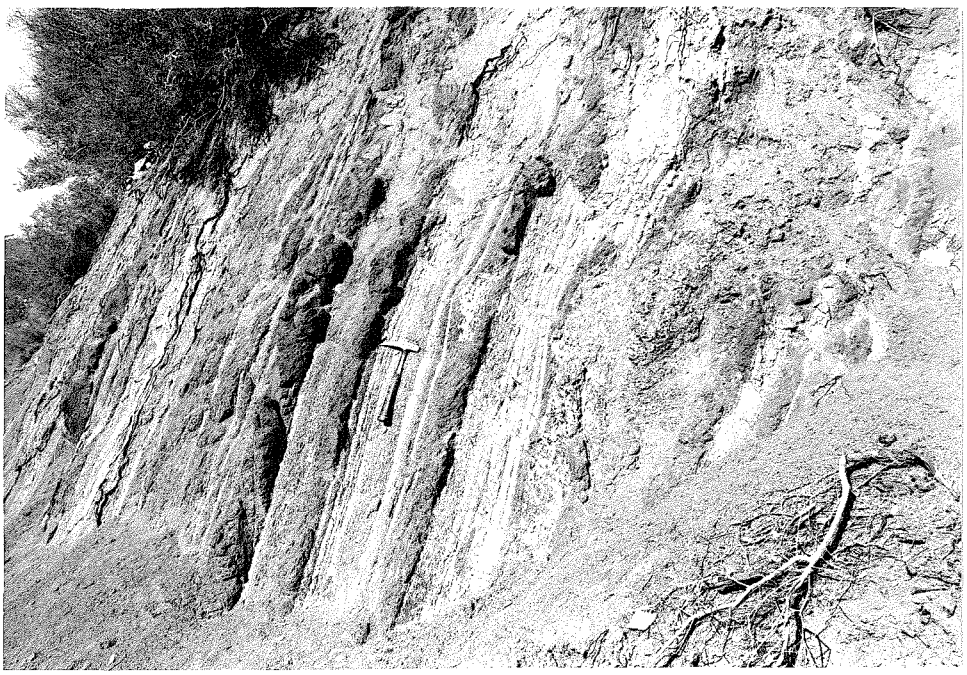

Figure 30. Cyclic repetition of graded layers in jotunite from the anorthosite block subunit of the jotunite unit near North Fork Saddle.

Figure 31. Anorthositic xenolith in layered, graded jotunite from the anorthosite block subunit of the jotunite unit near North Fork Saddle. Layers on the left accumulated on top of the xenolith and drape across it. Note that the xenolith appears to have been a poorly aggregated clot of large tabular plagioclase crystals.

centimeters wide, possibly due to partial assimilation. Layers in the gabbroic matrix commonly drape across both types of blocks. These blocks probably formed by stoping and subsequent sinking of blocks of gneiss from the roof and blocks of gabbro which crystallized near the roof.

Understanding the mode of formation of the angular anorthosite blocks is critical to any interpretation of the origin of the anorthosite-syenite body. It is evident that the mafic rocks of the syenite and jotunite units must be younger than the anorthosite blocks they include. These rocks may have formed adjacent to the floor of the chamber as a result of magmatic erosion of the floor rocks, and incorporation of large blocks of floor rocks into basal rocks accumulating from the new magna. Alternatively, intrusion of younger magma may have broken the blocks out of the walls of feeder dikes and carried them upward where they accumulated in the chamber, either by settling or flotation.

Several dikes in anorthosite in the central part of the body consist of large angular anorthosite blocks in a very mafic matrix. Blocks (10 centimeters to 3 meters) may comprise as much as half of the dike. Most dikes are less than 5 meters across and none could be traced farther than about 50 meters. Most are probably less than a few hundred meters vertically from the upper contact of anorthosite but a few are present more than 1000 meters below the contact. If the magma was very mafic, then the blocks might be expected to float upward into the chamber due to the density contrast. Even without a density contrast, magma flow could carry the blocks upward into the chamber. In the chamber, the blocks might accumulate by settling or by flotation,

depending on relative densities.

Anorthosite blocks have not been observed in rocks near the upper contacts of either normal syenite or the upper four jotunite subunits. A few blocks may have been overlooked, but certainly there is no concentration of anorthosite blocks near the tops of these subunits. This indicates that the blocks did not float within the chamber except perhaps locally or only for brief periods.

Anorthosite blocks apparently accumulated on the floor of the chamber. This is supported by abundant mineral and size graded layers in the mafic rocks surrounding anorthosite blocks. Layers in the mafic rocks clearly drape across the tops of blocks and are undeformed below them (Figures 28-31). A variety of crosscutting relationships in sequences of graded layers are similar to cross-bedding in sedimentary rocks and indicate the relative tops of the sequences. These relationships indicate that the blocks accumulated on the floor of the chamber.

Some blocks could have been derived from underlying dikes as de cribed above, but several types of evidence indicate that most of them were produced by erosion of the floor of the chamber. The blocks normally are exclusively of lithologies of the rocks of the anorthosite-leucogabbro unit immediately below the contact. Thus anorthosite blocks occur above anorthosite and leucogabbro blocks above leucogabbro. Dikes cutting through the anorthosite-leucogabbro unit should entrain blocks of diverse lithologies representative of the entire section. Blocks are found in rocks of the syenite and jotunite units only adjacent to areas which structural reconstruction suggests were immediately above the anorthosite-leucogabbro contact. If dikes had entrained the blocks, then blocks should be abundant at the base of each of the jotunite subunits,

each of which probably resulted from a major injection of new magma. Discordant gabbroic masses containing anorthosite blocks were not recognized in any rocks of the syenite and jotunite units. Near North Fork Saddle, several hundred meters of the underlying anorthosite-leucogabbro section may be absent, perhaps cut out by erosion on the floor of the chamber.

Other Structures

Several large (2-10 meter) wedge-shaped bodies of very coarse anorthosite occur in leucogabbro in the southeastern part of the body (Figure 32-34). The larger of these point outward from thick layers of anorthosite; several smaller wedges have bases along thin layers of coarse plagioclase and pyroxene (uralite). These are interpreted to have formed by flow of plagioclase crystal mush upward into overlying leucogabbro crystal mush. This diapiric rise of lower density plagioclase crystal mush may have occurred when the leucogabbro crystal mush was under tension, perhaps because it accumulated on a sloping floor (Figure 35a). Downslope sliding of leucogabbro crystal mush might have allowed the emplacement of the diapiric lobe without any upward bending of layers in the leucogabbro (Figure 35 b,c). If the overlying mush was completely unconsolidated, downward sliding might occur without deformation and crumpling of its layers. Some of the leucogabbro crystal mush may have been dragged along on the upslope side of the diapiric lobe (Figure 35d). The top of the lobe might have ultimately pierced the top of the crystal mush and grown upward directly into the magma, both by continued diapiric rise and by direct crystallization (Figure 35c). The plagioclase mush apparently was completely squeezed

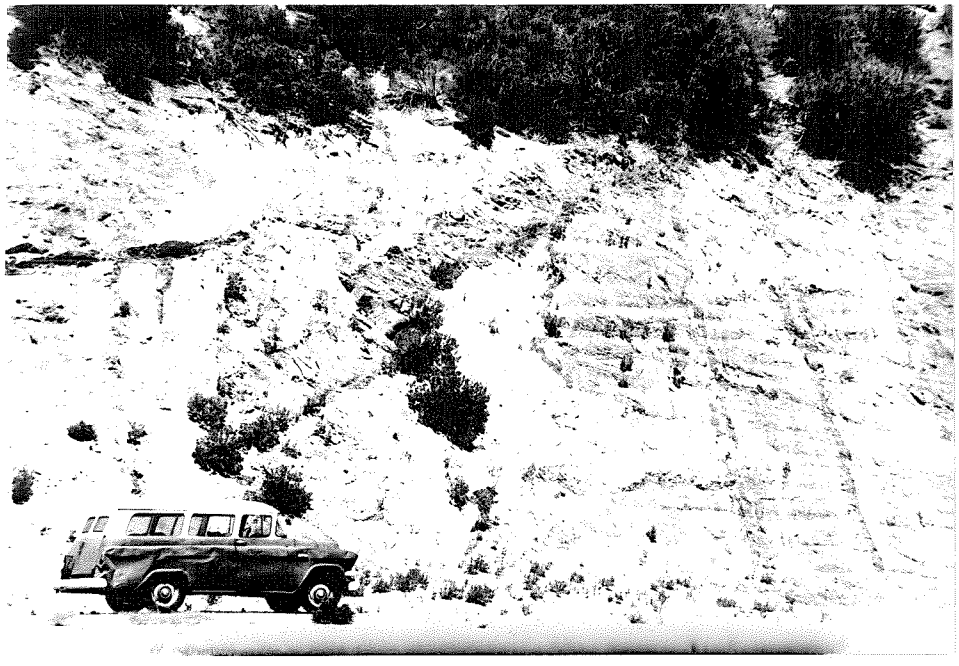

Figure 32. A large wedge extending from an anorthosite layer outward through about 4 meters of layered leucogabbro. A younger lamprophyric dike cuts off the anorthosite layer in the upper left. Note the two smaller anorthosite wedges higher in the cut (see also Figure 33). Main Fork Mill Creek.

Figure 33. Anorthosite wedges in leucogabbro (see Figure 32). The crescumulate layer on the right indicates that up was originally to the right. All three wedges have large pyroxene (uralite) crystals mainly along their lower sides. Note that the upper part of the top wedge contains unlayered leucogabbro.

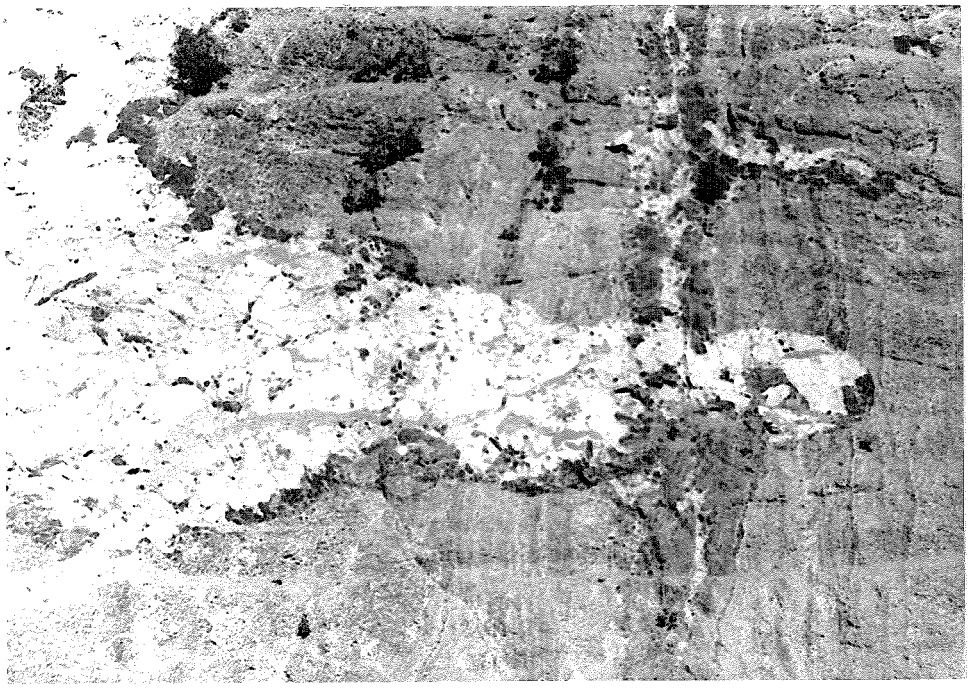

Figure 34. Closer view of the anorthosite wedge in Figure 32. Note the very coarse pyroxene (uralite) crystals along the right side of the main anorthosite layer and concentrated along the lower side of the wedge.

Figure 35. Proposed origin of anorthosite wedges which cut leucogabbro (see Figures 32-34). (a) A thick layer of plagioclase crystal mush overlain by a thin pyroxene-rich layer is buried beneath later-accumulated, layered crystal mush of leucogabbro composition. Accumulation either occurred on an initally sloping floor or else tilting during accumulation developed a slope resulting in tension within the poorly-consolidated crystal mushes. (b,c) Sliding of denser leucogabbro mush produces tension which allows the diapiric rise of the less dense plagioclase crystal mush. Because the diapir is rising into an area of tension, it causes very little upward bending of the leucogabbro layers. (d) On the down-slope slide of the lobe, the pyroxene-rich layer is folded upward while some of the overlying leucogabbro crystal mush is dragged along on the up-slope side of some lobes. (e) The top of the anorthosite diapir may pierce the top of the leucogabbro crystal mush. Direct crystallization of plagioclase on the top of the diapir may occur and locally deplete the magma in plagioclase constituents, resulting in subsequent direct crystallization of pyroxene on top of the diapir. The small plagioclase crystals in the diapir recrystallize at lower temperatures to produce the extremely coarse crystals typical of anorthosite throughout the San Gabriel body. (Possibly the recrystallization might have affected part of the adjacent leucogabbro, producing very coarse pyroxene cystals). At still lower temperatures, the pyroxene was uralitized in all the rocks.

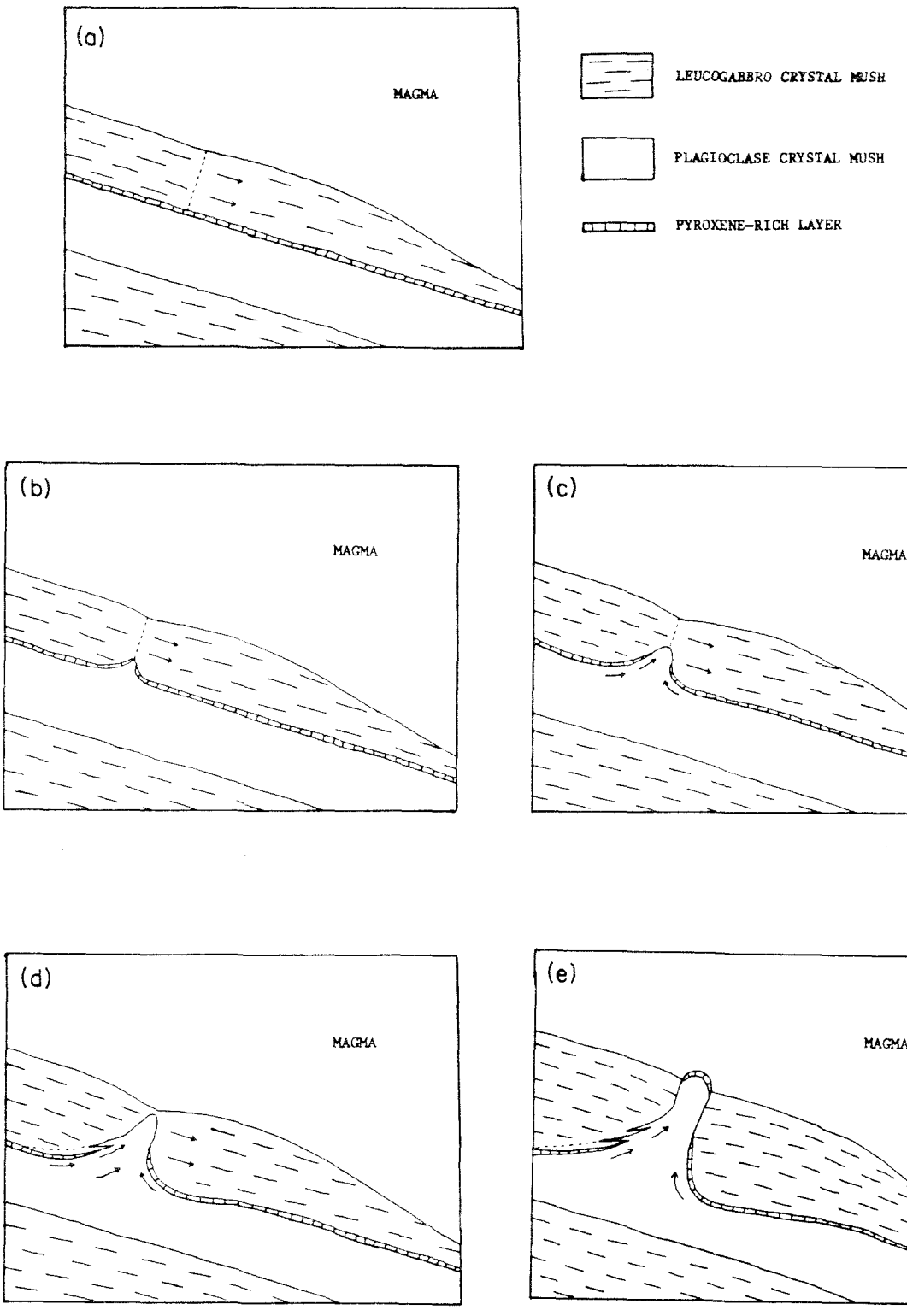
(a)
MAGMA
LEUCOGABBRO CRYSTAL MUSH
PLAGIOCLASE CRYSTAL MUSH
PYROXENE-RICH LAYER
(b)
MAGMA
(c)
MAGMA
(d)
MAGMA
(e)
MAGMA

Figure 35.

out of some layers. The plagioclase crystal mush probably contained small 0.5-3 centimeter crystals like those in the leucogabbro on either side. Postcumulous recrystallization produced the extremely coarse crystals now observed.

Cross-layering is observed in a few rocks. Some of these rocks are generally homogeneous except for thin 1 - 5 centimeter layers of slightly higher color index which are cross-layered at low angles. Rarely cross-layering up to 45° is present and in a few outcrops confused dune-like cross-layering covers many tens of square meters.

A few channel-like structures are present in mafic rocks of the jotunite unit in Pacoima Canyon and near North Fork Saddle (Figure 36).

All of the structures indicating the original orientation of layering are shown on Plate I and a summary of major indicators is shown in Figure 37. These data, combined with the areal distribution of lithologies and the orientations of compositional layering, aid in reconstruction of the original configuration of the anorthosite-syenite body (Figure 19).

SYNPLUTONIC TECTONISM

Introduction

Several types of evidence suggest that important synplutonic tectonism occurred during at least part of the crystallization of the San Gabriel anorthosite-syenite body. The large accumulations of anorthosite blocks along with associated slump structures, provide the best evidence of synplutonic tectonism. The characteristics of these block accumulations have been described above. They clearly accumulated on the floor of the magma chamber. As described below, the preferred

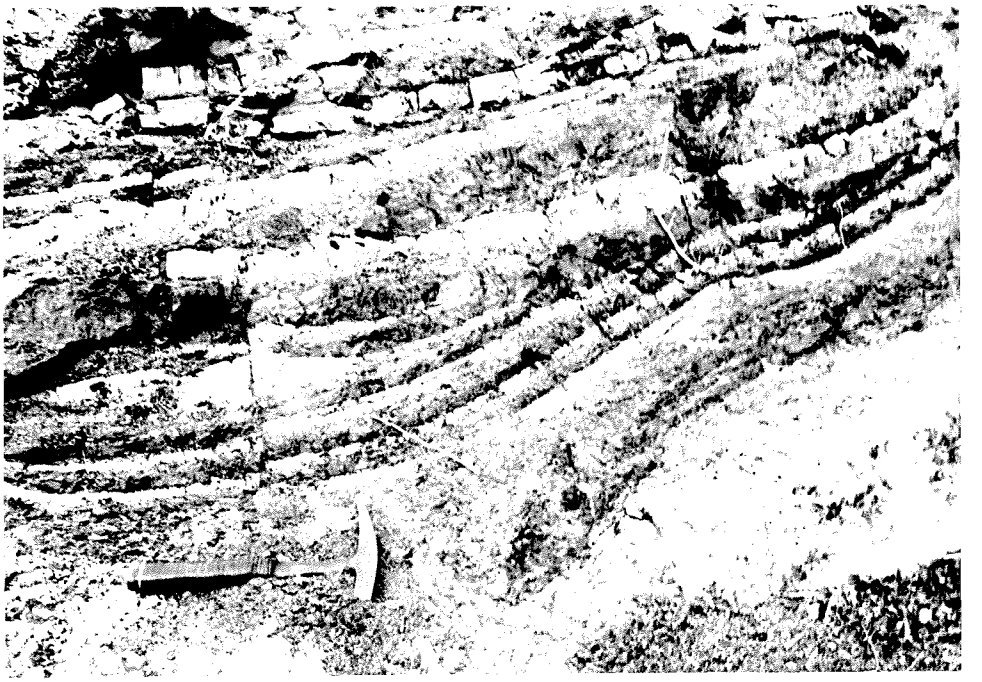

Figure 36. Channel structure defined by graded jotunite layers. From the upper jotunite subunit of the jotunite unit in Pacoima Canyon near the mouth of Spring Canyon.

Figure 37. Summary of major indicators showing original orientation of layering of rocks of the San Gabriel anorthosite-syenite body. Arrow indicates top of originally sub-horizontal layers (now mostly with steep dips). Major indicators include: (X) cross-layering, (G) density and/or size graded layers, (C) cresumulate layers, (S) slump structures.

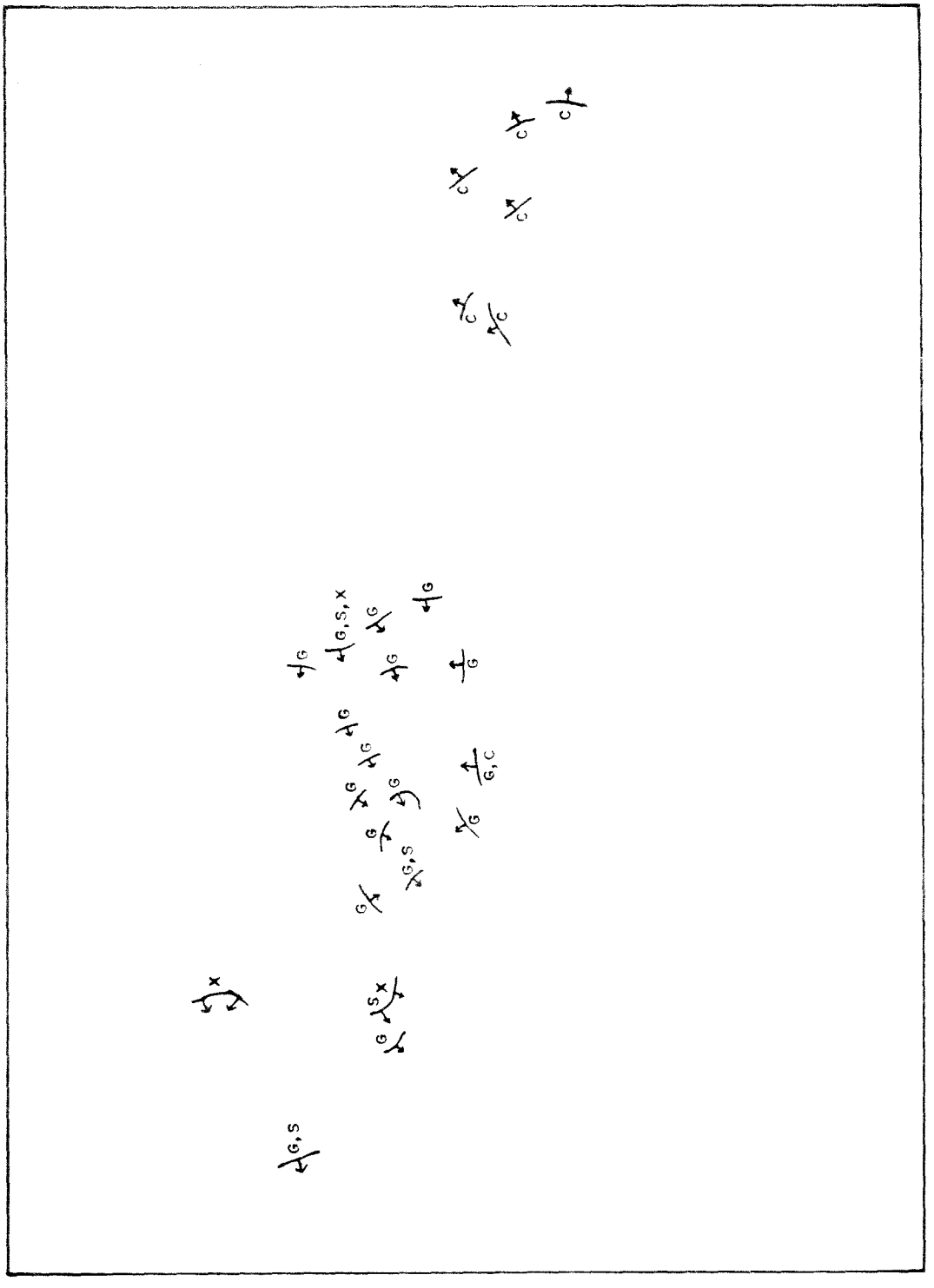

Figure 37.

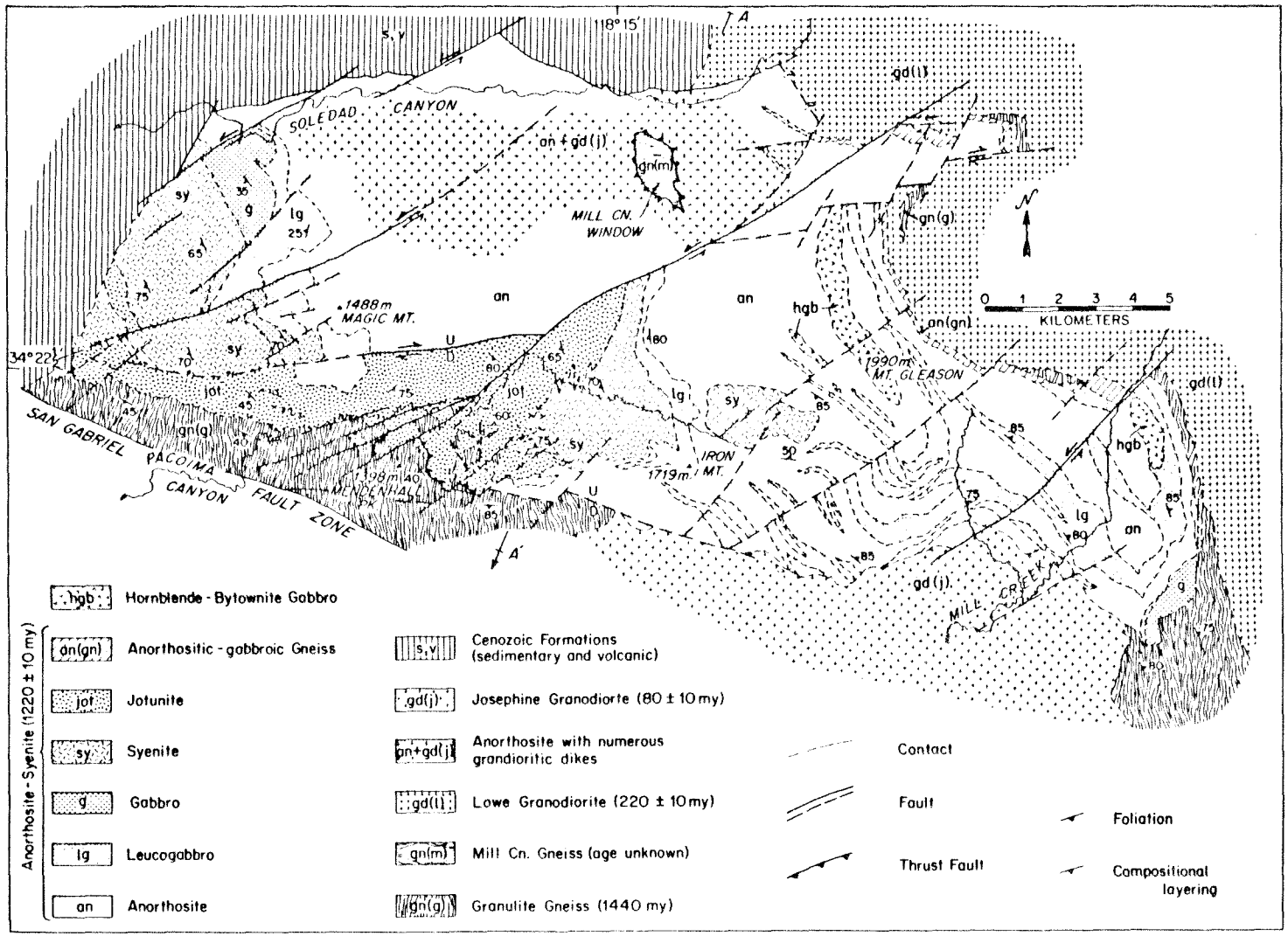

SIMPLIED GEOLOGIC MAP OF THE SAN GABRIEL ANORTHOSITE-SYENITE BODY, LOS ANGELES COUNTY, CALIFORNIA

Figure 37.

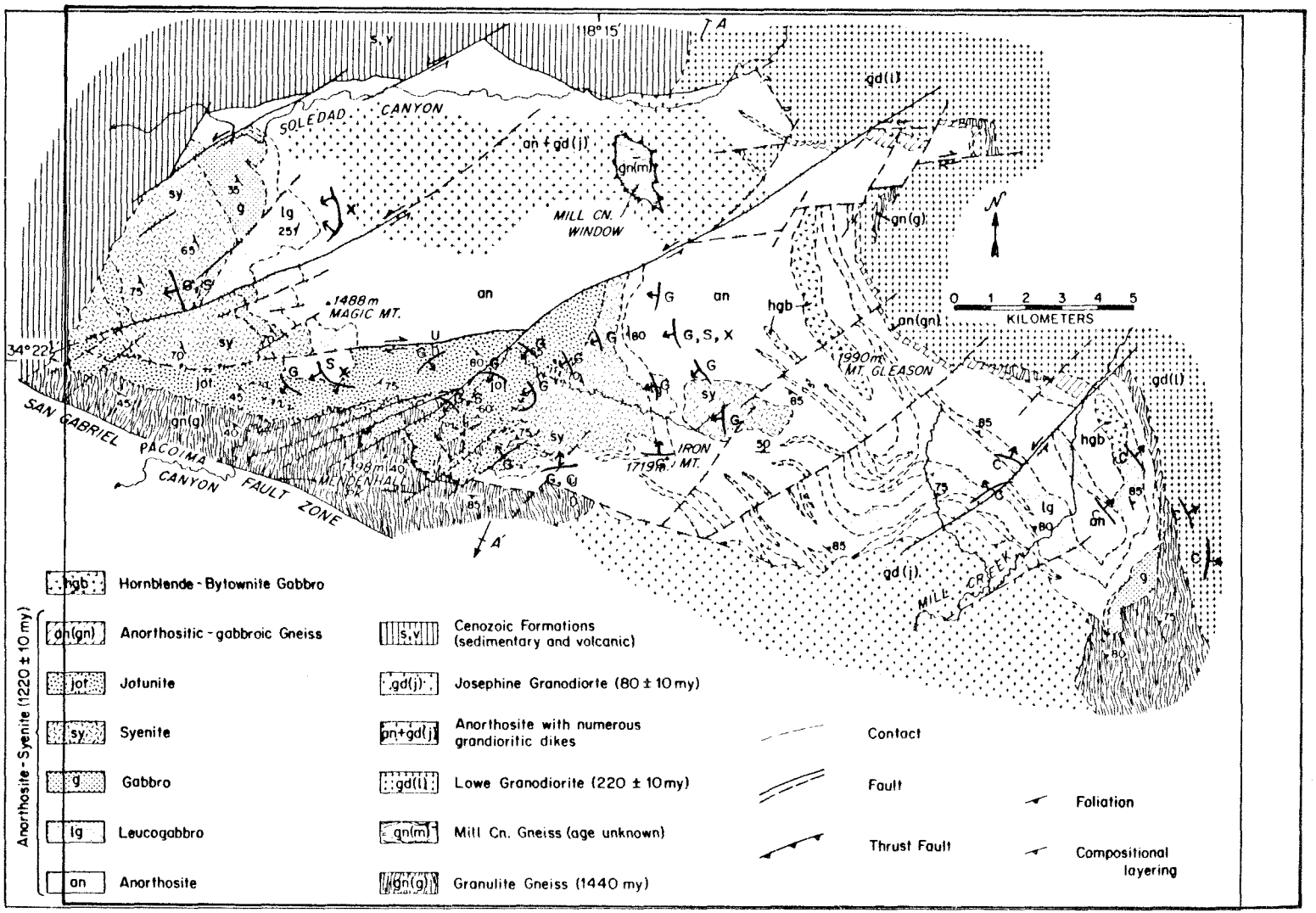

SIMPLIED GEOLOGIC MAP OF THE SAN GABRIEL ANORTHOSITE-SYENITE BODY, LOS ANGELES COUNTY, CALIFORNIA

Figure 37.

Figure 37.

explanation is that they originated when anorthosite blocks broke off of steep scarps on the floor of the chamber and sank or slid downward to accumulate nearer the base.

The configuration of the southeastern margin and the formation of diapiric structures in that area may owe their origin in part to synplutonic tilting. As discussed previously, the distribution of lithologies within the body may be in part the result of synplutonic tectonism. Much of the pervasive fracturing which has affected anorthosite in all parts of the body may be due to synplutonic tectonism, although some of the fracturing resulted from subsequent tectonic activity.

The best and most completely studied evidence of synplutonic tectonism is found in the Buck Canyon synform which is described below.

Buck Canyon Synform

Evidence of tectonic movements during the late stages of crystallization of the anorthosite-syenite body is best developed in and immediately north of the Buck Canyon synform. This is a west-plunging structure; massive anorthosite with minor amounts of leucogabbro in the east is overlain by 1500 to 1800 meters of the syenite unit in the west. The syenite unit consists mostly of massive syenite alterating with thinner sequences of layered, more mafic rocks of syenitic to jotunitic composition and includes a variety of gabbroic to ultramafic rocks at its base. The syenite unit thins abruptly both north and south of the synform axis and is overlain by rocks of the jotunite unit to the west. This structure is truncated by the Transmission Line fault to the west and northwest. The synform is defined by the thick syenite unit, whose

southern edge is poorly defined, but whose northern edge increases from about 300-600 meters to about 1800 meters over a distance of about 3 kilometers. Rocks of the syenite unit here are less homogeneous than those west of Magic Mountain. In the Buck Canyon synform, layered rocks present in the normal syenite subunit provide useful structural information bearing on the mode of origin and timing of the synform's development. Sections across the Buck Canyon synform are shown on cross sections D-D', E-E' and F-F' on Plate II, and a diagrammatic cross section is shown in Figure 38. The Buck Canyon synform is underlain by homogeneous massive anorthosite with very few leucogabbro interlayers except near North Fork Saddle, where about 400 meters of leucogabbro separates it from the overlying syenite. On the northern flank of the Buck Canyon synform (and also near Magic Mountain) the upper part of the anorthosite-leucogabbro unit is a complex zone as much as 100 meters thick in which numerous dikes and more irregular bodies of mafic to ultramafic rocks cut anorthosite, in a few instances constituting extremely coarse dike-breccias of anorthosite with a mafic or ultramafic matrix. Similar mafic dikes are present elsewhere in the anorthosite-leucogabbro unit, and scattered anorthosite dike-breccias are present at least a thousand meters below the upper contact, but it is only near this contact with syenite unit rocks that mafic dikes become volumetrically significant. These dikes are most conspicuously developed on the northern flank of the Buck Canyon synform. They are less conspicuous on its southern flank, and north and east of North Fork Saddle.

Rocks of the ultramafic syenite subunit immediately above the anorthosite contact are structurally and compositionally complex, especially along the axis and northern flank of the synform. They are

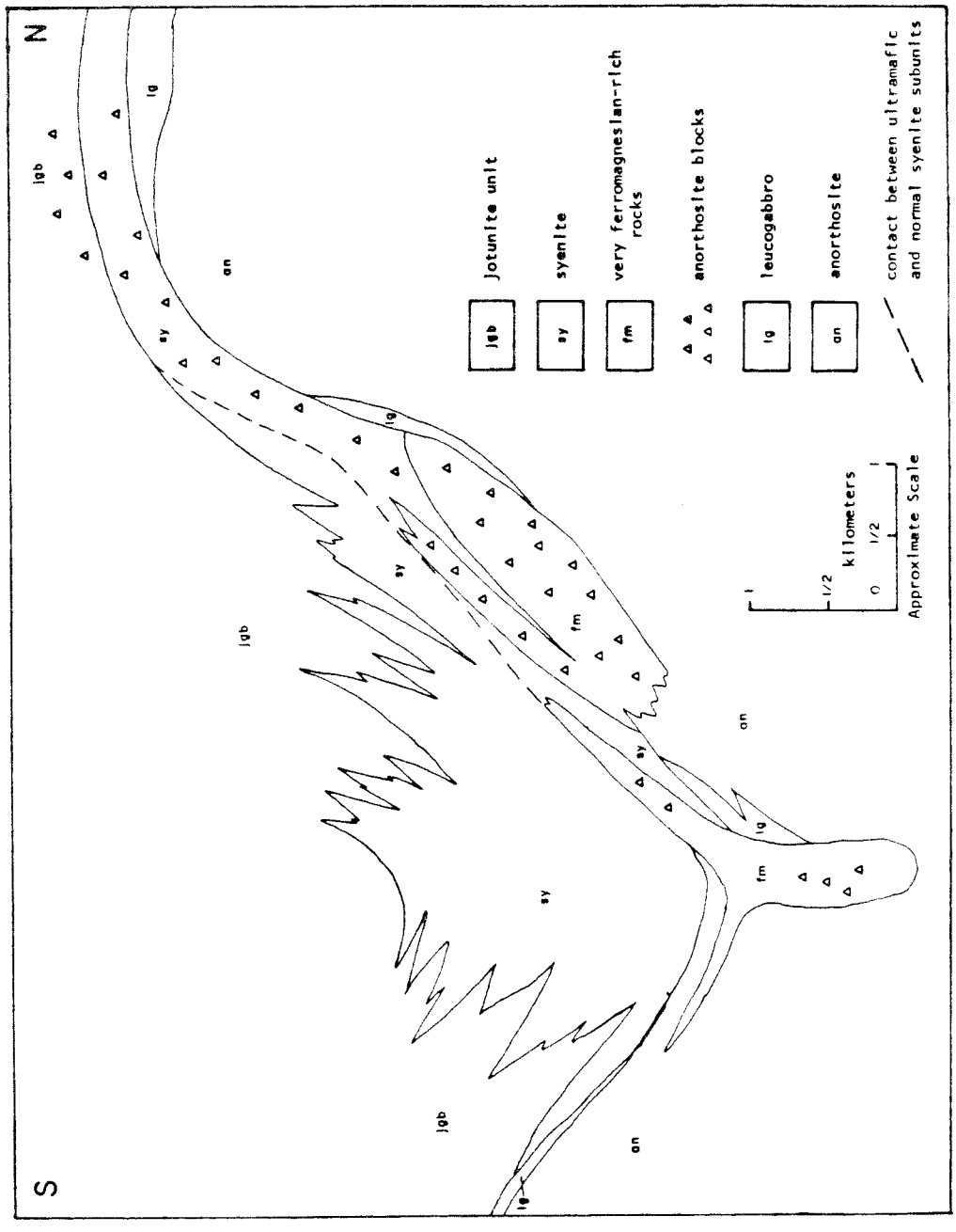

Figure 38. Diagrammatic cross section of the Buck Canyon synform.

300 to 900 meters thick in the axis of the synform, where they include normal syenite, anorthosite, gabbro, mangerite and jotunite, and large amounts of ultramafic rocks. Most rock types occur as layers a few meters to several tens of meters in thickness. A few fault and intrusive contacts are present, but most contacts are gradational changes in mineral proportions. Mineral and size graded layers are common in the more mafic rocks and verify that bottom crystal accumulation formed many of the rocks. Large blocks (commonly one meter to a few tens of meters) of anorthosite and sometimes other rock types are common within thick mafic or ultramafic layers. These mafic rocks sometimes display graded layering which drapes over the blocks. In one place abundant angular anorthosite blocks within very mafic rock forms a unit about 15-30 meters thick which extends about 800 meters along the north flank of the synform. This unit thickens and includes progressively larger anorthosite blocks toward the axis, where anorthosite blocks exceeding 30 meters diameter are present.

This zone was produced by bottom crystal accumulation, predominantly of ferromagnesian minerals, accompanied by massive slumping and rotation of large blocks, especially along the north flank of the synform. The direction of sliding and slumping is difficult to confirm but on the basis of slump structures and thickening of lithologic units, it was probably generally from east to west near North Fork Saddle, generally from north to south along the north flank of the Buck Canyon synform, and possibly included an east to west component along the axis of the synform. Scant directional evidence suggests movement from south to north on the south flank of the synform.

Within the synform, rocks of the ultramafic syenite subunit with common slump structures are overlain by massive homogeneous rocks of the normal syenite subunit. North of the synform, near North Fork Saddle, mafic rocks with common slump structures include all of the (much thinner) syenite unit, and include the anorthosite block subunit of the overlying jotunite unit. Thus, the zone of mafic rocks with abundant slump structures clearly transgresses the stratigraphic units (in this case based on the uppermost occurrence of syenite) although its total thickness of about 900 meters remains constant.

Within the synform, rocks of the normal syenite subunit are massive and homogeneous, but include a few layered units, commonly more mafic than syenite and usually containing antiperthite rather than mesoperthite. The layers are commonly graded and suggest that up was toward the west during crystallization and accumulation of these rocks. This is consistent with a variety of up indicators in the underlying mafic rocks of the ultramafic rocks of the ultramafic syenite subunit. A few small bodies (to tens of meters) of mafic rocks cut anorthosite below and syenite above, but there is no evidence of large-scale crosscutting, or any suggestion of a significant temporal hiatus between crystallization of the two subunits. Small-scale intrusive relationships are probably produced by small masses of mafic magma or crystal mush which were injected downward into underlying anorthosite, and later mafic bodies (probably related to the jotunite unit) which were intruded into both anorthosite and syenite. Thus, it appears that slumping occurred in the axis and along the flank of the synform during accumulation of the mafic part of the syenite unit, and that the normal syenite higher in the section crystallized later when the topographic relief of the bottom of the magma chamber may

have been considerably less. North of the synform, where a much smaller thickness of syenite accumulated, slumping occurred throughout its accumulation, and continued during accumulation of the lower part of the jotunite unit. This contrast can be explained if either the zone of abundant slumping or the major stratigraphic units (or possibly both) are time transgressive.

(1) If the slump horizon is time transgressive, then slumping occurred either in a limited area which migrated with time or else in two or more distinct episodes at different times.

(a) Slumping may have started near the present synformal axis and subsequently migrated up its north flank, so that relatively homogeneous syenite was crystallizing in its center while slumping was occurring high on its north flank. Near North Fork Saddle, slumping would have continued after complete crystallization of the syenite unit and involved the lower rocks of the jotunite unit.

(b) Accumulation of the lower 600-900 meters of the syenite unit may have been everywhere accompanied by slumping, and followed by accumulation of relatively homogeneous syenite only in the center of the synform. Following crystallization of the syenite unit, similar tectonic activity may have produced a renewed slumping near North Fork Saddle during accumulation of the lower part of the jotunite unit.

In either case, the presence of anorthosite blocks in the rocks of the jotunite unit near North Fork Saddle indicates that anorthosite must have been exposed on the floor of the magma chamber during their accumulation. This requires that the syenite unit must be absent somewhere nearby, probably to the north and east, just as

it thins and disappears between the axis and the southern edge of the synform.

(2) It is possible that the slumped rocks formed during a given time interval to produce a zone of relatively uniform thickness regardless of lithology (or stratigraphic unit). If all the slumped rocks formed synchronously, then the contact between the syenite and jotunite units must be time transgressive, and as much as 1200 meters of syenite crystallized in the synform after the overlying jotunite began to accumulate about 2.5 kilometers to the north. The uppermost syenite appears to lie stratigraphically 900 to 1200 meters higher in the axis of the synform than on either its north or south flanks. In Pacoima Canyon above the mouth of the North Fork, rocks of the two units appear to interfinger over nearly a thousand meters vertically. Perhaps these units formed in part simultaneously, and the zone of abundant slump structures might have formed at approximately the same time in all parts of the area.

The first is the preferred explanation of the relationships observed in and adjacent to the Buck Canyon synform. Jotunitic magma was apparently intruded after crystallization of much of the syenite and mixed with some of the remaining syenitic magma. Mixing of the magmas was incomplete so that interfingering of the two units occurred over about a thousand meters stratigraphically, although intrusion of jotunitic magma into syenite could account for some of the interfingering. Slumping occurred along the upper contact of the anorthosite-leucogabbro unit and apparently persisted longer near North Fork Saddle where the syenite unit is thin, than it did in the Buck Canyon

synform where the syenite unit is much thicker.

Origin of the Buck Canyon Synform

Rocks of the anorthosite-leucogabbro unit formed by bottom crystal accumulation mostly of plagioclase, and subsequent recrystallization of much of the rock (see chapter 4). Layering in leucogabbro was probably sub-horizontal and the upper contact is generally parallel to the layering. However, discordance of this contact in upper Pacoima Canyon is suggested by the approximately 400 meters of leucogabbro below the contact northeast of North Fork Saddle which is absent farther south, so that anorthosite is below the contact in the Buck Canyon synform to the southeast (Figure 38).

Rocks immediately above the contact contain abundant evidence of massive slumping as well as of continued bottom crystal accumulation, largely of ferromagnesian minerals. Evidence of bottom accumulation shows that anorthosite slump blocks accumulated on the floor of the chamber. Numerous mafic to ultramafic bodies intrude the underlying anorthosite near the contact. The presence of large angular anorthosite slump blocks 500 meters or more above the contact suggests that major tectonic movements much have occurred during accumulation of the slumped rocks. Local vertical relief of the upper contact of the anorthosite-leucogabbro unit must have exceeded 500 meters. Major tectonic movements were probably also responsible for fracturing the upper part of the anorthosite, and probably produced the oversteepened slopes from which the angular slump blocks were derived. Fractures in the upper part of the anorthosite within a few hundred meters of the contact were infilled either by the overlying melt from which mafic and

ultramafic rocks were accumulating or else by mafic crystal mush. Thus, near the contact many dikes and irregular bodies of mafic and ultramafic rock cut anorthosite, sometimes forming coarse anorthosite dike-breccias where fracturing was severe.

Recognized slump structures are uncommon in the underlying anorthosite-leucogabbro unit although this could be in part due to its different composition and the extensive recrystallization which has occurred. It is evident that accumulation of the rocks of the syenite unit began at a time of major tectonic movements which produced massive slumping and finally the Buck Canyon synform, with total structural relief of as much as 1500 meters, a steep northern flank, and perhaps a more gentle southern flank. These tectonic movements and accompanying slumping persisted through the accumulation of the lower part of the jotunite unit in at least one area north of the synform.

The exact orientation and nature of these tectonic movements are not known. The synform was probably asymmetric, and may even have approached a monocline with a steep north flank and a nearly flat floor to the south. Incomplete evidence suggests that slumping occurred from north to south into the axis of the synform. The anorthosite floor, probably fractured and broken, was at least intermittently exposed during formation of the slumped rocks, probably mostly to the north and east, towards the probable center of the anorthosite-syenite body. Slumping off of a steep scarp on the anorthosite floor near the Buck Canyon synform may have removed enough material to cut out as much as 400 meters of leucogabbro. However, the total volume of slump blocks is too little to account for the absence of that much leucogabbro, which may be in part the result of normal thinning of leucogabbro like that

seen in many places southeast of Mt. Gleason.

Other Synplutonic Tectonism

Gabbro in the upper part of the anorthosite-leucogabbro unit varies greatly in thickness in lower Pole Canyon. Parts of this rock contain anorthosite blocks, but no large-scale discontinuity has been recognized at its base and the anorthosite blocks are localized in an area only about 0.5 kilometer in diameter immediately south of Soledad Canyon. While the thick gabbro and overlying syenite to the west may have formed in a deep sag similar to the Buck Canyon synform, the absence of widespread anorthosite blocks and the apparantly gradational contacts between lithologies indicates that this area developed differently than the Buck Canyon synform.

Anorthosite blocks are present in the rocks of the ultramafic jotunite subunit in one small area south of Magic Mountain. It is probable that the three underlying jotunite subunits are not present in this area and that these rocks formed adjacent to a steep scarp on the floor of the chamber. This indicates that at least limited tectonism continued through the crystallization of the jotunite unit rocks.

Abundant anorthosite blocks are present in three tabular bodies of layered gabbro in rocks of the normal syenite unit in lower Oak Spring and Iron Canyons. The westernmost of these is 2 to 3 kilometers vertically above the basal contact of the syenite unit west of Magic Mountain. If these were eroded off of a tectonic scarp, then it must have been larger than that on the north flank of the Buck Canyon synform. Alternatively, these may be gabbroic sills intruded into syenite, although intrusive contact relationships were not recognized. The

blocks clearly accumulated on the floor during crystallization of these rocks, but the blocks could have been entrained by intruding magma and thus emplaced into a level considerably above that where they originated. Neither alternative is very attractive. If these rocks were formed adjacent to a tectonic scarp, then it is larger than any others recognized, and no other evidence of the scarp was recognized (however, this is an area where several Cenozoic faults of major displacement have seriously complicated structural reconstruction of the primary distribution of lithologic units). No definite intrusive contacts were recognized, and no other similar gabbroic intrusions containing numerous blocks were observed elsewhere in the anorthosite-syenite body. Thus, the origin of these bodies remains undetermined.

POST ANORTHOSITE STRUCTURE

MT. LOWE GRANODIORITE EMPLACEMENT

The northeast margin of the anorthosite-syenite body was profoundly affected by emplacement of the early Mesozoic (Silver, 1971) Mt. Lowe granodiorite (Figure 39), and was affected to a lesser extent elsewhere. The contact between the Mt. Lowe granodiorite and older anorthositic and metamorphic rocks trends northwest (N 20°W to N 60°W), usually dips steeply toward the granodiorite body (60-90° NE) and is approximately planar over distances of several kilometers. Rocks several hundreds to a few thousands of meters on either side of the contact show the effects of strong deformation parallel to it. There are very few places where Mt. Lowe granodiorite clearly cross-cuts the older rocks.

Mt. Lowe granodiorite near the contact has been very strongly deformed, such that the characteristic porphyritic rock is transformed

into a highly sheared augen gneiss in which the augen are hardly recognizable due to extreme elongation. The foliation gradually decreases toward the interior of the granodiorite body until it becomes a minor structural element several kilometers from the contact. The foliated marginal Mt. Lowe granodiorite is inferred to have been emplaced into its present position as a nearly solid crystal mush. Numerous fine to medium grained leucocratic dikes with compositional affinities to the Mt. Lowe granodiorite occur in augen gneiss near the contact and parallel to it and show little or no deformation, thus suggesting that emplacement occurred before cessation of magmatic activity.

Deformational effects of this emplacement are pronounced in the adjacent anorthositic rocks and Mendenhall gneiss. A thin, discontinuous screen of Mendenhall gneiss separates anorthositic rocks from Mt. Lowe granodiorite along about half of the contact. This gneiss was originally part of the roof of the anorthosite-syenite body.

Strongly deformed, partially recrystallized anorthositic rocks occur at the contact. Deformational layering and foliation is parallel to the contact and sub-parallel to primary igneous layering in less deformed anorthositic rocks farther from the contact. These deformed rocks are generally more mafic than the remainder of the anorthosite-leucogabbro unit; many of them are gabbro in average composition, especially in the Mill Creek area. These deformed mafic rocks probably represent differentiates which formed at the roof of the body, just as jotunite overlies leucocratic rocks farther west. Thin veins of hornblende gabbro formed by recrystallization of gabbro cross-cut primary layering in leucogabbro in a few places. Broader-scale cross-cutting

may also be present; there appears to be about 1500 meters more section present in Mill Creek than north of Mt. Gleason, although this may be a primary feature.

R.T. Phipps (1951) mapped a north-south fault at the Monte Cristo Mine about 360 meters west of, and parallel to the Mt. Lowe granodiorite contact. The ore-bearing rocks were emplaced along this fault. This fault, of unknown displacement, is older than sub-horizontal mafic dikes similar to those found in the Mt. Lowe granodiorite, and is oriented differently than the prominent Cenozoic fault sets in the area. It may be related to emplacement of the Mt. Lowe granodiorite.

Emplacement of the Mt. Lowe granodiorite apparently produced broad folds in the anorthosite-syenite body. The nature of this folding is described in the following section.

FOLDS

Two sets of major post-Precambrian folds appear to be present in the crystalline rocks of the western San Gabriel Mountains: an earlier one with approximately east-west axial planes; and a later one with north-northwest-trending axial planes. Some of these folds are poorly delineated and are of uncertain age. The north-northwest folds are generally parallel to the Mt. Lowe granodiorite contact and probably formed in response to its emplacement, although they were probably reactivated in Cenozoic time. East-west folding is evidenced by the Pacoima Canyon synform and a broad antiform farther north. The Pacoima Canyon synform formed (more or less) along part of the Precambrian Buck Canyon synform in middle to late Cenozoic time.

North-Northwest Folds

Several folds are sub-parallel to the early Mesozoic Mt. Lowe granodiorite contact and appear to have been produced by NE-SW compression accompanying its emplacement (Figure 39). The Mt. Gleason antiform extends about 13 kilometers southeast from the mouth of Mill Canyon, where otherwise unfamiliar gneisses are exposed in its core, to Mt. Gleason, where a large body of hornblende-bytownite gabbro is exposed on its northeast limb and lenses out toward the southwest, with only a small body exposed on that limb of the antiform. This antiform plunges toward the southeast at a low angle in Mill Canyon, toward the southeast at a moderate to high angle north of Mt. Gleason, and probably plunges toward the north south of Mt. Gleason.

The North Fork synform lies about 4 kilometers west of the Mt. Gleason antiform, and is inferred to extend about 10 kilometers between Soledad and Pacoima Canyons. Its axis probably crosses the road about 1.5 kilometers morthwest of North Fork Saddle where gabbroic layers and a few metamorphic xenoliths occur in anorthosite. To the south, its axis must lie between Rattlesnake and Spring Canyons, where its original southward plunge has been further steepened in the north limb of the younger Pacoima Canyon synform.

The Magic Mountain antiform lies about 4 kilometers west of the North Fork synform and is inferred to extend about 9 kilometers between Soledad and Pocoima Canyons. The anorthosite south of the Lonetree fault between Dagger Flat and Dorothy Canyons probably lies in the core of this antiform, whose original southward plunge has been further steepened in the north limb of the younger Pacoima Canyon synform. The numerous Mesozoic(?) granodioritic dikes south of Soledad Canyon are

Figure 39. Early Mesozoic structures developed mainly during emplacement of the Mt. Lowe granodiorite: (1) Magic Mountain antiform, (2) North Fork synform, (3) Mt. Gleason antiform.

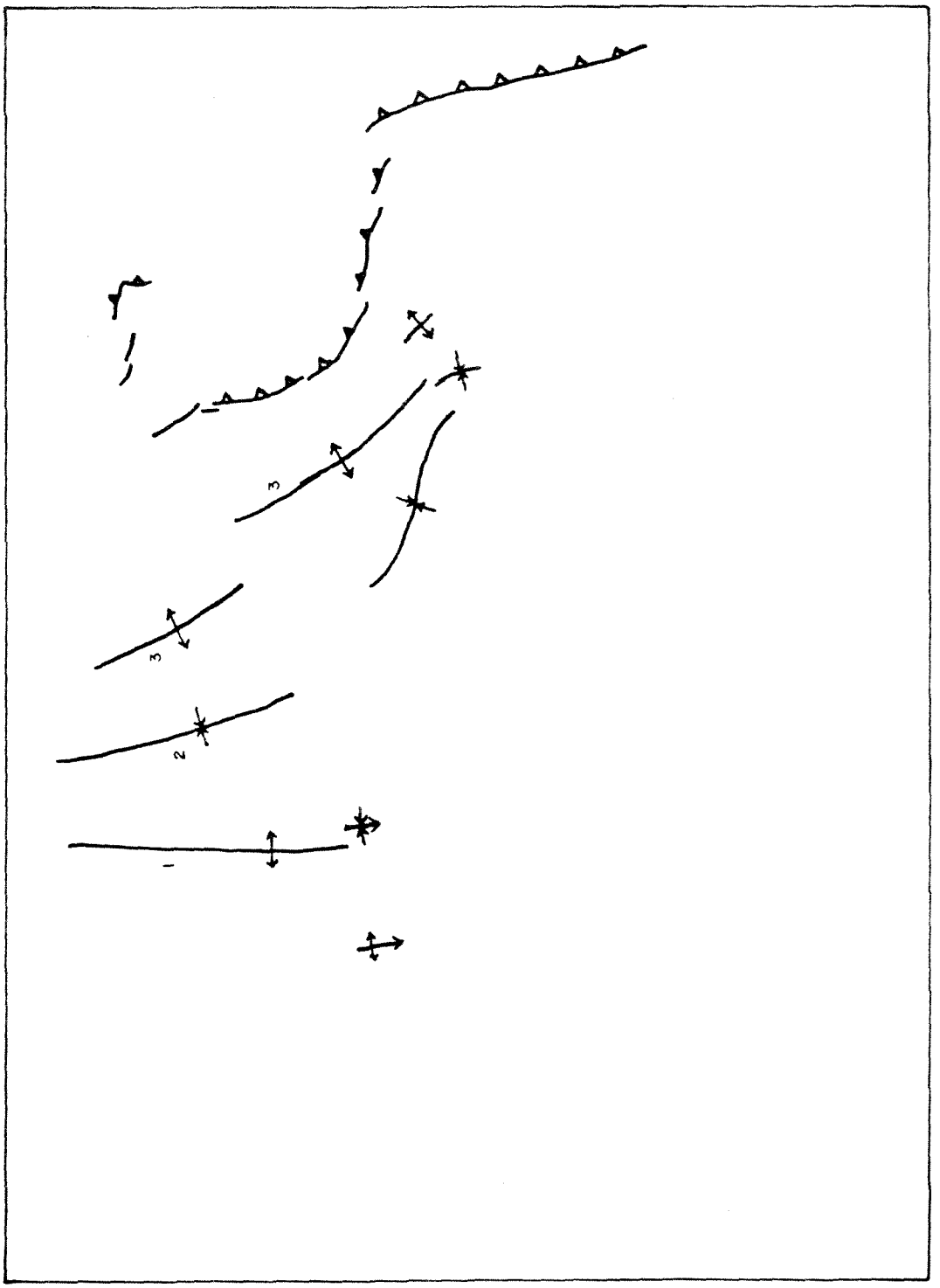

Figure 39.

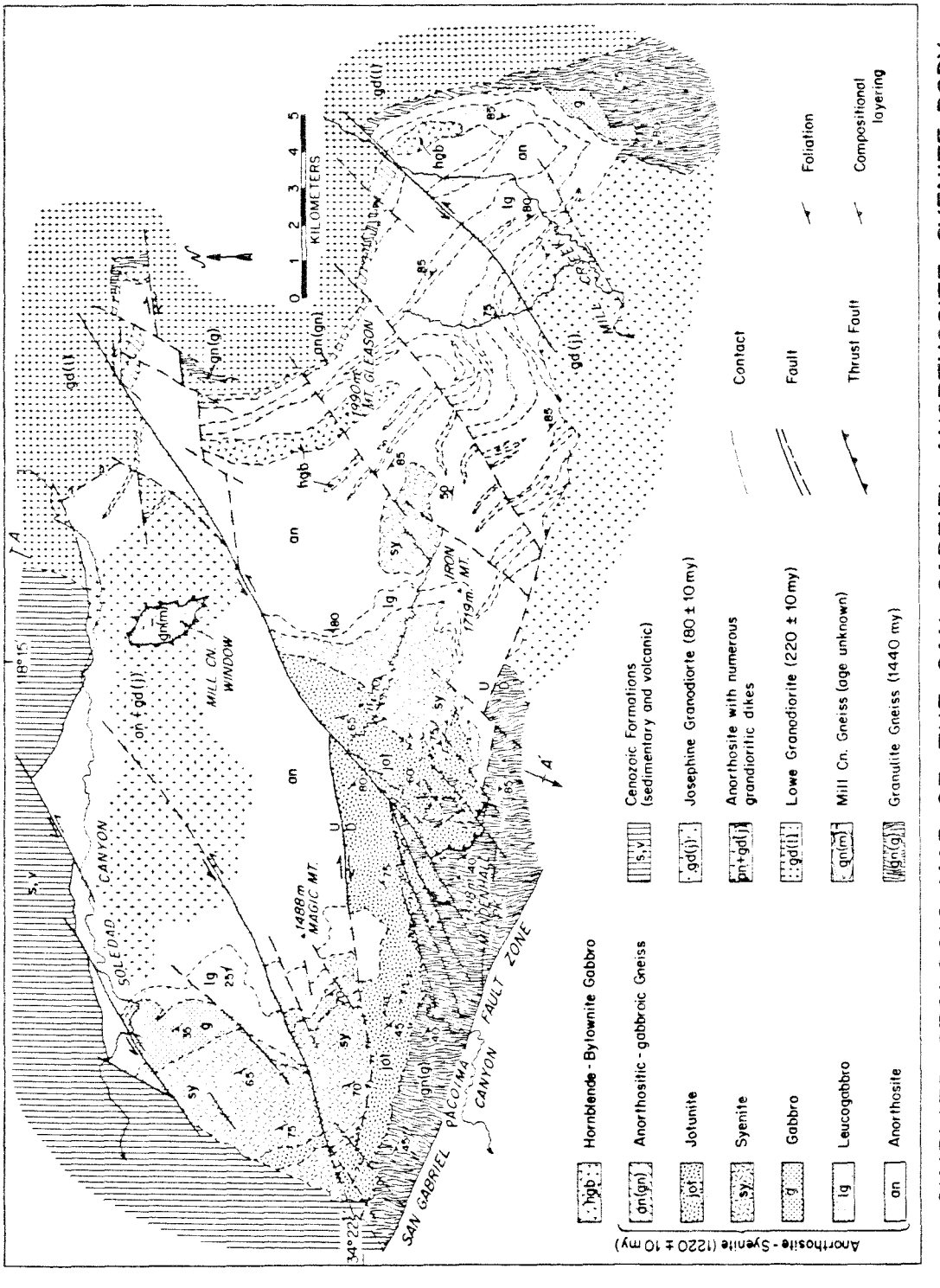

SIMPLIED GEOLOGIC MAP OF THE SAN GABRIEL ANORTHOSITE-SYENITE BODY, LOS ANGELES COUNTY, CALIFORNIA

Figure 39.

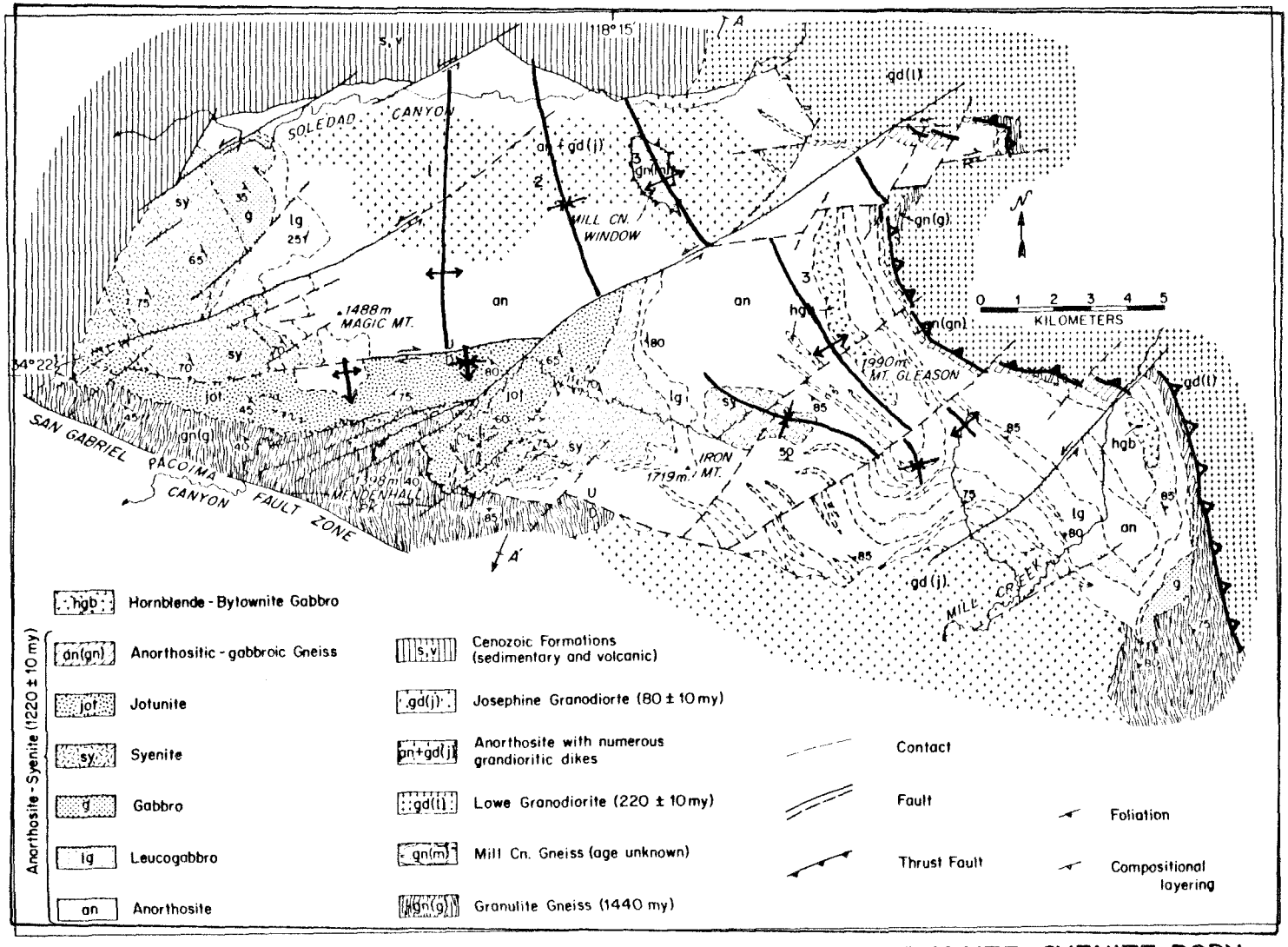

SIMPLIED GEOLOGIC MAP OF THE SAN GABRIEL ANORTHOSITE-SYENITE BODY, LOS ANGELES COUNTY, CALIFORNIA

Figure 39.

Figure 39.

almost entirely restricted to the anorthosite-leucogabbro unit, and appear to be concentrated in the fractured cores of the northern parts of the Mt. Gleason and Magic Mountain antiforms.

Several smaller north to northwest-trending folds are exposed in the core of the Pacoima Canyon synform between Pacoima Canyon and Mendenhall Ridge. On the basis of their trends, they are probably related to emplacement of the Mt. Lowe granodiorite. These structures could usually be defined only where the contact between jotunite unit rocks and Mendenhall gneiss is exposed.

East-West Folds

North-south compression of the anorthosite-syenite body probably occurred during and soon after deposition of the Oligocene(?) Vasquez formation which has been strongly affected by north-south compression (Leon Silver, personal communication). This deformation produced the east-west Pacoima Canyon synform which deformed the originally sub-horizontal contact between jotunite unit rocks and Mendenhall gneiss in and south of Pacoima Canyon (Figure 40). This fold steepened the southward plunging noses of the early Mesozoic folds north of Pacoima Canyon. The eastern part of this westward-plunging fold coincides in part with the Precambrian Buck Canyon synform which originally probably had a more northwesterly trend. In upper Pacoima Canyon, it is difficult to separate the structural evidence for this fold from that for the Precambrian Buck Canyon synform.

The broad westward-plunging Bear Canyon antiform lies about 5 kilometers north and parallel to the Pacoima Canyon synform. The structurally highest rocks in its core contain numerous granodioritic

Figure 40. Middle to late Cenozoic folds: (1) Bear Canyon antiform, (2) Pacoima Canyon synform.

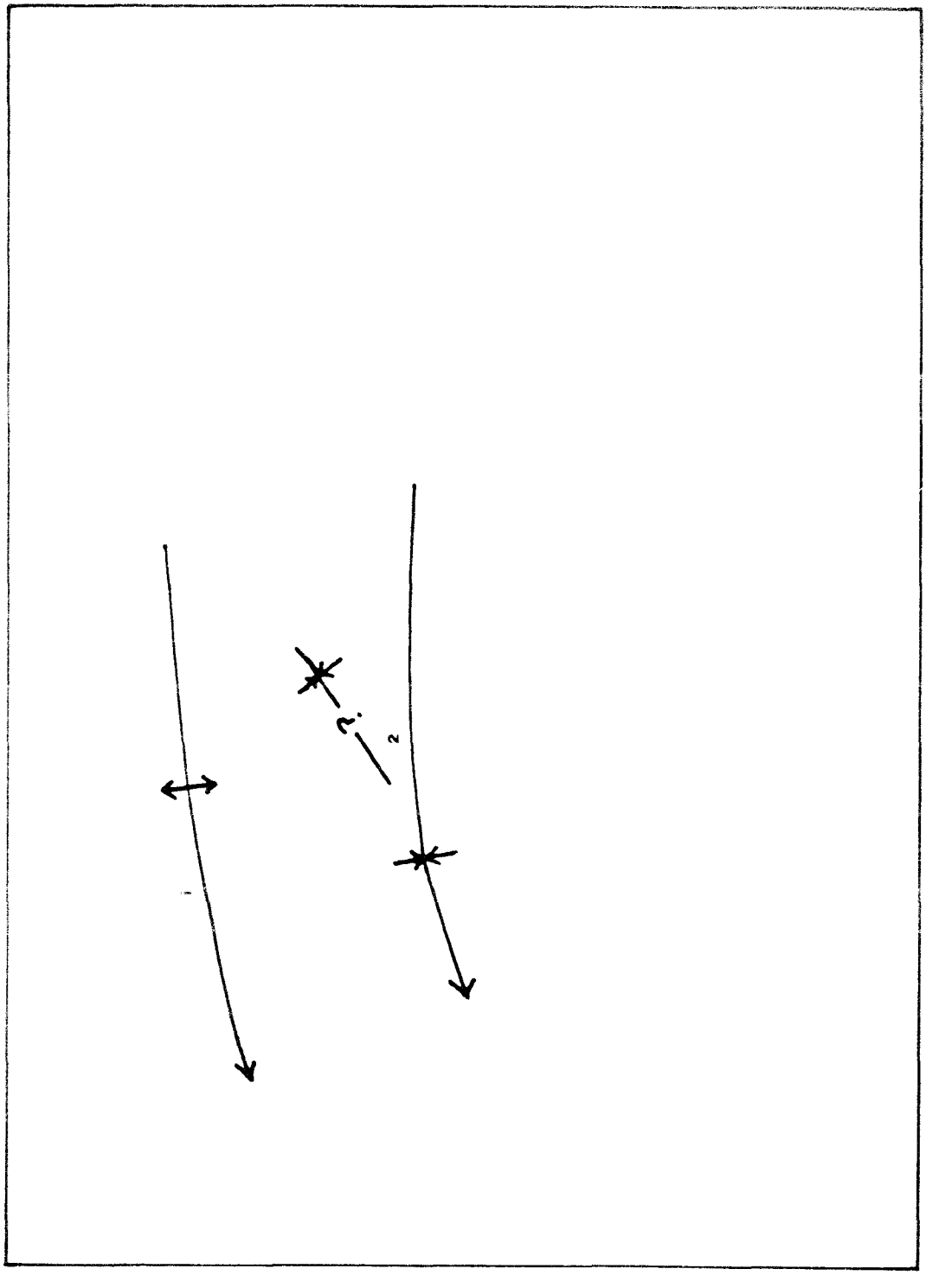

Figure 40.

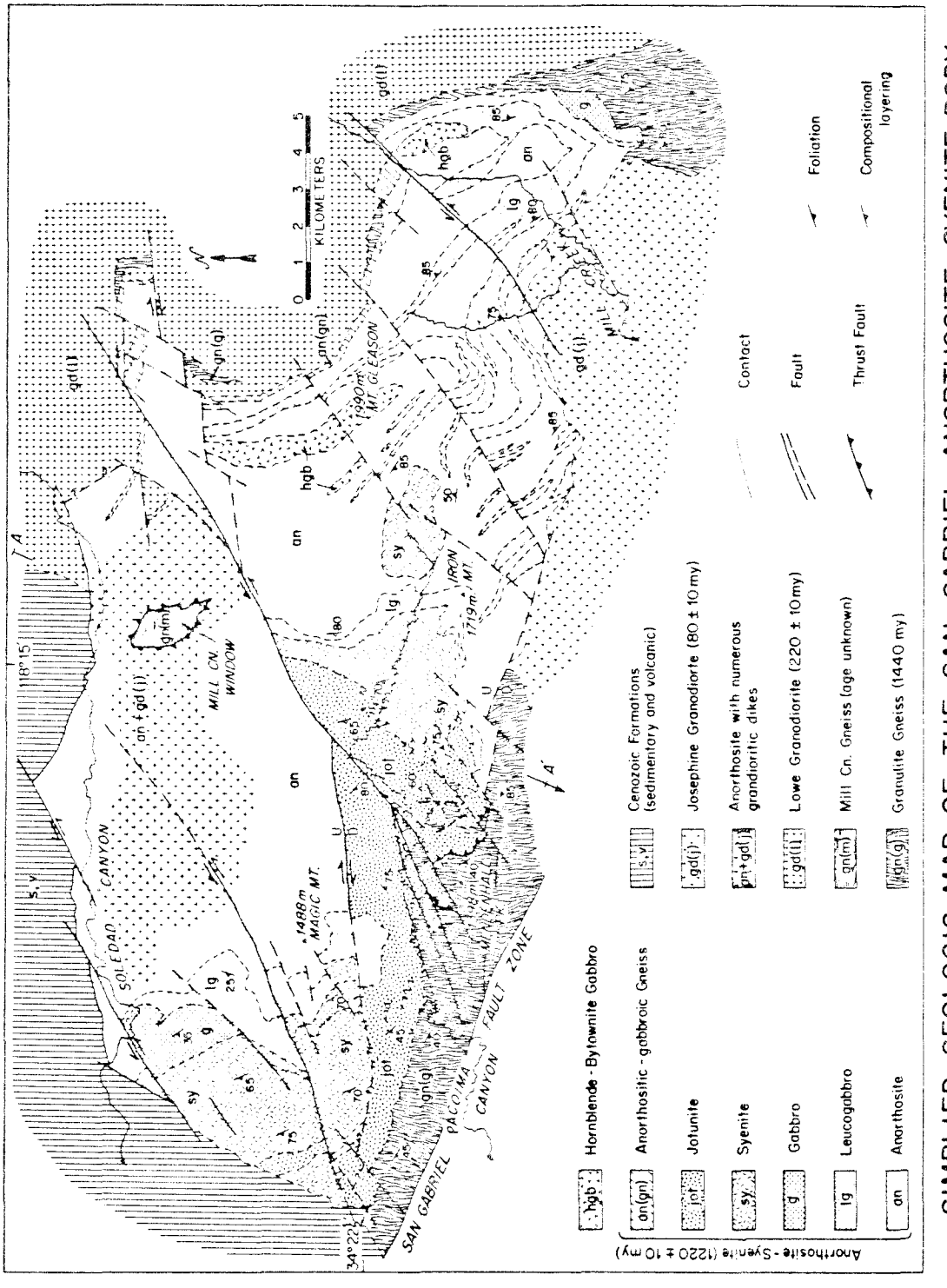

SIMPLIED GEOLOGIC MAP OF THE SAN GABRIEL ANORTHOSITE-SYENITE BODY, LOS ANGELES COUNTY, CALIFORNIA

Figure 40.

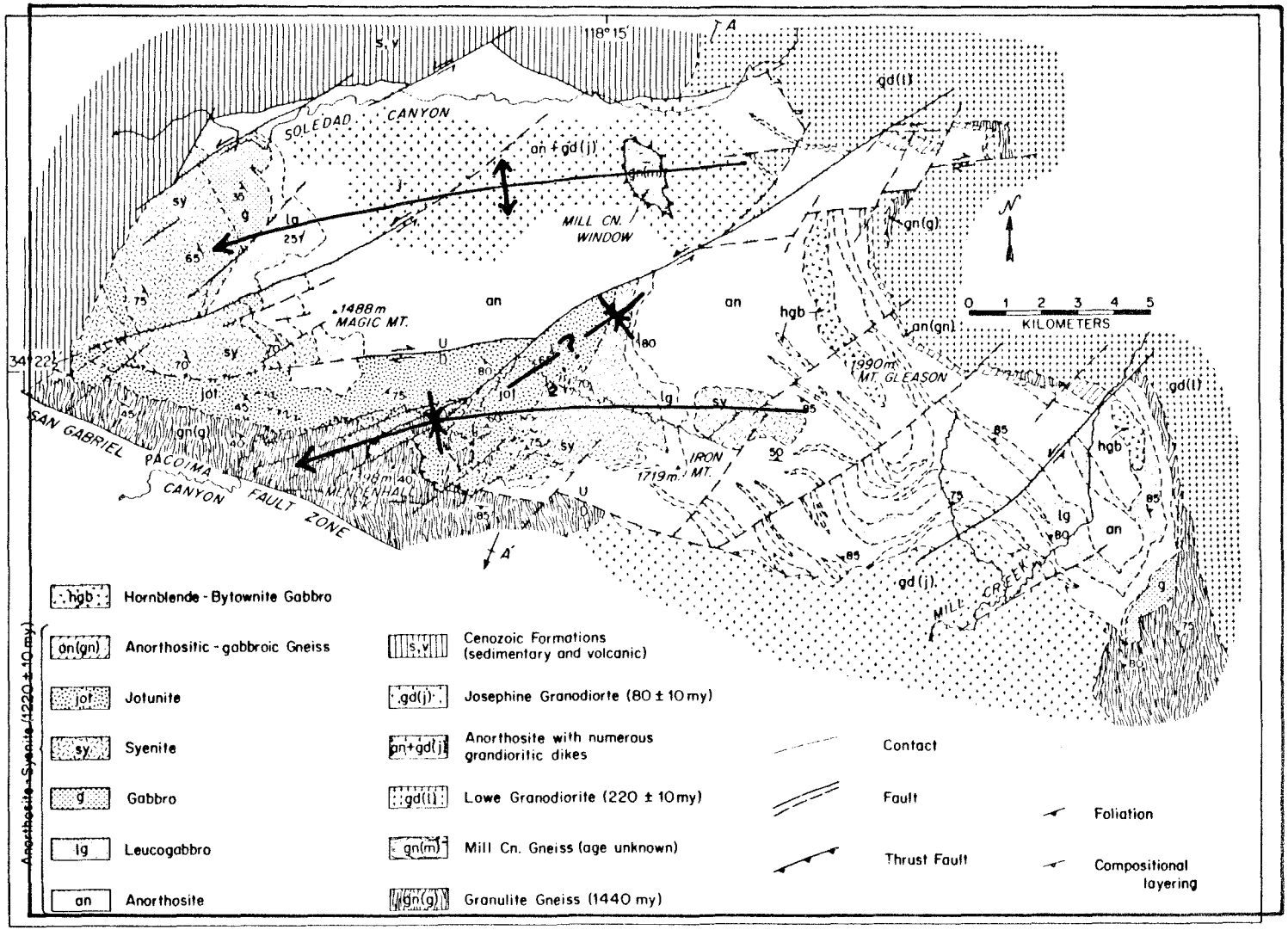

SIMPLIED GEOLOGIC MAP OF THE SAN GABRIEL ANORTHOSITE-SYENITE BODY, LOS ANGELES COUNTY, CALIFORNIA

Figure 40.

Figure 40.

dikes and include the gneisses in Mill Canyon. It may be responsible for the westward bend of the anorthosite-leucogabbro contact north of Magic Mountain. North of the San Gabriel Mountains, the Soledad Basin constitutes a broad, west-plunging syncline which is inferred to be of the same generation. Thousands of meters of structural relief were produced in rocks of the anorthosite-syenite body by folding during this episode of deformation.

Several small folds in lower Pacoima Canyon were probably formed during this deformation. A few hundreds of meters of uplift of the north side of lower Pacoima Canyon along numerous small east to northeast-trending faults may also have occurred at this time.

East-west Cenozoic faults probably formed during this same episode of deformation and northeast-trending left-lateral faults may be only slightly younger.

Reactivation of North-Northwest Folds

Reactivation of the north-northwest trending folds probably occurred during Cenozoic time. Evidence of this reactivation is the fact that the thrust sheet exposed in Mill Canyon, which includes late Mesozoic(?) granodioritic rocks, is folded by the Mt. Gleason antiform.

The Mill Canyon structure appears to be less tightly folded by this antiform than is the hornblende-bytownite gabbro on Mt. Gleason, so reactivation of an older structure seems to be indicated.

Warping on East-West Axes

Plio-Pleistocene and Recent warping caused uplift and is responsible for the most recent unroofing of anorthositic rocks in the San

Gabriel Mountains. This warping also affected upper Cenozoic rocks in the Soledad Basin to the north where sediments as young as Pleistocene in age (Saugus formation) have been affected. Minor dip-slip movement may have occurred on some faults at this time, perhaps reactivating some older faults such as the Lonetree or Soledad faults. This warping moved crystalline rocks south of Soledad Canyon upward relative to sedimentary and crystalline rocks north of Soledad Canyon. It is probably related to the continuing strain which was most recently expressed by the San Fernando earthquake in 1971, and perhaps by the Palmdale Bulge(?).

CENOZOIC FAULTS

The anorthosite-syenite body is cut by many high-angle, predominantly strike-slip, Cenozoic faults which have substantially modified its original form. Movement on these faults was probably at least in part concurrent, but two major sets and one minor set can be distinguished on the basis of the age of latest movement. Their absolute ages are undetermined, although they are all probably Oligocene and younger. An older, more or less east-west trending set of faults shows major strike-slip and dip-slip displacements and is cut by a set of northeast trending faults with important left-lateral displacement. Both sets are cross-cut by a set of small northwest trending faults with right-lateral and sometimes dip-slip displacements, most of which are too small to be traced for any distance and thus are not shown on the geologic map (Plate I).

A major zone of low-angle faulting is exposed in Mill Canyon in the north central part of the body. Smaller exposures of this zone

are present nearby in Mattox and Bootleggers Canyons.

Plate IV shows schematically the inferred distribution of the major lithologies of the San Gabriel anorthosite-syenite body prior to displacement on the Cenozoic faults which cut the body.

Older, Generally East-West Faults

Three major faults with generally east-west trends cross-cut the anorthosite-syenite body (Figure 41). Although they could be unrelated, they have similar trends, apparent displacements of comparable magnitude, and are all similarly offset by northeast-trending faults. From north to south these faults are: (1) the Soledad fault, which separates anorthosite from the Tertiary sedimentary and volcanic rocks of the Soledad basin, (2) the Lonetree fault, which lies entirely within the anorthosite-syenite body except in the northeast part of the area, and (3) the Slaughter Canyon fault, which in part separates the anorthosite-syenite body from older gneiss and younger intrusive rocks to the south.

Soledad Fault

The Soledad fault was named by Oakeshott (1954) who mapped it in the western part of the area covered in this report. This fault follows the general trend of Soledad Canyon for about 16 kilometers, and separates the Oligocene(?) or lower Miocene(?) Vasquez formation and the Miocene Mint Canyon formation on the north from anorthosite and related rocks on the south. Its trend is approximately east-west, varying between N 65° E and N 45° W, and it dips 30° to 70° north. It is offset by northeast-trending faults with left-lateral displacement and by northwest-trending faults with right-lateral displacement.

Figure 41. Older, east-west trending strike-slip faults of Cenozoic age: (1) Soledad fault, (2) Lonetree fault, (3) Slaughter Canyon fault.

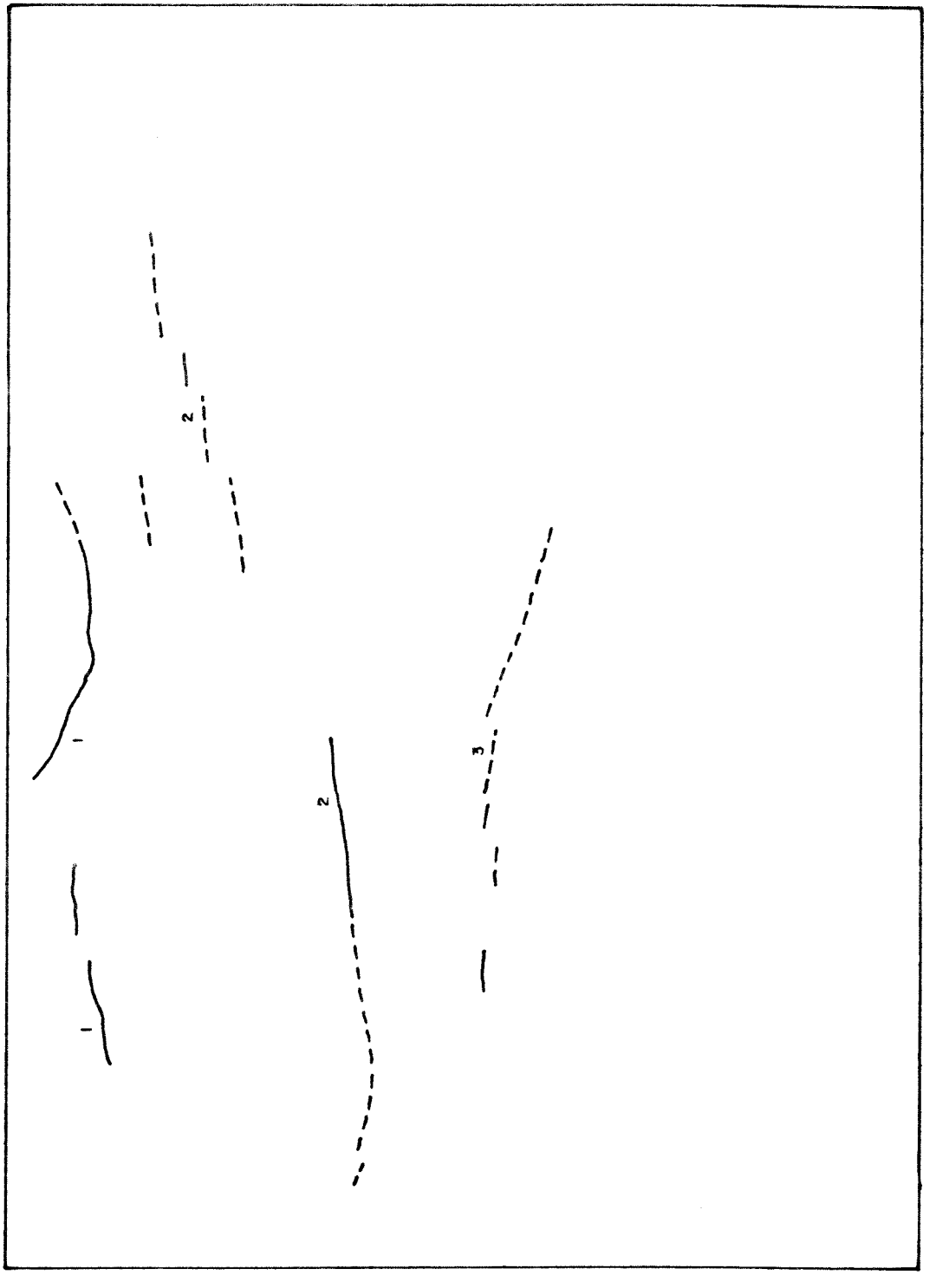

Figure 41.

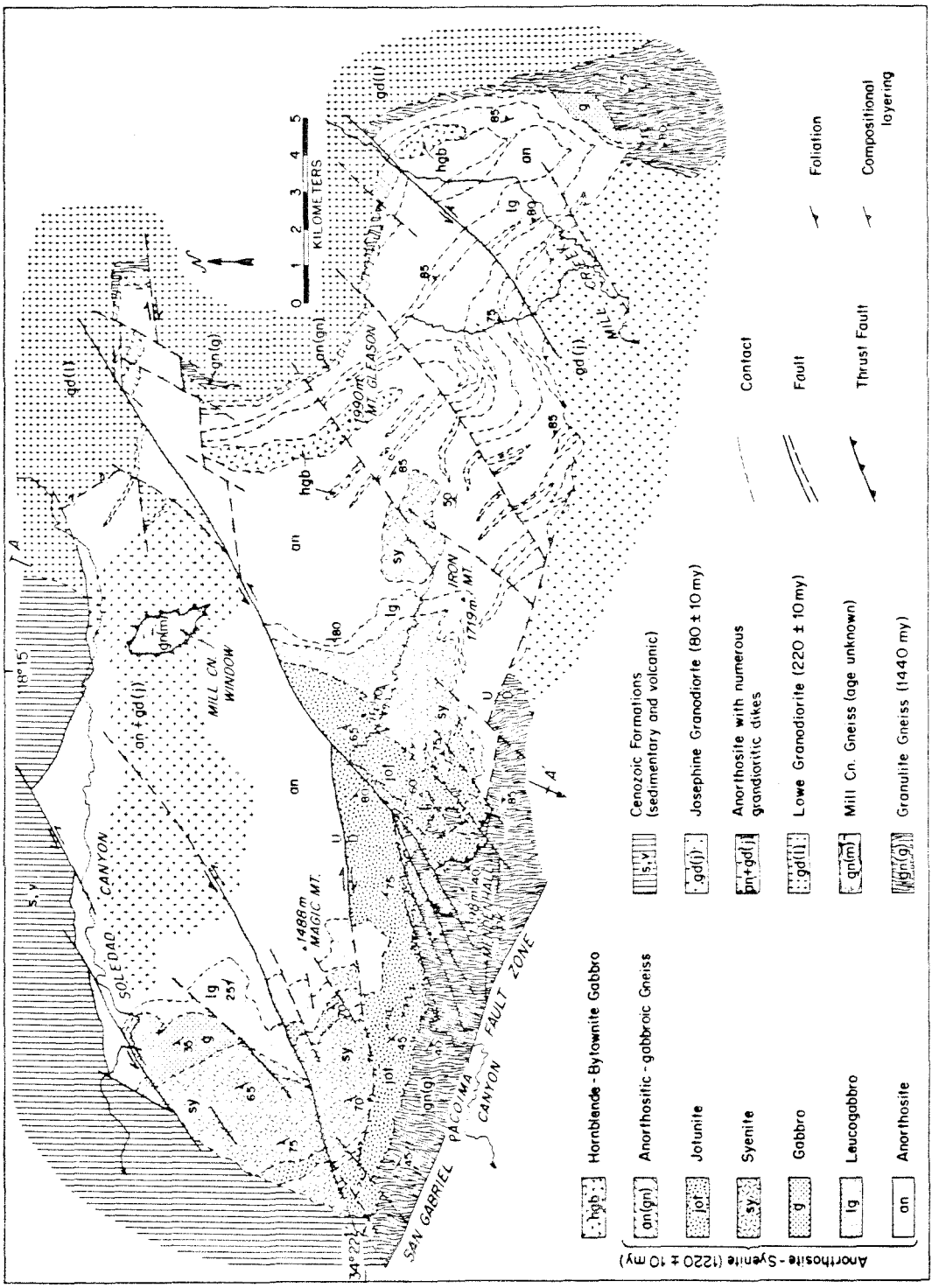

SIMPLIED GEOLOGIC MAP OF THE SAN GABRIEL ANORTHOSITE-SYENITE BODY, LOS ANGELES COUNTY, CALIFORNIA

Figure 41.

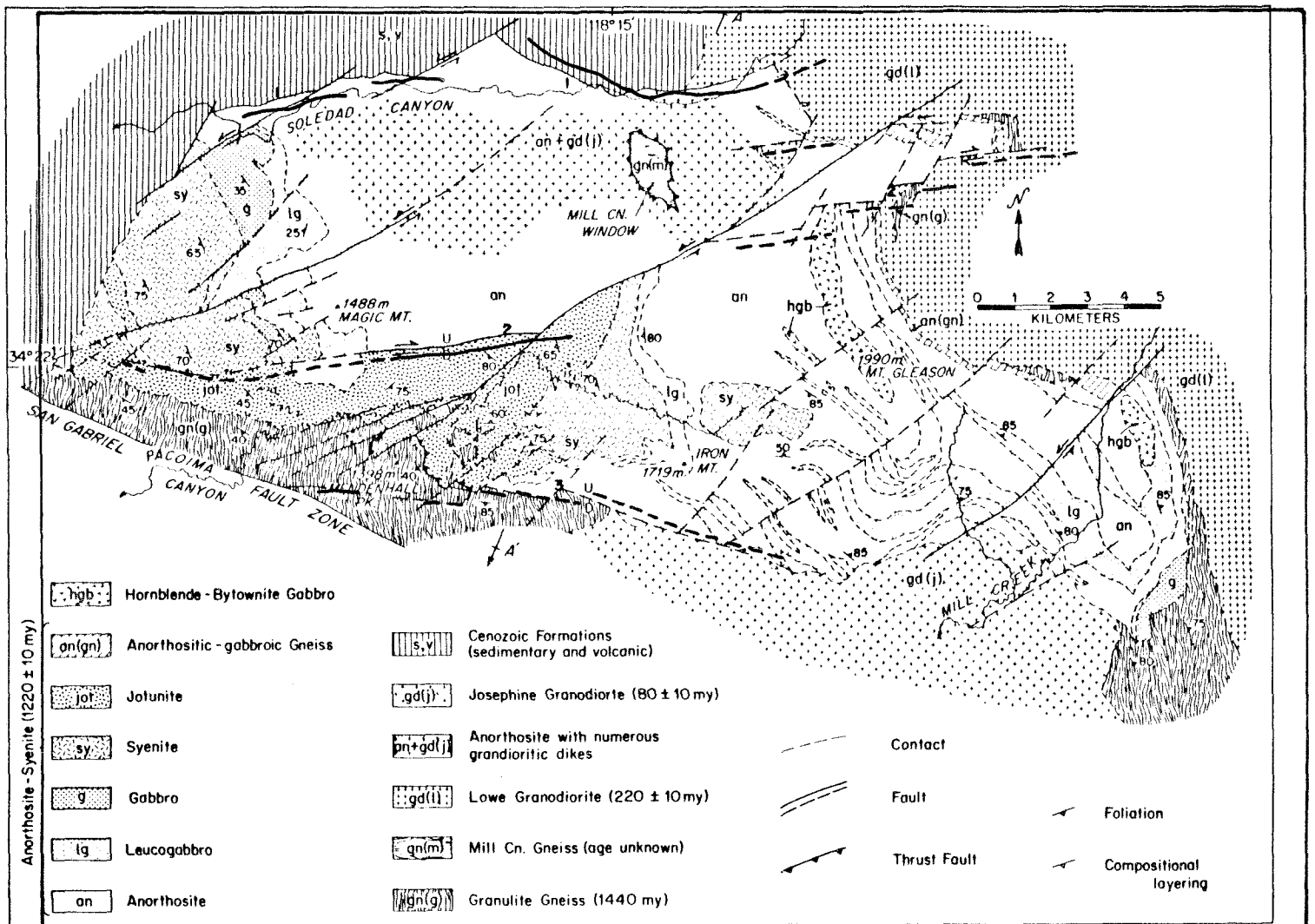

SIMPLIED GEOLOGIC MAP OF THE SAN GABRIEL ANORTHOSITE-SYENITE BODY, LOS ANGELES COUNTY, CALIFORNIA

Figure 41.

Figure 41.

Displacement on this fault is unknown, but is probably primarily dip-slip. Rocks on the north side are stratigraphically considerably higher, indicating major dip-slip displacement, north side down. However, there is some evidence that this may actually be a reverse fault along which Tertiary sediments have been dislocated upward and southward over Precambrian crystalline rocks (Leon Silver, personal communication). The fault which separates anorthosite from Vasquez formation sedimentary and volcanic rocks and Parker Mountain diorite between the mouths of Mill and Arrastre Canyons is probably a continuation of the Soledad fault. However, this fault shows apparent left-lateral displacement and could possibly be a continuation of the left-lateral Magic Mountain fault. In Upper Bootleggers Canyon, 1.5 kilometers to the south, another east-west fault probably has either major right-lateral displacement, or major dip-slip displacement (north side up). This fault could not be followed as far as Mill Canyon and could not be correlated with the Soledad fault.

Oakeshott (1958) infers the existence of the Soledad fault at least as early as upper Miocene based on the very coarse basal fanglomerate of the Mint Canyon formation seen on the north side of Soledad Canyon near the mouth of Agua Dulce Canyon. According to Jahns and Muehlberger (1954), the principal movement on this fault probably took place in pre-middle to lower Miocene time.

Lonetree Fault

The Lonetree fault can be followed from Upper Sand Canyon on the west about 18 kilometers through the middle of the anorthosite-syenite body to Aliso Canyon on the east. It is offset about

5 kilometers left-laterally by the northeast-trending Transmission Line fault in the center of the body. It is particularly conspicuous southeast of Magic Mountain where it juxtaposes white anorthosite against dark rocks of the jotunite unit. The eastern end of this fault could not be accurately located in the Sand and Bear Canyon areas but it must curve slightly to a north-west trend since it does not offset the jotunite-Mendenhall gneiss contact along the south side of Sand Canyon. Its trend varies between N 80° W and N 80° E and its dip is between 65° and 90° S. This fault offsets the steeply dipping anorthosite-Mt. Lowe granodiorite contact west of Aliso Canyon about 3 kilometers in a right-lateral sense. Southeast of Magic Mountain, juxtaposition of anorthosite against stratigraphically higher jotunite indicates large (at least a few thousand meters) dip-slip displacement on this fault, south side down. A few slickensides observed along this part of the fault indicate that the most recent displacement was predominantly dip-slip. Strike-slip movement on this part of the fault is probably about 2.6 kilometers in a right-lateral sense, based on the uncertain correlation of the western contacts of anorthosite with rocks of the jotunite or syenite units south of Magic Mountain.

The Lonetree fault has been mapped only within the crystalline rocks of the San Gabriel Mountains. It is post-Mt. Lowe granodiorite in age, and a Tertiary age is indicated if it was active at the same time as the Soledad fault. Oakeshott (1958) mapped a 5.5 kilometer long fault in Tertiary sediments parallel to and about 1.5 kilometers north of the San Gabriel fault starting about 1.5 kilometers west, and following the same trend as the western end of the Lonetree fault. This high angle fault is pre-Pliocene in age and has displaced upper

Miocene beds about 30 meters, north side up. It could possibly be a westward extension of the Lonetree fault, but it could also represent a more northerly and perhaps older part of the San Gabriel fault zone.

Slaughter Canyon Fault

The Slaughter Canyon fault forms about 8 kilometers of the southern margin of the anorthosite-syenite body, juxtaposing anorthosite and related rocks against Mendenhall gneiss in the west and Mt. Josephine granodiorite in the east. The eastern part of this fault was mapped by Oakeshott (1958) who called this segment the Condor Peak fault. This new usage, substituting "Slaughter Canyon fault" for Oakeshott's (1958) "Condor Peak fault" was adopted because an unequivocal exposure of this fault could not be located near Condor Peak, but the fault is exceedingly well exposed in and near to Slaughter Canyon.

This fault was traced 1.2 kilometers west of Slaughter Canyon, and is also exposed 3 kilometers farther west near the San Gabriel fault. Because of steep slopes and dense vegetation, this fault was seen in only a few places; the best exposure is in the canyon west of Slaughter Canyon. Along its projected trend, the anorthosite contact is quite linear, and the lack of intrusive relationships and the evidence of strong brecciation suggest the presence and approximate location of the fault.

The Slaughter Canyon fault is characterized by a 10-12 meter wide zone of crushed rock and several centimeters of extremely fine gouge. The fault plane is conspicuously cross-cut by numerous small faults with a few centimeters to several meters of displacement. It is also offset by several northeast-trending left-lateral faults. The fault plane is

nearly vertical and its strike changes from about N 85° near the San Gabriel fault in the west to about N 70° W near Condor Peak in the west.

Total displacement on the Slaughter Canyon fault is unknown, although rocks to the south (gneiss and granodiorite) are stratigraphically higher than the anorthositic rocks north of the fault, suggesting perhaps a few thousands of meters of dip-slip displacement, north side up. Possible right-lateral strike-slip displacement is suggested by a small area of anorthosite south of the fault in Trail Canyon which might be displaced from anorthosite in lower Fox Creek about 4.2 kilometers to the east and north of the fault. This fault was not mapped east of Condor Peak

Younger, Northeast-Trending Faults

Several northeast-trending faults with important left-lateral displacements transect the anorthosite-syenite body (Figure 42). Aggregate left-lateral displacement of about 11 kilometers occurs across the more important faults of this set and has altered the original shape of the anorthosite-syenite body by rotation in a counter-clockwise sense. Several other faults of this set are present in the Soledad basin as much as 13 kilometers north of Soledad Canyon. These faults offset the Soledad, Lonetree and Slaughter Canyon faults but appear to die out near the San Gabriel fault zone. In the Soledad basin faults of this set offset rocks as young as upper Miocene but do not offset lower Pliocene rocks. Displacement on these faults could, therefore, be no younger than upper Miocene.

Figure 42. Younger, northeast trending left-lateral faults of Cenozoic age: (1) Pole Canyon fault, (2) Oak Springs Canyon fault, (3) Magic Mountain fault, (4) Transmission Line fault, (5) Moody Canyon fault, (6) Laurel Canyon fault, (7) Gooseberry Canyon fault, (8) Bad Canyon fault, (9) Mendenhall fault, (10) Mt. Gleason fault, (11) Fox Creek fault, (12) Mill Creek fault.

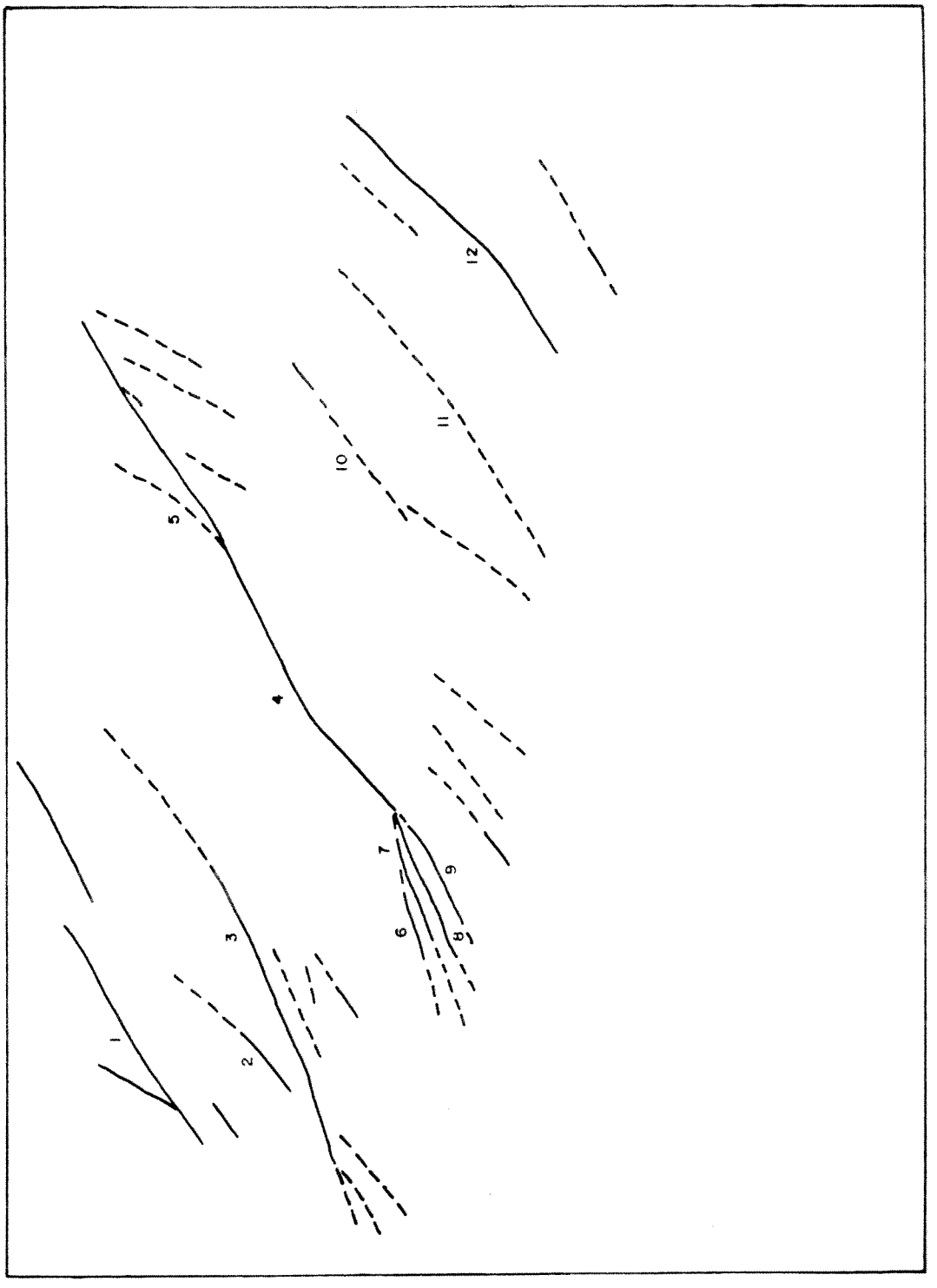

Figure 42.

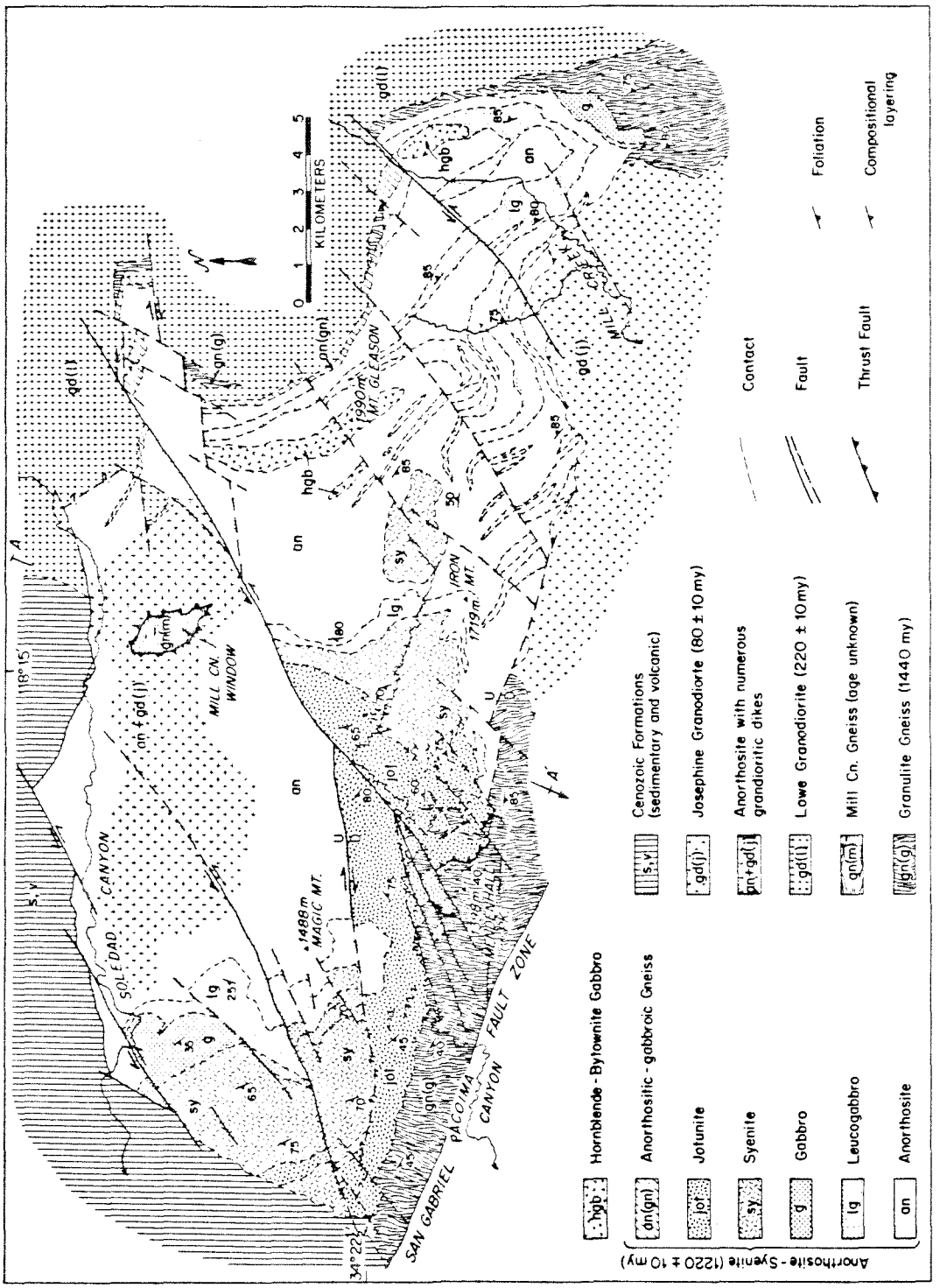
SIMPLIED GEOLOGIC MAP OF THE SAN GABRIEL ANORTHOSITE-SYENITE BODY,
LOS ANGELES COUNTY, CALIFORNIA
KILOMETERS
0 1 2 3 4 5
Hornblende - Bytownite Gabbro
Anorthosite - Syenite (1220 ± 10 my)
Anorthositic - gabbroic Gneiss
Jotunite
Syenite
Gabbro
Leucogabbro
Anorthosite
Cenozoic Formations (sedimentary and volcanic)
Josephine Granodiorite (80 ± 10 my)
Anorthosite with numerous granodioritic dikes
Lowe Granodiorite (220 ± 10 my)
Mill Cn. Gneiss (age unknown)
Granulite Gneiss (1440 my)
Contact
Fault
Thrust Fault
Foliation
Compositional layering
SOLEDAD CANYON
MILL CN. WINDOW
MAGIC MT.
1488m
IRON MT.
1719m
MT. GLEASON
1990m
MILL CREEK
SAN GABRIEL
PACOIMA
CANYON
FAULT ZONE
118° 15'
34° 22'

Figure 42.

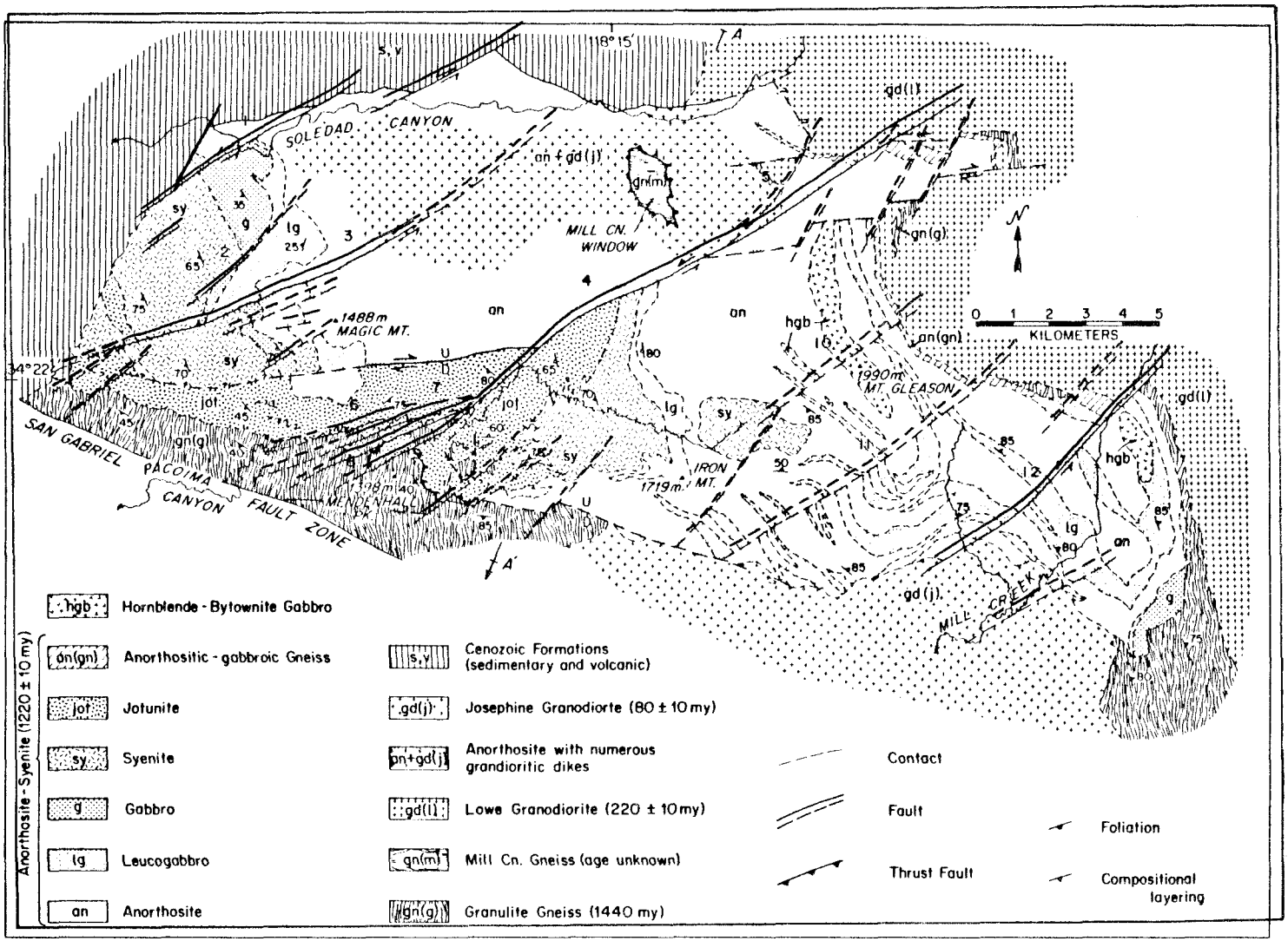

SIMPLIED GEOLOGIC MAP OF THE SAN GABRIEL ANORTHOSITE-SYENITE BODY, LOS ANGELES COUNTY, CALIFORNIA

Figure 42.

Figure 42.

Pole Canyon Fault

The Pole Canyon fault is exposed on either side of the mouth of Pole Canyon. It is particularly well-exposed about one kilometer east of Pole Canyon where it crosses Soledad Canyon and cuts through the highway tunnel and separates white anorthosite on the north from dark gabbroic rocks on the south. This fault is apparently concealed by alluvium in Soledad Canyon for about 3 kilometers east of the tunnel but beyond there it offsets the Soledad fault north of Soledad Canyon. West of Pole Canyon it separates syenite from conglomerate of the Mint Canyon formation. This fault dips about 60° to 75° S. and trends N 55° to 75° E.

The steeply-dipping contact between anorthosite and either gabbro or leucogabbro is offset about 1500 meters left-laterally across this fault and the low-angle Soledad fault has about 1800 meters of apparent left-lateral offset. These offsets suggest about 1500 meters left-lateral displacement and perhaps a few hundred meters of vertical displacement (south side up) on the Pole Canyon fault.

Oak Spring Canyon Fault

The Oak Spring Canyon fault is exposed in Oak Spring Canyon where it strikes N 45° E, dips 55° NW and separates syenite from gabbro. It was not located southeast of Rabbit Canyon and may merge with the Magic Mountain fault in Iron Canyon. Apparent right-lateral displacement of the steeply-dipping contacts between syenite and gabbro and between gabbro and leucogabbro is about 900 meters, although this contact probably makes a low angle to the fault so the true displacement is not certain. In Bear Canyon, about 3 kilometers to the northeast, the

shallow southwest-dipping, gradational contact between anorthosite and leucogabbro appears to be offset left-laterally about 300 meters. These differences in apparent offset could be explained by small left-lateral displacement and several hundred meters vertical displacement, south side up.

Magic Mountain Fault

The Magic Mountain fault is best exposed about 1.5 kilometers northwest of Magic Mountain where it juxtaposes anorthosite on the north against leucogabbro on the south. This fault is accurately located for about 9 kilometers between lower Sand and Bear Canyons and continues for about 8 kilometers farther east through pure anorthosite where it is only approximately located. This faults strikes between N 50° E and N 75° E and dips between 70° NW and 70° SE.

Three moderately to steeply dipping contacts northwest of Magic Mountain are offset left-laterally about 1200 meters and an anorthosite unit in lower Sand Canyon is similarly offset at least 900 meters by this fault. Vertical displacement along this fault is unknown, but might include a few hundred meters, south side up. A 3 kilometer fault parallel to and 600 meters south of the Magic Mountain fault north of Magic Mountain is part of the same fault system but shows about 370 meters apparent right-lateral offset of three contacts. However, these contacts dip at low angles to the west, and the same apparent offsets could be produced by about 250 meters of dip-slip displacement, south side up.

Transmission Line Fault

The Transmission Line fault bisects the anorthosite-syenite body and is the largest northeast-trending fault in the area, with about 5.5 kilometers of left-lateral displacement. It can be divided into two segments: (1) the central and northeastern part where most of the displacement occurs along a single break, and (2) the southwestern part in Pacoima Canyon where it breaks up into several closely spaced sub-parallel faults.

(1) The Transmission Line fault is a single break along most of its length between North Fork Saddle and Aliso Canyon. The actual fault plane was found only near North Fork Saddle in several places where it separates anorthosite from syenite. Between Arrastre and Aliso Canyons there is probably a single break which was located to within a few meters where it separates Mt. Lowe granodiorite from anorthosite. The middle 6.5 kilometers of this segment of the fault was only approximately located because of the presence of similar homogeneous anorthosite on either side of the fault.

Near North Fork Saddle, the fault dips 70° to 85° south, and it is also quite steep in Aliso Canyon. Its average strike is about N 60° E. The contact between anorthosite and Mt. Lowe granodiorite in Aliso Canyon shows about 1800 meters apparent left-lateral offset, but if the contact dips about 30 northeast, and a proposed 1100 meters total dip-slip displacement occurred, north side up, then about 3700 meters total left-lateral displacement is probable east of Arrastre Canyon. To the southwest, the Lonetree fault is offset left-laterally perhaps about 5200 meters, although the location of the intersection of its northeastern segment with the Transmission Line fault is uncertain.

If these estimates of displacement are correct, then the difference of about 1500 meters must be explained. The additional left-lateral displacement in the northeast may have occurred along several smaller faults sub-parallel to the Transmission Line fault. The Moody Canyon fault diverges toward the north-northeast and has about 900 meters apparent left-lateral offset, measured by offset of the northeastern anorthosite contact. However, this contact dips about 40° toward the northeast, so that dip-slip displacement on this fault could substantially change this figure. Southeast of the Transmission Line fault, two faults trending about N 30° E in upper Arrastre and lower Gleason Canyons show respectively about 450 meters and 600 meters apparent left-lateral offset of the steeply-dipping Lonetree fault. A third fault of similar trend east of Moody Canyon is postulated on the basis of the inferred location of the Lonetree fault west of Moody Canyon, and could have about 1100 meters apparent left-lateral offset. These four faults, as well as several smaller faults of similar trend and displacement are more than adequate to account for the smaller probable left-lateral offset observed on the main Transmission Line fault east of Arrastre Canyon.

Total left-lateral displacement on the Transmission Line fault is about 5200 meters near North Fork Saddle and is taken up in part by several related faults farther northeast. The presence of numerous granodioritic dikes intruded into anorthosite north of the Transmission Line fault, in contrast to the very few dikes south of the fault suggests possible large dip-slip displacement on this part of the fault, north side up. It is estimated that about 1100-1200 meters of dip-slip displacement occurred.

(2) Southwest of North Fork Saddle and especially southwest of the mouth of the South Fork of Pacoima Canyon, the Transmission Line fault breaks up into several branches, each taking up part of the total left-lateral displacement. Near the mouth of the South Fork, the main fault breaks up into at least four smaller faults with similar amounts of left-lateral displacement. These faults have more easterly trends, averaging about N 70° E and have dips of 70° to 90° in either direction. These faults could be traced through the Mendenhall gneiss only with difficulty and are approximately located southwest of the jotunite-gneiss contact.

The distribution of displacement over several faults and the change in trend occurs in proximity to the San Gabriel fault, the north branch of which is only about 1.5 kilometers south of and approximately parallel to Mendenhall Ridge. A similar splaying out of a related fault as it approaches the San Gabriel fault zone may occur on the Magic Mountain fault in lower Sand Canyon.

The Laurel Canyon fault is exposed near the mouth of Laurel Canyon and in Pacoima Canyon. The jotunite-Mendenhall gneiss contact shows about 1100 meters apparent left-lateral offset across this fault although comparable dip-slip displacement, north side up, could produce the same apparent offset.

The Gooseberry Canyon fault is exposed in Pacoima Canyon about 270 meters west, and also about 460 meters east of the mouth of Gooseberry Canyon. Apparent left-lateral offset of the jotunite-Mendenhall gneiss contact across this fault is about 460 meters. Possible small dip-slip displacement, south side up, is suggested by the presence of stratigraphically lower jotunite south of the fault in upper Laurel Canyon,

and would require somewhat greater actual left-lateral displacement. However, large topographic relief and the nature of the jotunite-gneiss contact, with large tabular bodies of each rock type in the other near the contact, make the argument for dip-slip displacement uncertain.

The Bad Canyon fault is exposed in Pacoima Canyon about 900 meters east of the mouth of Gooseberry Canyon. One, and possibly two jotunite-Mendenhall gneiss contacts are apparently offset about 1200 meters left-laterally across this fault. The magnitude and sense of possible dip-slip displacement is unknown.

The Mendenhall fault crosses the ridge about 450 meters north of Mendenhall Peak. Offsets of three jotunite-Mendenhall gneiss contacts of different attitudes, and of a Precambrian(?) thrust fault indicate about 1400 meters left-lateral, and about 250 meters north side up dip-slip displacement.

Three other faults farther southeast have similar trends and show a total of about 1200 meters apparent left-lateral displacement.

The four main breaks between Pacoima Canyon and Mendenhall Peak show a probable aggregate left-lateral displacement of about 4300 meters. The remaining 900 meters displacement measured on the Transmission Line fault farther northeast could be taken up along several smaller faults. At least one of these faults has significant north side up dip-slip displacement. Total vertical displacement of the jotunite-Mendenhall gneiss contact across lower Pacoima Canyon is probably at least 300 meters, north side up. Probably much of this displacement occurred along numerous small faults, some only a few meters apart, each with a few centimeters to a few meters of consistently north side up displacement. This type of distributed but consistent vertical

displacement can be seen in several places in Pacoima Canyon, especially where sub-horizontal mafic dikes cross large exposed faces.

Mt. Gleason Fault

The Mt. Gleason fault is exposed in upper Gleason Canyon 1.5 kilometers northeast of Mt. Gleason where it strikes N 60° E and dips 80° SE. It offsets the anorthosite-Mt. Lowe granodiorite contact about 90 meters right-laterally, although about 300 meters vertical displacement, south side down, would produce the same apparent offset. On the road west of Mt. Gleason, this fault is tentatively located as a zone of strong crushing. In Pacoima Canyon, 3 kilometers southwest of Mt. Gleason, this fault may offset the anorthosite-syenite contact a few hundred meters right-laterally. This fault could not be traced farther southwest, but another fault of similar trend probably offsets the anorthosite-syenite contact east of Indian Ben Saddle a few hundred meters left-laterally. This fault may continue south-west into Trail Canyon although it does not appear to offset the Slaughter Canyon fault.

Fox Creek Fault

The existence of this fault is inferred over a distance of more than 8 kilometers in anorthositic rocks south of Mt. Gleason. The straight 3 kilometer course of Fox Creek northeast of Condor Peak may be due to the presence of this fault. It probably offsets the contact between Mt. Lowe granodiorite and anorthosite about 300 meters left-laterally but apparently does not offset the Slaughter Canyon fault near Condor Peak.

Southeast of this fault, syenite is exposed at an elevation of 1580 meters on the ridge 3 kilometers south of Mt. Gleason. Syenite is not found at lower elevations and probably stratigraphically overlies the anorthosite as it does in the axis of the syncline across the fault 2.5 kilometers to the west. The axis of this syncline plunges at least 30° to the west, and if the small outcrop of syenite southwest of the fault is in normal stratigraphic sequence, then there must have been about 1200 meters dip-slip displacement on the Fox Creek fault, south side down, as well as about 600 meters of left-lateral displacement.

Mill Creek Fault

The Mill Creek fault was traced through anorthositic rocks for about 8 kilometers, from Fall Creek to upper Mill Creek. Its strike varies between N 45° E and N 65° E and it dips 80° NW in Middle Fork Mill Creek, the only place the fault plane was observed. The steeply dipping anorthosite-Mt. Lowe granodiorite contact is offset about 900 meters left-laterally, and the contact between anorthosite and Mt. Josephine granodiorite is offset about 1200 meters. Mendenhall gneiss forms a thin screen between anorthosite and Mt. Lowe granodiorite southeast of the fault but is absent northwest of the fault, which could suggest possible dip-slip displacement of a few thousand meters, north side up.

MILL CANYON STRUCTURE

Several types of gneissic rocks are exposed in the northern part of the area in and adjacent to Mill Canyon, some of them distinctly different from any other rocks observed in this study. These rocks

have been mapped by previous investigators (Jahns and Muehlberger, 1954, Jennings and Strand, 1969), but their unique significance was not recognized. Most of these rocks underlie a 2.5 X 1 kilometer area in one of the physiographically lowest parts of the anorthosite-syenite body. This exposure lies at the approximate intersection of the axis of the Mt. Gleason and Bear Canyon antiforms and thus occupies a structural high.

This study has demonstrated that these gneisses constitute several distinctive structural-lithologic units separated by sharp dislocation surfaces (Carter, 1971, Carter and Silver, 1972). Rocks exposed in Mill Canyon, in order from highest to lowest, include: (1) massive anorthosite cut by numerous granodioritic dikes, (2) lineated granodioritic gneiss, (3) gabbroic to anorthositic gneiss, and (4) layered amphibolitic gneiss (Plate V).

The gneisses in Mill Canyon are completely surrounded by massive anorthosite which is cross-cut by granodioritic dikes which resemble late Mesozoic(?) dikes elsewhere in the western San Gabriel Mountains. Exposures of these rocks are poor and the dike rocks are usually more resistant than anorthosite, so that usually all of the coarse float is granodiorite. Part of this material was previously mapped as granite (Jahns and Muehlberger, 1954, Oakeshott, 1958), but exposures suggest that about 20-35% of the rock is granodiorite and that the remainder is deeply weathered anorthosite. In this area, and elsewhere along Soledad Canyon, anorthosite has been affected by more severe fracturing, crushing and alteration than in the remainder of the anorthosite-syenite body.

Massive, lineated, granodioritic gneiss consists of quartz, plagioclase, potassium feldspar and a few percent biotite and muscovite. This is a catactastic rock which has a weak to strong liniation consisting of elongate rods of quartz-rich and feldspar-rich stringers which are sometimes paralleled by streaks of biotite. The edges of the quartz and feldspar grains are granulated and the entire rock displays a pronounced cataclastic fabric (Figure 43). Indistinct compositional layering is present in a few places.

Beneath the lineated granodioritic gneiss, a variety of layered gneissic rocks have compositions similar to anorthositic and gabbroic rocks of the anorthosite-syenite body. Most of these rocks are gabbroic, consisting of hornblende and plagioclase with smaller amounts of biotite, garnet, apatite and ilmenite. Cataclasis and recrystallization have strongly modified the original texture of this rock (Figure 44).

A few layers of anorthosite (1 to 20 meters) show the effects of extreme cataclasis and recrystallization along their margins but the largest have undeformed cores. Large boudin and weak mineral lineations are common in some parts of the gabbroic gneiss, but folds are much less conspicuous than in the underlying layered amphibolitic gneiss.

The Mill Canyon layered amphibolitic gneiss lies below all three of the previous lithologic units. It consists of alternating amphibolite and less abundant quartzo-feldspathic layers. Amphibolite consists of hornblende, plagioclase, and biotite with minor amounts of quartz, muscovite, potassium feldspar, epidote and chlorite. Quartzo-feldspathic layers consist of interlocking quartz, potassium feldspar and plagioclase with smaller amounts of biotite and hornblende. This rock was metamorphosed under amphibolite facies conditions. An early

Figure 43. Augen gneiss from the lineated granodiorite gneiss in Mill Canyon (crossed nicols, 7 x 11 mm. field).

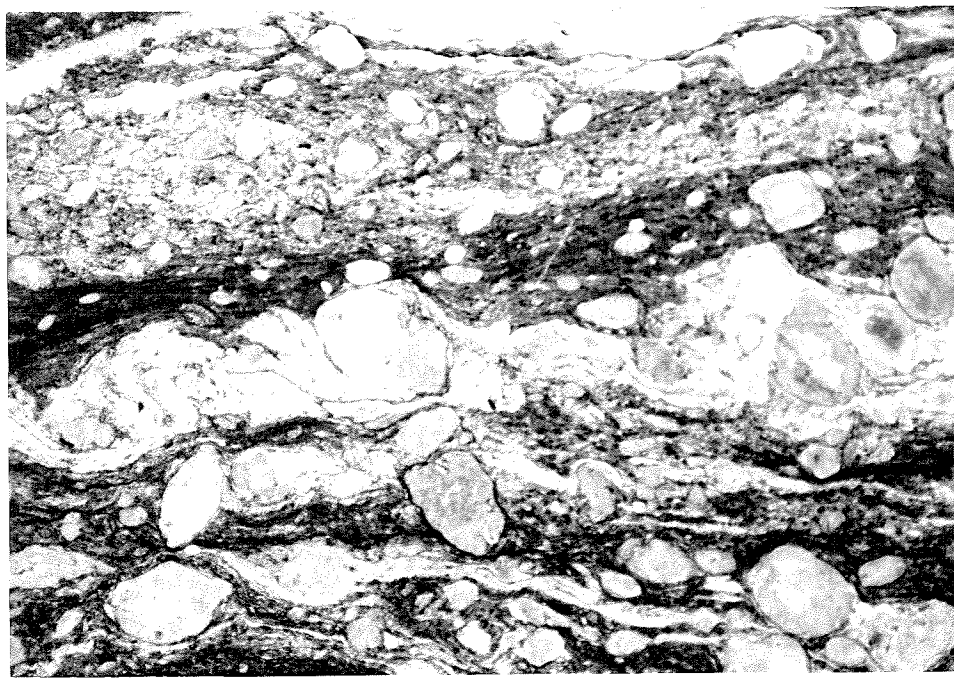

Figure 44. Gneiss from the Mill Canyon layered amphibolitic gneiss in Mill Canyon. Note that the augen appear to have been rolled during deformation (plane light, 7 x 11 mm. field).

generation of tight to isoclinal folds has been affected by a second generation of more open folds. The original metamorphic fabric has been modified by a superimposed cataclastic fabric which is usually less pronounced than that in the overlying granodioritic gneiss.

The massive anorthosite which surrounds the Mill Canyon structure is in fault contact with the three types of gneissic rocks. On the north, east and south sides, this is a low-angle fault surface which dips away from the gneiss at a low angle (Plate V). Abundant slickensides and a few mullion structures are present along this fault, and in most places the fault plane is underlain by 1 - 2 meters of fault breccia. This fault locally cross-cuts foliation and lineation in the underlying gneisses. Above the fault, anorthosite shows the effects of strong deformation which decreases in intensity over several tens of meters. Shearing, brecciation and fracturing are pronounced in anorthosite several hundred meters above the fault. These relationships demonstrate that the gneisses in Mill Canyon are exposed in a window and are separated from the overlying anorthosite by a major thrust fault. The western contact is a younger high-angle, probably dip-slip fault.

Within the window, the contact between the lineated granodioritic gneiss and the anorthositic to gabbroic gneiss is generally parallel to layering in the gabbroic gneiss, and anorthositic rocks along this contact appear to be more highly cataclasized than those farther from the contact. Several 1-4 meter lenses and irregular masses of anorthosite are surrounded by granodioritic gneiss several hundred meters from the contact east of Mill Canyon. These are interpreted to be xenoliths of anorthosite in granodiorite, both of which have been

affected by cataclastic deformation. A few granodioritic dikes cross-cut gabbroic gneiss and have also been affected by cataclasis. This contact is most reasonably interpreted as an original intrusive contact, of granodiorite with older anorthositic rocks, which has been modified by subsequent cataclastic deformaton. The magnitude of displacement along this contact during deformation is not known, but need not be large.

The contact between overlying granodioritic and anorthositic to gabbroic gneisses and underlying Mill Canyon layered amphibolitic gneiss is marked by strong deformation. Some catalastic rocks along this contact are mylonites. Well-developed lineation and boudin are found along this contact. Locally, it cross-cuts layering and foliation in the overlying granodioritic and anorthositic to gabbroic gneisses and in the underlying amphibolitic gneiss. These features suggest that significant low-angle displacement might have occurred along this contact, a suggestion which is supported by the fact that the underlying Mill Canyon amphibolitic gneiss does not resemble any other unit observed in this study.

Cross sections of the Mill Canyon exposure (Figure 45) show the observed and inferred relationships of the various lithologies. Indicated foliation orientations are based on measurements of representative orientations near the line of section. The fault and the underlying gneisses are exposed in Mattox Canyon about 0.5 kilometer west of Mill Canyon, and may be exposed about 1.5 kilometer east of Mill Canyon in upper Bootleggers Canyon.

Just west of Mattox Canyon an area of about 500 by 700 meters is underlain by strongly deformed gneisses. The gneisses are separated from

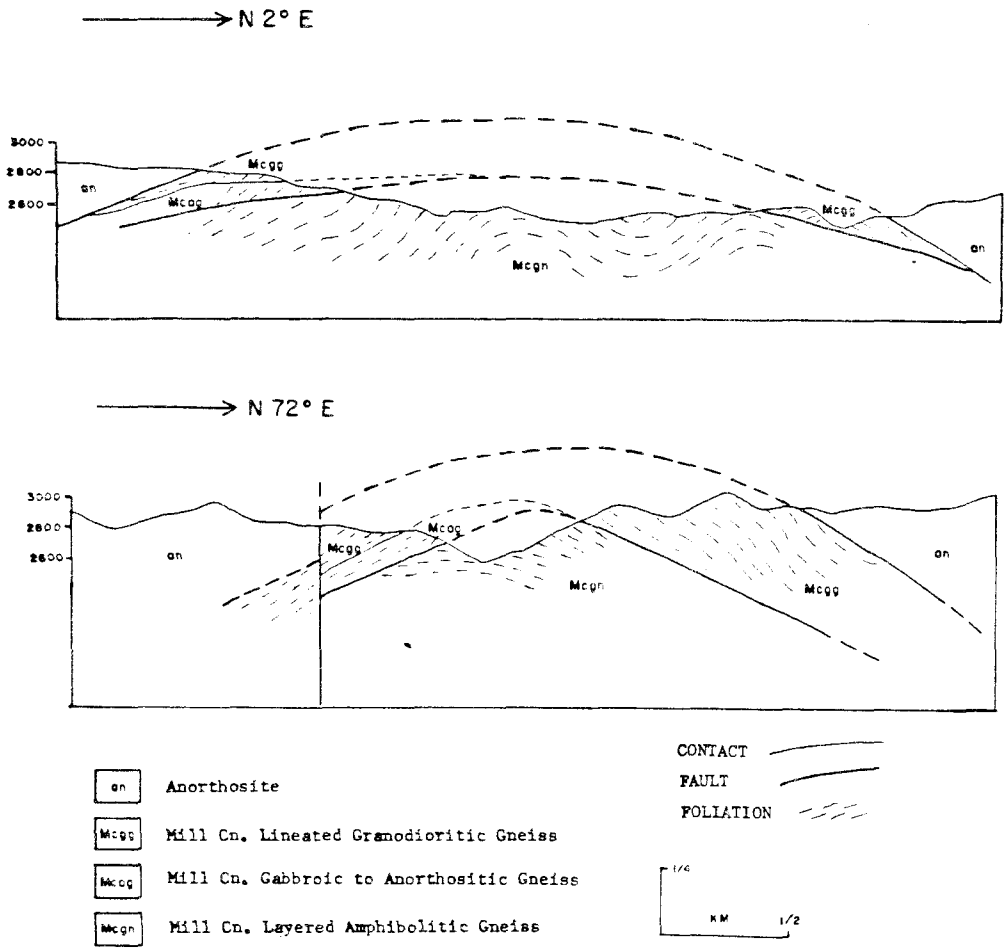

Figure 45 Geologic cross sections of the Mill Canyon structure. Foliations generalized after those measured near the lines of section.

overlying anorthosite by a contact which is nearly horizontal in part of the area. The eastern and western margins of the outcrop are bounded by high angle faults with north-northeast trends. The thrust contact could be located to within less than 1 meter in several places. Locally the fault cross-cuts foliation in the underlying gneiss, and within a few meters of the fault the underlying gneiss is brecciated and resembles the fault breccia in Mill Canyon.

Most of the gneisses in the Mattox Canyon window are lineated granodioritic gneiss. Mill Canyon layered amphibolite gneiss is exposed in a small area in the southeastern part of the window, in the inner part of a deep canyon where it probably underlies the granodioritic gneiss. Tight isoclinal folds are common in this rock. Highly cataclasized and recrystallized anorthositic and gabbroic gneisses are present in a very small area near the southern margin of the window.

A one-square-kilometer area between Bootleggers and Moody Canyons is also underlain by gneissic granodioritic rocks similar to those in Mill Canyon. This area is bounded on the southeast by a northeast trending high angle fault. The remaining contact between gneisses and surrounding anorthosite was located to within a few meters in a few places but its nature is uncertain. The similarity of the granodioritic gneiss in this area to those in Mill and Mattox Canyons and the fact that anorthosite completely surrounds the area suggests that this may be a third exposure of the thrust fault and underlying gneisses. If this is part of the same fault, then it must be steeply dipping on the south and southwest parts of the exposure. Poorly exposed lineated granodioritic gneiss is everywhere adjacent to the contact with surrounding anorthosite. Near its contact with anorthosite it commonly is strongly stained

with hematite and limonite but no fault breccia was found. A small 300 by 500 meter area surrounded by granodioritic gneiss consists of hornblende-biotite diroite with pronounced compositional layering on a scale of a few centimeters up to a meter or more. This resistant rock forms bold outcrops in which the layering and foliation is deformed by numerous folds 1 to 5 meters across with random axial orientations. Mineral foliation is usually parallel to layering, but cuts across layering in a few places, indicating that it is at least in part younger than the layering. This hornblende-biotite rock most closely resembles the Parker Mountain diorite part of the Mount Lowe granodiorite. In Bootleggers Canyon, the Parker Mountain diorite(?) was affected by post-emplacement deformation, which provided folds and crosscutting foliation, perhaps during the same thrusting episode which deformed the gneisses seen in the Mill Canyon and Mattox Canyon windows.

The designation "Mill Canyon thrust" is here applied to the low-angle structures exposed in Mill Canyon, including both the outer fault between the gneisses and overlying anorthosite, and the inner deformation zone between the Mill Canyon layered amphibolitic gneiss and the overlying grandioritic and gabbroic to anorthositic gneiss. Although the upper fault appears to cross-cut the lower deformation zone, they are sub-parallel and most likely are of similar age. If the granodioritic gneiss was produced by cataclasis of late Mesozoic(?) granodioritic rocks, then the age of thrust movement must be post-late Mesozoic(?), and it is probably pre-middle Miocene, based on the lack of evidence of major compression affecting rocks of that age in the Soledad basin.

Late Mesozoic(?) granodioritic rocks, anorthosite and related gabbroic rocks are all exposed in the plate overlying the Mill Canyon thrust within at most a few kilometers from Mill Canyon. Layered, folded amphibolitic gneiss resembling that exposed in Mill Canyon have not been observed anywhere else in the map area. The author is not personally acquainted with similar rocks anywhere in the central Transverse Ranges. It is probable, therefore, that the greatest magnitude of low-angle movement took place along the zone separating the Mill Canyon amphibolitic gneiss from the other gneisses in Mill Canyon rather than along the fault separating the gneisses from overlying anorthosite. The total magnitude of displacement is unknown, but could have been large. Preliminary observations of small-scale structures suggest that movement took place parallel to a line with a present northeast-southwest orientation.

It is evident that over an area of at least about 3 by 6 kilometers rocks of the anorthosite-syenite body are underlain by a tectonic floor. The evidence of strong cataclasis of rocks in Mill Canyon suggests that this tectonic floor may extend beneath a much greater part of the area. Pervasive fracturing, crushing and shearing of anorthosite along Soledad Canyon is more intense than in the rest of the body and extends for at least 6 kilometers west of the Mattox Canyon window. This may be due to proximity to the tectonic floor. It is possible that the entire anorthosite-syenite body is part of an allochthonous plate which may make up a large part of the San Gabriel Mountains. Similarities between the Mill Canyon thrust and the Vincent thrust in the eastern San Gabriel Mountains should be noted (Ehlig, 1958), although at present there is no concrete geologic evidence for correlation of the two thrust zones.

CHAPTER 4

FIELD PETROLOGY AND PETROGRAPHY

INTRODUCTION

This section describes the petrography of the rocks of the anorthosite-syenite body, the primary structures present in these rocks and inferences as to their origin. The field description and distribution of these rocks is included in Chapter 2 which includes the petrography of rocks other than those of the anorthosite-syenite body. Larger-scale structural features are described in Chapter 3.

The anorthosite-syenite body is divided into three stratigraphic units. In order from bottom to top of the body, determined from various structures as described previously, these units are: (a) the anorthosite-leucogabbro unit consisting of alternating layers of anorthosite, leucogabbro and norite, (b) the syenite unit consisting of a lower ultramafic syenite subunit and a normal syenite subunit, and (c) the jotunite unit, from the base upward consisting of the anorthosite block jotunite, the lower jotunite, the layered jotunite, the ultramafic jotunite and the upper jotunite subunits. The petrography and field petrology of the rocks will be described in the order listed.

ANORTHOSITE-LEUCOGABBRO UNIT

GENERAL

Rocks of this unit make up the greater part of the anorthosite-syenite body (perhaps as much as 70%) and form the lower part of the body. They range in composition from anorthosite to mafic gabbro. All gabbroic rocks show cyclic compositional layering on a scale of a few centimeters to a few meters. Nearly pure anorthosite makes up much of this unit, but in the southeast part of the body and toward the top of the unit, thick sequences of anorthosite alternate with thick sequences

of leucogabbro. A few masses of gabbro at the top of this unit are relatively thin except in the northwest where gabbro forms a thick sequence of layered rocks.

The cumulate rock terminology developed by Wager, Brown and Wadsworth (1960) is used in this section, although more general nomenclature is sometimes used because the above terminology requires interpretative textural conclusions not always warranted by the actual relationships seen. Rock names used are described in Chapter 2 and are ultimately based on the nomenclature developed by Goldschmidt (1916) to describe anorthosite and related rocks found in the Caledonian Mountains of Norway.

Nearly all of the rocks of this unit were apparently produced by bottom accumulation of crystals from a mgma of generally gabbroic composition. Tabular plagioclase crystals, 2-3 centimeters in diameter, are the only cumulate crystals in most of these rocks; ferromagnesian minerals in anorthosite and leucogabbro crystallized from the intercumulate magma. The upper rocks of this unit are more mafic, however, and pyroxene is probably a cumulate mineral in some parts of the gabbro in Pole Canyon. In anorthosite and most leucogabbro, primary cumulate textures have been extensively modified by postcumulous recrystallization, probably at near-solidus temperatures.

Outcrops show gradations from pure anorthosite with rare layers of leucogabbro (Figure 10) to compositionally layered leucogabbro (Figure 11) with only a few layers of anorthosite containing only slightly less than 10% ferromagnesian minerals. This gradation usually takes place over limited distances of a few tens to a few hundreds of meters and is the basis of the mapped anorthosite-leucogabbro contacts.

All of these cumulate rocks, including the almost pure anorthosite, probably crystallized under physical conditions similar to those which produced the cyclic compositional layering in the more gabbroic rocks. In the very plagioclase-rich rocks, any such layering was subsequently destroyed by postcumulous recrystallization which produced the massive unlayered anorthosite now observed.

There is very little compositional difference between plagioclase in anorthosite and that in adjacent leucogabbro (see Chapter 5). Anorthosite and leucogabbro probably accumulated under similar physical and chemical conditions and by similar mechanisms. The primary difference between them is whether or not minor amounts of pyroxene crystallized from the intercumulate magma. Crystallization of intercumulate pyroxene may have been controlled by rather minor shifts in conditions, so that the two rock types have the relationship of different igneous facies in a sequence of overall similarity. Anorthosite-leucogabbro contacts therefore may not represent time lines, although individual cyclic layers in an outcrop or in a limited area probably do very nearly represent time lines.

Unaltered pyroxene has not been observed in any rocks of the anorthosite-leucogabbro unit. In all of these rocks, primary pyroxene has been completely altered to fibrous aggregates of uralitic amphiboles. These uralite aggregates commonly display lamellar structures pseudomorphic alter original pyroxene exsolution lamellae, and commonly are oriented such that the original pyroxene cleavages can be determined.

ANORTHOSITE

Anorthosite consists of large anhedral crystals of calcic andesine, less than 10% other primary minerals and minor alteration minerals. Modes of several anorthosite specimens are given in Appendix A, although the typical anorthosite probably contains considerably more alteration minerals than do these specimens. Chemical analyses of two unusually fresh anorthosites and their calculated normative minerals are given in Chapter 5. One comes from near the top of the anorthosite-leucogabbro unit on Magic Mountain, and the other comes from near the bottom of the unit in Mill Creek, an estimated 4,500 meters stratigraphically below the top of the unit. Eight analyses of San Gabriel anorthosite reported by Oakeshott (1958) are also given in Chapter 5.

Anhedral, usually equant, andesine crystals in anorthosite average at least 3 to 6 centimeters in size but range up to two meters or more in extreme cases. The texture of the rock is typically inequigranular (Figure 46). Most plagioclase is calcic andesine with an average composition of about An_{45}; even the largest crystals show no evidence of compositional zonation. The composition of the plagioclase is similar through the entire anorthosite-leucogabbro unit: rocks stratigraphically as much as 6000 meters apart contain plagioclase of almost identical composition. A more complete description of plagioclase compositional variations is presented in Chapter 5.

Thin rims of some crystals are slightly more sodic (An_{30-40}). Small, commonly euhedral, inclusions of amphibole, apatite and oxide are present in many andesine crystals but do not define any obvious zonal patterns. Exsolution of extremely small potassium feldspar lamellae is observed in some plagioclase crystals, especially near their

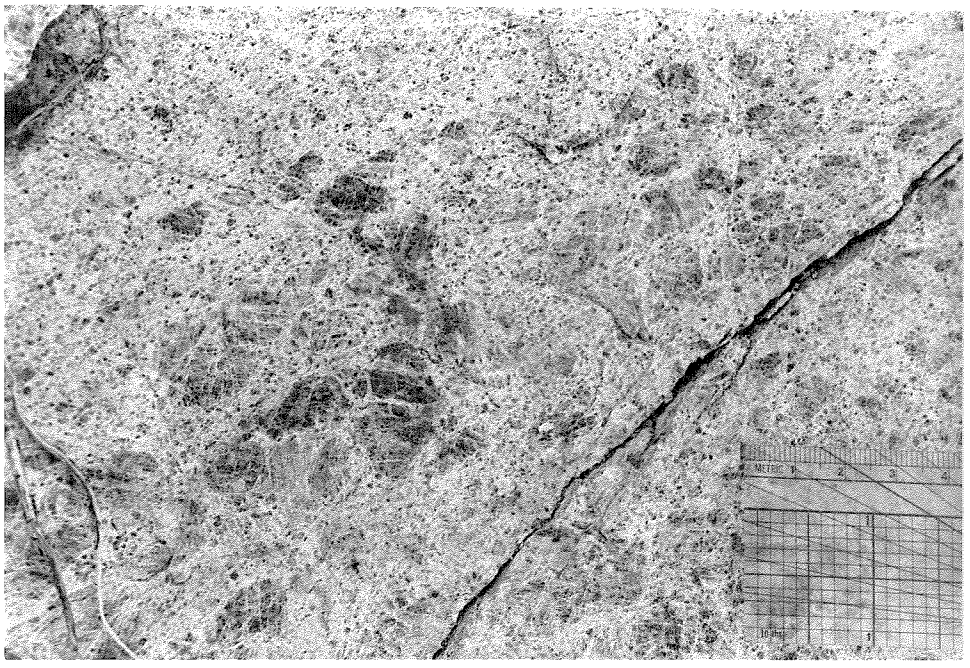

Figure 46. Anorthosite showing coarse andesine crystals (5 centimeters or greater) broken by numerous fractures. Alteration has accentuated the boundaries of the fragments and has produced an apparently much finer-grained rock in much of the exposure. Ridge east of Mill Creek about 1.5 kilometers south of Monte Cristo Creek.

margins. Andesine in anorthosite of the San Gabriel Mountains is probably much less antiperthitic than is andesine in anorthosite from many other massif anorthosites of otherwise similar composition (Anderson and Morin, 1969, Emslie, 1975).

Most andesine crystals show polysynthetic twinning according to both the albite and pericline laws but the twin lamellae are usually sparsely developed, in many instances wedge out towards the center of the crystal and vary greatly in width within the same crystal. Fractures, undulatory extinction, and partitioning of individual crystals into smaller domains of slightly different optical orientation is evidence of post-crystallization deformation which may have produced much of the twinning. In some instances polysynthetic twins are truncated by fractures and may have formed by strain deformation at the time of fracturing. Carlsbad twins are not present in plagioclase in anorthosite. Interstitial pyroxene(uralite) and ilmenite are present in small amounts in most anorthosite. Pyroxene(uralite) and ilmenite grains are usually less than about 1 centimeter in size and often are sub-ophitic in texture. Minute apatite crystals locally accompany ilmenite. Other primary minerals include trace amounts of spinel, garnet and zircon.

Late crystallized minerals include small equant 0.5-1.0 millimeter grains of quartz, albite and potassium feldspar (microcline or orthoclase) along boundaries between andesine crystals. These minerals are sometimes concentrated in the interstices between andesine crystals and less commonly are found along irregular cracks within them, indicating that fracturing occurred prior to crystallization of these minerals. Albite does not form rims on andesine crystals, which are essentially unzoned in most cases.

Deuteric alteration caused uralitization of original pyroxene and produced sericite, epidote and perhaps some amphibole and traces of other unidentified alteration products in the feldspar. Sericite and epidote commonly occur as very fine scattered grains evenly distributed throughout andesine crystals but are also sometimes present as concentrations of larger 0.5 to 1.0 millimeter grains between andesine crystals and along cracks within them. Leucoxene-sphene formed by alteration of primary ilmenite.

LEUCOGABBRO

Important primary minerals in leucogabbro were andesine and pyroxene with smaller amounts of ilmenite, apatite, and biotite. Modes of several specimens are given in Appendix A. The two main textural types are (1) ophitic leucogabbro and (2) non-ophitic leucogabbro.

Ophitic leucogabbro consists of a coarse-grained, inequigranular (2-15 centimeter or more) plagioclase matrix surrounding 5-25 centimeter pyroxene(uralite) crystals which ophitically enclose numerous 0.5-5 centimeter, usually tabular, plagioclase crystals which are often oriented parallel to compositional layering in the outcrop (Figures 47, 48, 49). Abundance of the pyroxene(uralite) crystals is variable. In extreme cases little or no plagioclase matrix is present, but in other cases as much as 90% of the rock is matrix. Pyroxene(uralite) crystals, although anhedral, are commonly slightly ellipsoidal parallel to compositional layering in the outcrop. Gradual increase and decrease of the abundance of the pyroxene(uralite) produces most of the compositional layering observed. Although the size of the pyroxene(uralite) crystals

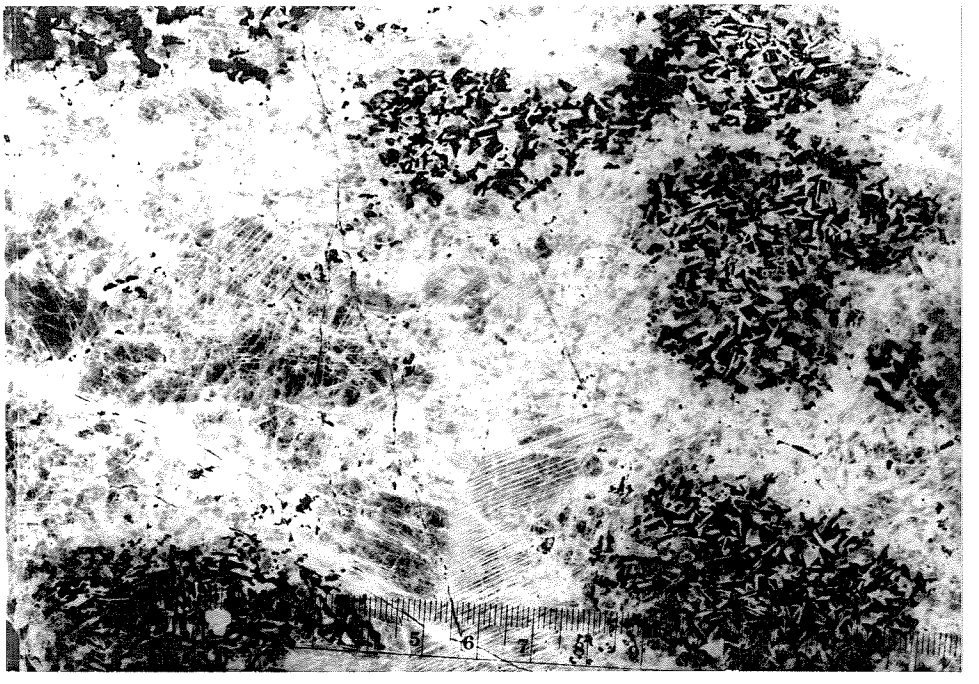

Figure 47. Ophitic leucogabbro (1055A), with well-preserved pseudomorphs of amphibole after large primary pyroxene crystals. The thin tabular plagioclase included in the pyroxene(now uralite) contrasts with the coarser anhedral plagioclase which surrounds the dark mineral aggregates. Scale is centimeters.

Figure 48. Part of a single large pyroxene crystal (now uralite) in ophitic leucogabbro from Mill Creek. The preferred orientation of plagioclase laths is much more pronounced than in most leucogabbro. Scale is centimeters.

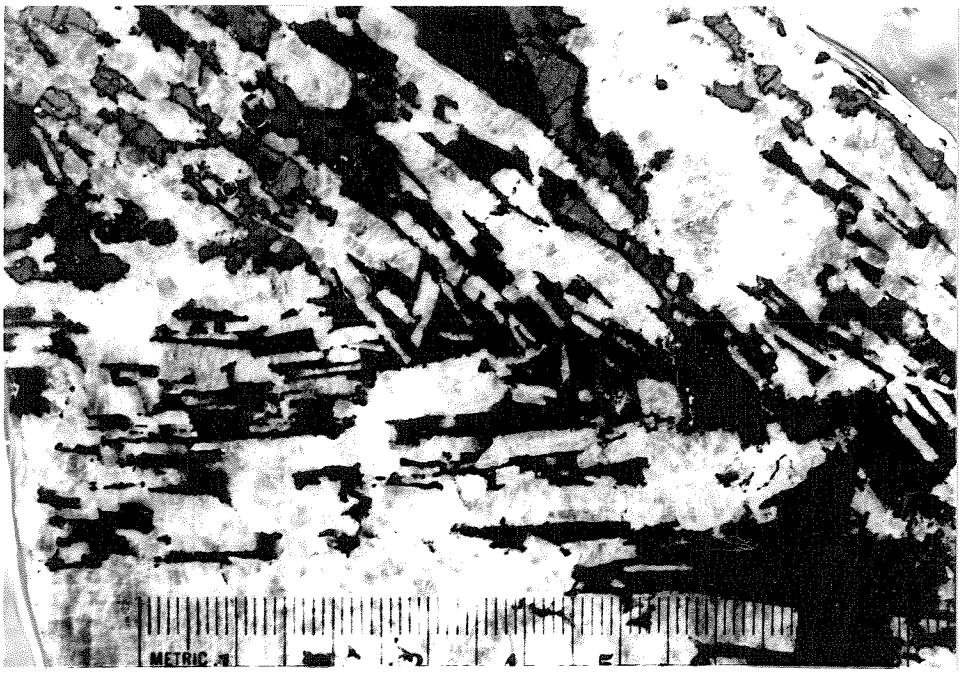

Figure 49. Part of a single large proxene crystal (now uralite) in orphitic leucogabbro from Mill Creek. Note the abrupt change in orientation of the included plagioclase laths in the upper half of the field and the presence of a single large crystal of ilmenite between the laths in the upper part of the field. Scale is in centimeters.

ranges from 3 to more than 25 centimeters, in any single outcrop they are all of similar size, usually varying by less than a factor of two. Plagioclase crystals in the matrix do not show any preferred orientation.

Non-ophitic leucogabbro shows little or no preferred mineral orientation and consists of subhedral to anhedral, equant 2-6 centimeter plagioclase crystals sub-ophitically enclosed by pyroxene (uralite) crystals of similar size (Figure 50). Leucogabbro of this type grades into anorthosite by decrease of the pyroxene(uralite) content, but with little change of size or shape of the plagioclase. Sub-ophitic pyroxene(uralite) crystals are commonly 2-4 centimeters and can reach 10-20 centimeters, and contain no included plagioclase laths.

Where non-ophitic leucogabbro is in contact with ophitic leucogabbro, it shows a well-defined contact with large ophitic pyroxene (uralite) crystals over only a few millimeters (Figure 51), but grades into the coarse plagioclase matrix over several centimeters by decrease of sub-ophitic pyroxene(uralite).

Most of the more leucocratic leucogabbro (10-25% ferromagnesian minerals) which is commonly associated with many anorthosite interlayers is of the ophitic type. As the color index of leucogabbro increases, it is more commonly the non-ophitic type. However, both types are present in many outcrops where the two types most commonly occur as irregular patches of either type within the other. In a few instances, however, 25 centimeters zones of non-ophitic leucogabbro appear to cut across the ophitic leucogabbro.

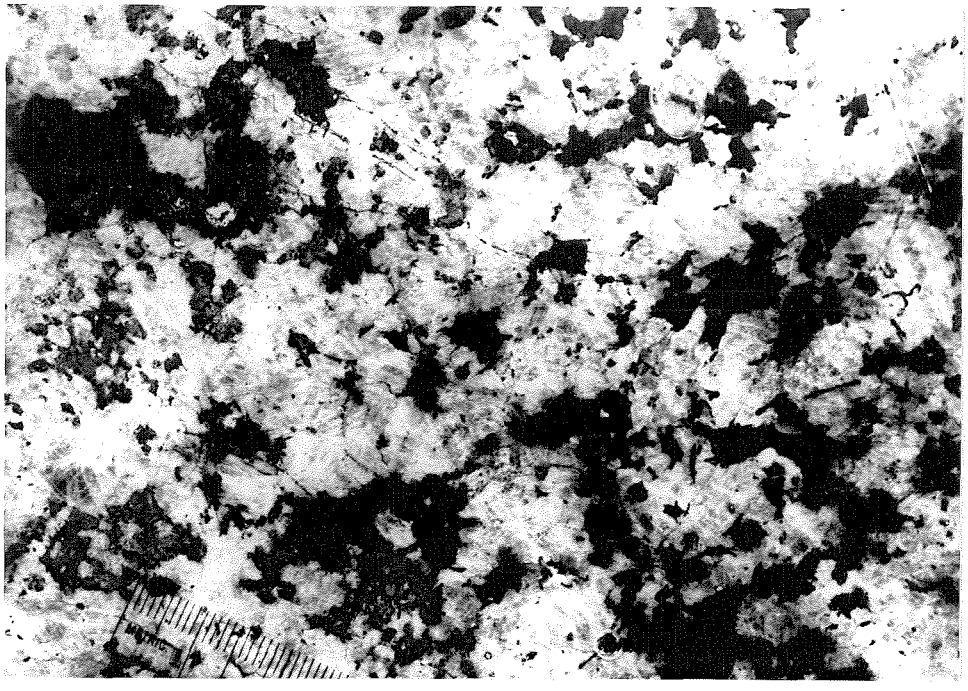

Figure 50. Non-ophitic leucogabbro (1055B) in which both plagioclase and pyroxene (now uralite) have been recrystallized. Scale is in centimeters.

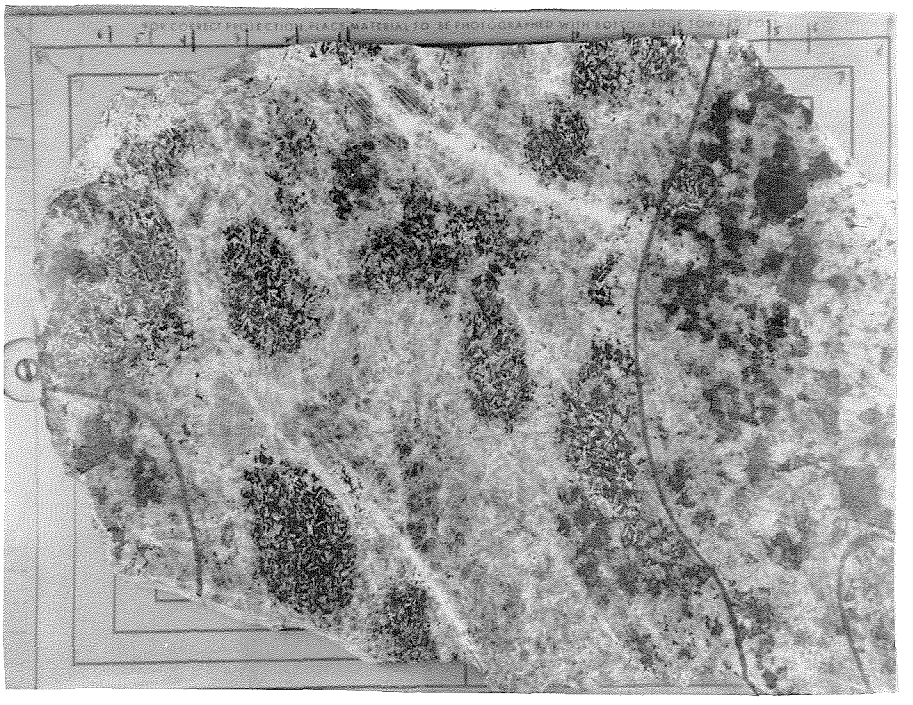

Figure 51. Ophitic leucogabbro (center) adjacent to non-ophitic leucogabbro. Approximate boundaries are marked. Both ophitic leucogabbro (1055A) and non-ophitic leucogabbro (1055B) have been chemically analyzed. (See Chapter 5). Top scale divisions are 16 millimeters apart. From the Middle Fork of Mill Creek.

The plagioclase in both rock types is calcic andesine (An_{40-50}) with very little compositional variation, either between different parts of a hand specimen or outcrop or between rocks from different parts of the body. The feldspar is usually unzoned; slight zonation of the margins of oriented tabular crystals might be present, but is almost always masked by alteration. The oriented tabular crystals are usually polysynthetically twinned according to the albite law, with individual twin lamellae that often extend the length of the crystal. Many of these tabular crystals also display carlsbad twin pairs. Plagioclase in the anorthosite matrix and in non-ophitic leucogabbro rarely if ever shows carlsbad twinning but is polysynthetically twinned according to the albite and pericline laws. These polysynthetic twins are similar to those in the anorthosite.

Uralite formed by alteration of original pyroxene which sub-ophitically overgrow large anhedral plagioclase crystals or ophitically enclose numerous small tabular plagioclase crystals. Relict pyroxene is extremely rare in leucogabbro, but pseudomorphic features indicate the existence of primary pyroxene. Relict pyroxene cleavage traces exist in many uralite pseudomorphs, and some show thin darker bands which are probably pseudomorphic after pyroxene exsolution lamellae (Figures 52,53). The textures of the uralite pseudomorphs resemble textures of unaltered pyroxene in gabbroic rocks of the jotunite unit. Similar-appearing uralitic alteration has strongly affected most rocks of the syenite and jotunite units but relict orthopyroxene is present in some of them. Relict hypersthene was not found in rocks of the anorthosite-leucogabbro unit, but is reported in these rocks by Oakeshott (1958) and Higgs (1954). One boulder of non-ophitic

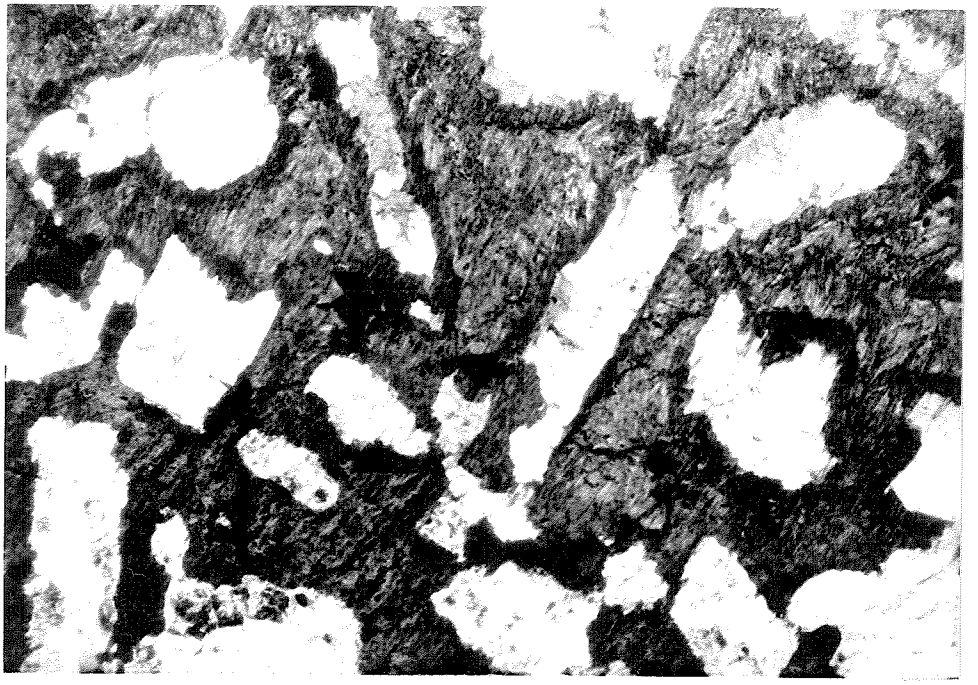

Figure 52. Cumulate plagioclase and intercumulate pyroxene (now uralite) in ophitic leucogabbro. Note the reaction rim, which is blue-green hornblende generally perpendicular to the contact between plagioclase and uralite. (plane light, 7 x 11 millimeter field).

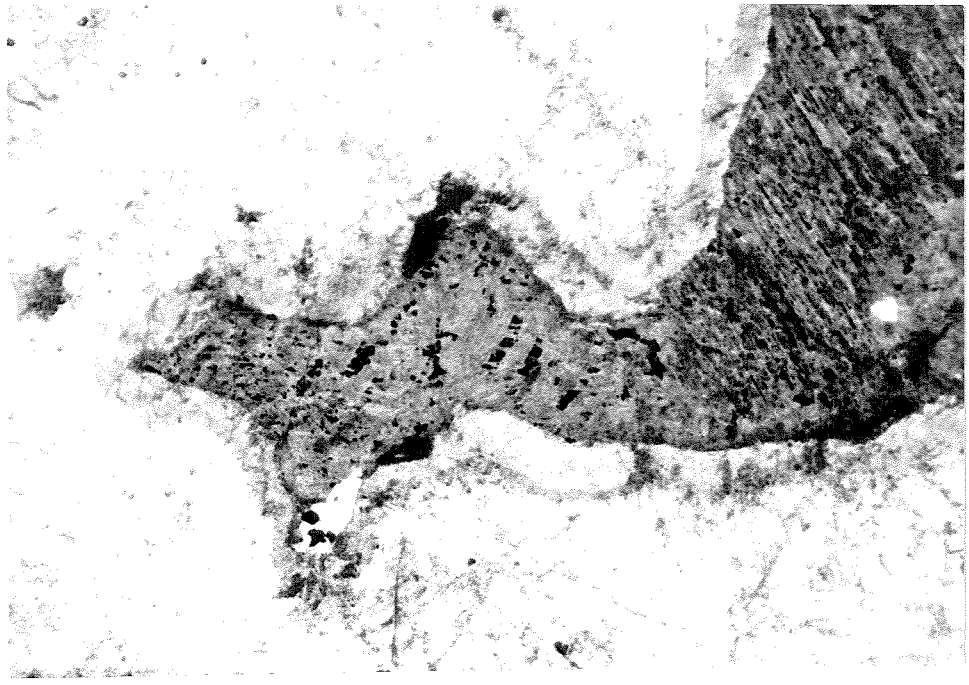

Figure 53. Relict lamellae, both coarse and fine, mostly defined by their greater abundance of opaques, in coarse uralite from non-ophitic leucogabbro, (plane light, 7 x 11 millimeter field).

leucogabbro from the Middle Fork of Mill Creek contains abundant unaltered clinopyroxene.

Most of the uralite in rocks of the anorthosite-leucogabbro unit was probably originally orthopyroxene, but part of it (10-20%) is darker and may be pseudomorphic after clinopyroxene. This second type of uralite is marginal to the lighter uralite, sometimes sub-ophitically rimming it, suggesting that it grew after the orthopyroxene(?). It is darker in color, mainly due to darker green hornblende and fine opaque inclusions and occurs as distinctly smaller areas (Figure 54). Distinct lamellar structures are not observed in this second uralite type, and it is sometimes spatially associated with late-crystallizing biotite, apatite and ilmenite. The grain size, shape and textural position of this uralite relative to that of the orthopyroxene(?) uralite is similar to the relationship of late-crystallizing clinopyroxene in unuralitized rocks containing predominantly orthopyroxene in the jotunite unit. The similarity in texture, lack of pseudomorphic lamellae and distinct difference in appearance from the normal uralite is the reason that this second uralite type is thought to have formed after original clinopyroxene.

A third, still darker, even more opaque-rich pseudomorph type is present in a few specimens (Figure 54) and may represent altered olivine, suggested by comparison with pseudomorphs containing relict olivine in rocks of the jotunite unit.

Ilmenite is present as small intergranular crystals in both major types of leucogabbro and also as larger, 2-10 centimeter crystals ophitically enclosing plagioclase tablets with a texture very similar to that of pyroxene(uralite) in ophitic leucogabbro (Figure 49).

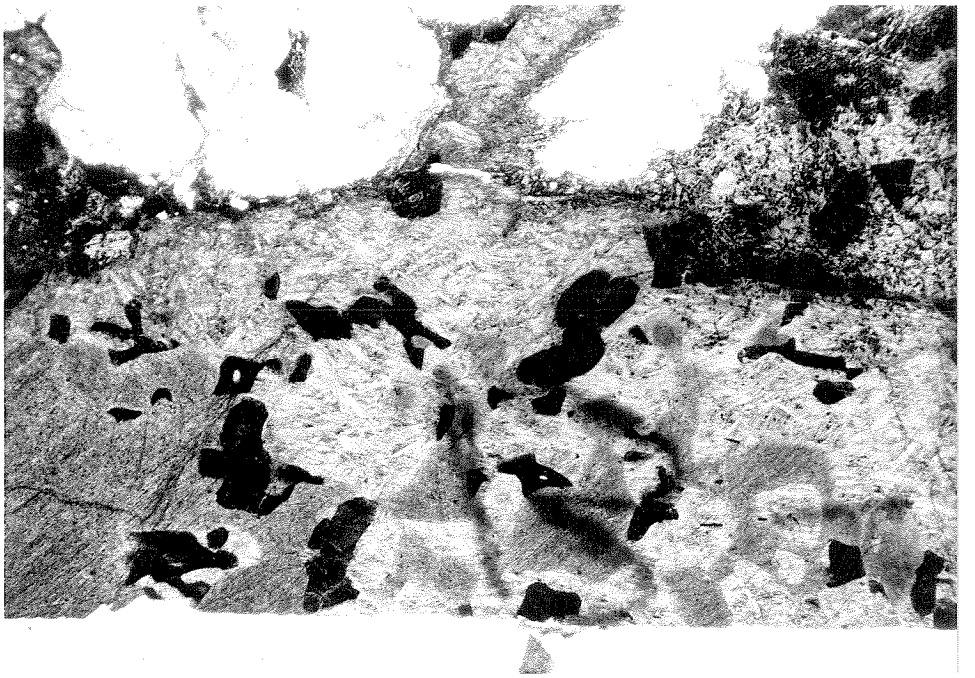

Figure 54. Ferromagnesian pseudomorph (uralite) in non-ophitic leucogabbro (1055B). Besides the thin rim of hornblende which grew around the original ferromagnesian mineral, three types of alteration can be distinguished: (1) coarse grained light grey material, (2) finer grained darker material, and (3) fine grained, very dark material. These three types of uralite may have formed by replacement of: (1) hypersthene, (2) augite and (3) olivine (plane light, 7 x 11 millimeter field).

Apatite is a late, intergranular mineral usually accompanying ilmenite. Small amounts of biotite, quartz, albite and potassium feldspar are intergranular late stage primary minerals.

Other than the uralitization of primary ferromagnesians, alteration of leucogabbro is similar to that observed in anorthosite, except that plagioclase has been extensively modified where it adjoins pyroxene (uralite). Altered plagioclase forms 0.1-0.5 millimeter rims on crystals and usually consists of many very fine-grained, fan-shaped, mymerkite-like intergrowths which abut the plagioclase-uralite contact and fan out into the plagioclase crystal (Figure 55,56). The mineralogy of these rims is unknown; some of it has an index of refraction distinctly lower than that of andesine, but the refractive index and birefringence of some of it resembles that of an epidote mineral. Similar alteration is present along all andesine-uralite contacts in all the leucogabbro examined.

Fine grains of epidote, sericite and muscovite, chlorite and hornblende are scattered through most andesine crystals. They were produced by deuteric and hydrothermal alteration similar to that observed in anorthosite, but they are considerably more abundant, due to the more mafic composition of the rock.

The average composition of leucogabbro was estimated in the field, and point counts were made on several scales. Point counts on single thin sections, on slabs with 2 and 5 millimeter grids, and on one road cut with a 30 centimeter grid along the lower 1.5 meters of the exposure are given in Appendix A. This latter point count may be most representative of the modal composition of leucogabbro in this unit.

Figure 55. Fine-grained reaction rim between plagioclase and uralite in ophitic leucogabbro (1055A, crossed nicols, 2.06 x 3.19 mm field).

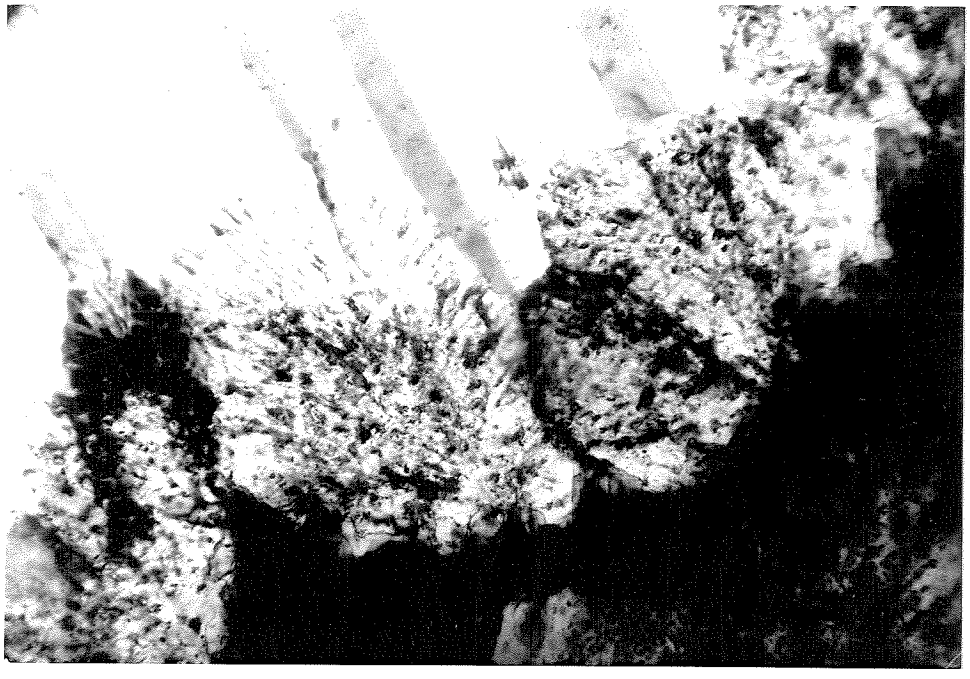

Figure 56. Detail of Figure 55 showing the fine-grained, fan-shaped, mymerkite-like intergrowths of unknown mineral in plagioclase adjacent to the contact with uralite (1055A, crossed nicols, 0.50 x 0.76 millimeter field).

Nearly all leucogabbro is compositionally layered on a scale of a few centimeters to a few meters. Individual mafic layers usually do not contain more than about 25-35% ferromagnesian minerals, but alternate with other layers which may contain about 10-15% ferromagnesian minerals or less. The average ferromagnesian content of leucogabbro is about 20±5%, but all intermediate color index values to anorthosite can be found. Textures are similar in the compositionally different layers. Contacts between layers are moderately sharp to gradational, and are nearly always planar and parallel to each other. No evidence of either size or density grading is seen in these layers. Thirty centimeter to two meter related dikes, mostly mafic gabbro or ultramafite, are present in many outcrops and generally are subparallel to the layering. Post-emplacement shearing and alteration commonly has obscured primary structure in leucogabbro, especially the preferred orientation of plagioclase crystals. Less commonly, leucogabbro is massive and nearly homogeneous with only faint compositional layering. This is more characteristic of the more mafic leucogabbro and gabbro.

Coarse layers and lenses consisting of crystals up to a meter or more in major dimension are present in some leucogabbro exposures, especially in the southeast part of the body. These layers are usually 30-100 centimeters thick and 1-100 meters long, lensoid to tabular, and are approximately parallel to the normal compositional layering. They consist of coarse anorthosite cores commonly surrounded by a discontinuous rim of equally coarse pyroxene(uralite) and locally ilmenite. Most of these layers are asymmetric, with most of the marginal ferromagnesian minerals on one side of the coarse anorthosite. In a few of

these bodies the coarse plagioclase crystals are oriented perpendicular to the layering and have the appearance of having grown from a solid substratum into adjacent magma. These layers are interpreted to represent crescumulate growth on the floor of the magma chamber (Figure 24). In the southeastern part of the body, many of the coarse layers show the plagioclase-pyroxene(uralite) asymmetry to some degree and always in the same sense.

A few of these layers along Mill Creek exhibit distinctive forms not observed elsewhere in the body. The most striking are several large wedge-shaped bodies of extremely coarse anorthosite seen in road-cuts near Mill Creek Campground. In cross section they are situated with their bases along coarse anorthosite layers and with points which extend outward and crosscut adjacent leucogabbro layers (Figures 32, 33, 34). Coarse pyroxene(uralite) crystals are present mainly along the wedge-side of the layer at its base and are usually more abundant along the edge of the wedge than the other. All of these wedge-shaped bodies point in the same direction, and adjacent crescumulate layers indicate that this direction was originally up. A few similar wedge-shaped bodies are poorly exposed about 1.5 kilometers to the southeast. These anorthosite wedges may have originated by the injection of fine-grained plagioclase crystal mush upward into overlying leucogabbro crystal mush. The origin of these structures is illustrated in Figure 35.

GABBRO

Gabbro contains plagioclase(andesine) and 35-65% ferromagnesian minerals, most of which were probably originally orthopyroxene, now altered to uralite. Some of the darker uralitic pseudomorphs may

represent altered clinopyroxene or even olivine although no relics of any primary ferromagnesians have been observed. Ilmenite and apatite are common primary minerals, and biotite and some hornblende may be in part primary. Quartz, biotite, hornblende and other amphiboles, epidote and chlorite are products of alteration of the primary ferromagnesians, and epidote and sericite were produced by alteration of the andesine.

Gabbro consists of coarse (2-10 millimeter) subhedral to anhedral andesine and uralitized aggregates of ferromagnesian minerals with interstitial ilmenite, apatite and sometimes biotite and hornblende. Elongate plagioclase crystals display a slight preferred orientation parallel to compositional layering in some leucocratic layers, but this does not appear to be a general characteristic of most gabbro. As in parts of the leucogabbro, the ferromagnesian minerals sub-ophitically enclose andesine.

Alteration of the ferromagnesian minerals in gabbro has been as pervasive as in leucogabbro, and has produced even more abundant alteration minerals. Fracturing and brecciation is similar to that in anorthosite but is less obvious because of the smaller amount of plagioclase. Polysynthetic twinning (albite and pericline) of plagioclase resembles that in anorthosite.

Uralite pseudomorphs are rimmed by a 0.05-0.5 millimeter layer of radially-oriented fibrous blue-green hornblende, which in turn is sometimes surrounded by an external rim of granular epidote. In the core of the pseudomorph, the original mineral is altered to a fine-grained aggregate of fibrous amphiboles and granular epidote, opaque and quartz, and sometimes includes small amounts of biotite, chlorite, and

plagioclase. Pseudomorphs after clinopyroxene lamellae(?) in orthopyroxene(?) are not so common as in leucogabbro or jotunite, and both biotite and quartz are much more common, especially in the Pole Canyon area.

Near its contact with syenite, gabbro contains plagioclase which has a mottled appearance. This plagioclase appears to be more sodic (An_{25-40}) and is made up of very irregularly intergrown domains. Crystals in some of these rocks seem to have irregular 0.01-0.5 millimeter 'bleached' patches whose nature is not otherwise known. Twinning is scarce or absent in this plagioclase. Alteration is pervasive in rocks containing this mottled feldspar, even more so than in gabbro away from the syenite contact, and both quartz and biotite produced by alteration are unusually abundant. The normative feldspar of the one analyzed rock of this type (1032) is Ab_{70} An_{20} Or_{10}, more albite-rich than any other analyzed rock of the anorthosite-syenite body. Although the reasons for these features are not understood, it appears to be related to their proximity to the syenite unit.

Gabbro is compositionally layered, with 2 centimeter to 3 meter layers of alternating ferromagnesian-rich and ferromagnesian-poor rock with gradational contacts. In Pole Canyon this primary compositional layering persists for distances up to 60 meters or more. Compositional layering is less well developed in coarser-grained gabbro in Big Tujunga Canyon. In some areas, especially in Big Tujunga Canyon, numerous mafic gabbro to ultramafite dikes intrude gabbro, usually sub-parallel to the layering. Asymmetric coarse lenses and layers similar to those present in leucogabbro have not been observed in gabbro, but a few examples of plagioclase crystals perpendicular to compositional layering have

been observed in gabbro. The apparent absence of asymmetric layers may be because the mafic adjacent layers mask the ferromagnesian-rich part of any asymmetric layers present. In one outcrop in Lynx Gulch, branching Willow Lake-type plagioclase crystals are present in gabbro (Figure 25).

Some of the more mafic gabbro east of lower Pole Canyon shows poorly developed compositional layering and contains numerous large angular blocks of anorthosite. The rocks of this area resemble those of the ultramafic syenite and the anorthosite block jotunite subunits which lie stratigraphically higher in the body. Due to poor exposures, these rocks were not studied in the same detail as some of the similar rocks higher in the sequence in the Buck Canyon synform. It is probable that all of these rocks were formed in a similar manner, but at different times.

POSTCUMULOUS RECRYSTALLIZATION OF ANORTHOSITE AND LEUCOGABBRO

All anorthosite and nearly all leucogabbro of this unit have been strongly affected by postcumulous recrystallization which has pervasively modified the original textures and finer-scale structures of these rocks. Understanding the nature of the recrystallization is important to understanding the anorthosite-syenite body and so this interpretative discussion is included here, following the mineralogical and textural descriptions of the rocks. Figure 57 illustrates the proposed sequence of textural development which produced the present textures of anorthosite and leucogabbro.

All anorthosite and leucogabbro formed by the bottom accumulation of 0.5 to 3 centimeter andesine laths (the only exceptions are the

crescumulate layers). Most andesine crystals probably were about 1 centimeter long and were tabular parallel to the (010) plane. These laths accumulated on the floor of the magma chamber to form a loose unconsolidated crystal mush in which the laths commonly (but not always) had a preferred orientation parallel to the floor (Figure 57a).

The crystal mush slowly completed its crystallization by either the adcumulous or the heteradcumulous processes (Wager, Brown and Wadsworth, 1960) such that the intercumulate magma crystallized while remaining in continuous diffussive equilibrium with the overlying magma. Anorthosite resulted when andesine alone crystallized from the intercumulate magma by the adcumulous process. Intercumulate andesine had the same composition as cumulate andesine because intercumulate magma remained in diffusive equilibrium with the large reservoir of overlying magma. Intercumulate andesine overgrew primary cumulate andesine to fill in all the pore space to produce an essentially pure andesine rock (except for minor ferromagnesian minerals crystallized from trapped residual intercumulate magma) made up of 1-3 centimeter unzoned andesine crystals probably with a preferred orientation (Figure 56b).

Leucogabbro resulted when pyroxene nucleated in the intercumulate magma so that both andesine and pyroxene crystallized from the intercumulate magma by the heteradcumulous process. Intercumulate andesine had the same composition as primary cumulate andesine because of diffussive equilibrium between intercumulate magma and the overlying magam. Intercumulate pyroxene grew from widely-spaced nuclei to form large crystals ophitically enclosing numerous cumulate andesine laths. Elsewhere andesine crystallized to completely fill in the intercumulate pore space and produced a locally pure andesine rock surrounding the

Figure 57. Sequence of textural development during accumulation, intercumulate crystallization and postcumulous recrystallization of anorthosite and leucogabbro. (a) Plagioclase crystals tabular parallel to the (010) plane accumulated on a sub-horizontal floor, usually with at least a slight preferred orientation. Anorthosite resulted when (b) intercumulate magma crystallized plagioclase by the adcumulous process, and (c) postcumulous recrystallization produced very coarse, inequigranular textures. Ophitic leucogabbro resulted when: (d) intercumulate magma crystallized both plagioclase and pyroxene by the heteradcumulate process, and (e) postcumulous recrystallization produced coarse anorthosite matrix between large ophitic pyroxene crystals. Non-ophitic leucogabbro resulted when: (f) further post recrystallization affected both plagioclase and pyroxene. (g) Subsequent to recrystallization, fluids circulating along fractures caused limited introduction of ferromagnesian minerals and alteration of plagioclase.

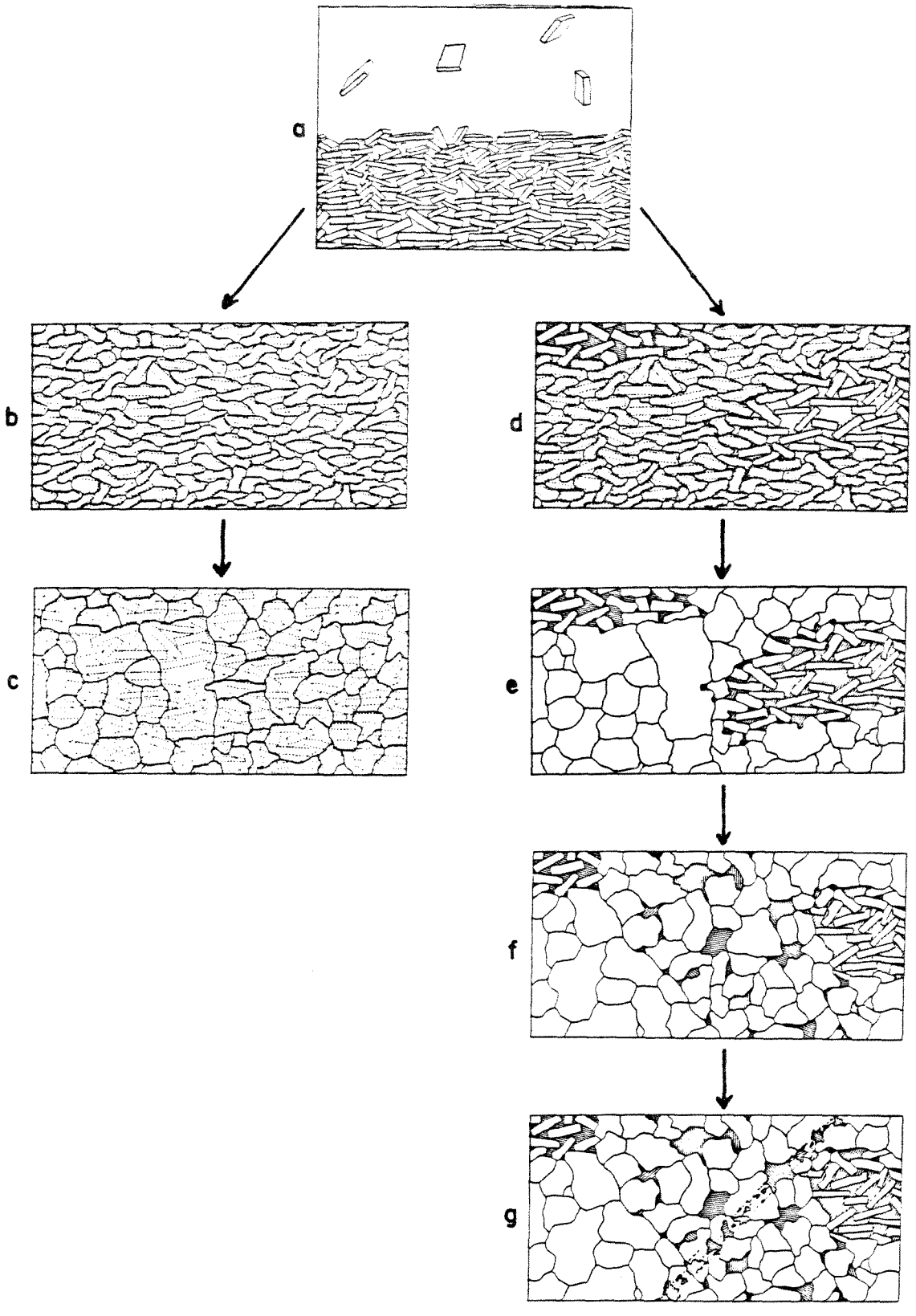

Figure 57.

large pyroxene crystals (Figure 57d). Leucogabbro probably formed most readily when the magma was closest to the plagioclase-pyroxene cotectic. However, slower rates of diffusion might also have favored formation of leucogabbro.

These rocks apparently remained at high temperatures for a long period of time as more cumulate rocks formed above them and very little heat was lost downward into the hot, previously accumulated rocks. During this extended period of elevated temperature, postcumulous recrystallization affected all the pure andesine rocks. In pure anorthosite as well as the anorthosite matrix of leucogabbro, a few andesine nuclei began to grow at the expense of the others until the rock consisted of a few much larger crystals commonly 10 to 25 centimeters in size but sometimes much larger (to about 150 centimeters). The process is conceived to have been similar to that by which numerous minute aragonite and calcite crystals in a carbonate sediment diagenetically recrystallize to form the much larger calcite crystals of micrite. Figure 57c shows the resultant anorthosite in which the large andesine crystals show no dimensional preferred orientation and have no compositional zonation (dashed lines outline the original cumulate laths and do not represent compositional differences). Figure 57c shows the resultant leucogabbro consisting of large ophitic pyroxene crystals surrounded by a matrix of coarse, unzoned, randomly oriented andesine crystals. The only cumulate andesine laths remaining are those enclosed in pyroxene and apparently protected by their host from the recrystallization process (Figure 47). There is only one observed example of a primary cumulate andesine lath partially enclosed in pyroxene(uralite) which has only partially recrystallized to a new

orientation where it was in contact with plagioclase in the anorthosite matrix surrounding its mantling pyroxene(uralite) (Figure 58).

In some instances leucogabbro underwent further recrystallization which affected the pyroxene as well as andesine. This affected rocks generally rich in pyroxene (average about 25%) and may have been facilitated by the presence of more fluids in these rocks. In parts of the rock the andesine and pyroxene together recrystallized to form a more granoblastic texture consisting of equidimensional equant andesine crystals subophitically surrounded by anhedral pyroxene crystals of similar size (Figure 57f). A single outcrop may contain both ophitic leucogabbro with a few cumulate andesine laths and totally recrystallized non-ophitic leucogabbro (Figure 51). Gabbro is the only rock of this unit which has not undergone postcumulous recrystallization. Most gabbro formed by bottom accumulation of both pyroxene and andesine and probably completed its crystallization by the heteradcumulous process. The resultant rock apparently contained sufficient amounts of pyroxene which separated the andesine crystals so that recrystallization never became an important process.

Deuteric alteration, especially along fractures, produced white alteration of andesine and sometimes introduced secondary ferromagnesian minerals (Figure 57g).

Following primary bottom accumulation, intercumulate crystallization and postcumulous recrystallization, all the rocks of this unit were affected by the pervasive alteration which produced uralite pseudomorphs after the original ferromagnesians in all of the rocks.

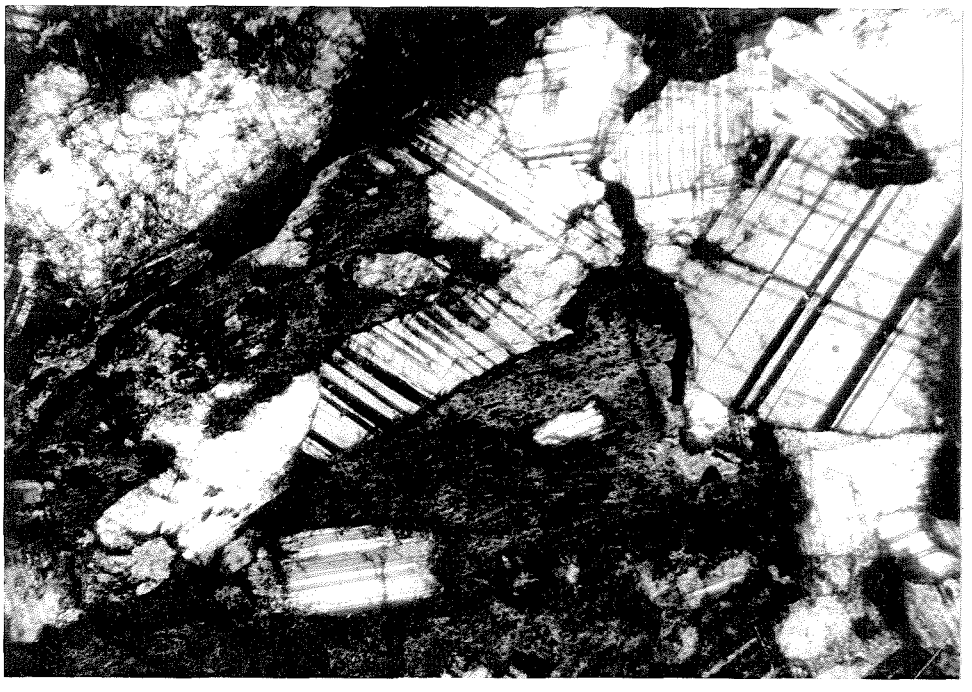

Figure 58. Tabular cumulate plagioclase crystal (left and center) near the margin of intercumulate-crystallized pyroxene (now uralite) in ophitic leucogabbro. Recrystallized granoblastic-texture anorthosite is present in the upper right corner. Part of the original cumulate plagioclase has been recrystallized to the same optic orientation as that of one of the granoblastic crystals external to the ophitic pyroxene (now uralite) (1055A, crossed nicols, 7 x 11 millimeter field).

SYENITE UNIT

The syenite unit is extremely variable in thickness, probably due to the shape of the magma chamber at the time of its emplacement and crystallization. The syenite sequence in the Buck Canyon synform contains several thick interlayers of more mafic layered rocks of mangerite or jotunite composition. The thicker syenite sequence in Iron and Rabbit Canyons, west of Magic Mountain, is more homogeneous and contains only a few mafic layers (except for later crosscutting gabbroic rocks), nearly all of which are near its base. This suggests some difference in either magma composition or crystallization conditions between the two areas. In the Buck Canyon synform, syenite is interlayered with the overlying jotunite over stratigraphic intervals of about 2000 meters (cross sections E-E' and F-F', Plate II). The interlayering does not appear to be intrusive, and may indicate variations in composition and/or crystallization conditions within the chamber. The basal part of this unit consistently contains more mafic and even ultramafic rocks in the Buck Canyon synform. The syenite unit has been subdivided into the lower ultramafic syenite subunit which occurs in the Buck Canyon synform and in a small area south of Magic Mountain, and the overlying normal syenite subunit.

ULTRAMAFIC SYENITE SUBUNIT

The basal part of the syenite unit in Buck Canyon synform is strongly compositionally layered with abundant mafic layers which commonly show mineral grading suggesting that they were formed by bottom accumulation. Layering in these rocks is parallel to their basal contact with the anorthosite-leucogabbro unit, and suggests

that at least some, if not all, the syenite suite formed under conditions favorable for gravity accumulation. Thus primary layering observed in syenite is generally concordant with layering in the underlying and overlying units and was probably originally sub-horizontal. West of Magic Mountain, where syenite is in contact with gabbroic rocks of the anorthosite-leucogabbro unit, there are fewer ultramafic rocks along the basal contact but the underlying gabbroic rocks are more mafic than those in the Buck Canyon synform. On the south flank of Magic Mountain, there is about 500-600 meters of anorthosite breccia in a matrix of gabbroic rocks (shown as leuco-gabbro on Plate I) which may be equivalent to the ultramafic syenite subunit.

The most abundant rocks of the ultramafic syenite subunit are gabbro and ferrogabbro with smaller amounts of ultramafite and leuco-gabbro. The ferromagnesian minerals are usually completely altered but probably consisted mainly of pyroxene but with a little olivine in some rocks. A few rocks contain unaltered augite, hypersthene and iron-rich olivine (see Chapter 5). Apatite and ilmenite are major constituents of many of the more mafic rocks. Biotite and hornblende crystals were produced by the pervasive alteration, which also produced fibrous amphiboles, chlorite and epidote. These mafic rocks contain variable amounts of feldspar (usually 5-50%) which is either plagioclase (andesine), oligoclase to andesine antiperthite or mesoperthite. There is no apparent correlation between feldspar composition and either color index or vertical position within the ultramafic syenite subunit.

Large angular 0.5-30 meter fragmented blocks of other rock types are common in the ultramafic syenite subunit. The most abundant blocks

are anorthosite, but both leucogabbro and syenite blocks are also present. Mineral graded layers are common in the more mafic matrix between the blocks, and these layers sometimes drape over the angular blocks (Figure 28).

NORMAL SYENITE SUBUNIT

This subunit consists almost entirely of uniform unlayered equigranular syenite consisting of equant (1-3 millimeter) crystals of feldspar and altered ferromagnesian minerals. This subunit varies in thickness from a few tens of meters near North Fork Saddle to a minimum of 3500 meters west of Magic Mountain. It is probably the most homogeneous of all the subunits, but small amounts of leucosyenite (less than 10% ferromagnesians) and of ferrosyenite (greater than 40% ferromagnesians) are present in a few places. Scarce ferromagnesian-rich syenitic layers 10-60 centimeters thick and intervals of such layers to 15 meters thick have gradational contacts with normal syenite. They are most common in the Buck Canyon synform. These mafic layers are less potassic than normal syenite, often consisting of mangerite or jotunite, and commonly show excellent mineral grading.

Typical syenite is comprised of mesoperthite and ferromagnesian pseudomorphs, with accessory plagioclase(oligoclase), ilemite, apatite, zircon, and perhaps biotite and quartz. Mesoperthite and ferromagnesian pseudomorphs are equant anhedral 1-3 millimeter crystals and aggregates which give the rock an allotrimorphic-granular texture quite in contrast to the ophitic to subophitic textures of the gabbroic and jotunitic rocks. Because of its generally dark color, much syenite was previously mapped as gabbro (Higgs, 1954, Oakeshott, 1958, Crowell, 1962). Only limited

compositional variation is present in many outcrops; individual hand specimens are nearly always homogeneous in composition and texture. Probably some of the biotite is of primary origin, but much was produced by secondary alteration.

Mesoperthite crystals consist of a fine, regular intergrowth of about equal proportions of potassium feldspar and plagioclase (Figures 59, 60). The index of refraction of the plagioclase lamellae indicates that it is sodic oligoclase rather than albite. Coarser marginal plagioclase patches which are optically continuous with the plagioclase lamellae are sodic oligoclase. The lamellae formed by subsolidus exsolution from originally homogeneous alkali feldspar with a composition of about Or_{50-65} Ab_{44-29} An_{6}. Mesoperthite shows microcline twinning in a few coarser more leucocratic rocks. The exsolved feldspar lamellae commonly coarsen near the crystal edges where they form relatively coarse (0.01-0.1 millimeter) zones of interlocking feldspar 0.05-0.2 millimeters wide between adjacent mesoperthite crystals (Figures 59,60). These "swapped borders" (Ramberg, 1962) appear to have formed either during final interstitial crystallization or during subsolidus exsolution, since they are usually optically continuous with exsolution lamellae.

Ferromagnesian aggregates pseudomorphic after original equant 1-3 millimeter crystals are the other major textural constituent of most syenite. Biotite and quartz are the most abundant alteration minerals but hornblende is also usually abundant. The inner parts of the pseudomorphs are made up predominantly of fine, 0.01-0.05 millimeter quartz and green hornblende with smaller amounts of biotite, epidote, and chlorite (Figures 61,62). The centers are surrounded by coronas

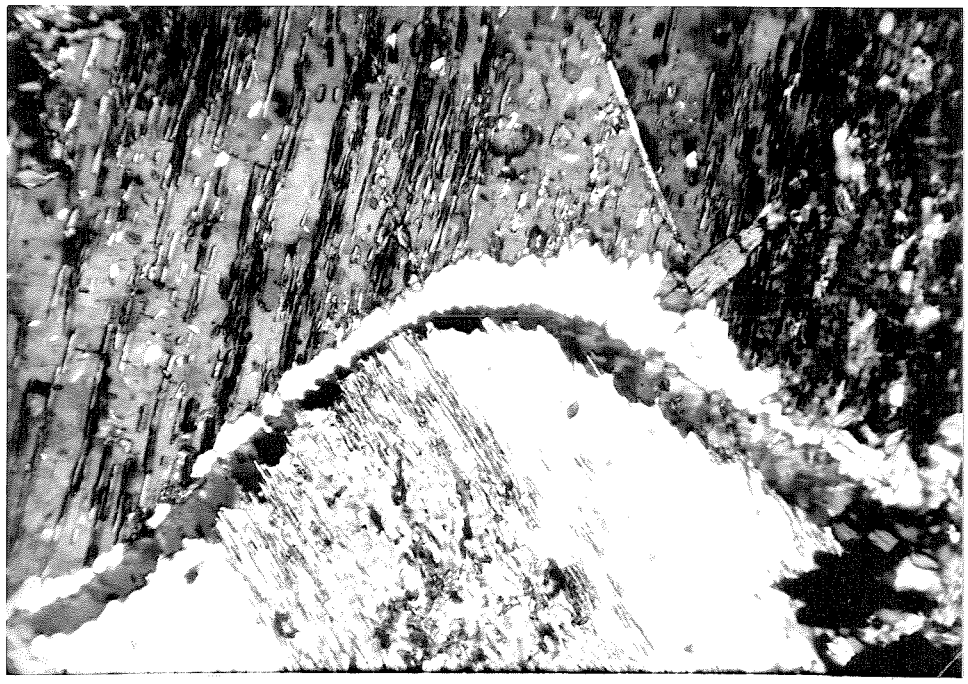

Figure 59. Swapped borders at the contact of two mesoperthite crystals in altered syenite. Note that the original contract was relatively smooth, but outward growth of plagioclase (albite-oligoclase) from the contact was irregular, preferentially growing along the exsolution direction in the adjacent mesoperthite. Both mesoperthite crystals contain numerous needles of amphibole (oriented preferrentially along the exsolution directions) produced during alteration of this rock (crossed nicols, 0.50 x 0.76 millimeter field).

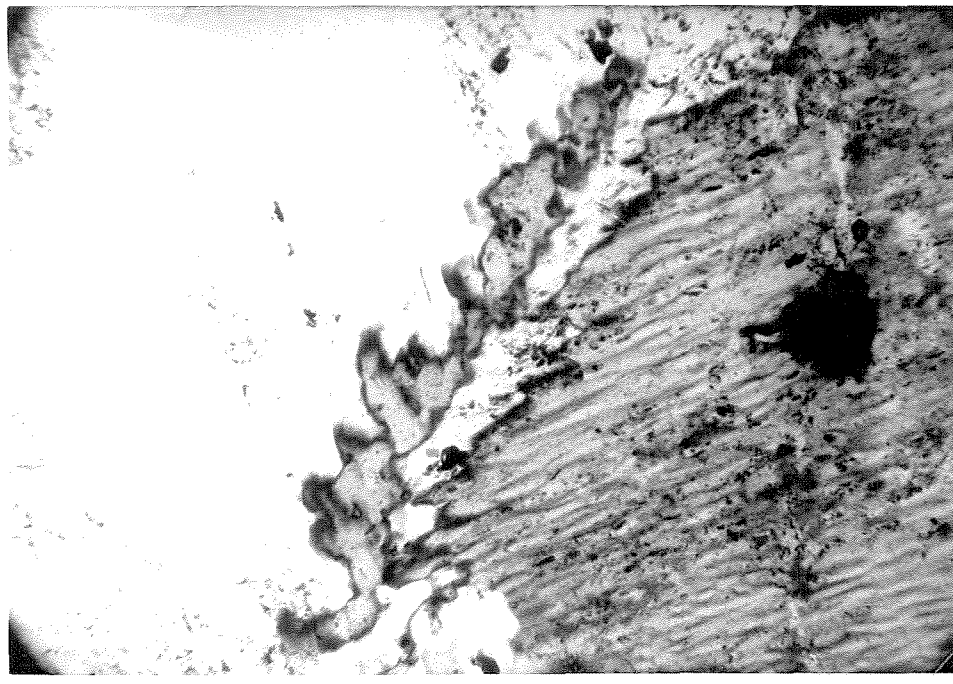

Figure 60. Swapped borders at the contact of two mesoperthite crystals in leucosyenite. Note the penetration of each plagioclase (albite-oligoclase) border parallel to the exsolution direction of the adjacent crystal (crossed nicols, 0.48 x 0.74 millimeter field).

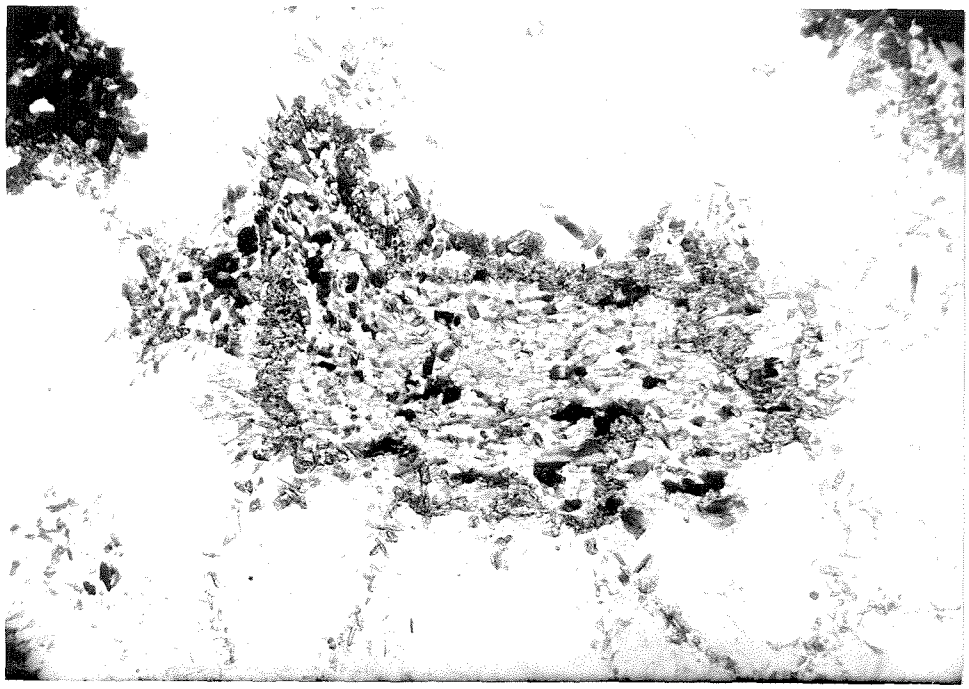

Figure 61. A replacement aggregate after a primary ferromagnesian mineral (proxene?) in syenite. Hornblende and epidote are abundant in the rim, and the central part contains abundant quartz, hornblende, biotite and chlorite (111C, plane light, 1.99 x 3.02 millimeter field).

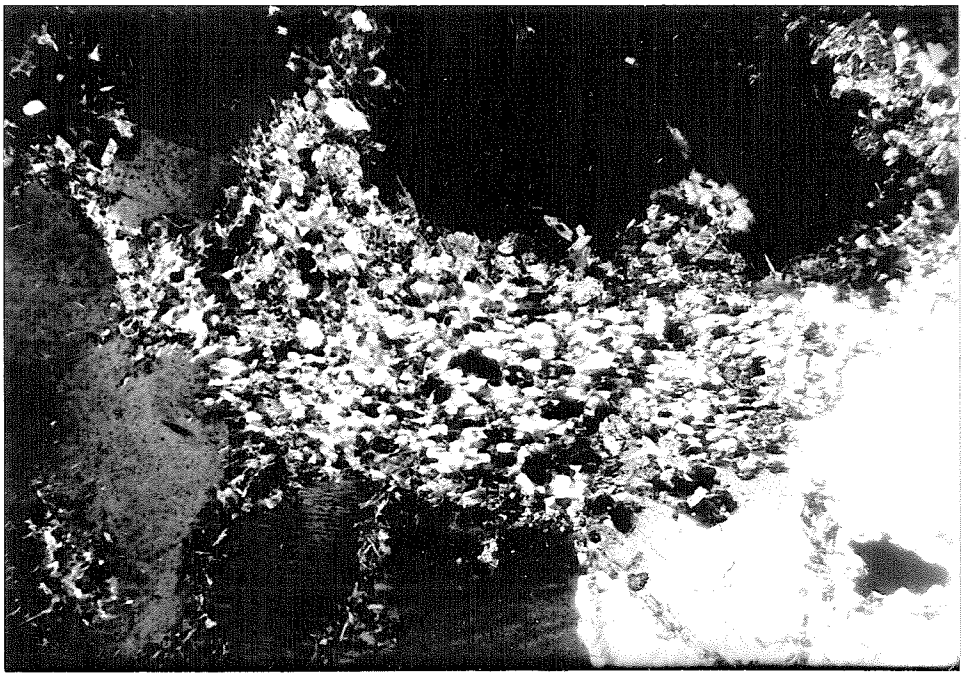

Figure 62. Same field as Figure 61. (111C, crossed nicols, 1.99 x 3.02 millimeter field).

of coarser, more continuous ferromagnesian material, usually radiating aggregates of hornblende or biotite (Figure 63). The proportion, distribution and size of these alteration minerals varies, but the average compositions of the pseudomorphs are similar. In the more greatly altered rocks biotite replaces feldspar several millimeters away from the pseudomorphs and also surrounds ilmenite.

The original ferromagnesian mineral is not known. Hornblende-rich vs. hornblende-poor bands within the fine grained core of some pseudomorphs suggest coarse exsolution lamellae in original pyroxene similar to those observed in hypersthene in jotunite near the top of the body (Figures 64,65). However, few pseudomorphs show this and some of them could have been augite or olivine. A few samples of syenite in Iron and Rabbit Canyons contain fresh olivine and augite (Figure 58), and on the south limb of the Buck Canyon synform one specimen contains largely unaltered hypersthene. In both places the rocks containing unaltered ferromagnesians appear to be relatively high in the syenite unit. No rocks containing unaltered ferromagnesians have been found anywhere in the lower half of the normal syenite subunit. The hypersthene-bearing rock contains both mesoperthite and antiperthite as equant, 1-3 millimeter, complexly sutured and intergrown crystals which give the rock a distinctive textural appearance. The hypersthene is subophitic and contains two sets of exsolved clinopyroxene lamellae, indicating inversion from original pigeonite. The feldspar is more altered to sericite, epidote, etc. than observed in most syenite but hypersthene shows almost no uralitization. The other syenites with unaltered ferromagnesians contain equant subhedral 1-3 millimeter crystals of augite, olivine and mesoperthite. The augite has no

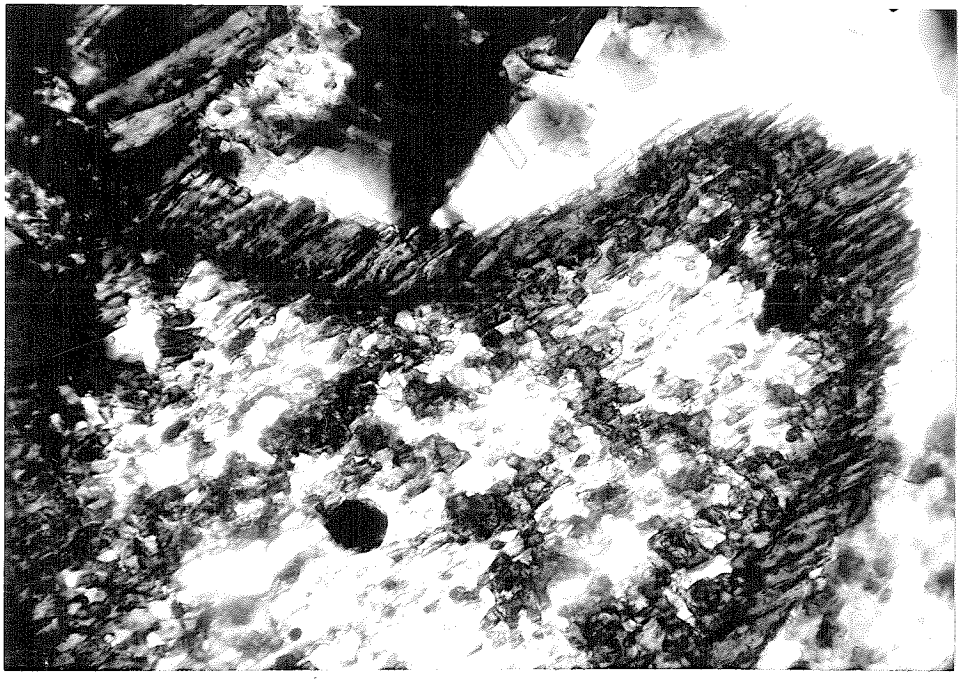

Figure 63. Pseudomorph after proxene(?) in syenite. Blue-green hornblende of the rim is all optically continuous, probably controlled by the orientation of the proxene(?) it replaced (1030A, plane light, 0.48 x 0.74 millimeter field).

Figure 64. Ferromagnesian pseudomorphs in syenite. Note the wide rims of blue-green hornblende and the relict lamellar structure in one pseudomorph. (1030A, plane light, 1.99 x 3.02 millimeter field).

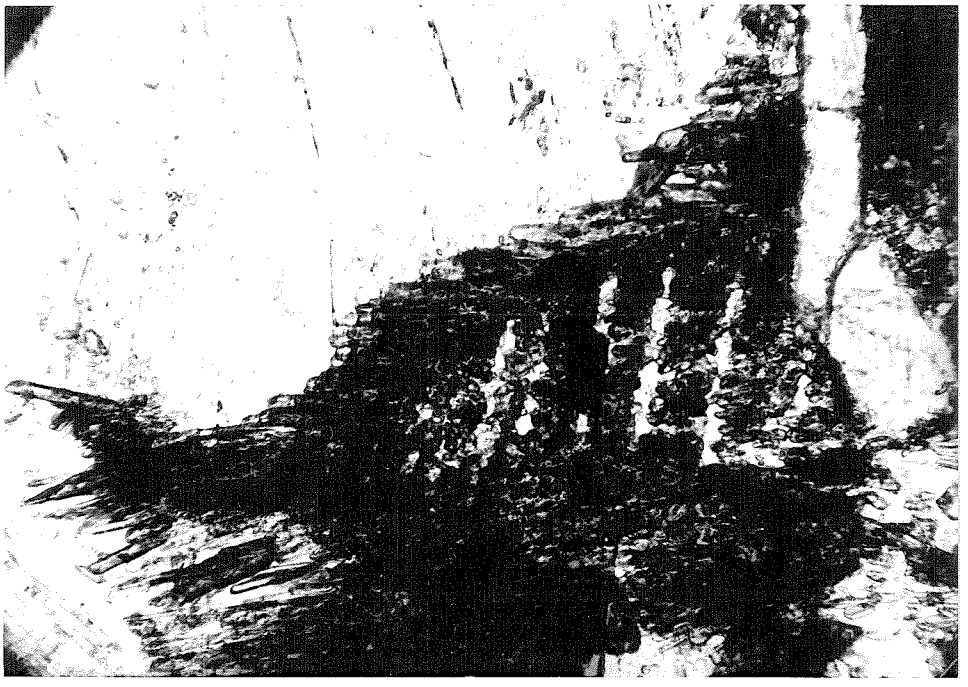

Figure 65. Enlarged detail of lamellae in a ferromagnesian pseudomorph in syenite. Relict lamellae suggest that the original ferromagnesian mineral in syenite was a pyroxene (1030A, plane light, 0.48 x 0.74 millimeter field).

exsolution lamellae or twins and is commonly slightly zoned, with calcium-depleted cores (2V=35-40) grading continuously outward to calcium-enriched rims (2V=55-60). Olivine is iron-rich (about Fa_{65}), unzoned, and almost completely unaltered. The ferromagnesian minerals are surrounded by thin rims (0.05 millimeters) of fine radiating hornblende in all these rocks.

Large abundant (to 1%) interstitial zircon crystals are usually associated with the ferromagnesian minerals in syenite. Accessory interstitial ilmenite is common and is often altered to leucoxene-sphene and surrounded by biotite. Large abundant euhedral to subhedral apatite crystals are usually associated with ilmenite and the ferromagnesian pseudomorphs. Small amounts of fine-grained interstitial albite, orthoclase and quartz are late stage minerals.

Especially in the upper part of the normal syenite subunit, a few thin layers of coarser, 5-10 millimeter mesoperthite crystals occur in otherwise homogeneous 1-3 millimeter syenite. These layers have gradational boundaries, are commonly 0.5-3 meters in length and 1-2 centimeters in width, and are discontinuous, grading into normal syenite at their ends. These veins probably formed by local recrystallization soon after primary crystallization. These veins are usually sub-parallel to the contacts of the unit and to the rare primary compositional layering, but are so variable in some outcrops that their orientations are not shown on the geologic map.

Leucosyenite is exposed along the ridge west of Iron Mountain and along the ridges on either side of Iron Canyon about 2 kilometers west of Magic Mountain. Both of these exposures are located near the base of the normal syenite subunit. Leucosyenite consists entirely of

equant 1-6 millimeter mesoperthite crystals (Figures 66,67). It commonly occurs as irregular 5-30 centimeter patches with sharp contacts sometimes slightly elongate parallel to the apparent structural orientation of the rock determined from nearby compositional layering or contacts. Uncommon bodies of leucosyenite a few meters to a few tens of meters in size occur in both places.

JOTUNITE UNIT

The jotunite unit is comprised of a diverse assemblage of generally mafic rocks which include jotunite, mangerite, gabbro, leucogabbro, ferrojotunite, ferrosyenite and ultramafite. Rhythmic layering is present in many rocks and mineral grading is common. The original orientation of layers in this unit was probably sub-horizontal and appears to be generally concordant with layers in the underlying syenite unit. Abundant evidence of slumping suggests continued tectonic activity during crystallization of the jotunite unit. Consistent trends of rock or mineral compositions as a function of vertical position have not been recognized in this unit or in individual subunits. The subunits are described below in order from lowest to highest.

ANORTHOSITE BLOCK SUBUNIT

Rocks of the anorthosite block subunit are mostly gabbroic, consisting primarily of andesine (much of it antiperthitic) and ferromagnesian aggregates. These rocks are usually deeply weathered; many of them were studied by means of grain mounts rather than thin sections. Andesine (An_{35-45}) is the most common feldspar, but antiperthite (An_{25-35}) is present in some rocks. Mesoperthite is the predominant

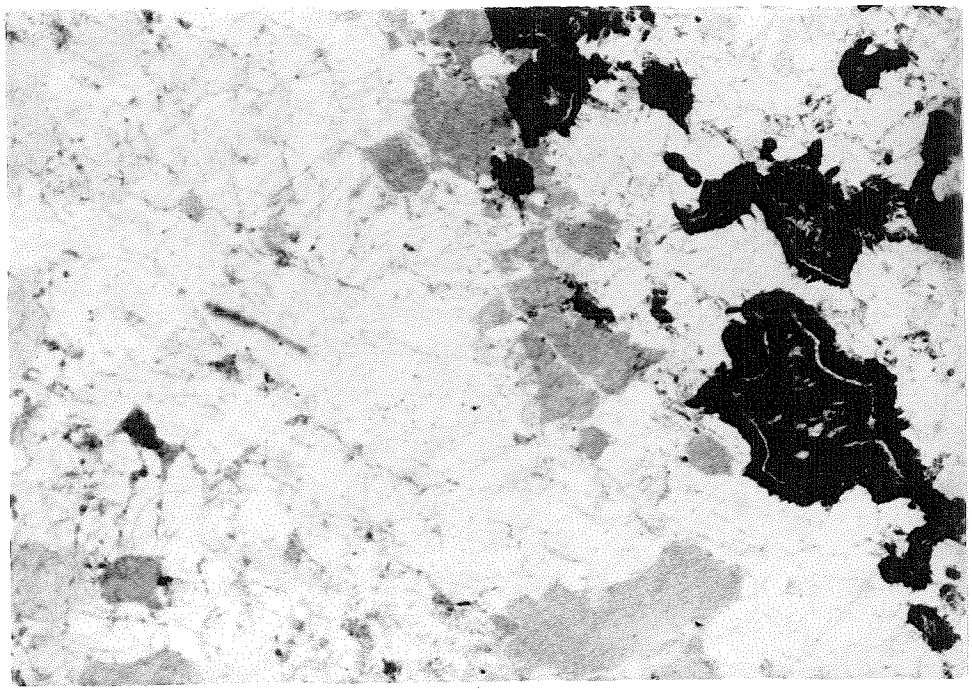

Figure 66. Contact of leucosyenite (left) with normal syenite (right). Other than a possible slight coarsening of the mesoperthite lamellae in leucosyenite, the only difference is the presence or absence of ferromagnesian minerals (plane light, 7 x 11 millimeter field).

Figure 67. Same field as Figure 66. Note the slightly coarser texture of mesoperthite in leucosyenite, and the faint microcline twinning which is present in many crystals in leucosyenite (crossed nicols, 7 x 11 millimeter field).

feldspar in some of them, mostly near the contact with rocks of the underlying syenite unit. Subhedral to anhedral feldspars crystals (1-3 millimeters) are sometimes slightly elongate parallel to compositional layering. Ilmenite and apatite are abundant accessory minerals and 0.5-2 millimeter biotite crystals are common, especially near the contact with rocks of the syenite unit. Blue-green hornblende and quartz are common fine-grained products of alteration of the primary ferromagnesian minerals, and epidote, chlorite and muscovite are other common alteration minerals.

Large anorthosite slump blocks are abundant in rocks of this subunit. Mineral graded layers are common and frequently drape over blocks or are deformed beneath them (see Chapter 3). A variety of other structures present in these rocks include channel-like structures, cross-layering and fine-scale deformation structures resembling those formed in unconsolidated sediments. Slump and sedimentation structures in these rocks suggest transport towards the west or southwest from an area east or northeast of North Fork Saddle. Anorthosite must have been exposed on the floor of the chamber in this area where it was broken up and then displaced downward within a gabbroic or jotunitic magma from which bottom crystal accumulation, mainly of ferromagnesian minerals, was occurring.

LOWER JOTUNITE SUBUNIT

Most rocks of this subunit are jotunitic but some mangerite and syenite are interlayered with jotunite. Compositional layering (sometimes graded) is present in a few exposures, but most of this subunit is massive. The jotunite contains about 30-45% ferromagnesian

minerals and consists of 3-10 millimeter equant to slightly tabular andesine (An_{30-35}) crystals subophitically surrounded by later-crystallizing ferromagnesian pseudomorphs after original pyroxene. The feldspar is not compositionally zoned and usually contains several percent of fine exsolved lamellae of potassium feldspar. The ferromagnesian pseudomorphs were probably originally pyroxene because they are similar in minerology and microscopic appearance to pseudomorphs containing relict hypersthene in rocks of the overlying layered jotunite subunit. Accessory ilmenite and apatite occur in these rocks. Leucoxene-sphene, biotite, blue-green amphibole, chlorite, epidote and white mica were produced by deuteric alteration.

LAYERED JOTUNITE SUBUNIT

This subunit is characterized by strongly developed (usually 5-30 centimeters) compositional layering. Individual layers are persistent for tens of meters. The average composition of individual layers varies, usually within the range of 20-60% ferromagnesians. The average composition of layers in different parts of this subunit is variable, but in a single outcrop individual layers are all similar in average composition (Figure 21). Many layers display conspicuous mineral grading (Figure 23). Lower parts containing 35-50% ferromagnesians may grade upward to zones containing about 10-25% ferromagnesians, with relatively sharp contacts with adjacent layers. The compositional difference between top and bottom is commonly not so great, but it is distinct.

The rocks of this subunit are all jotunite, most with color indices between 20 and 60 although the extremes range from 10 to 80. These rocks consist of antiperthite plates 2-10 millimeters long and elongate

subophitic ferromagnesian minerals of similar size oriented parallel to the layering. Oriented subhedral tabular feldspar crystals (An_{30-40}) contain abundant exsolution blebs or lamellae which are often unevenly distributed through the crystal in distinct 1-2 millimeter patches of abundant exsolved potassium feldspar (figure 68). There is no suggestion of any kind of zonal arrangement of the antiperthitic areas within andesine crystals, and no other compositional zonation was recognized.

Most of the primary ferromagnesian minerals have been completely altered to fine grained amphiboles, epidote and micas. Relict lamellar structure can be seen in some pseudomorphs which were probably originally hypersthene or pigeonite. A distinctly different pseudomorph type which contains abundant opaque oxides was probably originally olivine, based on its similar appearance to alteration rims around olivine in other rocks. Rocks containing relict ferromagnesian minerals, either predominantly iron-rich hypersthene (inverted pigeonite) (Figure 54) or else predominantly augite and fayalitic olivine (Figure 68) can be traced along strike into rocks with partially to completely altered ferromagnesians.

These are interpreted to be adcumulate rocks in which andesine (An_{30-40}) and pigeonite or sometimes olivine and augite were primary cumulate minerals. Adcumulate growth of andesine and pyroxene occurred from the interstitial magma, from which interstitial ilmenite and apatite also crystallized. Adcumulate growth of pyroxene produced subophitic overgrowth of the unzoned plagioclase tablets. Upon cooling, inversion of pigeonite to hypersthene caused exrolution of clinopyroxene lamellae in hypersthene. Exsolution of feldspar during cooling produced antiperthite which exsolved in some areas more than others.

Figure 68. Oriented cumulate antiperthitic andesine tablets in jotunite. Note the presence of both albite and carlsbad twinning which is characteristic of cumulate plagioclase in most jotunite (crossed nicols, 7 x 11 millimeter field).

Deuteric fluids completely altered hypersthene, augite and olivine in most of the rocks of this subunit.

Rare anorthositic inclusions in layered jotunite consist of coarser (5-20 millimeter) antiperthitic andesine crystals in masses usually about 5-8 centimeters wide and 10-25 centimeter long oriented parallel to the layering. The feldspar is similar in composition and texture to that in the adjacent jotunite. In contrast to the large angular anorthosite blocks present in other parts of the jotunite unit, these inclusions have irregular, gradational contacts and look as if they were originally masses of poorly-aggregated crystals. These inclusions may represent either plagioclase rafts which sank more slowly than plagioclase in the normal rock, or poorly-consolidated blocks broken off of some higher surface, perhaps the roof, which then sank and were included within the normal rocks.

Near the top of this subunit a few coarser (1-15 centimeter) feldspathic veins or irregular bodies crosscut some of the graded jotunite layers (Figure 69). Plagioclase is frequently oriented perpendicular to the margins of these veins and biotite is a common constituent (Figure 70). Similar feldspathic rocks are also common in the two overlying subunits. These zones probably formed by recrystallization, perhaps facilitated by fluids, along fractures in the cumulate rocks.

ULTRAMAFIC JOTUNITE SUBUNIT

Ultramafic jotunite subunit rocks characteristically have color indices between 50 and 100. These are allotrimorphic-granular to hypidiomorphic-granular rocks with 5-10 millimeter anhedral, sometimes

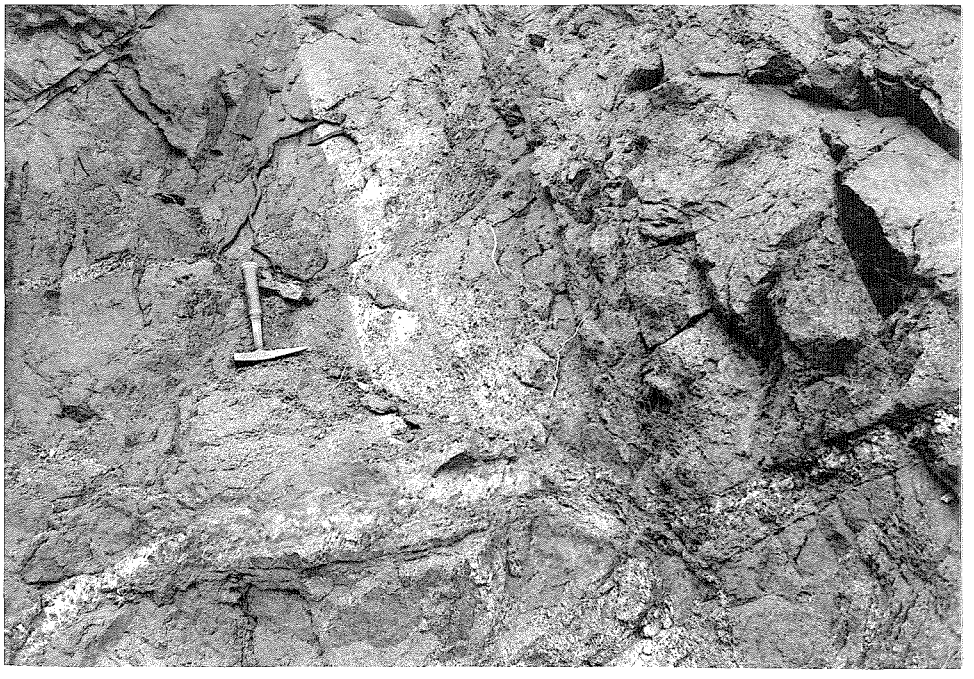

Figure 69. Graded layer in the layered jotunite subunit of the jotunite unit. Note the zone of coarser, more feldspathic recrystallized jotunite crosscutting the primary layering. Near the mouth of the South Fork of Pacoima Canyon.

Figure 70. Graded layers of jotunite from the layered jotunite subunit of the jotunite unit in Pacoima Canyon near the mouth of Bad Canyon. Note the coarser, recrystallized jotunite in the lower right corner crosscutting primary layering. A younger unrelated dike follows part of the contact. The feldspathic margin of the recrystallized rock contains coarse plagioclase crystals oriented perpendicular to the contact.

slightly elongate crystals of olivine, augite, feldspar, ilmenite, apatite and sometimes red-brown hornblende (Figures 71,72). They commonly have a distinct oriented fabric and fine-scale but often indistinct compositional layering. A few of the thicker layers are mineral graded. These rocks are mixtures of various proportions of two types of feldspar and ferromagnesians.

The feldspar in most of these rocks is andesine (An_{40-45}) with no exsolved potassium-feldspar. Locally, antiperthite and even mesoperthite are present. No consistent stratigraphic variation in feldspar compositions has been recognized. Compositional zoning is not seen in feldspar crystals, and the feldspar is usually remarkably free of sericitic alteration, as compared to feldspars in most other rocks of the anorthosite-syenite body. Elongate, lensoidal aggregates of anhedral feldspar are common in some rocks and their form suggests that original coarse crystals (1-3 centimeters) might have later recrystallized to form the observed aggregates.

The ferromagnesian minerals are predominantly olivine and augite, but deep red-brown hornblende is common. Ilmenite and apatite together invariably make up about 35% of the total non-feldspar component of the rocks and green spinel is a common accessory. The rocks commonly contain oriented aggregates of 3-10 millimeter equidimensional, anhedral unzoned olivine crystals (about Fa_{62}). Subhedral to anhedral, slightly elongate augite crystals (about En_{34} Fs_{22} Wo_{44}) are not zoned and contain no pyroxene exsolution lamellae. Some augite crystals contain numerous well oriented 0.001 by 0.01-0.1 millimeter opaque rods. Red-brown, strongly pleochroic anhedral hornblende overgrows earlier-formed olivine, augite, ilmenite and apatite and appears to be the latest

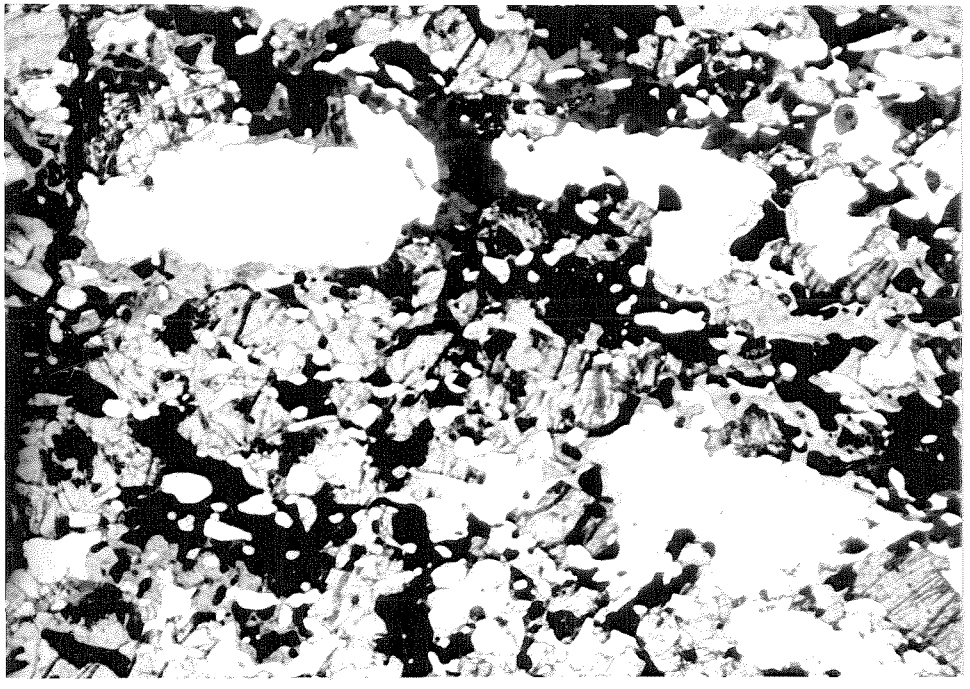

Figure 71. Ferrogabbro from the ultramafic jotunite subunit of the jotunite unit. Cumulate layering is defined by oriented apatite (small clear crystals) and andesine (large clear crystals). Olivine, augite and ilmenite are other major constituents of the rock. Late-crystallized dark red-brown hornblende is present in the upper center of the field (102, plane light, 7 x 11 millimeter field).

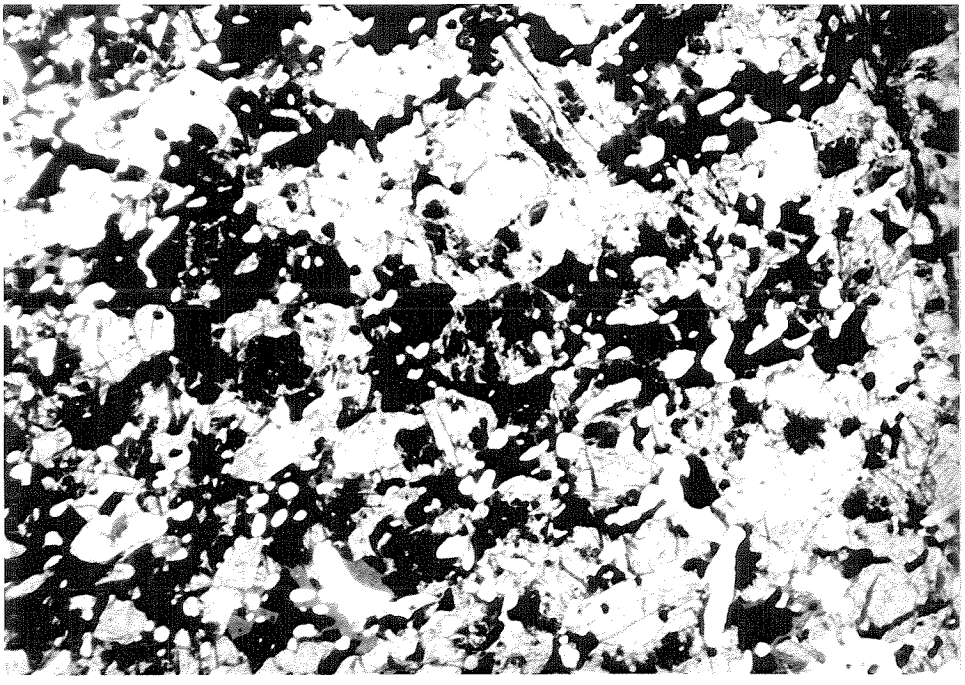

Figure 72. Ultramafite from the ultramafic syenite subunit of the jotunite unit. Cumulate layering is defined by oriented apatite (small clear crystals). Olivine, augite and ilmenite are other major constituents of the rock (102, plane light, 7 x 11 millimeter field).

primary mineral to crystallize (Figure 73). Ilmenite and apatite probably crystallized after most of the olivine and augite. Dark green spinel (hercynite or pleonaste, 0.1-1.0 millimeters) is intergrown with ilmenite from which it may have formed by granular exsolution.

Coarse, feldspar-rich veins similar to those described in the previous section crosscut primary layering in a few outcrops.

UPPER JOTUNITE SUBUNIT

The upper jotunite subunit consists predominantly of coarse plagioclase-antiperthite (An_{30-40}) and uralitized pyroxene. Olivine, now altered, was a major constituent of some rocks, and minor amounts of primary hornblende, biotite, ilmenite and apatite are also common. Orthopyroxene was probably the original pyroxene in most rocks, but relict augite is sparsely present. Coarse feldspar-rich veins commonly cut primary layering.

This subunit is relatively massive, but fine-scale, often poorly defined compositional layering is present in some places, most often in 3-30 meter horizons alternating with much thicker sections which show little or no compositional layering. Most of the layered rocks of this subunit show abundant evidence of slumping, most of which probably occurred in a plastic crystal mush. (Figures 12, 13, 22). The common density grading of layers is sometimes extreme, with thin nearly holo-leucocratic tops underlain by much thicker (0.2-3 meter) ultramafite bases (Figure 74).

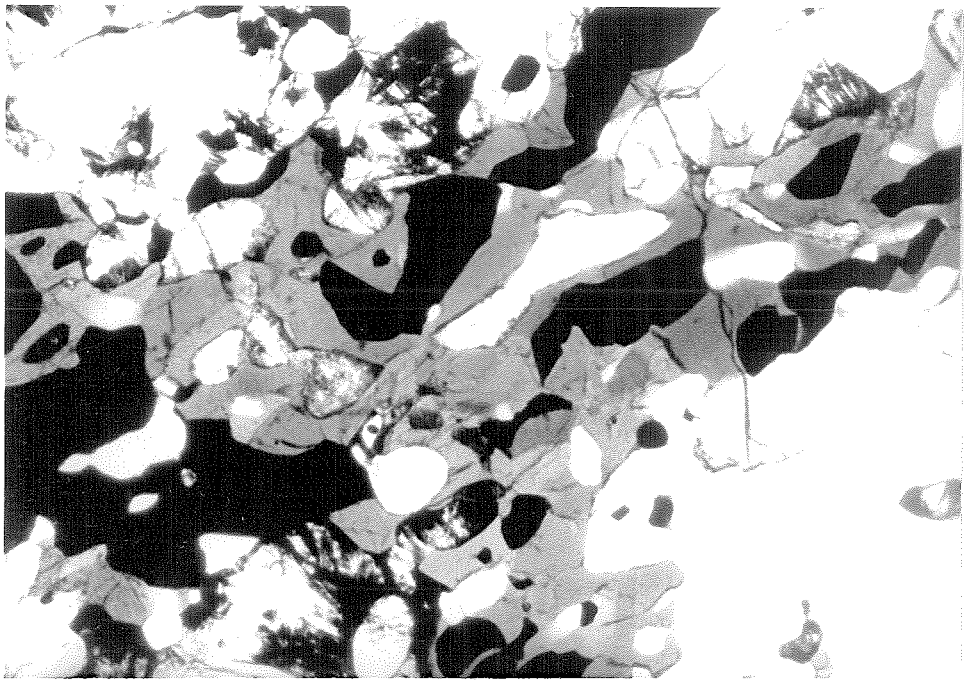

Figure 73. Ferrogabbro from the ultramafic jotunite subunit of the jotunite unit. Plagioclase (An_{45}) is present in the lower right corner; other minerals include olivine, augite, apatite, and ilmenite. Red-brown hornblende (with strong absorption) is abundant and generally grows around ilmenite in these rocks (102, plane light, 1.99 x 3.02 millimeter field).

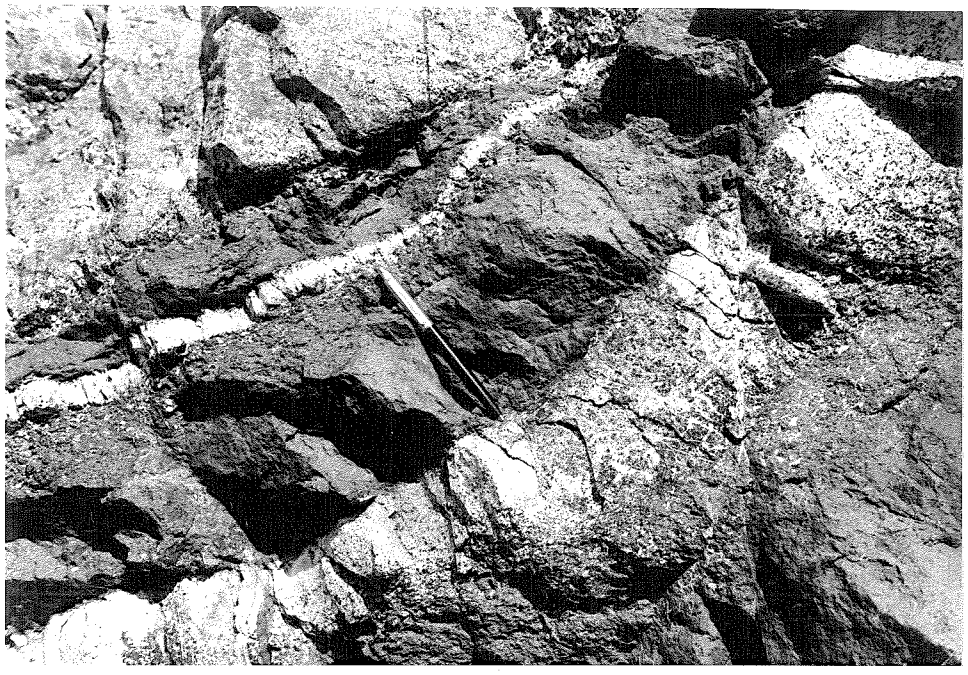

Figure 74. Graded layers in the upper jotunite subunit of the jotunite unit in Pacoima Canyon near the mouth of Spring Canyon. The thick layer on the lower right displays mineral grading to lower color index toward the upper left, and the ferromagnesian pseudomorphs in its ultramafite base grade to smaller size toward the upper left.

CHAPTER 5

ROCK AND MINERAL CHEMISTRY

INTRODUCTION

This section describes the chemical compositions of the various rocks making up the San Gabriel anorthosite-syenite body as well as some of the individual minerals in the rocks. Chemical analyses of 20 rocks are reported and are plotted on several variation diagrams used to discuss some of the chemical characteristics and apparent liquid variation trends of the anorthosite-syenite body. These diagrams are used to compare the compositions of these rocks with those of other anorthosite-syenite suites and to address important questions such as the possible consanguinity of the magmas which crystallized the rocks of the body. An approximate bulk chemical composition for the overall plutonic complex is estimated, using selected analyses of representative rocks and their estimated volumetric abundance based on the maps and cross-sections. Some data on the compositions of individual minerals are presented, particularly for the feldspars and the major ferromagnesian minerals (pyroxenes and olivine). This study has not obtained all of the key mineral compositions which would be needed to discuss chemical variations due to fractional crystallization in the magmas. Exsolution and other fine-scale intergrowth textures characteristic of both of these mineral groups are described. A discussion of high temperature sub-solidus mineralogical changes involving the processes of inversion, recrystallization and uralization is presented.

ROCK COMPOSITIONS

DATA

Chemical analyses were obtained by conventional wet chemical methods for a total of 20 selected rocks from the San Gabriel anorthosite-syenite

Table I: Chemical Analyses of Rocks of the San Gabriel Anorthosite-Syenite Body

	Anorthosite-Leucogabbro Unit					"Gabbro"
Sample	18	276	1033	1055A	1055B	1032
Chemical Analyses						
SiO_2	58.20	46.45	53.39	52.22	49.78	57.15
TiO_2	0.05	4.95	0.16	0.85	1.12	1.17
Al_2O_3	26.82	16.28	27.27	23.93	23.58	19.84
Fe_2O_3	0.36	3.12	0.47	1.02	1.76	1.90
FeO	0.19	9.32	1.01	2.81	3.86	4.45
MnO	0.01	0.15	0.01	0.02	0.04	0.08
MgO	0.18	5.46	0.08	2.46	3.54	1.08
CaO	7.41	9.87	9.95	10.07	9.60	4.34
Na_2O	6.16	2.95	5.50	4.68	4.25	7.10
K_2O	0.52	0.17	0.64	0.36	0.40	1.57
H_2O+	0.43	1.27	0.68	0.87	1.36	0.89
H_2O-	0.32	0.35	0.41	0.26	0.45	0.44
P_2O_5	0.05	0.03	0.06	0.02	0.02	0.36
S	0.01	0.01	0.04	0.05	0.05	0.04
Total	100.71	100.38	99.67	99.62	99.81	100.41
C.I.P.W. Norms						
Q	4.37	0.33				
Or	3.08	1.02	3.84	2.16	2.41	9.36
Ab	52.13	25.26	41.88	40.20	36.43	60.25
An	36.46	31.07	38.55	43.91	45.01	17.80
Cor	2.78					
Nep			2.88		0.14	0.19
Di		14.82	0.99	5.41	2.00	1.31
Hy	0.45	13.30		1.19		
Ol			0.64	3.84	8.29	5.10
Mgt	0.46	4.58	0.69	1.50	2.61	2.78
Hem	0.04					
Ilm	0.09	9.52	0.31	1.64	2.17	2.24
Ap	0.12	0.07	0.15	0.05	0.05	0.87
Py	0.02	0.02		0.10	0.10	0.08

Table I: (Continued)

	Ultramafic Syenite Subunit		Ultramafic Jotunite Subunit	
Sample	335	387	61	102
Chemical Analyses				
SiO_2	40.99	24.77	42.06	27.61
TiO_2	4.58	8.07	4.22	5.90
Al_2O_3	9.61	3.24	9.13	5.38
Fe_2O_3	7.41	10.06	12.42	6.57
FeO	17.20	26.54	13.37	29.33
MnO	0.42	0.44	0.41	0.58
MgO	4.28	12.13	3.38	8.94
CaO	7.71	7.74	8.19	9.06
Na_2O	2.34	0.28	2.28	0.86
K_2O	1.96	0.12	1.35	0.13
H_2O+	0.81	1.40	0.81	0.59
H_2O-	0.61	0.85	0.53	0.37
P_2O_5	2.54	4.76	2.44	4.98
S	0.03	0.05	0.01	0.24
Total	100.49	100.45	100.60	100.54
C.I.P.W. Norms				
Q			7.32	
Or	11.67	0.72	8.02	0.77
Ab	19.93	2.40	19.39	7.28
An	10.01	7.33	10.72	10.44
Di	9.95	0.06	11.62	1.67
Hy	17.30	15.93	10.82	5.35
Ol	5.35	31.51		41.32
Mgt	10.82	14.79	18.11	9.53
Ilm	8.76	15.55	8.06	11.21
Ap	6.16	11.61	5.90	11.98
Py	0.06	0.10	0.02	0.45

Table I: (Continued)

	Syenite-Quartz Syenite				
Sample	5B	111	708	1030A	1030B
Chemical Analyses					
SiO_2	72.51	58.11	62.03	53.21	54.80
TiO_2	0.30	0.85	0.39	1.43	1.56
Al_2O_3	12.76	17.81	17.65	14.88	14.81
Fe_2O_3	2.17	3.09	1.38	4.71	2.33
FeO	1.27	4.51	3.06	9.72	10.96
MnO	0.03	0.15	0.08	0.24	0.24
MgO	0.01	0.63	0.29	1.05	1.21
CaO	0.86	4.05	2.58	4.12	4.51
Na_2O	3.27	5.02	5.26	4.41	4.36
K_2O	5.46	3.80	6.61	3.92	4.34
H_2O+	0.70	1.16	0.59	0.84	0.41
H_2O-	0.39	0.33	0.26	0.79	0.72
P_2O_5	0.03	0.26	0.08	0.36	0.47
S	0.00	0.03	0.04	0.05	0.12
Total	99.76	99.80	100.30	99.73	100.84
C.I.P.W. Norms					
Q	31.20	4.25	0.19	23.61	25.72
Or	32.70	22.84	39.29	38.02	36.98
Ab	28.03	43.19	44.74	9.42	8.05
An	4.08	15.11	5.07		
Di	0.04	3.09	6.33	7.82	9.83
Hy	0.10	4.63	1.36	9.30	5.03
Mgt	3.19	4.56	2.01	6.96	3.39
Ilm	0.58	1.64	0.75	2.77	2.97
Ap	0.73	0.64	0.19	0.88	1.13
Py		0.06	0.07	0.10	0.23

Table I: (Continued)

	Jotunitic Gabbro				Hornblende-Bytownite Gabbro
Sample	11	32	100	1052	230
Chemical Analyses					
SiO_2	48.29	48.09	53.88	38.23	41.34
TiO_2	2.40	2.49	0.30	3.83	1.12
Al_2O_3	14.40	15.61	17.94	14.51	29.11
Fe_2O_3	3.54	2.76	1.56	7.27	3.70
FeO	12.77	10.25	8.03	12.49	3.85
MnO	0.27	0.25	0.22	0.25	0.09
MgO	3.61	3.38	3.42	4.70	2.83
CaO	7.21	7.27	7.59	10.18	16.17
Na_2O	3.72	4.40	4.66	2.95	1.01
K_2O	1.37	1.11	0.92	0.95	0.14
H_2O+	0.66	1.59	0.72	1.90	1.08
H_2O	0.22	0.40	0.38	0.66	0.32
P_2O_5	1.68	2.18	1.14	2.49	0.04
S	0.08	0.00	0.12	0.03	0.02
Total	100.22	99.78	100.88	100.44	100.82
C.I.P.W. Norms					
Q			0.18		
Or	8.14	6.64	5.45	5.72	0.83
Ab	31.63	37.68	39.48	20.52	4.97
An	18.66	19.82	25.37	24.01	74.93
Nep				2.66	1.96
Di	5.30	1.91	4.10	8.99	4.40
Hy	19.24	14.80	19.61		
Ol	3.07	3.84		13.76	5.23
Mgt	5.16	5.20	2.27	10.75	5.40
Ilm	4.58	4.79	0.57	7.42	2.14
Ap	4.06	5.31	2.75	6.11	0.10
Py	0.15		0.23	0.06	0.04

Table II: Chemical Analyses of San Gabriel Anorthosite from Oakeshott (1958, p32)

Sample	OA-1	OA-2	OA-3	OA-4	OA-5	OA-6	OA-7	OA-8
Chemical Analyses								
SiO_2	55.23	56.42	53.66	53.50	56.88	52.50	53.04	56.56
TiO_2	0.04	0.08	0.03	0.14	0.17	0.15	0.12	0.08
Al_2O_3	27.32	26.96	29.28	28.27	25.95	27.94	25.48	26.09
Fe_2O_3	0.12	0.47	0.23	0.61	0.18	0.79	0.86	0.29
FeO	0.86	0.86	0.82	0.77	1.12	1.29	0.34	0.77
MgO	Tr	Tr	0.00	0.34	0.36	1.14	0.46	0.22
CaO	9.58	8.20	11.12	10.78	8.06	10.28	7.88	8.04
Na_2O	5.64	5.48	4.16	4.39	6.12	4.56	3.29	5.64
K_2O	0.39	0.97	0.27	0.12	0.44	0.48	1.08	0.85
P_2O_5	0.04	0.06	Tr	0.07	0.06	Tr	0.04	0.04
C.I.P.W. Norms								
Q		2.96	4.04	3.82	1.22		13.30	2.62
Or	2.32	5.76	1.60	0.72	2.62	2.86	6.89	5.10
Ab	48.09	46.59	35.34	37.51	52.12	38.91	30.06	48.40
An	47.64	40.50	55.41	53.57	39.86	51.45	41.94	40.20
Cor	0.31	2.14	1.94	1.51	0.91	1.25	5.05	1.39
Hy	0.84	1.06	1.27	1.54	2.54	3.39	1.24	1.61
Ol	0.45					0.69		
Mgt	0.18	0.69	0.33	0.89	0.26	1.16	0.81	0.43
Hem							0.37	
Il	0.08	0.15	0.06	0.27	0.33	0.29	0.25	0.15
Ap	0.10	0.15		0.17	0.15		0.10	0.10

body. Because of the large grain size of most of these rocks, samples weighing from 4 to 50 kilograms were crushed and then split to obtain representative aliquots of powder. Analyses were performed by several analysts at the Japan Analytical Chemistry Research Institute, Tokyo, and are shown in Table I. Descriptions of the analyzed rocks are given below. Eight additional analyses of anorthosite from the San Gabriel body, reported by Oakeshott (1958), are shown in Table II and have been considered in the following discussion.

ANALYZED ROCKS

The analyzed rocks are described below in the same order as they appear in Table I.

SG-18: Anorthosite from the south side of Magic Mountain. This rock lies very near the top of the anorthosite-leucogabbro unit. The outcrop is massive, coarse, inequigranular anorthosite which shows very little alteration.

SG-276: Leucogabbro from the crest of the ridge about 1.5 kilometers west-southwest of Magic Mountain. This rock comes from the upper part of the anorthosite-leucogabbro unit. The bouldery outcrop consists of coarse uralitized leucogabbro with poorly developed compositional layering.

SG-1033: Anorthosite from the Middle Fork of Mill Creek about 0.5 kilometer above its mouth. It lies in the lower part of the anorthosite-leucogabbro unit. Thin layers of leucogabbro (10-40 centimeters) alternate with thicker layers of anorthosite (20-50 centimeters). This sample was collected from one of the thicker anorthosite layers.

SG-1055A and B: Leucogabbro (Figures 47, 50, 51, 54, 55, 56, 58) from a small tributary on the west side of the Middle Fork Mill Creek, about 1.5 kilometers above its mouth. These specimens lie in the lower part of the anorthosite-leucogabbro unit, about 1/3 of the way above its base. Both specimens come from a slab sawed out of a boulder (about 30 x 45 x 60 centimeters) collected from an outcrop of typical uralitized leucogabbro in the creek bottom. Similar leucogabbro crops out discontinuously along the creek bottom for about 10 meters in either direction, and similar but more weathered rock is present on the walls of the canyon above the outcrop. Part of the slab consists of ophitic leucogabbro (1055A) and the rest of the slab consists of non-ophitic leucogabbro (Figure 51). One reason for analyzing this pair of rocks was to determine the extent of compositional changes accompanying postcumulous recrystallization of these rocks.

SG-1032: Sodic gabbro from the gabbro which forms the upper part of the anorthosite-leucogabbro unit in the northwest part of the body in lower Pole Canyon. This lithology consists of coarse grained uralitized gabbroic rocks which are mineralogically layered on a scale of 2 - 25 centimeters. This sample comes from one of the more leucocratic, less altered layers. The strong sodium-enrichment of this rock may be characteristic of much of the "gabbro", especially that within a few hundred meters of the syenite unit. Because of its sodium-rich character, a special symbol is used to designate this rock on the diagrams below.

SG-335C: Ferrosyenite (Figures 97, 98) from the ridge about 800 meters southeast of Iron Mountain near Indian Ben Saddle. This rock

comes from the ultramafic syenite subunit in the axis of the Buck Canyon synform. The very mafic rocks are deeply weathered in most places, especially along numerous closely spaced (2 - 20 centimeters) joints. Unweathered and unuralitized rock is present between joints and appears to vary from syenite to ultramafite over distances of a few meters. Thus, the rock is probably layered on a scale of a few meters, although this couldn't be confirmed on the exposure. The sample is homogeneous, with a crude lamination defined by elongate concentrations of light and dark minerals. Centimeter-scale compositional layering is present in similar rocks within 30 meters of the outcrop. This rock is part of a large mass extending from the axis of the Buck Canyon synform into anorthosite (Figure 38). Blocks of anorthosite are included within this mass which was probably intruded into anorthosite as either a magma or a crystal mush.

SG-387C: Ultramafite from the road about 2.5 kilometers west-northwest of Indian Ben Saddle. This rock comes from the ultramafic syenite subunit near the axis of the Buck Canyon synform. The outcrop appears to be homogeneous although a slight preferred orientation of mineral grains is visible. This is from a 3 meter or thicker layer in a sequence of unuralitized rocks which includes nearby layered ferrogabbro (some of it jotunitic).

SG-61: Ferrosyenite (Figure 111) from the Magic Mountain Road about 2600 meters southwest of Magic Mountian. This unuralitized rock is part of the ultramafic subunit of the jotunite unit. This rock is exposed in several small boulder outcrops along the top of a small ridge just north of the road. All the exposures are similar although some nearby rocks contain much less feldspar (ultramafite). Variations

in color index define crude 2 - 4 meter layering which is parallel to elongate ferromagnesian concentrations and elipsoidal 1 - 2 centimeter feldspar (mesopherthite) aggregates. This rock is anomalous compared to others of the jotunite unit, hardly any of which contain mesoperthite. This rock could represent either interlayered syenite unit rock or rock intruded into the jotunite unit, although in the field, it appears to be a normal part of the ultramafic jotunite unit. Because of its anomalous composition, it is shown with a separate symbol on the diagrams below.

SG-102C: Ferrodiorite (Figures 71, 72, 73) from Pacoima Canyon, about 430 meters west of the mouth of Rattlesnake Canyon. This is a completely unuralitized rock from the ultramafic subunit of the jotunite unit. The rock shows a fine-scale layering due to elongate concentrations of light and dark minerals and the preferred orientation of mineral grains, but otherwise is unlayered. Similar mafic rocks 10 - 20 meters away show compositional layering, some of it graded.

Solsy-5b: Quartz syenite from Ten-Hi, about 11 kilometers northeast of the map area.

SG-111: Syenite (Figure 61) from the Mt. Gleason road about 6 kilometers west of Mt. Gleason. The rock comes from the relatively thin part of the syenite unit just north of the Buck Canyon synform. The outcrop consists of homogeneous, unlayered uralitized syenite. Other gabbroic to anorthositic rocks are found elsewhere in the roadcut as little as 10 meters from this outcrop.

SG-708: Syenite from the ridge about 3.5 kilometers west of Magic Mountain. This uralitized rock lies near the base of the syenite unit. It comes from a small (10 meter) outcrop of slightly more

resistant syenite surrounded by similar, less resistant syenite. The rock is unlayered and almost completely homogeneous except for irregular patches (0.2 - 1 meter) of more leucocratic syenite. This rock is typical of much of the lower part of the syenite unit west and northwest of Magic Mountain.

SG-1030A and B: Syenite (Figures 63-65, 86) from outcrops about 50 meters apart near the mouth of Rabbit Canyon. These rocks lie in the highest part of the syenite unit exposed west of Magic Mountain. Both rocks come from large outcrops of homogeneous, unlayered syenite. Both contain rare mesoperthite megacrysts (1 - 3 centimeters) although these are more common in SG-1030A, and both samples contain rare large segregations of ferromagnesian minerals. Both samples are very similar in texture and color index, but the ferromagnesian minerals have been completely uralitized in 1030A, while olivine and augite are only slightly uralitized in 1030B. The appearance of the ferromagnesian aggregates in 1030A suggests that pyroxene was originally the dominant dark mineral, with only small amounts of olivine, while both pyroxene (augite) and olivine are abundant in 1030B. No obvious contact was observed between these two rocks in almost continuous exposure along the creek. One reason for analyzing this pair of rocks was to determine the extent of compositional changes accompanying uralitization of similar rocks.

SG-111: Jotunitic gabbro from Pacoima Canyon, about 650 meters below the mouth of the North Fork. This rock lies approximately at the contact between the lower jotunite and the layered jotunite subunits. The outcrop shows well-developed compositional layering, with a few layers reaching syenite composition about 20 meters

(across the strike) to the east. This sample comes from a 2 - 4 meter horizon in which all the rocks are moderately mafic, layering is indistinct and minerals (particularly antiperthite) display a slight preferred orientation. The rock is broken by numerous closely spaced joints (2 - 10 centimeters), along which weathering has occurred, but it is largely unaltered, and unuralitized otherwise.

SG-32: Jotunite from Pacoima Canyon at the mouth of the South Fork. This rock is probably part of the layered jotunite subunit. The outcrop is from a 3 - 4 meter thick zone of homogeneous rock showing very little compositional layering. Nearby rocks exhibit compositional layering, some of it graded. This is an antiperthite rock in which primary ferromagnesians have been completely uralitized.

SG-100C: Jotunitic gabbro (Figure 94) from Pacoima Canyon, about 250 meters west of the mouth of the South Fork. It lies in the jotunite unit and probably comes from the layered jotunite subunit, but possibly from the upper jotunite or ultramafic jotunite subunits. The outcrop appears to be nearly homogeneous, with a fine-scale layering resulting from elongate aggregates of unuralitized ferromagnesian minerals and a slight preferred orientation of antiperthitic andesine crystals.

SG-1052: Jotunitic gabbro dike from Pacoima Canyon about 0.6 kilometer southwest of the mouth of Dagger Flat Canyon. This rock comes from a gabbroic dike crosscutting Menhenhall gneiss about 0.4 kilometer from the contact of the jotunite unit. The dike varies in width up to about 6 meters and consists of mafic uralitized gabbro containing tabular plagioclase crystals which show a distinct

preferred orientation. Irregular areas with slightly different color indices are present, but do not define recognized compositional layering. This rock is the most likely, of all rocks analyzed, to have the composition of an actual magma, assuming the intruded magma did not contain suspended plagioclase tablets.

SG-230E: Hornblende-bytownite gabbro from the west side of the ridge about 800 meters northwest of the crest of Mt. Gleason. This rock is part of the hornblende-bytownite gabbro which is probably not a primary lithology of the anorthosite-syenite body. The rock occurs in several small outcrops and is homogeneous, with a strong lineation produced by parallelism of elongate, primary hornblende crystals.

DISCUSSION

Most of the rocks of this body are cumulates and some of them are greatly enriched in plagioclase or ferromagnesian minerals compared to the magmas which produced them. It is arguable that none of these rocks precisely matches the compositions of the magmas from which they directly crystallized. Any interpretations based on the following variation diagrams must keep this in mind.

The following categories of rocks are differentiated by symbols: (1) rocks from the anorthosite-leucogabbro unit (□); (2) rocks from the syenite unit (○); (3) rocks from the jotunite unit (△); and (4) anorthosite from Oakeshott (1958) (+). A further symbol is used for unusual hornblende-bytownite gabbro (230) (x), whose chemistry cannot be easily related to the three main units of the San Gabriel anorthosite-syenite body. High color index cumulate rocks in the syenite and jotunite units are also indicated (⊕ , ⊿). Plagioclase-enriched

anorthositic cumulate rocks (those with wt % Al_2O_3 20%) are also indicated on the diagrams (⊟ , and all +). The "gabbro" from Pole Canyon (1032) is part of the anorthosite-leucogabbro unit, but is anomalously sodium-rich and is designated separately (⊠). A ferrosyenite from the jotunite unit (61) is anomalously rich in alkali feldspar compared to other rocks of the jotunite unit and is designated separately (⏃). A jotunitic dike cutting Mendenhall gneiss above the roof of the body (1052) is the only rock which very likely represents a liquid composition and is designated separately (▲). Paired analyses (1030A and B and 1055A and B) are connected by a line. The compositional range of rocks of the anorthositic suite from the Adirondack Mountains (Emslie, 1973) is shown on several of the diagrams.

(1) Wt. % Alkalis-Total iron as FeO-MgO (Figure 75): The strongly iron-enriched character of this suite is evident, as is its trend toward alkali-enrichment. Specimens 1055A and 1055B are plagioclase-enriched leucogabbros from near the base of the body and have the lowest FeO/FeO+MgO ratios (0.61). Other than these rocks (and the extremely plagioclase-enriched anorthosites), all other rocks have relatively similar ratios averaging around 0.80 - 0.85. Thus, there is rather poor documentation of an early trend toward enrichment of iron over magnesium in rocks of this suite since no very magnesian rocks are present. A possible trend of magmatic evolution is shown on this diagram.

(2) Wt. % normative Anorthite-Albite-Orthoclase (Figure 76): Most of the rocks fall near a line which might represent a possible trend of differentiation. Almost all of these rocks fall within the field of "normal" (vs. sodic or potassic) rocks (Irvine and Barager, 1971). Exceptions include: specimen 387 which is an extremely ferromagnesian-

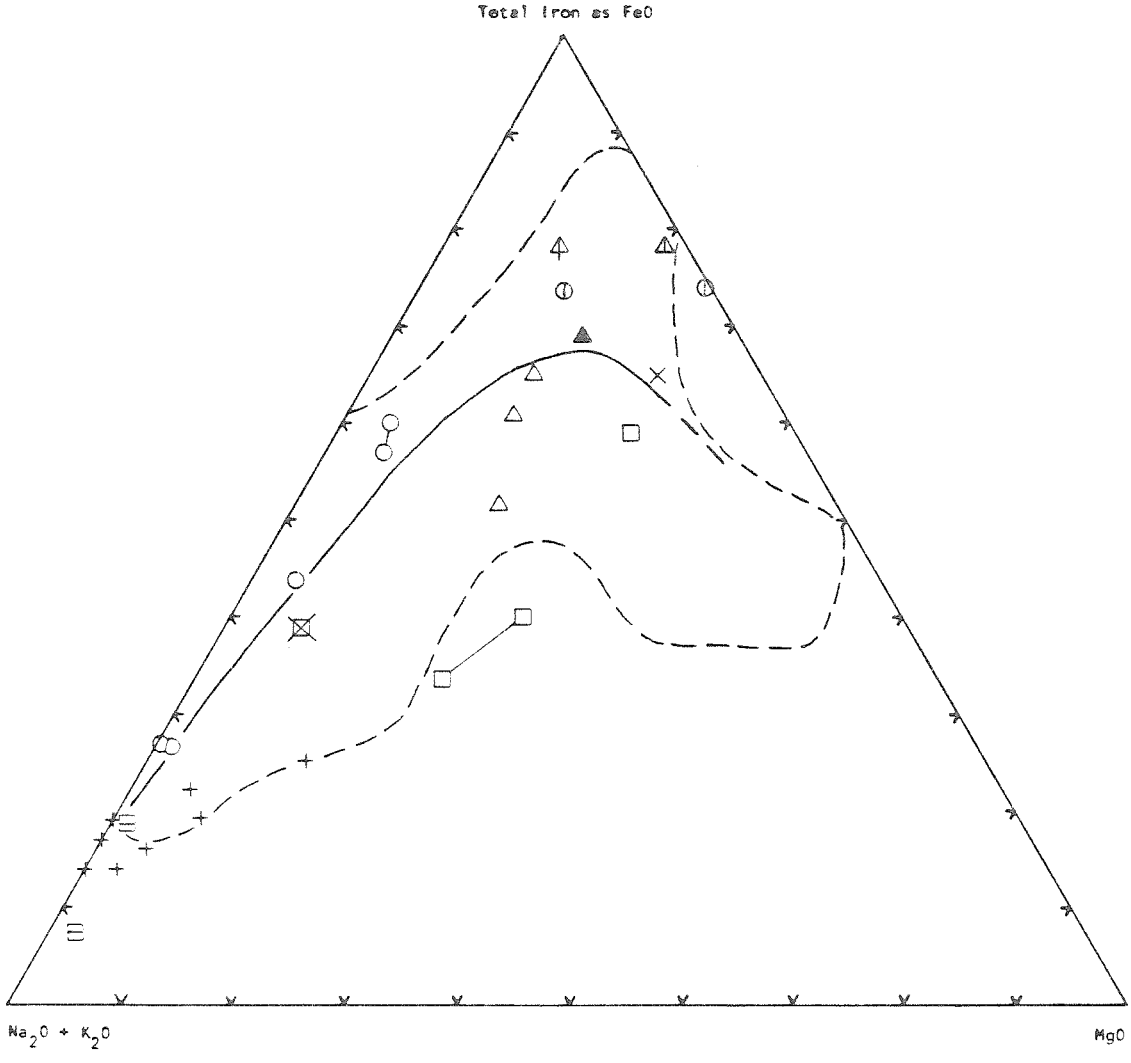

Figure 75. Weight percent K_2O+Na_2O vs. total iron as FeO vs. MgO. Symbols explained in text. Dashed line indicates field defined by rocks of the Adirondack Mountains (Emslie, 1973). Heavy line--possible magmatic trend for the San Gabriel body.

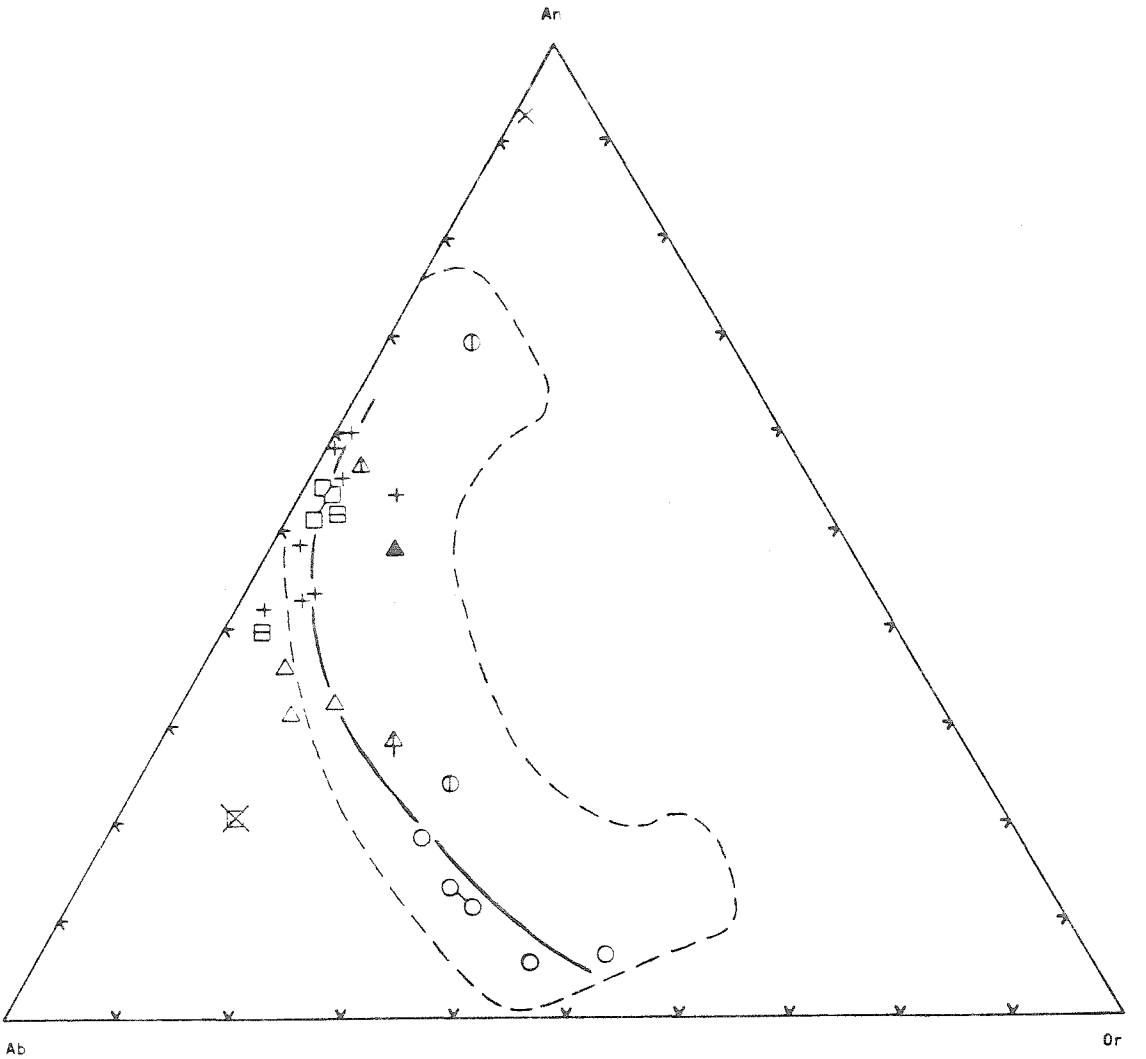

Figure 76. Normative An-Ab-Or. Symbols explained in text. Dashed line indicates field defined by rocks of the Adirondack Mountains (Emslie, 1973). Heavy line--possible magmatic trend for the San Gabriel body.

enriched cumulate rock with less than 11% normative feldspar and large amounts of CaO in the abundant augite; specimen 1052 which is from a jotunite dike cutting granulite which may have contaminated the dike and thus produced abnormally high K_2O contents; and specimen 1032 which is a plagioclase-pyroxene (uralite) sodic gabbro from near the top of the anorthosite-leucogabbro unit and contains albite-rich plagioclase and an anomalous microscopic texture.

(3) Wt % Al_2O_3 vs. normative An/An+Ab (Figure 77): The four ferromagnesian-enriched cumulates have anomalously low Al_2O_3 contents because of their low feldspar contents. All other analyses fall above or only slightly below the calcalkalic vs. tholeiitic dividing line, and this high Al_2O_3 character is maintained well below An/An+Ab ratios of 35, where most calcalkalic and tholeiitic suites tend to merge (Irvine and Baragar, 1971). Two distinct groups of analyses are distinguishable: (a) those with high Al_2O_3 (23% - 29%) and intermediate An/An+Ab (40 - 60) which include all anorthosites and leucogabbro from low in the anorthosite-leucogabrro unit; and (b) those with lower Al_2O_3 (13% - 20%) and intermediate to low An/An+Ab (mostly 10 - 40) which include leucogabbro and gabbro from high in the anorthosite-leucograbbo unit and all rocks from the syenite and jotunite units.

(4) Wt. % K_2O vs. SiO_2 (Figure 78): Only two analyses of this suite have wt % SiO_2 above 58%, but this may be in part a sampling effect. Syenitic rocks are abundantly represented members of this suite in the San Gabriel Mountains and elsewhere in Southern California. Quartz-bearing syenites are uncommon in the San Gabriel Mountains and 3 of 5 analyzed syenites have wt. % SiO_2 less than 58%. However, quartz syenite is an abundant member of this suite in the Orocopia, Little Chuckawalla

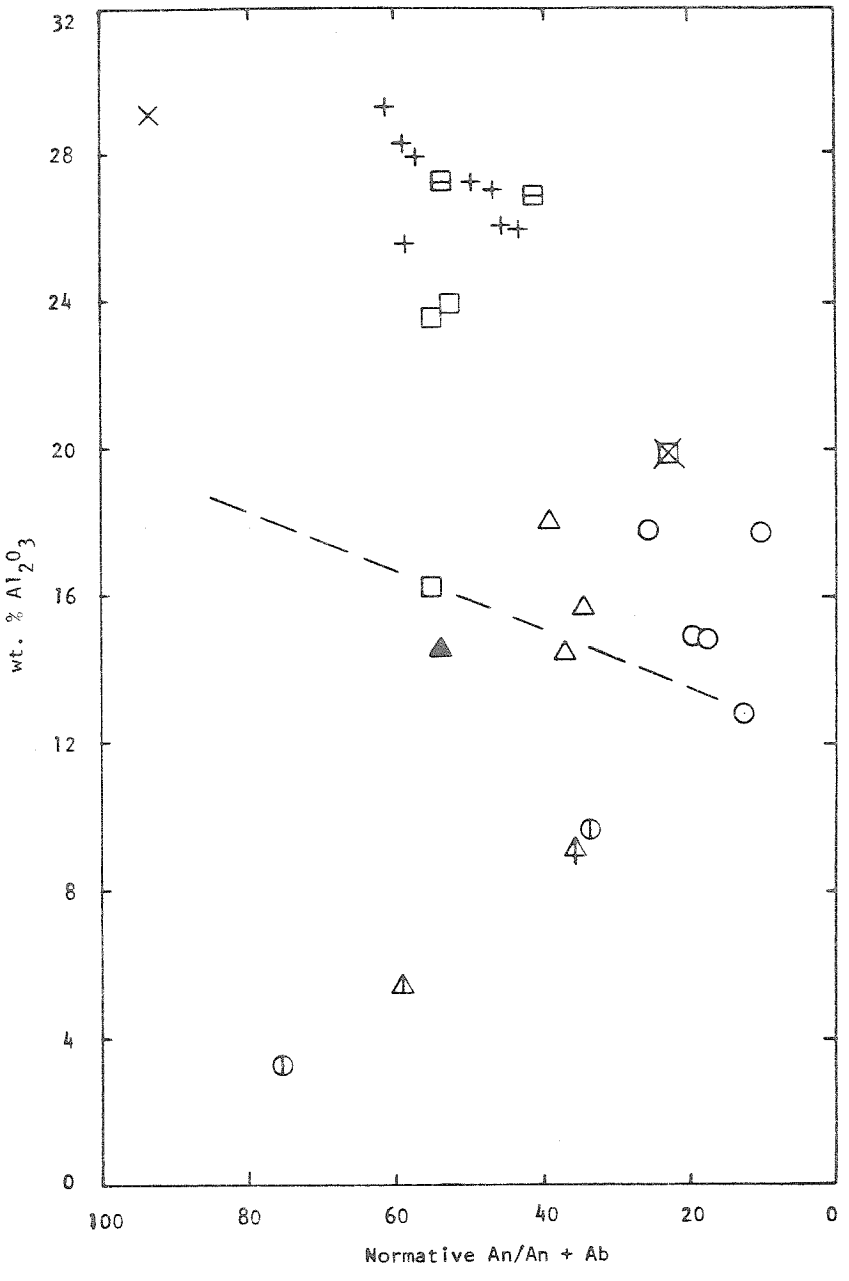

Figure 77. Weight percent Al_2O_3 vs. normative An/An+Ab. Symbols explained in text.

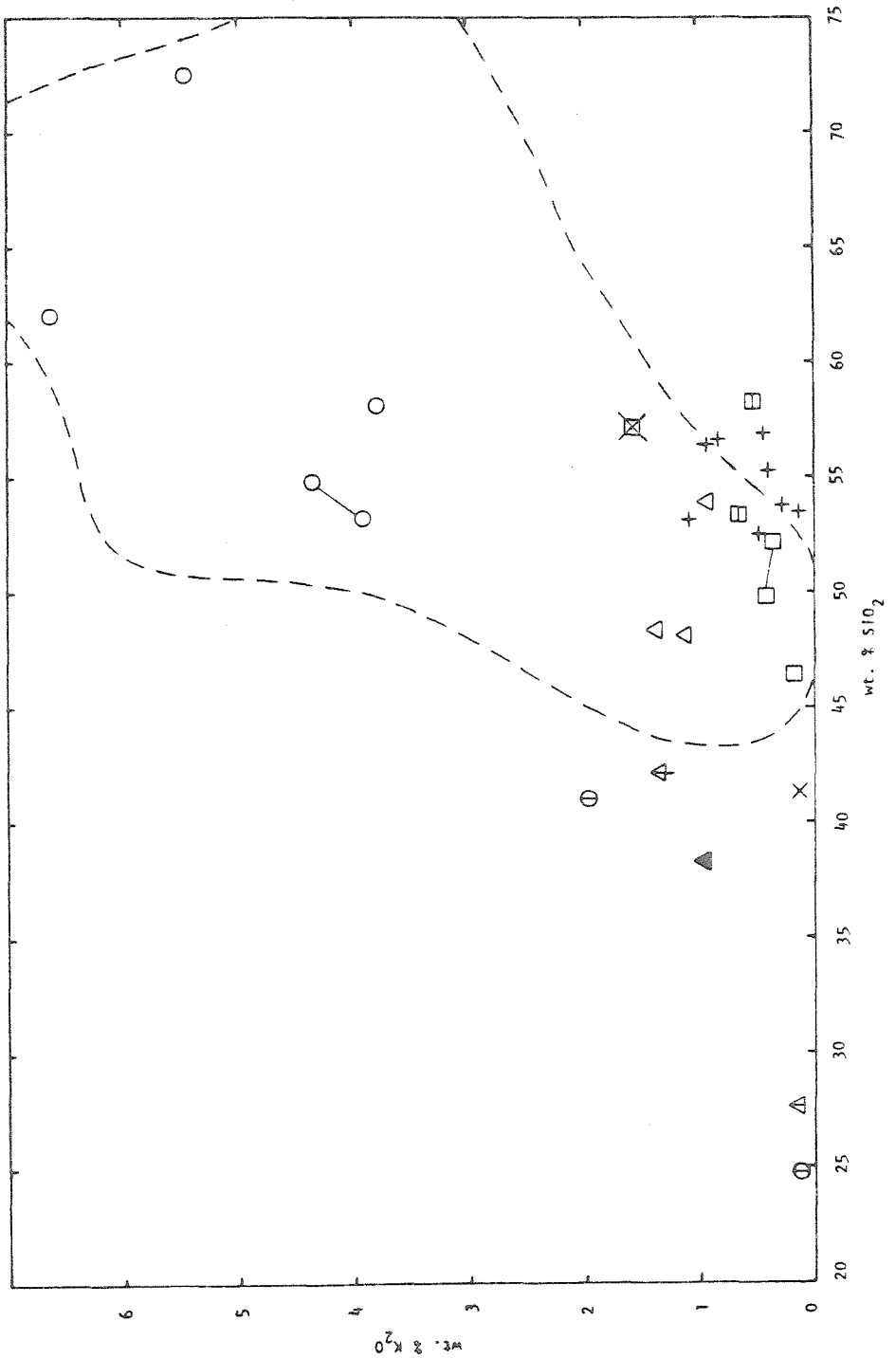

Figure 78. Weight percent K_2O vs. SiO_2. Symbols explained in text. Dashed line indicates field defined by rocks of the Adirondack Mountains (Emslie, 1973).

and Eagle Mountains and north of the Soledad Basin. Rocks from the anorthosite-leucogabbro unit mostly have low K_2O contents in the SiO_2 range of 50% - 58% comparable to those of calc-alkalic suites (Dickenson, 1969). Compared to rocks from the anorthosite-leucogabbro unit, most rocks from the jotunite unit have higher K_2O contents at given SiO_2 contents, and those from the syenite unit have still higher K_2O contents at given SiO_2 contents.

(5) Wt % MgO vs. total iron as FeO in rocks with more than 80% normative feldspar (Figure 79): If the anorthositic rocks of this suite are essentially plagioclase cumulates, then the intercumulous material in these rocks may be regarded as samples of trapped liquid minus the plagioclase components. This interstitial material should range in composition from that of the original liquid (if little adcumulus diffusion occurred) to compositions significantly enriched in magnesium (as iron preferentially diffused out during adcumulus growth). Lower MgO/FeO values, therefore, should approximate those of the original liquids while higher values should reflect the greater diffusive communication between pores and the magma reservoir (Emslie, 1973). All of these rocks have MgO/FeO ratios less than 4:6 and most have ratios less than 3:7. Thus, it can be inferred that liquids co-existing with cumulus plagioclase from which the anorthosite formed, rarely, if ever, had MgO/FeO ratios exceeding 3:7. This level of iron enrichment is high, but is also characteristic of the other rocks of this suite, suggesting a possible genetic relationship between anorthosite and the other rocks of the anorthosite-syenite body.

(6) Wt. % P_2O_5 vs. differentiation index (1/3 SiO_2 + K_2O-FeO-MgO-CaO) (Figure 80): Rocks of this suite can be divided into two groups:

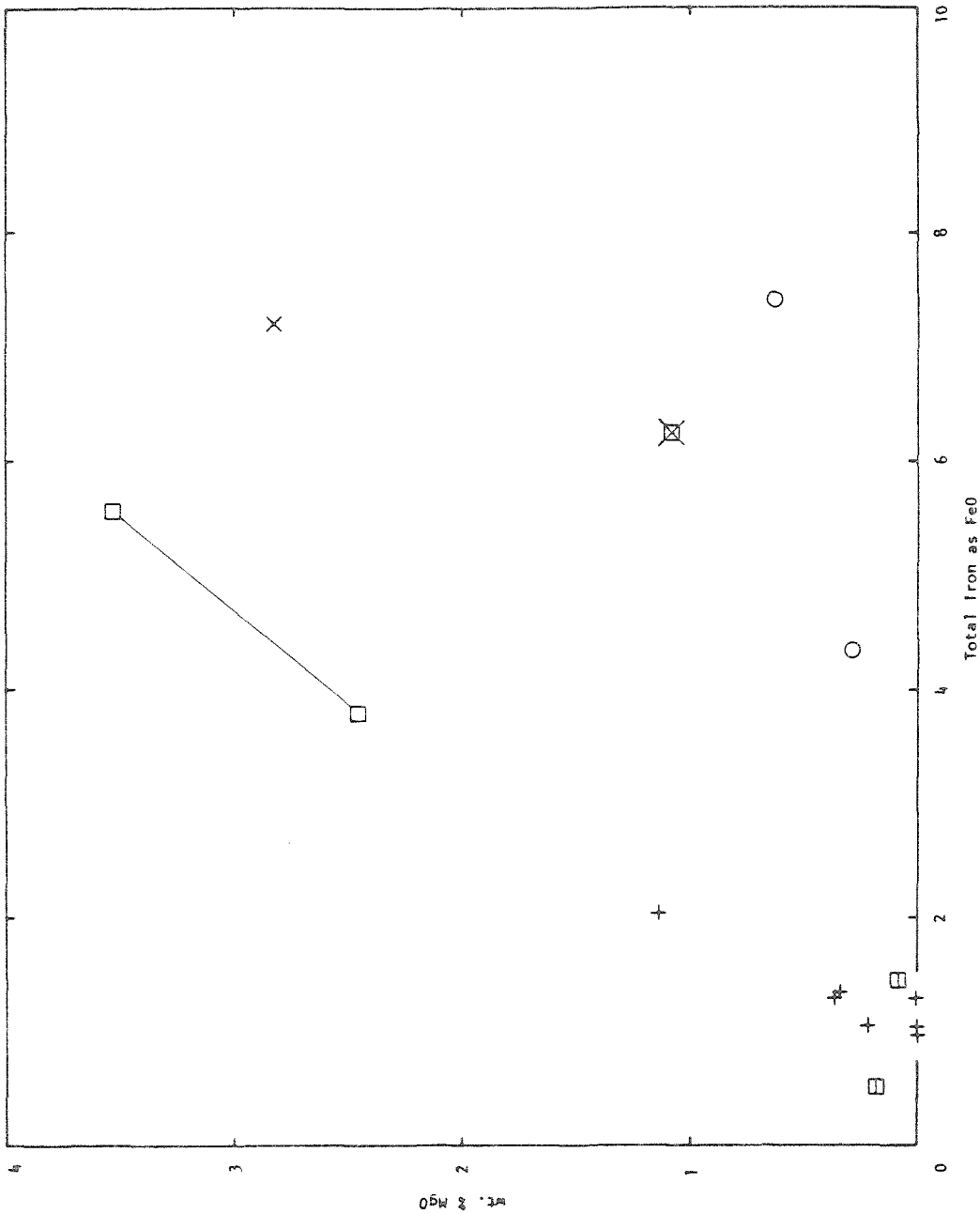

Figure 79. Weight percent MgO vs. FeO. Symbols explained in text.

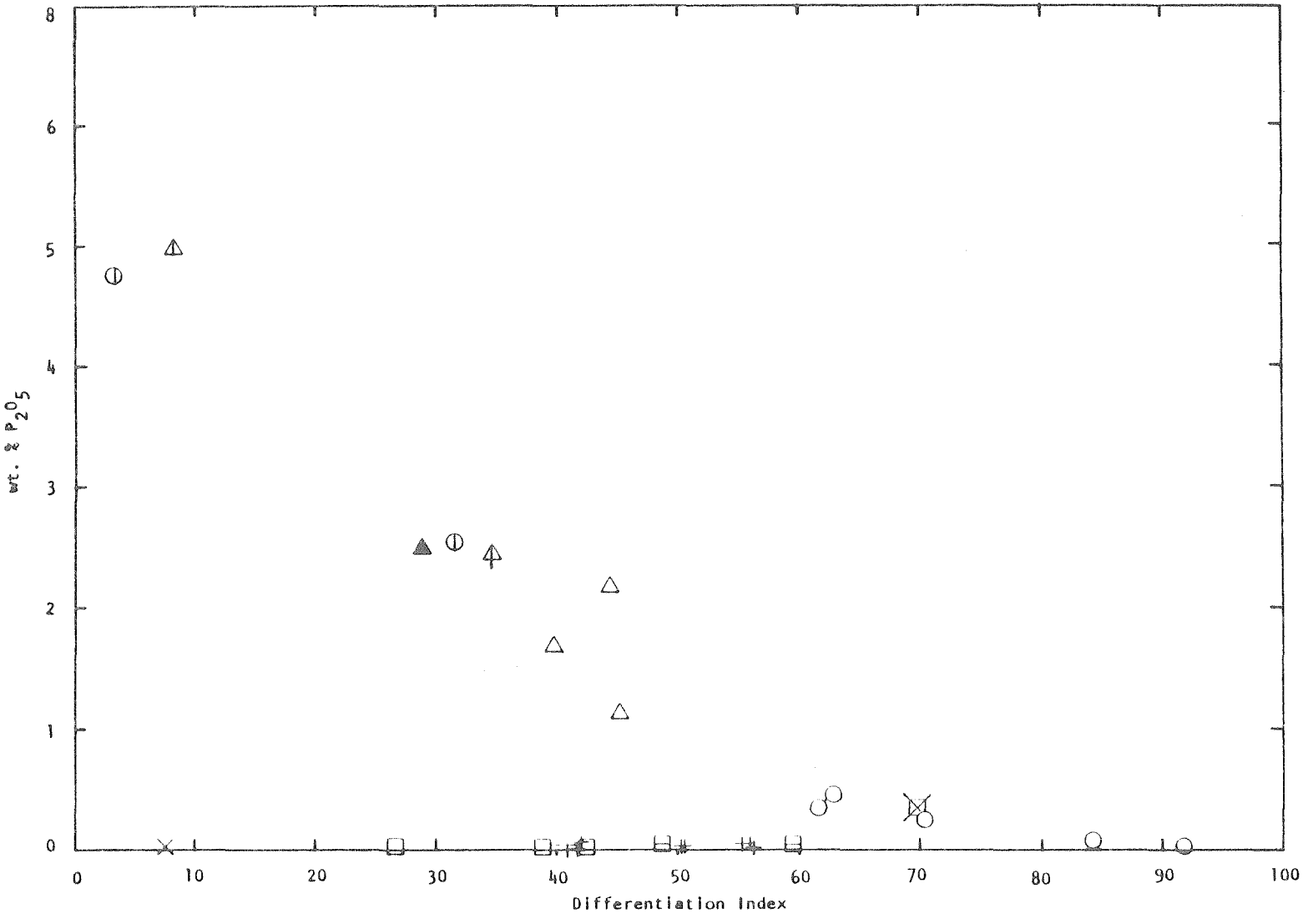

Figure 80. Weight percent P_2O_5 vs. Differentiation Index. Symbols explained in text.

(a) those with uniformly low P_2O_5 contents regardless of their differentiation index are rocks of the anorthosite-leucogabbro unit in which apatite apparently was not a cumulate mineral and so all of the P_2O_5 is that in the trapped intercumulate magma, the proportion of which was apparently nearly constant in all rocks; and (b) those with high P_2O_5 contents at low differentiation index and decreasing P_2O_5 with increasing differentiation index represent rocks of the syenite and jotunite units formed when apatite apparently was a cumulate mineral. It appears that the P_2O_5 content of the syenite and jotunite magmas decreased with increasing differentiation. Two anomalous rocks are specimen 276 (leucogabbro) which has cumulate ilmenite but not cumulate apatite and specimen 100 (jotunite), which has cumulate apatite but not cumulate ilmenite.

(7) Wt. % TiO_2 vs. CaO+MgO (Figure 81): Rocks of this suite can be divided into two groups: (a) rocks which plot along the upper curve represent rocks of the syenite and jotunite which apparently formed when ilmenite was a cumulate mineral; and (b) rocks which plot along the lower curve are from the anorthosite-leucogabbro unit and formed when ilmenite was not a cumulate mineral. In both sets of rocks, the TiO_2 content of the magma decreases with decreasing MgO and CaO. Rocks of this suite do not appear to have lower TiO_2 contents at MgO+CaO values above 10% as they do in the Morin suites (Philpotts, 1966). Note that two rocks from near the top of the anorthosite-leucogabbro unit, leucogabbro (276) and sodic gabbro (1032) lie near the upper curve and so probably formed when ilmenite was a cumulate mineral, and one rock from the jotunite unit (100) lies near the lower curve and so probably formed when ilmenite was not a cumulate mineral.

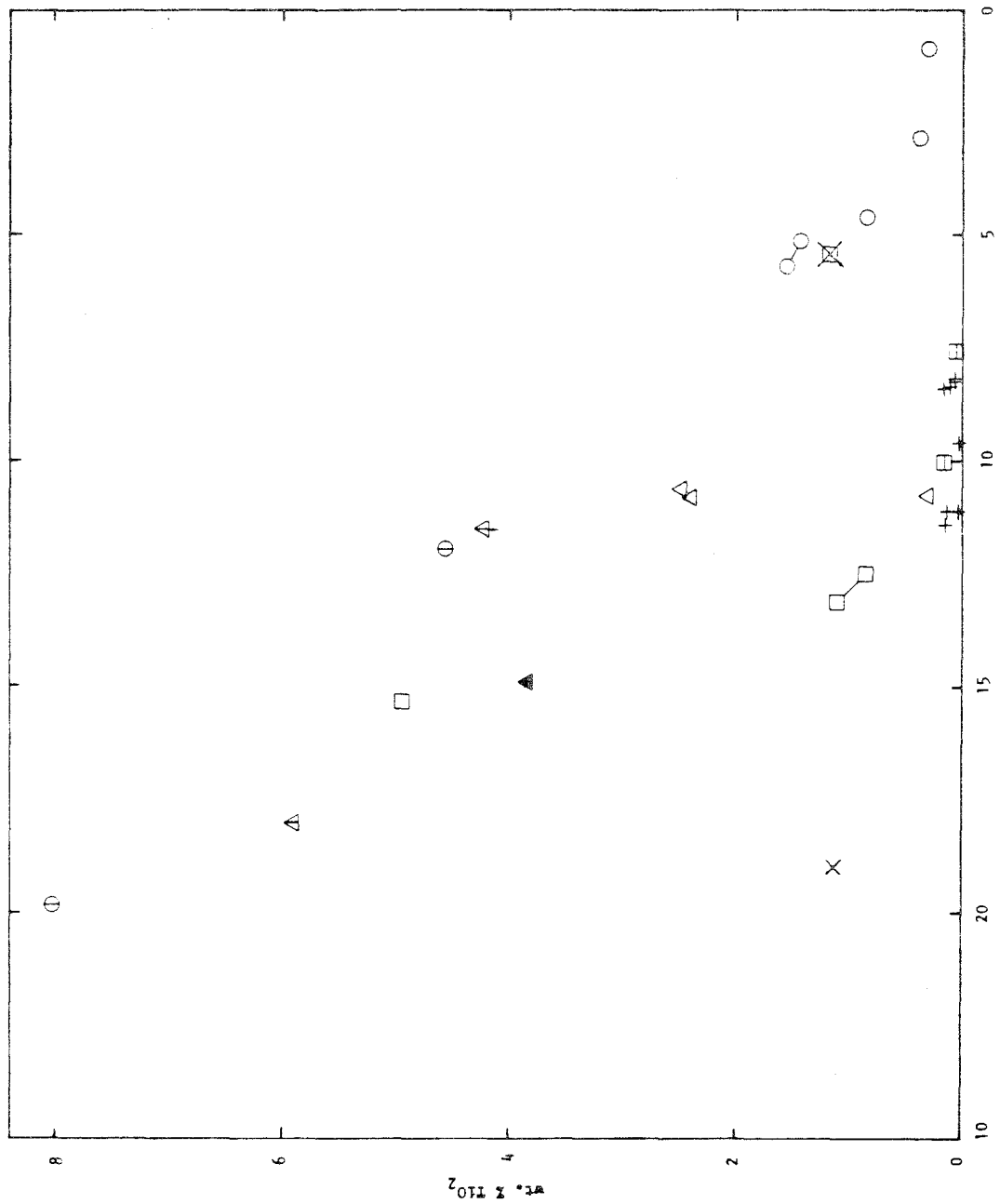

Figure 81. Weight percent TiO_2 vs. CaO+MgO. Symbols explained in text.

(8) Wt. % normative apatite vs. ilmenite + magnetite (Figure 82): Philpotts (1967) pointed out that some oxide-rich deposits associated with anorthositic rocks contain apatite in proportions of about 1 apatite to 3 opaque oxides by weight. He suggested that the constant proportions were due to formation of an apatite-ilmenite immiscible liquid. There is a very rough positive correlation between the variables in Figure 82, but the points do not lie along the line of 1:3 ratio shown on the diagram. This suggests that a more likely alternative to liquid immiscibility is accumulation of apatite and oxide minerals by crystal settling.

(9) Two syenite specimens from adjacent outcrops were analyzed (1030 A and B): The uralitized syenite (1030A) has about twice the H_2O+ compared to unuralitized syenite (1030B) and a slightly higher ferric to ferrous iron ratio. Other than these two differences, the two rocks are compositionally very similar. These differences suggest that the uralitization process involved addition of water and oxidation of some of the iron, but that it did not result in major bulk rock chemical changes.

(10) Two leucogabbro specimens from the same outcrop were analyzed (1055 A and B, Figure 51). These analyses of ophitic leucogabbro (1055A) and non-ophitic leucogabbro (1055B) show that the iron to magnesium ratio is essentially identical, apparently unchanged by the process of recrystallization. Other differences, including higher titanium, magnesium, and total iron in 1055B are probably due to its higher color index. The similar iron to magnesium ratios and alkali contents indicate that the process of recrystallization did not produce major bulk rock compositional changes in these leucogabbros.

The chemical analyses indicate that all rocks of this body are relatively iron-rich, that they contain relatively high levels of TiO_2 and

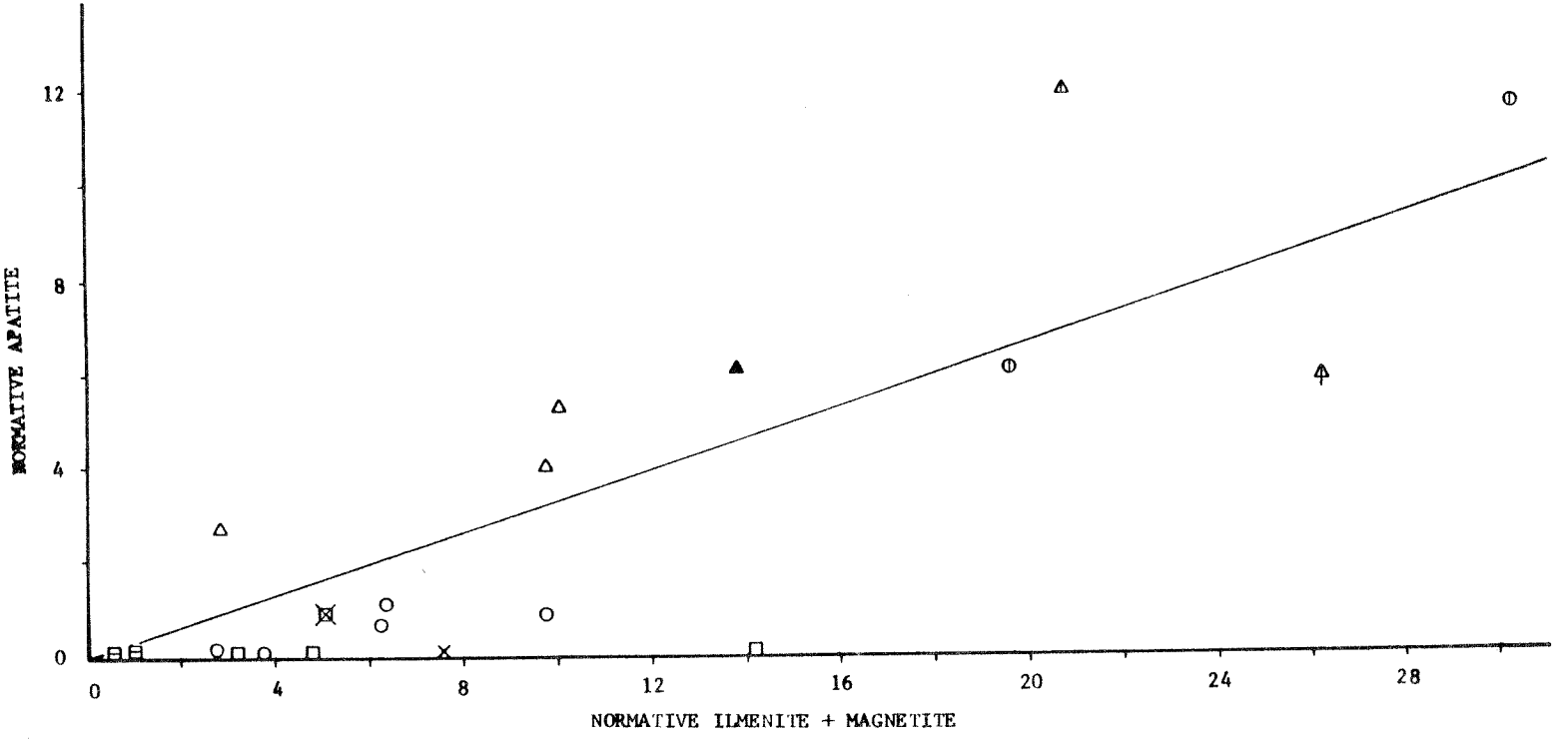

Figure 82. Normative apatite vs. ilmenite + magnetite. Line indicates apatite/oxide ratio of 1:3. Symbols explained in text.

P_2O_5 compared to many other igneous suites and that they share a number of other common chemical characteristics. Rocks of this suite form crudely defined lines on several variation diagrams but there is considerable scatter. On several of the diagrams (AFM, An-Ab-Or, SiO_2-K_2O) rocks of each of the three units define fields with very little overlap with the fields of the other units (Figure 83). It may be possible for rocks of the three units to be derived from the same parent magma by fractional crystallization or some other process. However, it seems more likely that some of the magmas which produced these rocks must have been independently generated, even though mixing of magmas occurred and they were all generated at about the same time and probably due to the same fundamental thermal or tectonic disturbance.

AVERAGE COMPOSITION

The average composition of the anorthosite-syenite body, as presently exposed in the western San Gabriel Mountains, was approximated by estimating the percentage of each major lithology present in the original body and multiplying the estimated average chemical composition of each lithology by its estimated proportion of the original body. Elsewhere, in the Soledad Basin a few kilometers to the north, and east of the San Andreas fault in the Orocopia, Chuckawalla and adjacent ranges about 250 kilometers to the southeast, exposed rocks of this body are predominantly syenitic. However, these exposures are either smaller, less well-exposed or structurally more fragmented than the San Gabriel exposure.

The anorthosite-leucogabbro unit is estimated to comprise about 73% of the total body and to include about 63% anorthosite, 32% leucogabbro and 5% gabbro. The syenite unit is estimated to comprise about 13% of

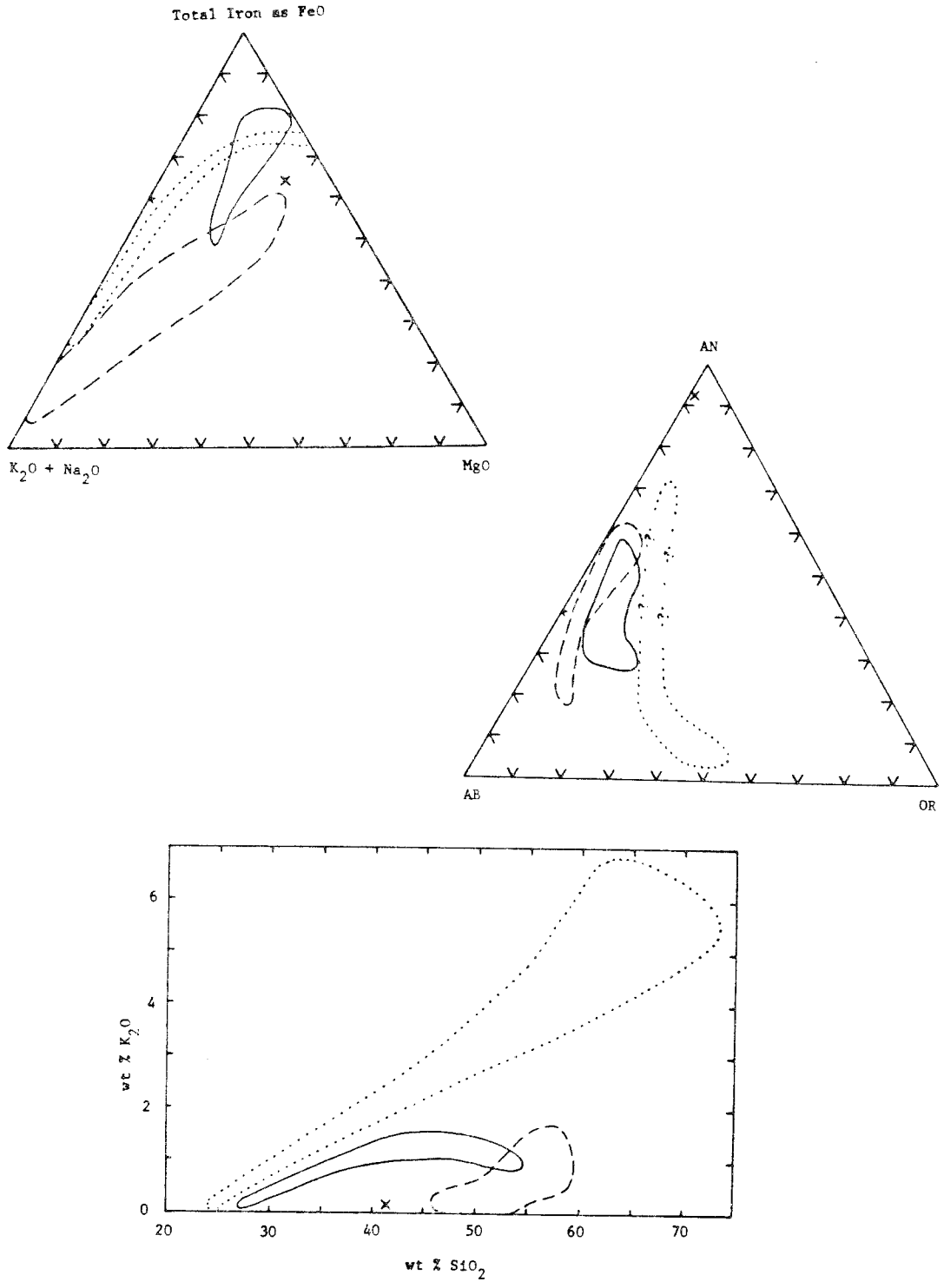

Figure 83. Comparison of the three units of the anorthosite-syenite body on AFM, An-Ab-Or and K_2O vs. SiO_2 diagrams. Dashed line, anorthosite-leucogabbro unit; dotted line, syenite unit; solid line, jotunite unit; (x), hornblende-bytownite gabbro (probably not part of the primary rock assemblage of the anorthosite-syenite body). Compare with Figures 75, 76, and 78.

the total body and to include about 90% syenite and 10% mafic rocks of the ultramafic syenite subunit. The jotunite unit is estimated to comprise about 14% of the total body and to include about 80% jotunite and 20% mafic rocks of the ultramafic jotunite subunit. These estimates indicate that the anorthosite-syenite body, as presently exposed in the San Gabriel Mountains, consists of about 46% anorthosite, 23% leucogabbro, 4% gabbro, 12% syenite, 11% jotunite and 4% ultramafite rocks. Table III lists the analyzed specimens thought to best characterize each of these six lithologies, and the resulting proposed average composition calculated from these data.

MINERAL COMPOSITIONS

Compositional data on minerals of the San Gabriel anorthosite-syenite body have been obtained by conventional flat stage thin section techniques and supplemented with a limited number of electron microprobe analyses. Approximate data from thin sections were used to outline ranges of compositional variations and to choose the specimens from which the more accurate electron microprobe data were obtained. These compositional data are incomplete--data are presented for typical examples of some of the major minerals but their detailed compositional variations were not determined. This section serves as a starting point for more detailed future work on mineral variations in the San Gabriel anorthosite-syenite body.

There is a gross mineralogical variation from the anorthosite-leucogabbro unit upward through the syenite and jotunite units. However, consistent compositional variations of individual minerals has not been

Table III: Proposed Average Composition of Each Lithology and of the Entire Anorthosite-Syenite Body in the San Gabriel Mountains

Lithology	Anorthosite	Leucogabbro	Gabbro	Syenite	Jotunite	Ultramafite	Average	Average
Analyses and Proportions used to calculate averages	18(1/2) + 1033(1/2)	276(1/3) + 1055A(2/3)	1032	708(1/2) + 1030A(1/2)	11(1/3) + 32(1/3) + 100(1/3)	102C(1/3) + 335(1/3) + 287(1/3)	Compo. of the Entire Body	Compo. Less Water
Estimated percentage of each lithology in the entire body	46	23	4	12	11	4		
SiO_2	55.80	50.30	57.15	57.62	50.09	31.12	53.07	53.73
TiO_2	0.10	2.22	1.17	0.91	1.73	6.18	1.16	1.17
Al_2O_3	27.05	21.37	19.84	16.27	15.98	6.08	22.06	22.33
Fe_2O_3	0.41	1.72	1.90	3.04	2.62	8.01	1.64	1.66
FeO	0.60	4.98	4.45	6.39	10.35	24.36	4.48	4.54
MgO	0.13	3.46	1.08	0.67	3.47	8.45	1.70	1.72
CaO	8.68	10.00	4.34	3.35	7.36	8.17	7.98	8.08
Na_2O	5.83	4.10	7.10	4.84	4.26	1.16	4.99	5.05
K_2O	0.56	0.30	1.57	5.26	1.13	0.74	1.17	1.18
H_2O+	0.55	1.00	0.89	0.72	0.99	0.93	0.76	
H_2O-	0.36	0.64	0.44	0.52	0.33	0.61	0.46	
MnO	0.01	0.06	0.08	0.16	0.25	0.48	0.08	0.08
P_2O_5	0.06	0.02	0.36	0.22	1.67	4.09	0.41	0.42
S	0.03	0.04	0.04	0.05	0.07	0.11	0.04	0.04

recognized within individual subunits or units. For example, calcic andesine with no exsolved potassium-feldspar is abundant in the anorthosite-leucogabbro unit and is present in some rocks in the syenite and jotunite units as well, while antiperthitic sodic andesine is common in the latter two units and occasionally present in the former. Similarly, iron-rich olivine-augite assemblages are present in apparently normal stratigraphic position near the base of the syenite unit, and in several parts of the jotunite unit. Some of the important processes which affected the mineralogy of these rocks, such as postcumulous recrystallization, uralization of the primary ferromagnesians and exsolution in the feldspars have occurred in rocks from most or all parts of the body. Consequently, it is more appropriate to discuss the detailed mineralogy and some of the processes which affect it in this separate section rather than with the preceding general petrographic descriptions of the individual units and lithologies.

FERROMAGNESIAN MINERALS

General

Common primary ferromagnesian minerals in rocks of the San Gabriel anorthosite-syenite body include olivine, hypersthene (inverted pigeonite), augite, traces of uninverted pigeonite, red biotite, red-brown hornblende, and oxides. Important secondary ferromagnesian minerals include blue-green hornblende, fibrous uralite (amphibole), chlorite, and biotite. This section presents limited compositional data on olivine, the pyroxenes and secondary amphiboles.

Complete uralization of pyroxene and olivine is usual in all parts of the body but unaltered pyroxene and olivine is present in a few rocks

of the ultramafic and normal syenite subunits and throughout the jotunite unit (perhaps most commonly in the layered and ultramafic jotunite subunits). Figure 84 shows the approximate distribution of some of the unuralized rocks in the different parts of the anorthosite-syenite body and Appendix A gives the estimated modes of several rocks containing unaltered ferromagnesians. Unuralized rocks of the normal syenite subunit exhibit 0.2 - 3 millimeter granoblastic textures suggesting that they may have undergone recrystallization (Figure 85); the other unuralized rocks usually exhibit cumulate-like textures (Figure 68). The color index of unuralized rocks ranges from less than 25 to 100 with no apparent systematic variation with position in the body. The compositions of the feldspars in unuralized rocks is variable: a few contain plagioclase with compositions between An_{50} and An_{70} (based on flat-stage thin section observations); many contain slightly to moderately antiperthitic plagioclase with compositions between An_{25} and An_{40} (jotunite) and others contain highly antiperthitic plagioclase (mangerite) or mesoperthite (syenite). Antiperthitic plagioclase-bearing rocks are most common in the jotunite unit, but a few labradorite-bearing rocks are present in the ultramafic syenite subunit and a few mesoperthite-bearing rocks are present in the jotunite unit. Thus, the unuralized rocks do not display any systematic variation of feldspar composition with position in the body, nor is there any apparent systematic variation of feldspar composition as a function of color index.

There are some consistent patterns in rocks with unuralized ferromagnesians. It is evident that most rocks fall into two general ferromagnesian assemblages: (1) abundant olivine and augite with little or no orthopyroxene, and (2) abundant orthopyroxene with smaller amounts of

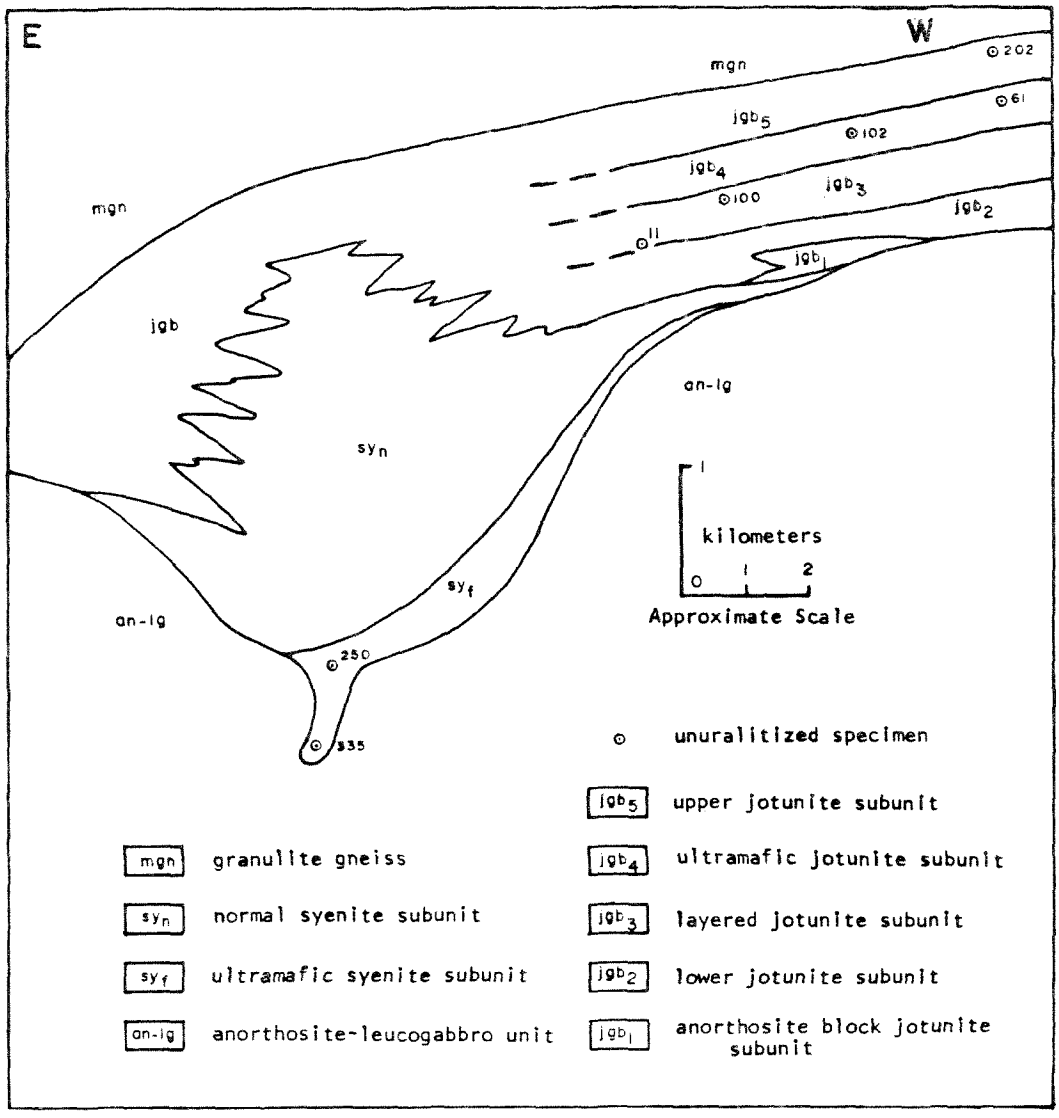

Figure 84. Diagrammatic section illustrating distribution of rocks with analyzed unuralitized ferromagnesians.

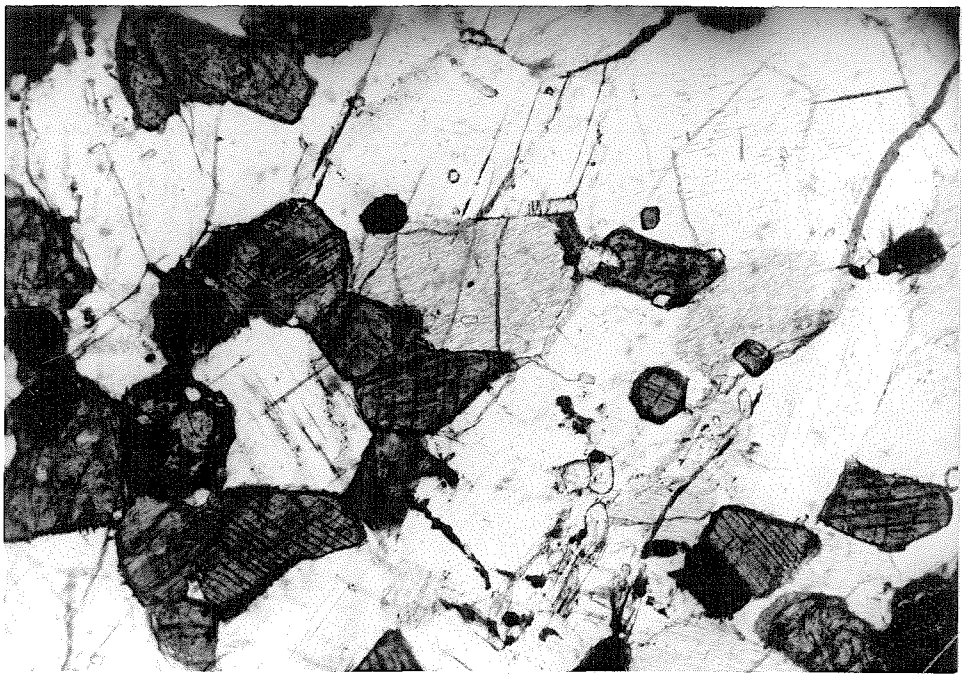

Figure 85. Granoblastic texture of mesoperthite, augite, and olivine in syenite. (plane light, 1.99 x 3.06 millimeter field).

augite and no olivine. Most of these rocks also contain several percent of either red-brown hornblende or red biotite (but rarely both) which were among the last minerals to crystallize, mostly as rims around pyroxene, olivine and especially the opaque oxide (Figure 73). Apatite and oxide together nearly always constitute about 35% of the non-feldspar part of the rocks, a proportion which seems to remain constant in rocks with color indices ranging from 25 to 100.

Pyroxene and olivine range from less than 1 millimeter equant crystals in some granoblastic rocks, through 1-10 millimeter equant to ophitic crystals in various rocks with cumulate textures, to occasional very large (to 20 millimeter) irregular hypersthene and skeletal olivine crystals. Many of these rocks have no secondary amphiboles but others show all degrees to almost complete alteration of the primary ferromagnesians (Figure 86).

Composition of Pyroxene and Olivine

The approximate compositions of some ferromagnesians based on flat stage thin section observations is included in Appendix A. More accurate compositions of pyroxenes and olivine in seven specimens were obtained with the electron microprobe. These data include analyses of olivine in three hypersthene in two, augite in seven, and zoned augite-pigeonite crystals in two specimens. Most of these specimens were collected before the structure of the body was well understood and, consequently, they come from widely separated locations and the exact position of some of them in the stratigraphic sequence is uncertain. For example, specimen 335 lies near the base of the ultramafic syenite subunit but was probably intruded into this structural position, specimen 100 lies near a

Figure 86. Granoblastic syenite. Note the darker rims of blue-green hornblende around augite, the uralitic alteration of the margins of the augite crystals, and the olivine partially altered to opaque oxide and overgrown by augite which is now partially uralitized (1030B, plane light, 1.99 x 3.06 millimeter field).

large fault in an area where the ultramafic jotunite subunit is absent and so its position in the vertical sequence is uncertain, and specimen 202 lies many kilometers from most other specimens in an area where the different jotunite subunits could not be distinguished. The approximate location of each specimen in the sequence is shown diagramatically in Figure 84.

The average compositions of each mineral in these specimens are shown in Figure 87. Compositional variation with vertical position is not very evident; the $FeSiO_3/FeSiO_3+MgSiO_3$ ratio of augite in each rock is plotted as a function of probable relative vertical position in the sequence in Figure 88. With the exception of a few small (1 millimeter or less) zoned pigeonite-augite crystals in two rocks, pyroxene and olivine crystals appear to be either unzoned or only very slightly zoned (at most 2% variation). For this reason, only the average compositions of the 2 to 25 points analyzed are plotted in Figures 87 and 88. Most rocks containing unaltered ferromagnesians display structural evidence indicating their origin by bottom crystal accumulation. Because of this, the composition of the rocks and their constituent minerals would be expected to vary systematically with vertical position if the rocks formed from a single differentiating magma. Figure 88 shows that such a systematic variation does not exist, and that the lowest rock in the sequence (335-ferrosyenite from the ultramafic syenite subunit) actually contains the most iron-rich augite. This rock is, therefore, the most highly differentiated of the rocks analyzed, and even though it was probably intruded into its present position, it is part of the lowest of the stratigraphic units with unaltered ferromagnesians. In contrast, the other rock from this subunit (250) contains considerably less iron-enriched

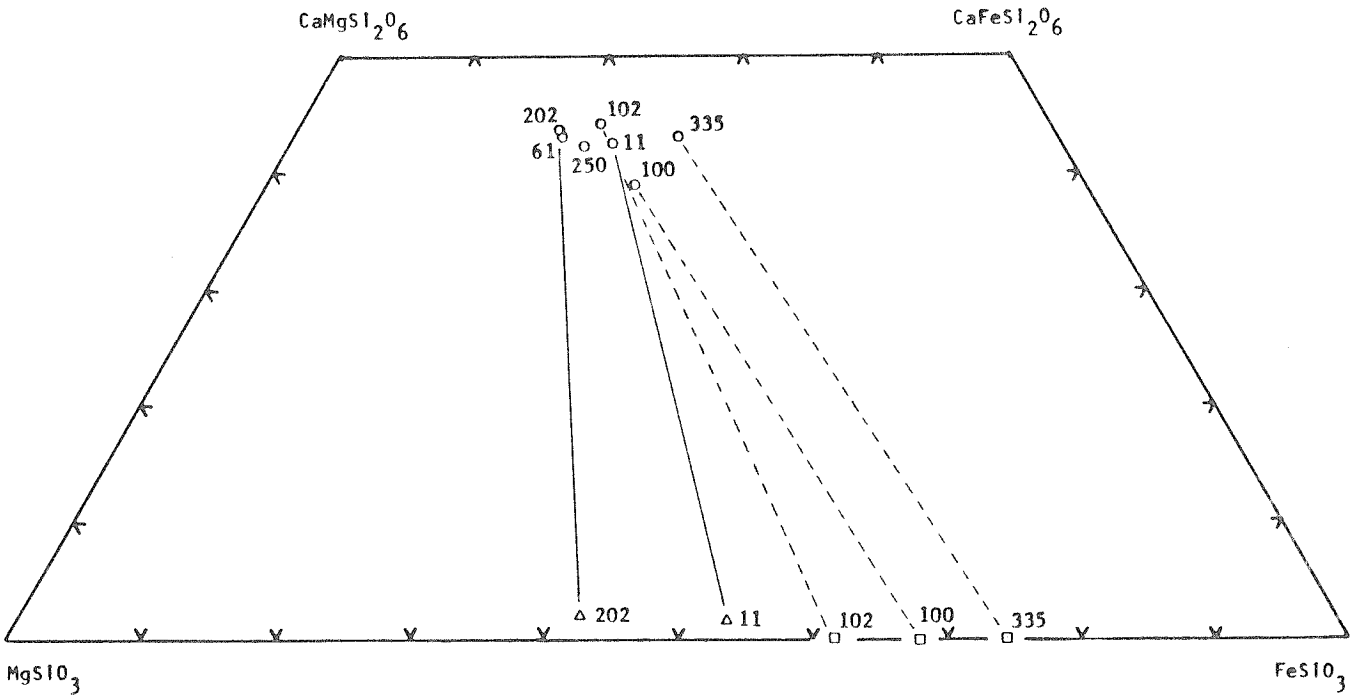

Figure 87. Average composition of pyroxene and olivine in unuralitized rocks. Squares indicate olivine, circles indicate augite and triangles indicate hypersthene. Lines connect coexisting minerals in the same rock. Sample numbers are indicated (see Figure 84).

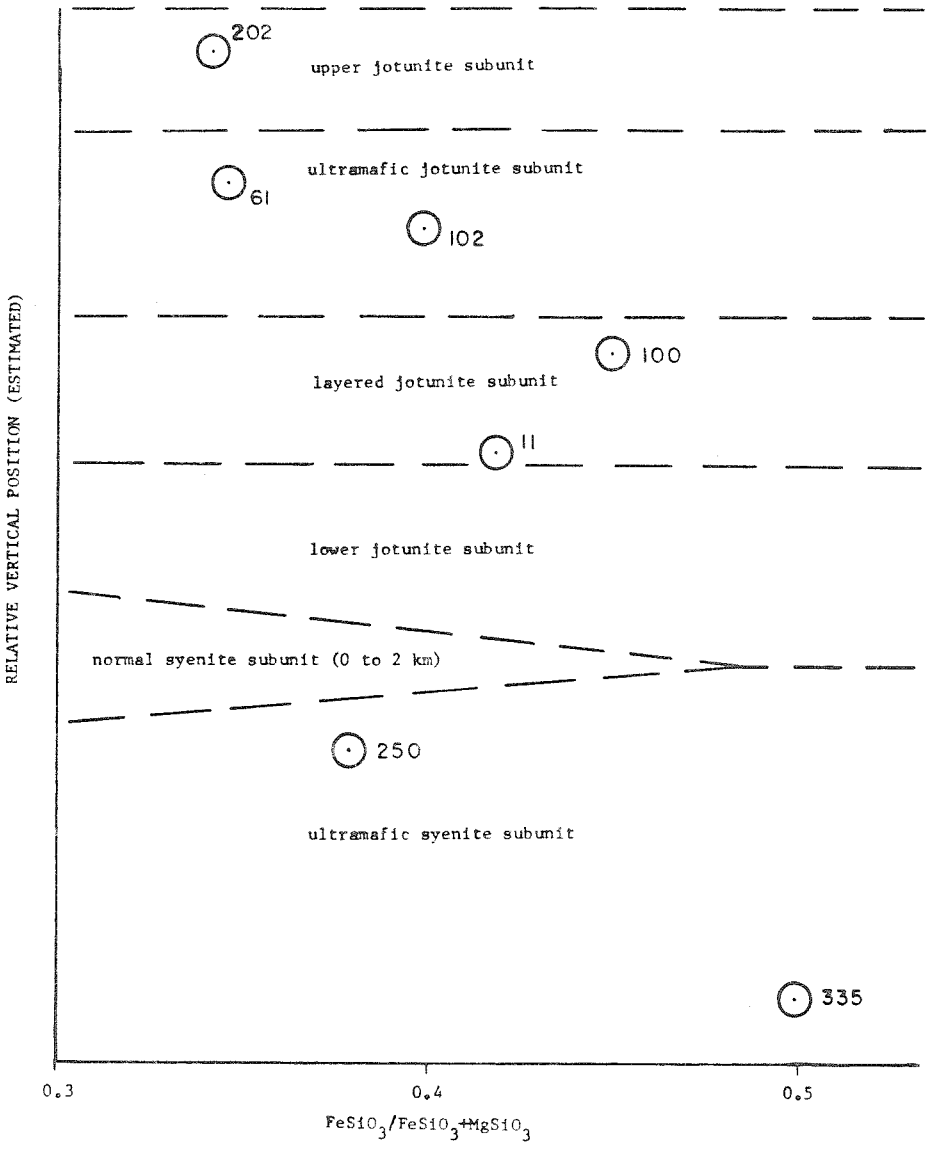

Figure 88. Average composition of augite versus estimated vertical position in the syenite and jotunite units. Approximately 3 to 4 kilometers vertical section, excluding the normal syenite subunit (see Figure 84).

ferromagnesians. Rocks from the jotunite unit have ferromagnesians with variable compositions, generally less iron-enriched in the higher subunits compared to the lower subunits.

Since the structural evidence indicates that these rocks formed by bottom accumulation, it seems most likely that the total sequence (ultramafic syenite and all jotunite subunits) was produced by a series of magma injections, each of at least slightly different composition. Major injections of new magma could have produced each individual subunit. However, in several instances, substantially different compositions are present within an individual subunit, so either compositions changed substantially due to differentiation within individual subunits, or else several injections of new magma occurred during formation of some subunits. It is not possible to answer these questions with the present data. Many samples collected to date in this study are of uncertain relative vertical position in the rock sequence, in part due to the necessity of correlation over long distances along the strike. Sporatic preservation of unaltered ferromagnesian minerals makes it difficult to obtain a sequence of specimens through individual subunits at a given location.

The data do suggest that repeated injection of new magma occurred during formation of the syenite and jotunite units. Non-systematic vertical variation of color index, feldspar composition, pyroxene and olivine composition, and the non-parallelism of augite-olivine tie lines all might be explained as the result of multiple magma intrusions.

Pyroxene Exsolution and Inversion

Hypersthene in all of these rocks contains lamellae which appear to have originated by exsolution. Most hypersthene exhibits 2 sets of clinopyroxene lamellae (Figure 89). The earlier coarser lamellae exsolved parallel to the (001) plane of primary pigeonite, and after inversion of pigeonite to hypersthene the later finer lamellae exsolved parallel to the (100) plane of the hypersthene (Deer, et al., 1978). Some large hypersthene crystals consist of two to ten or more domains containing sets of coarse exsolution lamellae of different orientations (Figure 90). These domains of differently oriented lamellae in a single hypersthene crystal show that a single hypersthene crystal has formed by inversion of several differently oriented, contiguous pigeonite crystals, each of which exsolved its own set of lamellae prior to inversion. This probably occurred because inversion did not take place immediately when the temperature dropped below the stability field of pigeonite. After cooling below the inversion temperature, nucleation of hypersthene occurred somewhere in one of the pigeonite crystals and the inversion spread through the original crystal and on into other contiguous pigeonite crystals. Thus, this texture probably results from the relatively rapid growth of the first hypersthene nucleus compared to the rate of formation of new nuclei. In the usual case, all contiguous pigeonite crystals were inverted to a single hypersthene crystal which exsolved a second set of fine clinopyroxene lamellae parallel to its (100) plane (Figure 91).

There are uncommon examples of coarse clinopyroxene lamellae which extend across the contact between two differently oriented hypersthene crystals (Figure 92). This resulted when a second hypersthene nucleus

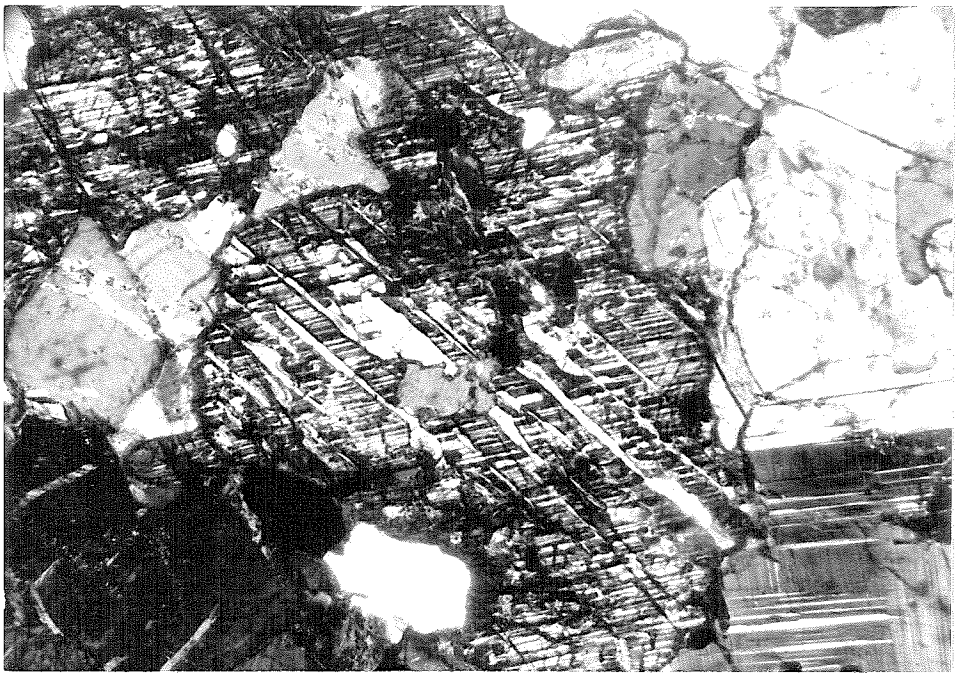

Figure 89. Part of a large hypersthene crystal (inverted pigeonite) exhibiting two sets of clinopyroxene lamellae. Note the irregular changes in thickness and occasional coalescence of adjacent lamellae of the coarser set (crossed nicols, 2.06 x 3.19 millimeter field).

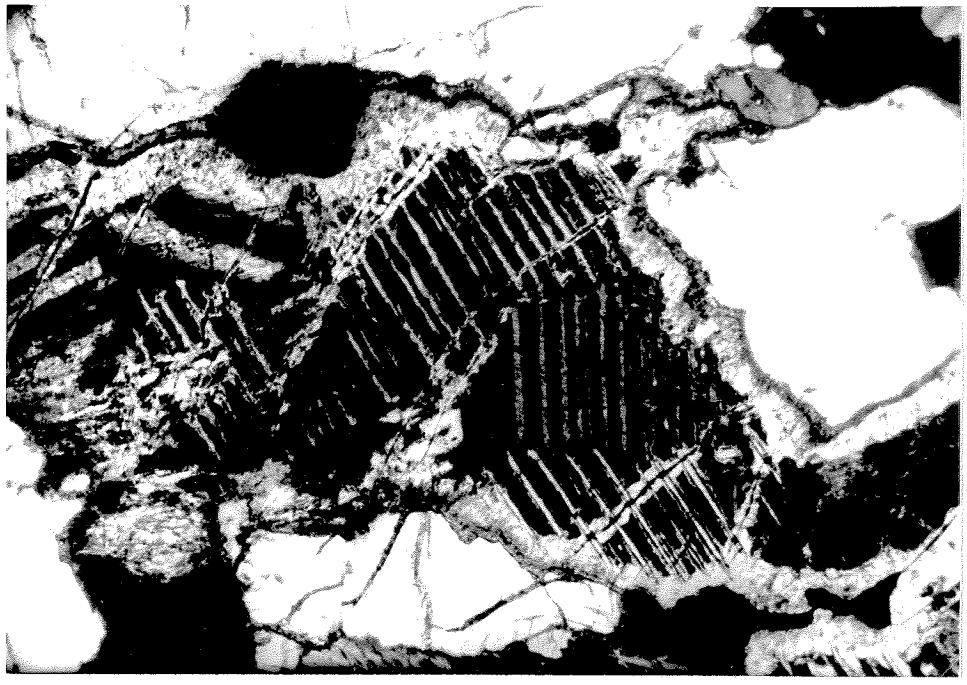

Figure 90. Several differently oriented sets of coarse exsolution lamaellae in a single hypersthene crystal (at extinction). Note the dark rims (blue-green hornblende) on pyroxene, and the lighter, fibrous uralite formed interior to the rims and along cracks. Note the anti-perthite in the upper right corner (crossed nicols, 2.06 x 3.19 millimeter field).

Figure 91. A single large hypersthene crystal in jotunite, containing sets of coarse augite lamellae of several different orientations. Each set of coarse lamellae exsolved from a separate pigeonite crystal along the (001) plane. When inversion occurred, a single hypersthene crystal nucleated and grew to transform all the different pigeonite crystals. Upon inversion, exsolution produced the set of fine lamellae parallel to the (100) plane of hypersthene (sub-horizontal). (crossed nicols, 7 x 11 millimeter field).

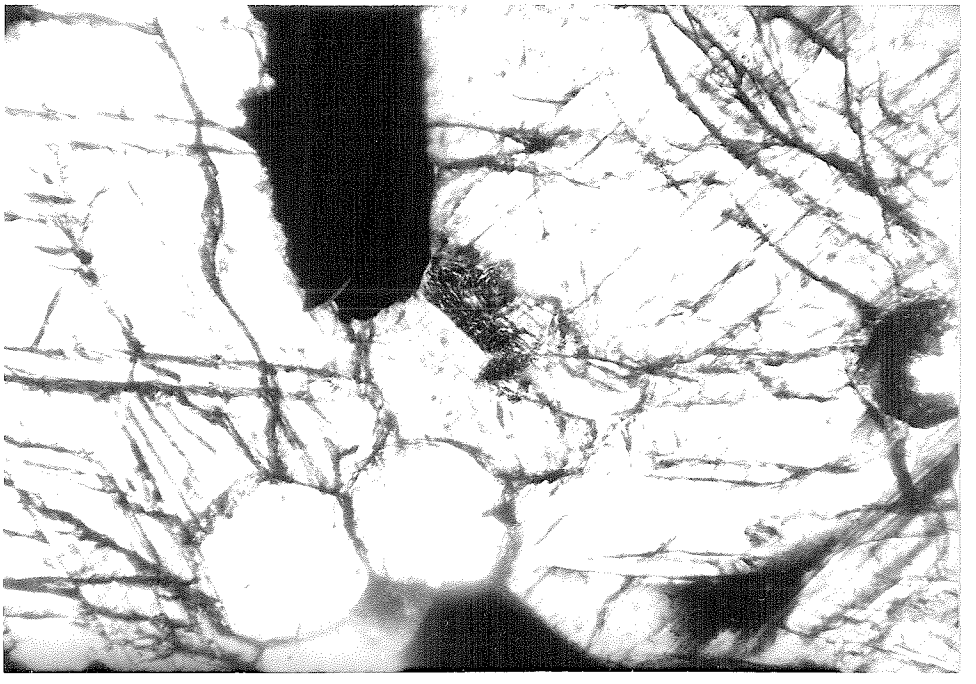

Figure 92. Part of a contact between two differently oriented hypersthene crystals. The contact runs through the apatite and ilmenite grains near the center of the field. Coarse horizontal augite lamellae, exsolved parallel to the (001) plane of a single pigeonite crystal are present in both hypersthene crystals. (plane light, 0.50 x 0.76 millimeter field).

formed somewhere in a contiguous group of pigeonite crystals before all the pigeonite was inverted to the first orientation. This would produce two hypersthene crystals of different orientations which might have a contact which cuts through a domain which originated as a single pigeonite crystal. Examples of this relationship are uncommon, which indicates that growth of hypersthene nuclei was relatively rapid compared to the rate of formation of new nuclei during cooling of these rocks.

Eight specimens contain small amounts of uninverted pigeonite, some as small (less than 1 millimeter) irregular uninverted patches in the cores of hypersthene crystals, and some as very small (less than 0.4 millimeter) zoned pigeonite-augite crystals (Figures 93, 94). The compositional ranges of two pigeonite-augite crystals in a rock from the jotunite unit are shown in Figure 95. One of the pigeonite-bearing rocks is from a dike in gneiss forming the roof of the anorthosite-syenite body, five are from the jotunite unit and two are from the syenite unit. The dike rock is almost completely uralized but the others have undergone at most about 25% uralization of the primary ferromagnesians. The color index ranges from 25 to 65 and the plagioclase composition is about An_{25-20} in the pigeonite-bearing rocks. The feldspars of all of these rocks contain substantial exsolved potassium feldspar which ranges from an estimated 5% to 50% or more of the total feldspar. The presence of uninverted pigeonite in these rocks suggests that cooling was sufficiently rapid that inversion ceased before all pigeonite disappeared. These are apparently deep-seated rocks but structural uncertainties permit the possibility that all the pigeonite-bearing rocks could have crystallized within one to two kilometers of the roof of the intrusion. The presence of uninverted pigeonite might indicate that at least some rocks of the San Gabriel anorthosite-syenite body crystallized at relatively shallow depth.

Figure 93. A large pyroxene crystal in jotunite (note the tabular cumulate plagioclase crystals). Most of the crystal is hypersthene (inverted pigeonite) but a core of uninverted pigeonite remains (near extinction). The central part of the zoned pigeonite core is calcium-depleated relative to its rim in contact with hypersthene. (crossed nicols, 2.06 x 3.19 millimeter field).

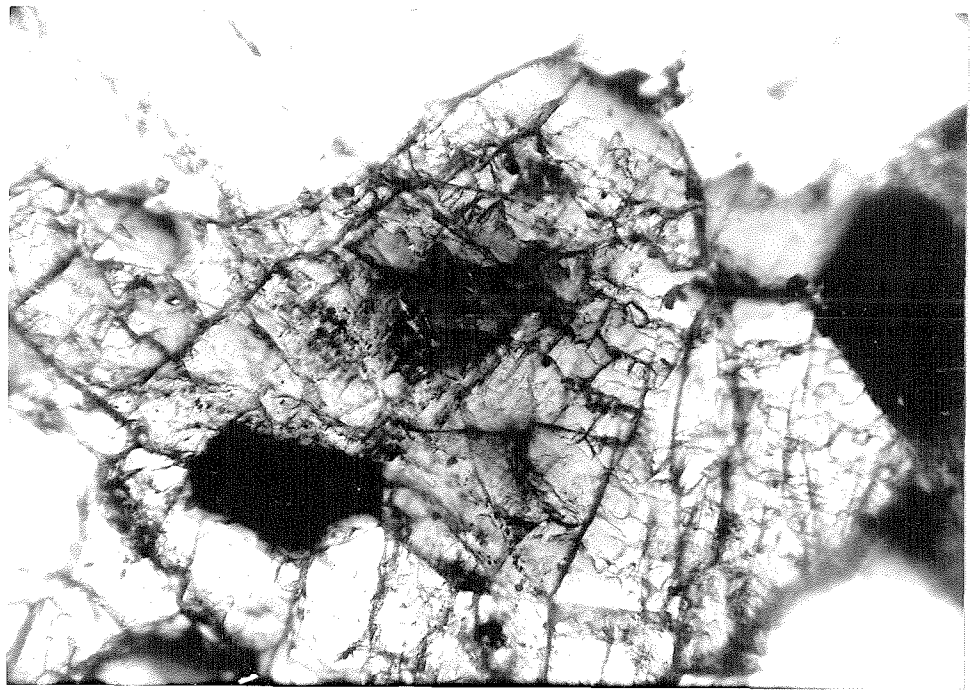

Figure 94. Zoned pigeonite-augite crystal in jotunite. The central pigeonite is near extinction. (100, crossed nicols, 0.50 x 0.76 millimeter field).

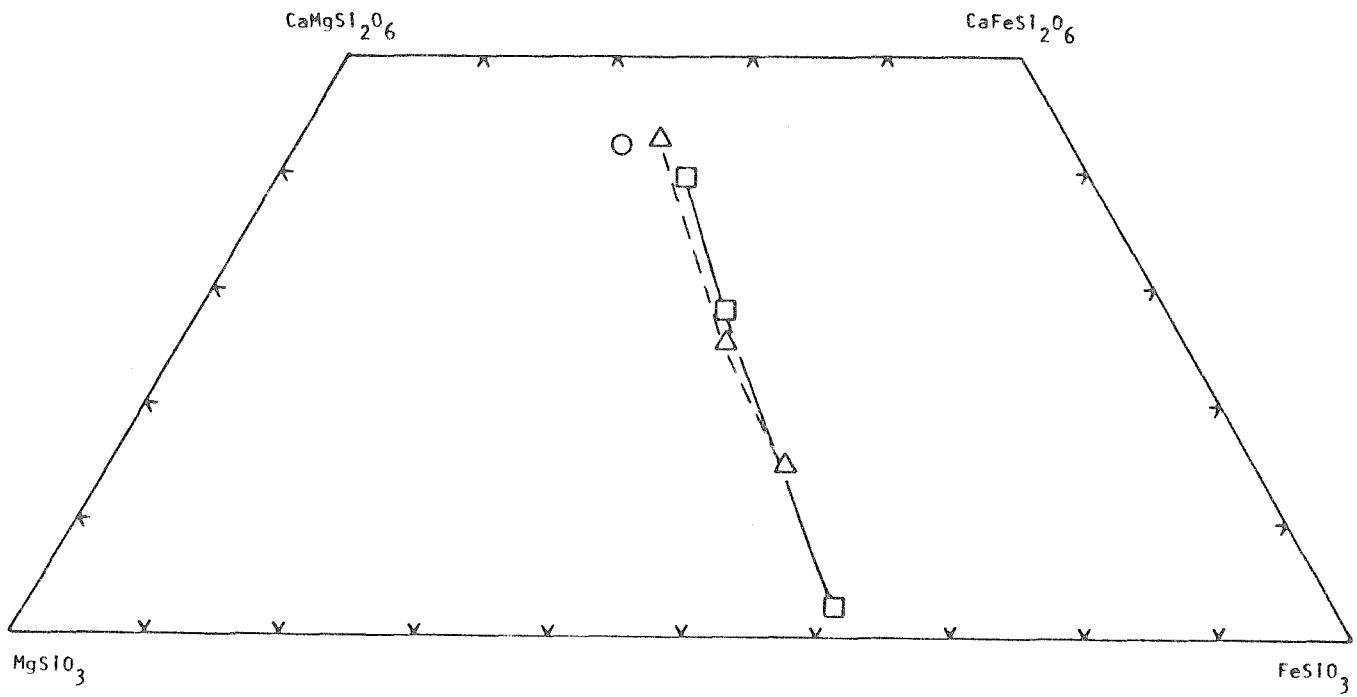

Figure 95. Compositions of zoned pigeonite-augite crystals in jotunite (11). Triangles and squares are two different crystals, each with gradual compositional change between the Ca-rich and Ca-poor extremes. Circle is composition of most augite (unzoned) in the rock.

Inclusions

Striking patterns of opaque oxide inclusions in pyroxene are common in some rocks of the anorthosite-syenite body. In several jotunite rocks large hypersthene crystals contain cores of graphically intergrown opaque oxide and hypersthene (Figure 96). These intergrowths suggest that hypersthene grew around an original mineral which later broke down to form a mixture of oxide and hypersthene. Comparison of these textures with those of some olivine-pyroxene rocks (Figure 86) suggests that the original mineral might have been olivine.

A second pattern of opaque oxide inclusions is present in augite in a few augite-olivine rocks. This pattern consists of numerous minute (0.01 - 0.001 millimeter) lamellae intergrown in at least two directions (Figures 97, 98). These lamellae are very abundant in the cores and are much less abundant or completely absent in the rims of the augite. Electron microprobe analyses of augite from specimen 335 shows that the cores and the rims are almost identical in composition.

Uralitic Alteration of Pyroxene and Olivine

One of the most striking features of the San Gabriel anorthosite-syenite body is the characteristic pervasive uralization of the primary ferromagnesians in almost all of its rocks. Pseudomorphic lamellae, cleavage traces and crystal form, along with occasional relict pyroxene, indicates that pyroxene underwent the normal sequence of crystallization, cooling and exsolution described above (Figure 99). In the usual sequence, primary pyroxene was first overgrown by rims of radiating blue-green hornblende and, subsequently, underwent alteration to uralite.

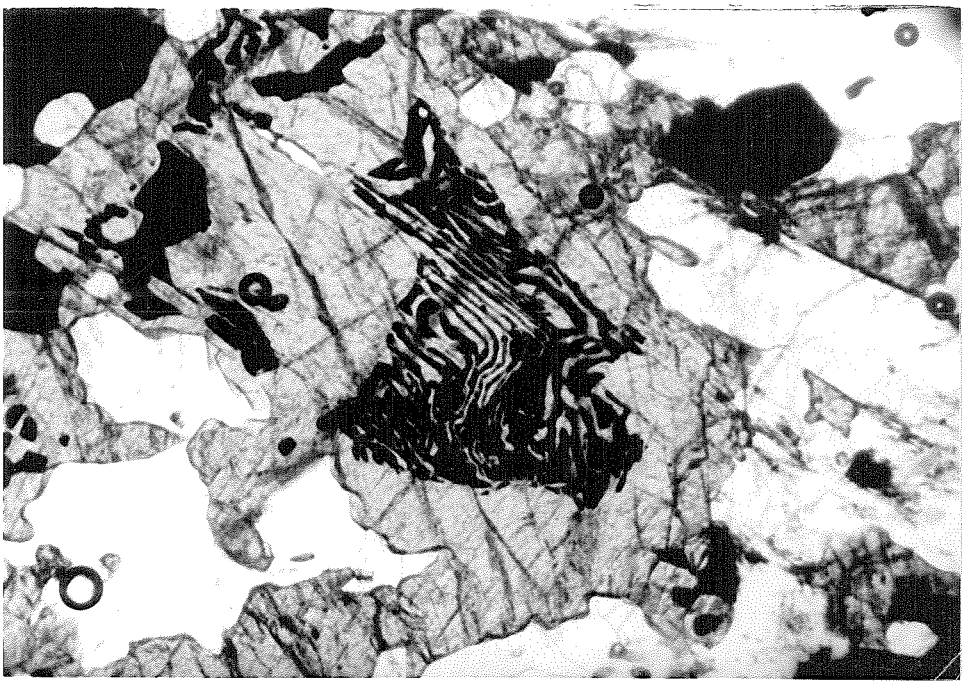

Figure 96. Graphic intergrowth of opaque oxide and hypersthene in the core of a larger hypersthene crystal. Note that the hypersthene in the core is of slightly different optical orientation than that of the surrounding crystal (plane light, 2.06 x 3.19 millimeter field).

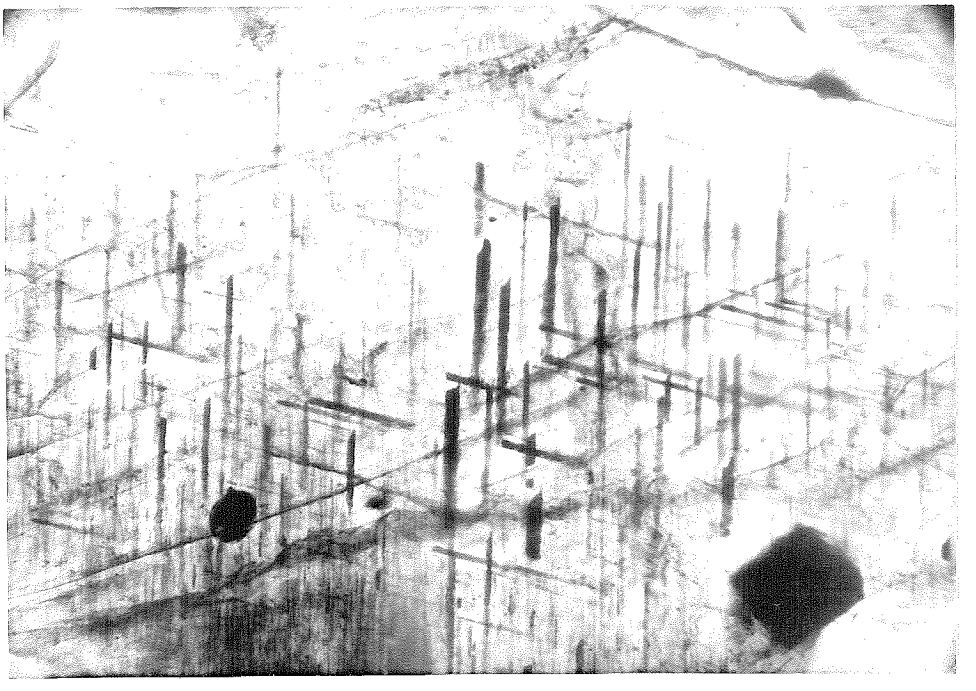

Figure 97. Fine opaque oxide lamellae in augite. Three zones can be distinquished: (1) marginal parts of the crystal contain no oxide lamellae, (2) more central parts contain numerous coarse lamellae, and (3) the core contains numerous very fine lamellae, most of them in the same orientation. (335, plane light, 0.50 x 0.76 millimeter field).

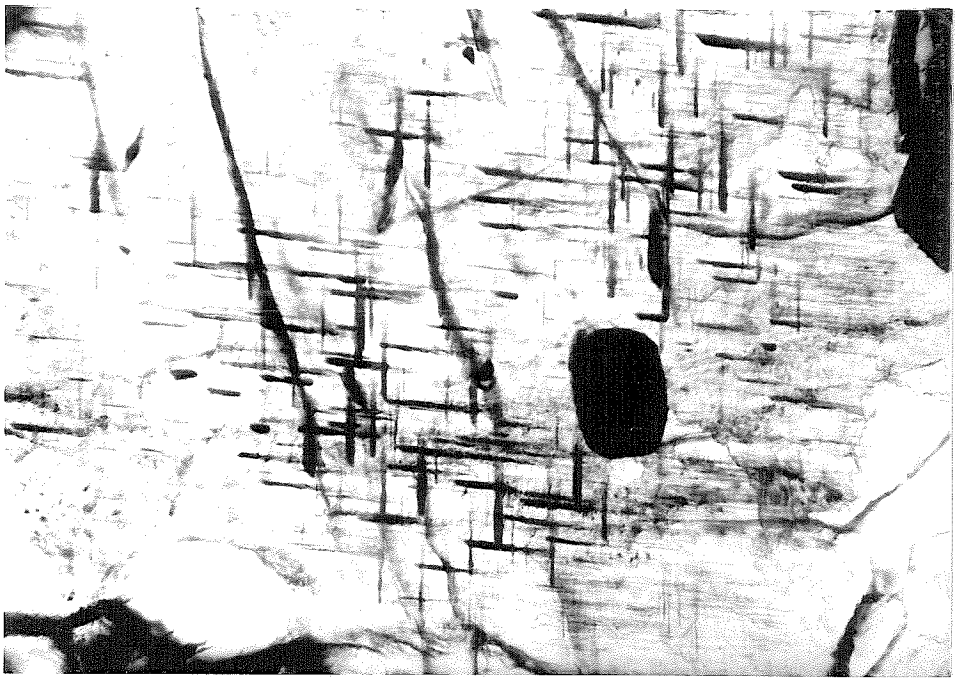

Figure 98. Two sets of fine opaque oxide lamellae in the central part of an augite crystal in ferrosyenite. (335, plane light, 0.50 x 0.76 millimeter field).

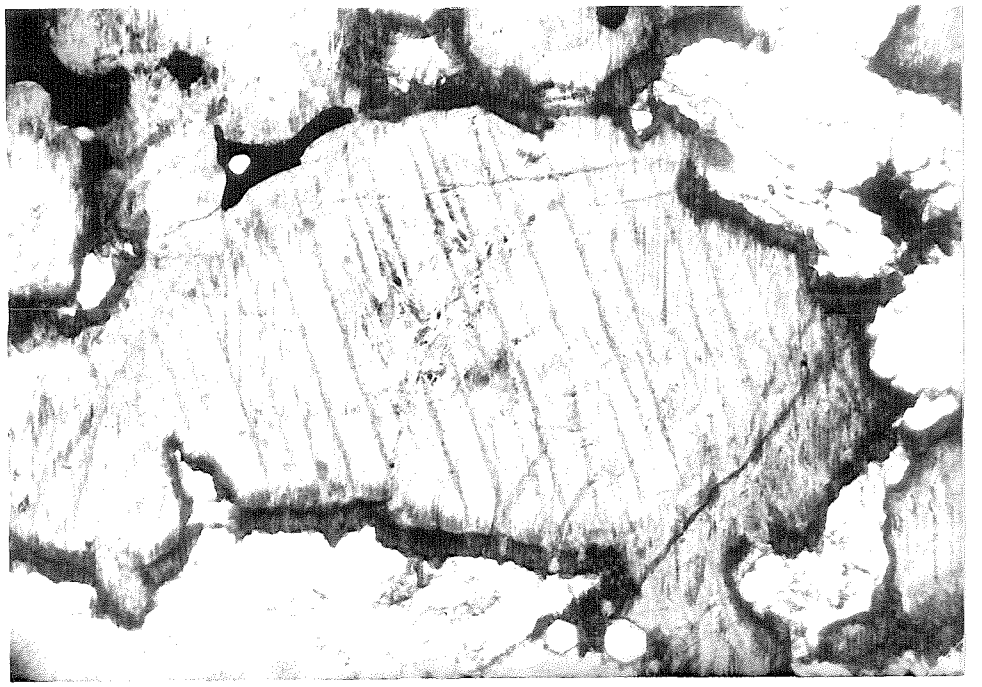

Figure 99. Uralite pseudomorph after primary pyroxene, with a rim of blue-green hornblende. All the pyroxene has been altered to uralite, but both coarse and fine lamellae are visible, the latter as zones of abundant very fine opaque oxide grains. (plane light, 2.06 x 3.19 millimeter field).

Partially uralized pyroxenes are altered on their margins and along fractures (Figure 100). Complete uralization occurred in nearly all rocks of the anorthosite-leucogabbro unit and in most rocks of the syenite and jotunite units. In these rocks the degree of uralization appears to be uniform, even in the cores of crystals which were more than a meter in diameter. Uralization is uniform throughout the anorthosite-leucogabbro unit, showing no recognized relationship to any geographic area, geologic contact or deformation zones.

In rocks of the syenite unit, alteration aggregates commonly resemble those in the underlying rocks, but frequently are bordered by wider rims of blue-green hornblende, and contain biotite, quartz, chlorite and epidote along with the uralitic amphibole. A few of the pyroxene rocks (with or without olivine) of the jotunite unit contain relict unaltered ferromagnesians, but only the iron-rich olivine-augite rocks in the ultramafic syenite and ultramafic jotunite subunits show complete absence of uralitic alteration. In these late, iron-rich rocks brown hornblende and red biotite are late-forming minerals which overgrow olivine and pyroxene.

Electron microprobe analyses of alteration amphiboles were obtained in two leucogabbro specimens: 1055B from near the base of the anorthosite-gabbro unit and 276 from near its top. Both interior uralite and blue-green hornblende rims were analyzed in 1055B, and interior uralite was analyzed in 276. The average compositions of these three amphiboles are shown in Table IV and are plotted on a graph of formula proportion ($K_2O + Na_2O$) vs. formula proportion FeO in Figure 101.

There is a regular variation of alkali content with iron content as well as with Fe/Fe+Mg ratio in all analyzed amphiboles from a given

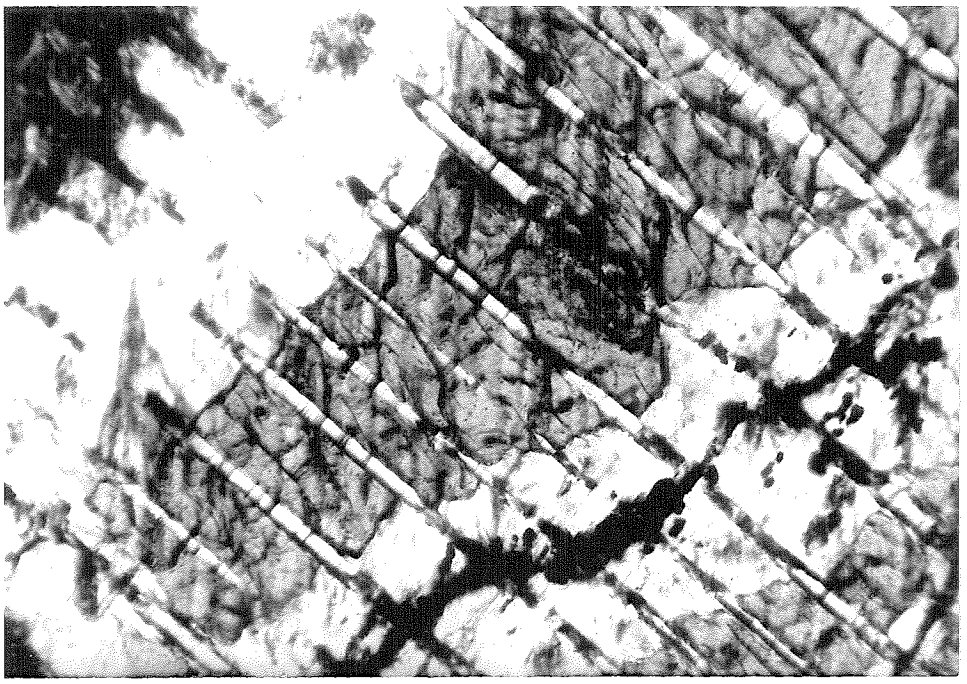

Figure 100. Uralitic alteration of a hypersthene crystal, both marginally and along a crack through the crystal. Clinopyroxene lamellae extend outward into zones of altered hypersthene. Note the concentration of opaque oxide in the areas of altered clinopyroxene lamellae, leaving ghost lamellae in the uralite after complete alteration of all pyroxene. (crossed nicols, 0.50 x 0.76 millimeter field).

Table IV: Compositions of Representative Amphiboles (Electron Microprobe, 10 micron spot)

1055B-15 Blue-green hornblende rim around uralite.

$(K_{0.06}Na_{0.39})Ca_{1.87}(Mg_{2.47}\ Fe_{1.84}Mn_{0.02}Ti_{0.03}Al_{0.76})(Si_{6.53}Al_{1.47})O_{22}(OH_{1.92}F_{0.06}Cl_{0.02})$

1055B-12 Amphibole from interior uralite

$(K_{0.02}Na_{0.26})Ca_{1.83}(Mg_{3.02}Fe_{1.63}Mn_{0.02}Ti_{0.04}Al_{0.46})(Si_{6.97}Al_{1.03})O_{22}(OH_{1.98}Cl_{0.02})$

276-5 Amphibole from interior uralite

$(K_{0.08}Na_{0.32})Ca_{1.44}(Mg_{2.30}Fe_{2.17}Mn_{0.02}Ti_{0.05}Al_{0.52})(Si_{6.64}Al_{1.36})O_{22}(OH_{1.98}Cl_{0.02})$

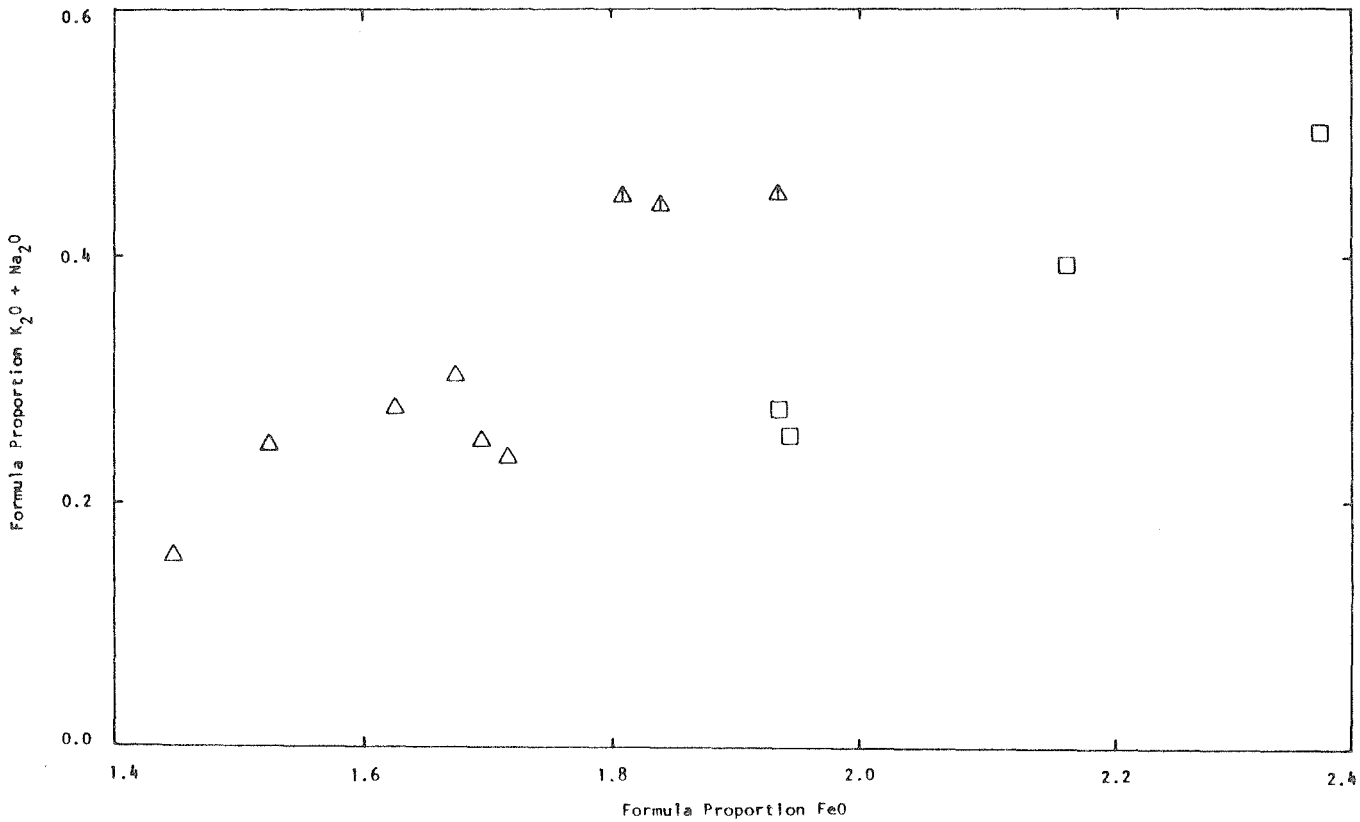

Figure 101. Compositions of amphiboles in uralite pseudomorphs after pyroxene. Triangles are from leucogabbro 1055 (open triangles are interior uralite, triangles with bars are blue-green hornblende rims). Squares are from leucogabbro 276.

rock. Both alkalis and iron increase toward the margin of the pseudomorph with the highest levels found in the blue-green hornblende rim. The iron content and Fe/Fe+Mg ratio increases from the inner to the outer part of the blue-green hornblende rim, but total alkalis and Na/Na+Ca remain constant.

The above observations need to be extended. The correspondence of electron microprobe analyses of individual amphibole crystals with the bulk composition of the uralite pseudomorph must be determined, as well as the uniformity of uralite and blue-green hornblende compositions within a single psuedomorph and in a given specimen. Compositional changes accompanying uralization should be determined, and it may ultimately be possible to determine the type of original pyroxene by analysis of uralite pseudomorphs. Compositional variations of uralite along the strike and across the strike of layered gabbroic rocks and in the vicinity of recrystallized jotunitic rocks may yield information concerning the nature of the fluids which produced uralization and the way in which they migrated through the rocks.

FELDSPARS

General

Feldspars are the most abundant minerals in the San Gabriel anorthosite-syenite body. The feldspars range from intermediate through sodic plagioclase to alkali feldspar. Much plagioclase more sodic than An_{35} is generally antiperthitic, containing variable amounts of small lamellae, blebs or patches of potassium feldspar. Most of the alkali feldspar is mesoperthitic, consisting of a very fine intergrowth of

lamellae of potassium feldspar and oligoclase. Feldspars have been studied extensively in thin section, and the electron microprobe has been used to analyze feldspars in several rocks and grain mounts.

Rocks of the anorthosite-leucogabbro unit contain plagioclase commonly between An_{35} and An_{55} in composition. Rocks of the syenite unit contain some plagioclase as clacic as An_{40} but most of them contain predominantly mesoperthite alakli feldspar. Most rocks of the jotunite unit contain antiperthitic plagioclase between An_{20} and An_{40} in composition. Several outcrops of feldspathic hornblende gabbro near the northeastern margin of the anorthosite-syenite body contain zoned bytownite or labradorite. The coarser gabbros contain plagioclase cores at least as calcic as An_{90} overgrown by plagioclase which, in some cases, is at least as sodic as An_{40}. These hornblende-bytownite gabbro bodies are not considered part of the primary rock assemblage of the anorthosite-syenite body, and they are not discussed further in this section.

Composition

The compositions of feldspars in rocks of the syenite and jotunite units were obtained using conventional thin section techniques. The electron microprobe was used to obtain compositions in four polished thin sections of three analyzed specimens: 1055A and B and 276 (leucograbbros respectively from near the bottom and near the top of the anorthosite-leucogabbro unit). Additional microprobe data were obtained on feldspar grain mounts made from 40 specimens collected along Angeles Forest highway in Mill Creek and along the Mt. Gleason-Magic Mountain road east of North Fork Saddle (Plate I).

Analyses of individual crystals in thin section show variation of 2% - 3% anorthite content, but this variation is not consistent with systematically more sodic rims and calcic cores. The statistics are poor, but concentric compositional zoning does not appear to be present in feldspars of the anorthosite-leucogabbro unit.

Cumulate plagioclase tablets surrounded by uralite in ophitic leucogabbro (1055A-1) have compositions between An_{49} and An_{52}. In the same thin section, plagioclase from the anorthosite matrix (1055A-1) has compositions between An_{47} and An_{50} (Figure 102). Plagioclase in non-ophitic leucogabbro from the same outcrop has compositions ranging from about An_{49} to An_{53} (Figure 102).

The electron microprobe was used to analyze plagioclase in polished grain mounts of 40 specimens collected along two traverses through parts of the body. Traverse 1 was collected in roadcuts of the Angeles Forest highway along Mill Creek (Plate I). Specimens were collected at 20 stations through a total stratigraphic thickness of about 5640 meters for an average spacing of about one station every 300 meters (Figure 103). In the south, the lowest 700 meters of this section has been cut out by younger intrusives, but specimen 1 comes from a xenolith about 500 meters stratigraphically below the base of the continuous section. To the north, a strike slip fault has cut out about 940 meters of the upper part of the section. In this area the body consists of several alternating subunits of anorthosite and layered leucogabbro (Plate I). At each station, from one to five specimens were collected, including each of the various lithologies in the outcrop. Most analyses were of plagioclase from massive anorthosite, but in 4 instances plagioclase from leucogabbro was also analyzed and in 2 instances crescumulate plagioclase was also analyzed.

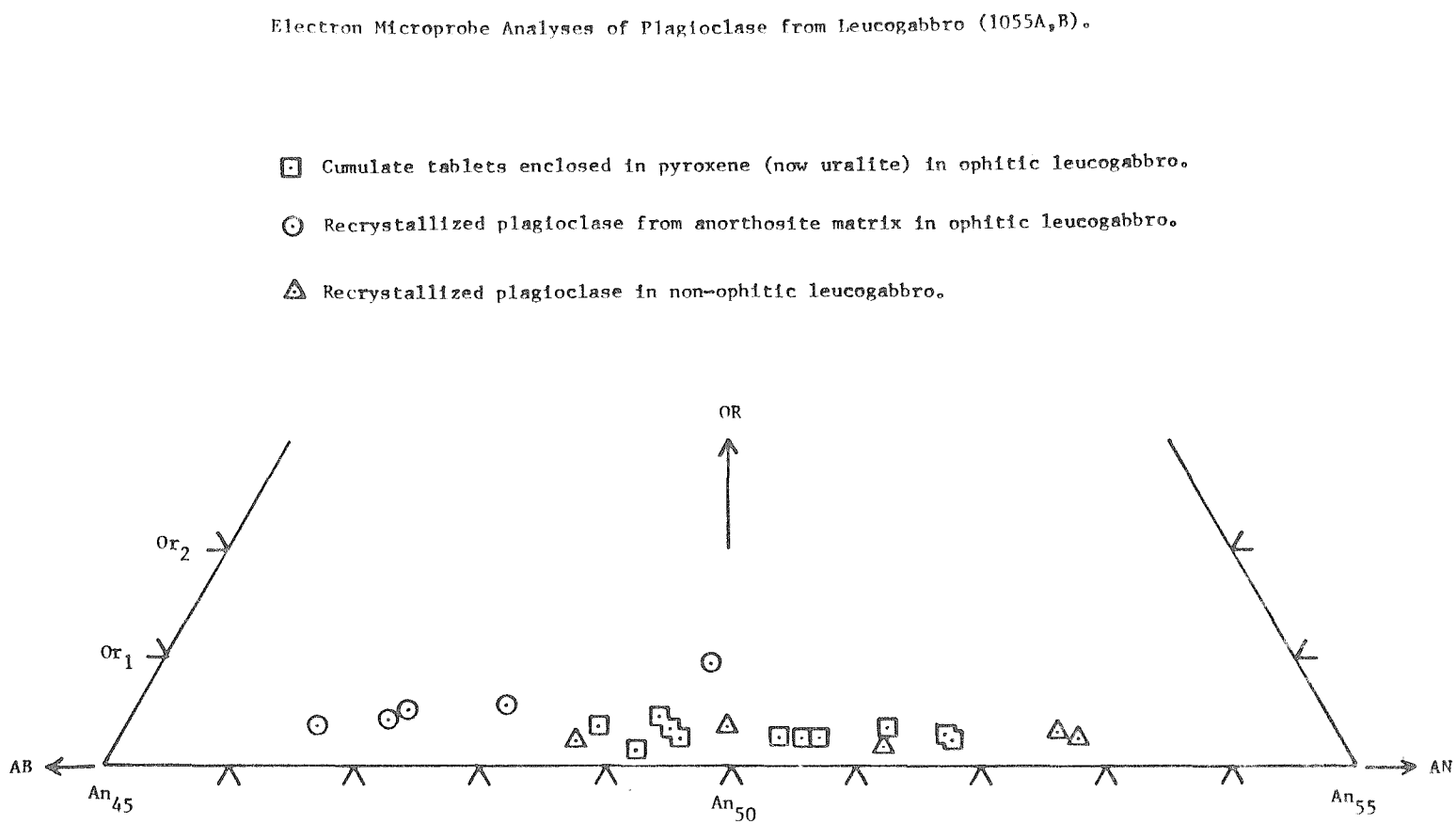

Figure 102. Compositions of plagioclase in leucogabbro (1055A and B).

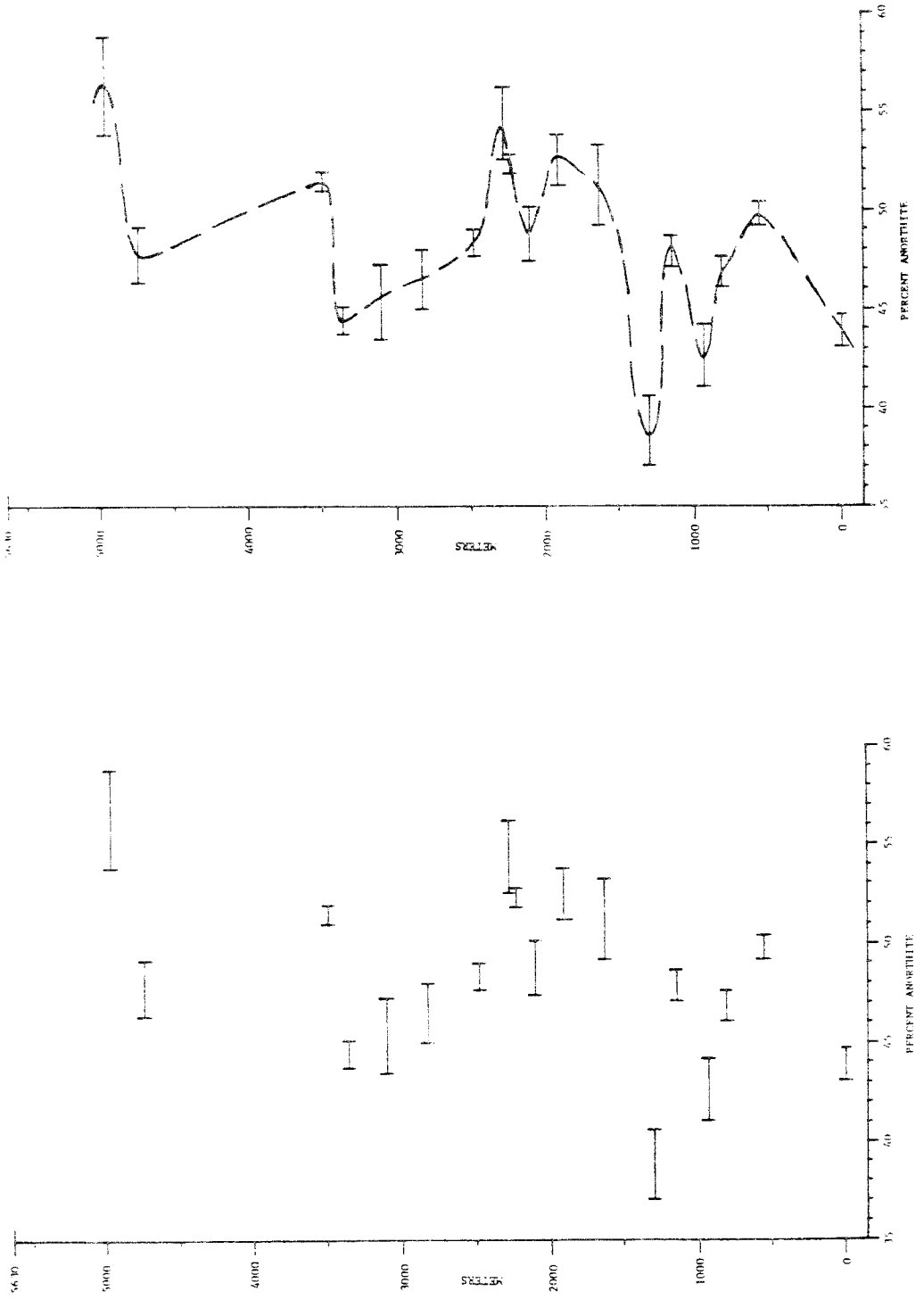

Figure 103. Plagioclase compositions in traverse one, along Mill Creek.

Traverse 2 was collected along the Magic Mountain-Mt. Gleason ridge east of Sold (Plate I), at 14 stations through an estimated stratigraphic thickness of about 3600 meters for an average of about one station every 250 meters (Figure 104). Layering is generally absent in this section. Stratigraphic position is estimated by projection of structures 1 to 2 kilometers away from the line of section and is subject to substantial possible error. In this area, the body consists almost entirely of massive anorthosite. The lower 700 meters of the section includes some leucogabbro, but not in mappable units, and the remainder of the section is entirely massive anorthosite. At one station, plagioclase from leucogabbro as well as anorthosite was analyzed, but all other specimens are anorthosite.

Each specimen was about 2 centimeters on a side. Because of the coarse grain size of most anorthosite, each anorthosite specimen may come from a single crystal. About 20% of each specimen was crushed and fragments of the resulting power were analyzed. Two to six fragments were analyzed from each specimen. Within individual fragments, the composition typically varies by 1% - 2% anorthite while within all fragments of a specimen the composition typically varies by 2% - 4% anorthite. The data from polished thin sections indicate that the total range in 6 analyzed crystals in non-ophitic leucogabbro is about 3% anorthite. The range in 4 crystals in the anorthosite matrix of ophitic leucogabbro is about 3% and that in 3 cumulate crystals in ophitic leucogabbro is also about 3% anorthite (Figure 102). More analyses of fragments from each specimen would probably extend the total compositional range, and all grains in some specimens may have come from a single large crystal. However, the compositional variability in a single specimen appears to

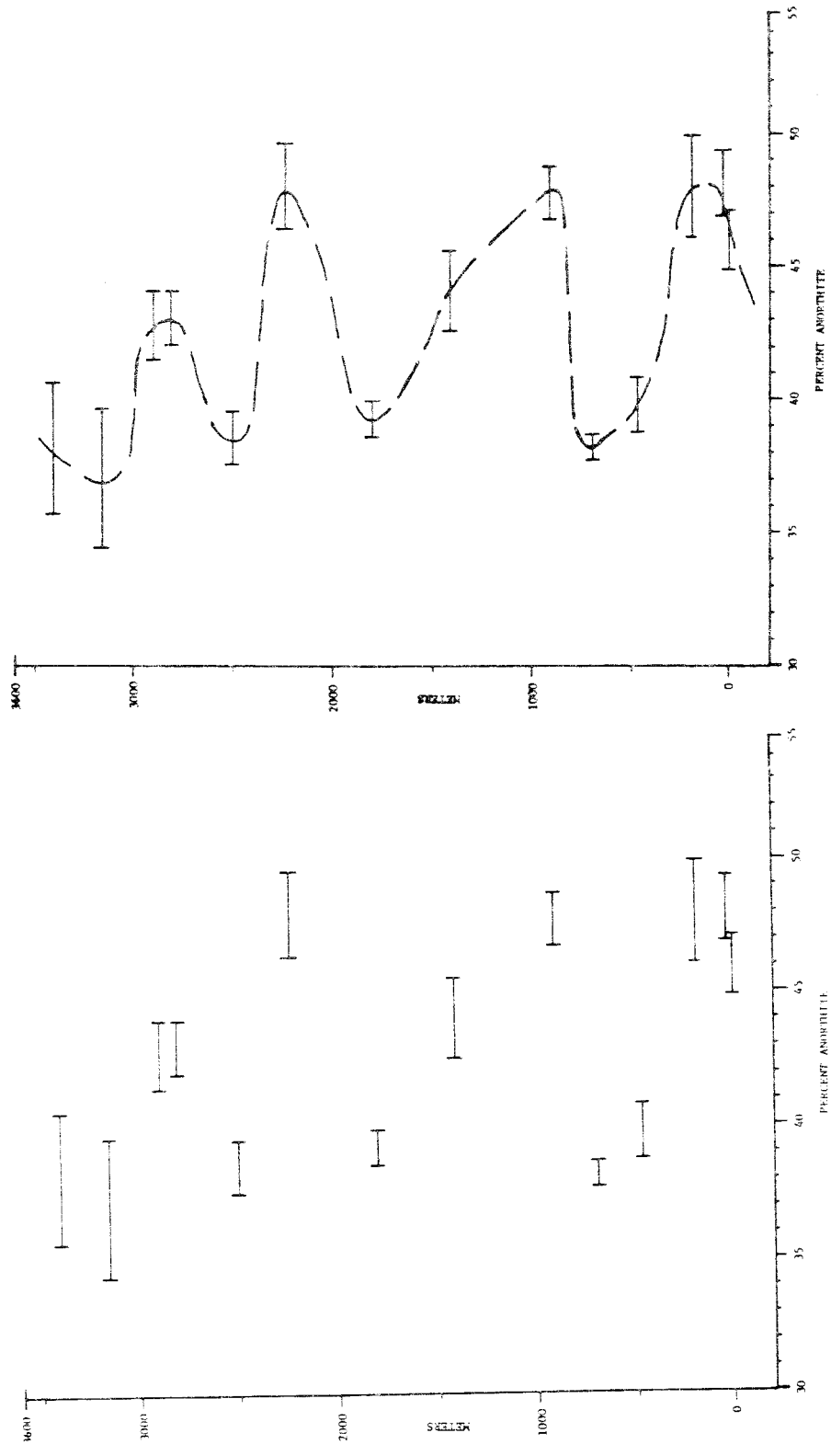

Figure 104. Plagioclase compositions in traverse two along the road east of Sold.

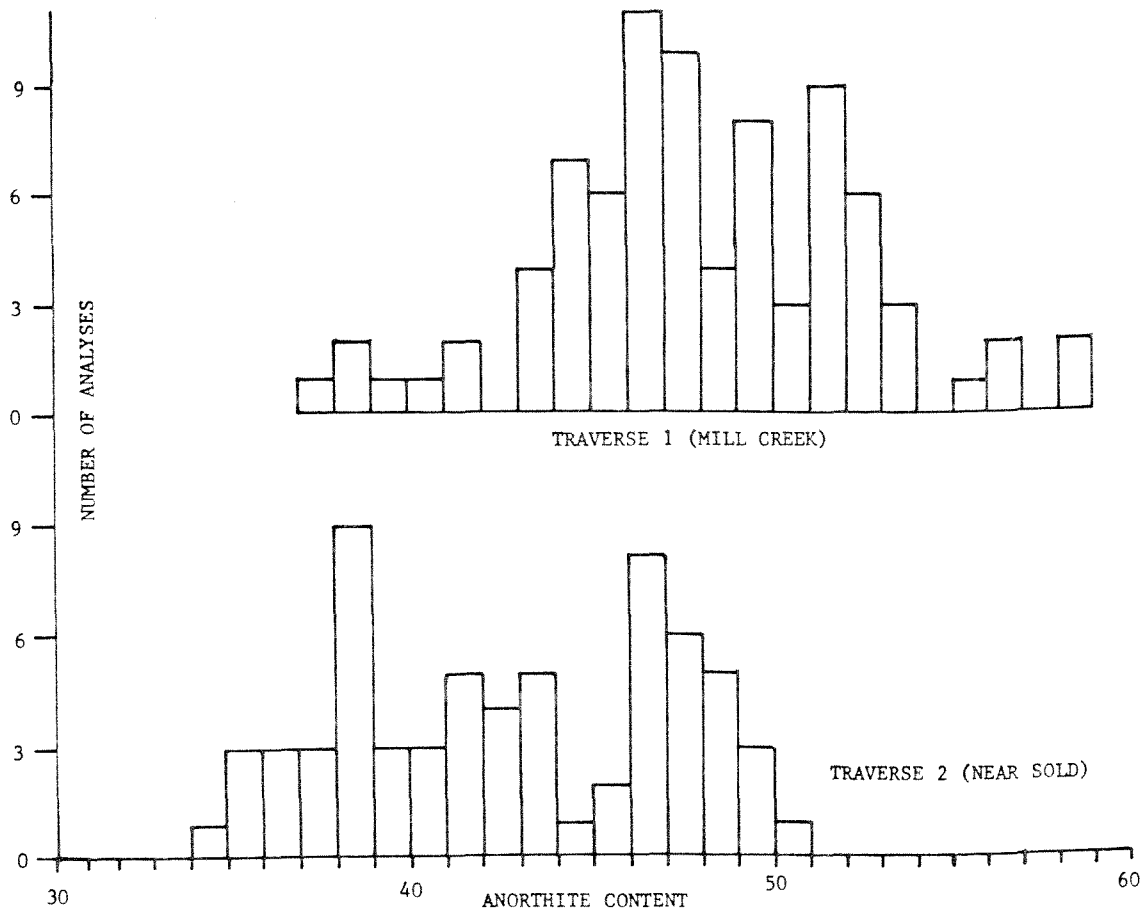

Figure 105. Histograms of plagioclase compositions on two traverses through the anorthosite-leucogabbro unit.

be considerably less than that between different specimens from different stations. Compositional variations of 3% to 4% in single plagioclase crystals indicate that postcumulous recrystallization did not result in compositionally homogeneous plagioclase crystals.

The results of these analyses are shown in Figures 103 and 104. The stratigraphic position of each station is indicated along with the average composition and the total range of the 2 to 8 individual analyses. Specimens from traverse 1 have a total range of average anorthite contents from 38% to 57% and those from traverse 2 have a total range from 36% to 48%. Figure 105 shows histograms of the compositions in each traverse and of the total of all analyses.

In traverse 1, the specimen at about 4900 meters is an altered, partially recrystallized rock whose composition may be anomalous. Excluding this specimen, compositions of specimens in this traverse fluctuate within an approximate band with a width of about 11% - 15% anorthite content. Within this band there may be a slight tendency toward increase in anorthite content toward the top of the section, although it could as well be interpreted as fluctuation within the same limits throughout the section, particularly if the specimen at about 1300 meters is not included.

In traverse 2, compositions of specimens fluctuate within an approximate band with a width of about 10% - 12% anorthite content. Within this band, there appears to be a tendency toward decrease in anorthite content toward the top of the section (about 5% - 6%).

It appears that there are cyclic compositional variation in both traverses. In each traverse, plagioclase alternately shifts toward more sodic and more calcic compositions. The data appear to be consistent with more rapid changes toward calcic compositions and more gradual changes toward sodic compositions. Each traverse might consist of

several "plagioclase units," each of which starts with calcic compositions and gradually changes toward more sodic compositions. These compositional variations in both traverses could be explained as the result of the competing processes of fractional crystallization toward more sodic plagioclase and intrusion of new magma capable of crystallizing more calcic plagioclase.

The average thickness of 7 plagioclase units in traverse 1 is 840 meters and the average of 4 units in traverse 2 is 900 meters. The 800 - 900 meter average thicknesses of plagioclase units in the anorthosite-leucogabbro unit is similar to the estimated thicknesses of the individual subunits of the jotunite unit, each of which was probably produced by intrusion of new magma into the chamber. The compositional variations in traverse 1 correspond approximately with contacts between anorthosite and leucogabbro. Most plagioclase units consist of lower anorthosite and upper leucogabbro, although the data are not sufficient to indicate if this is always true.

If all plagioclase was originally of about the same composition, then uralitization of primary pyroxene might have caused the loss of calcium and aluminum from plagioclase and resulted in more sodic plagioclase in leucogabbro. However, the existence of similar compositional variations in traverse 2, which contains very little leucogabbro, argues against this possibility and suggests that the variation is a primary feature of anorthosite and leucogabbro.

The fact that the compositional variations correspond with anorthosite-leucogabbro contacts in traverse 1 suggests that, for each plagioclase unit, the original magma was on the plagioclase side of the plagioclase-pyroxene cotectic and initially crystallized plagioclase

almost exclusively. Fractional crystallization of this magma produced successively more sodic plagioclase and drove the magma toward the cotectic curve. Toward the top of each plagioclase unit, the magma was thus closer to saturation in pyroxene components and pyroxene was progressively more easily crystallized from either interstitial magma, stagnant bottom layers or immediately above crescumulate plagioclase layers, so that predominantly leucogabbro was produced. Intrusion of new magma which mixed with the earlier fractionated magma would have driven the resultant magma away from the cotectic curve and caused crystallization of more calcic plagioclase to again produce nearly pure anorthosite.

Traverse 1 has almost twice the total compositional variation of traverse 2, reaching extreme compositions about 6% - 10% more anorthite-rich than any in traverse 2. If substantial amounts of calcium and aluminum had been removed from the bulk plagioclase during uralitization, then traverse 1 should contain less calcic plagioclase than traverse 2; the more calcic compositions in traverse 1 argue that uralitization may have had little effect on the bulk plagioclase compositions (although thin reaction rims of plagioclase in contact with uralite may be deficient in calcium and aluminum). If the magma chamber was thicker toward the center (traverse 2) than toward the margin of the body (traverse 1), and if each new pulse of magma was of nearly uniform thickness throughout the body (perhaps forming a layer at the top of the chamber), then the new magma might mix with a smaller proportion of fractionated magma near the margin, where more calcic plagioclase might mark the beginning of each plagioclase unit. Alternatively, if new magma was intruded near the margin of the body and first began to crystallize there before much mixing or fractionation occurred, then plagioclase in the marginal rocks

should be more calcic than that in the more central rocks. The difference in compositions in the two traverses also suggests the possibility of persistent lateral inhomogeneties in the magma chamber.

Many of the above suggestions remain speculative. The persistence of anorthosite and leucogabbro subunits over long distances in the southeast part of the body suggests that the plagioclase units are also of large lateral extent. However, even though structural reconstruction of the body suggests that the top of the section in traverse 1 (north end) should correspond with the top of the section in traverse 2 (west end), it has not been possible to correlate individual plagioclase units between the two traverses. It is possible that the plagioclase units were produced by intrusions of new magma but that each intrusion affected only part of the magma chamber and so individual plagioclase units are not correlative throughout the body.

At 4 stations specimens of both anorthosite and leucogabbro were analyzed. In all cases there is overlap of the compositions of the paired specimens: in two cases the leucogabbro average is about 1% more sodic and in the other two cases the leucogabbro is about 2% more calcic than the adjacent anorthosite. These figures are compatible with identical compositions in the two adjacent lithologies, and suggest that uralitization has not significantly changed the bulk plagioclase composition. At two of the above stations crescumulate plagioclase is about 1% and about 3% more sodic than the average plagioclase from adjacent anorthosite and leucogabbro.

Figure 106 plots the orthoclase versus anorthite content of all analyses. This shows an average of about $Or_{0.3}$ at An_{59} increasing to about $Or_{0.8}$ at An_{35}. Felcspars from the Morin Complex, Quebec, which

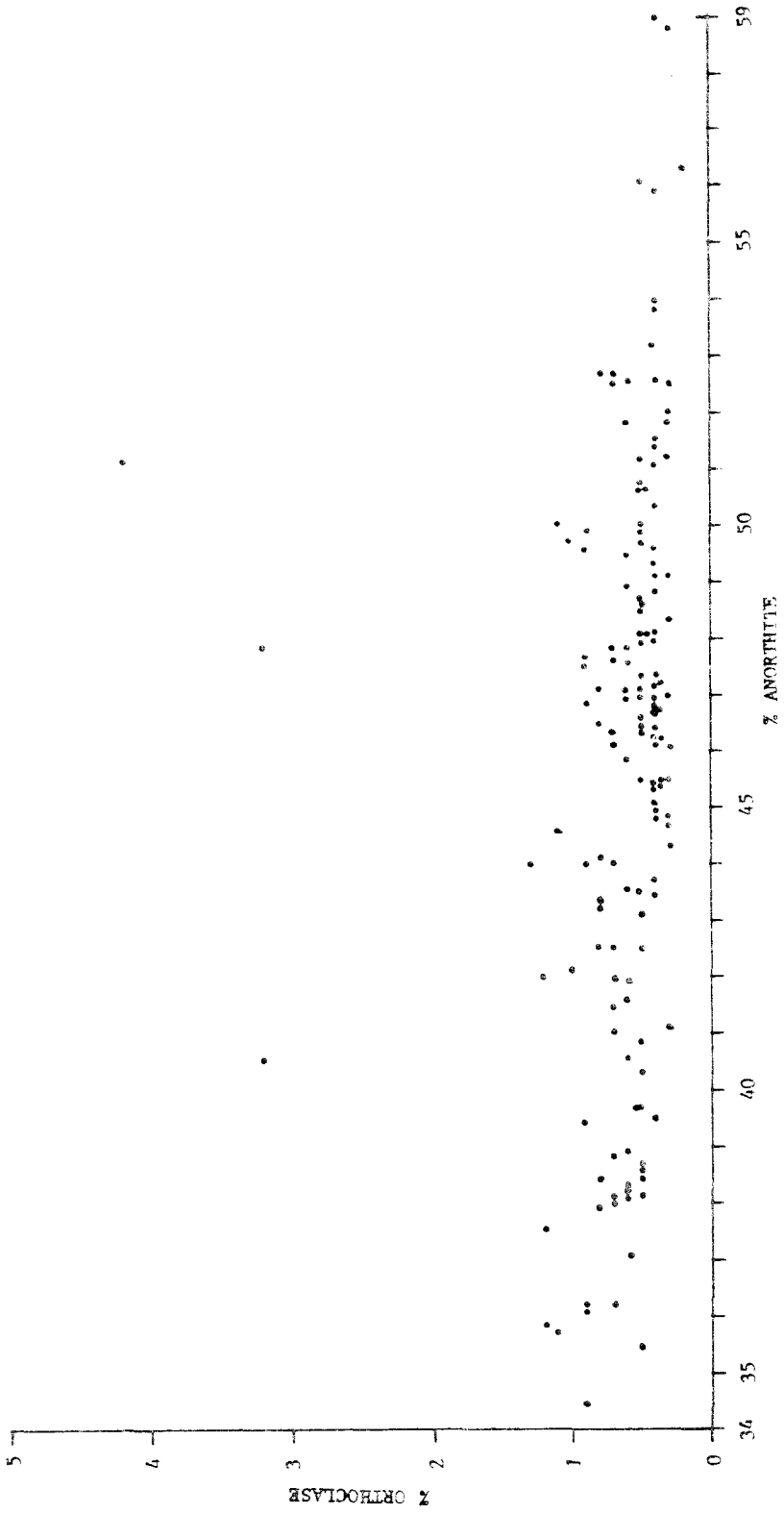

Figure 106. Orthoclase content of analyzed plagioclase.

range between An_{44} and An_{50} average about 5 mole percent Or except for two which have been recrystallized (Emslie, 1975). Since plagioclase from the anorthosite-leucogabbro contains very little antiperthite, the bulk plagioclase crystals probably have Or contents of less than 1%.

Ryder, et al. (1975) have analyzed plagioclase from 122 specimens from the anorthosite-leucogabbro and jotunite units. Their data indicate a compositional range in rocks of the anorthosite-leucogabbro unit which is almost identical to that measured in this study. The present study (traverses 1 and 2) indicates that, in detail, compositional variations are more complex than suggested by the above authors who show, for example, that almost all of traverse 1 should have compositions more calcic than An_{48} (their Figure 4).

Recrystallization

As described in Chapter 4, nearly all rocks of the anorthosite-leucogabbro unit have undergone postcumulus recrystallization which has produced extremely large plagioclase grains in anorthosite and in plagioclase-rich parts of leucogabbro (Figure 57). Comparison with cumulate plagioclase tablets preserved in large ophitic uralite pseudomorphs after pyroxene shows that the degree of enlargement during recrystallization commonly is one and may even reach two orders of magnitude. Similar postcumulous enlargement of plagioclase grains in cumulate rocks of the Bushveld intrusion has been described by Cameron (1969). The existence of compositional variability of 3% - 4% within individual recrystallized plagioclase crystals suggests that original compositional variations within and between adjacent cumulate crystals were not homogenized during recrystallization.

The potential which drove the recrystallization might have been residual strain energy, surface energy or the change from a high temperature disordered structure to a low temperature ordered structure. It seems unlikely that residual strain energy drove the recrystallization since the cumulate plagioclase tablets show little optical evidence of strain. Recrystallization of micron-size crystals to millimeter sizes results in an extremely large decrease in surface area per unit volume, but recrystallization of millimeter to centimeter-size crystals to tens of centimeter sizes results in relatively little decrease in surface area per unit volume. Therefore, it seems unlikely that the decrease in residual strain or in surface energy alone could have been sufficient to drive the extensive recrystallization observed. It seems most likely that the transition from a high temperature disordered to a low temperature ordered structure is the driving energy which produced the recrystallization. Mueller (1970) has proposed a two-step mechanism of ordering in some silicates which requires that order-disorder equilibrium can be attained at temperatures below the lower temperature limit of cation ordering only through recrystallization, and not by thermal annealing which does not result in recrystallization. Data concerning the structural states of plagioclase in the rocks of this body must be obtained before more can be said about the nature of the driving energy which produced recrystallization.

It is possible that high fluid contents facilitated postcumulous recrystallization in these rocks. The San Gabriel body contrasts with many anorthosite massifs in its hydrated ferromagnesian assemblages which indicate that water pressures must have been relatively high at some time soon after crystallization of its rocks. Compared to other

anorthosite massifs, the San Gabriel body also probably has developed unusually abundant rocks with extremely coarse textures in anorthosite and leucogabbro, and this may be due to recrystallization occurring in a more hydrous system than those which have produced most other anorthosite suites. Coarse recrystallized zones of jotunite which crosscut primary layering in the jotunite unit contain considerably more biotite than unrecrystallized jotunite and so probably underwent recrystallization in a relatively water-enriched system. Whole-rock chemical analyses of ophitic leucogabbro and of adjacent non-ophitic (completely recrystallized) leucogabbro shows that the latter is slightly higher in H_2O+, in ferric/ferrous iron, and in K_2O. The differences are minor, but are consistent with the presence of an elevated fluid pressure during crystallization. However, compositional inhomogeneities in recrystallized plagioclase might suggest that water pressures were relatively low during the recrystallization which preceded uralitization.

Exsolution

Nearly all rocks of the anorthosite-leucogabbro unit contain plagioclase with little or no associated alkali feldspar. The only exceptions are small amounts of intergranular alkali feldspar, rare antiperthite near the rims of a few crystals and very albite-rich plagioclase in some gabbro near the top of the unit. Electron microprobe analyses of 149 plagioclase fragments from this unit (Figure 105) show that it normally contains less than 1% potassium feldspar. In marked contrast to these rocks, rocks of the syenite and jotunite units nearly always contain feldspars consisting of intimately associated plagioclase and alkali

feldspar. Most rocks of the syenite unit contain large amounts of fine mesoperthite (Figures 59, 60), and most rocks of the jotunite unit contain antiperthitic plagioclase (Figure 68).

The antiperthite occurs as irregular domains, patches, blebs or lamellae but there is no obvious systematic distribution of these various morphologies in rocks of the jotunite unit. The estimated percentages of potassium feldspar in antiperthitic plagioclase ranges from less than 1% to as much as 25% - 30%, but there does not seem to be any systematic variation in the jotunite unit. Figures 107-110 show typical examples of antiperthite from the jotunite unit. Exsolved potassium feldspar is often concentrated along twin boundaries or along fractures, and sometimes shows one or more preferred orientations. Most of these intergrowths probably formed by normal exsolution reactions considered to be responsible for antiperthites in most anorthositic rocks (Carstens, 1967), but limited discontinuous precipitation along grain boundaries probably also occurred (Figure 111).

Mesoperthite of the syenite unit consists of nearly equal amounts of oligoclase and potassium feldspar in a very fine intergrowth of thin (about 0.01 millimeter) lamellae (Figure 59). A striking feature of most syenite is the prominent development of swapped borders between adjacent mesoperthite grains (Figures 59, 60). Ramberg (1962) explained these textures as the result of unmixing of alkali feldspar during which the intergranular albite layer which nucleated parallel to lamellae in one grain grew mainly by replacing potash feldspar in the adjacent grain. The tendency of albite to grow by replacing an adjacent grain inclined at some angle to the original grain is explained in terms of the lattice strain created during growth of the albite.

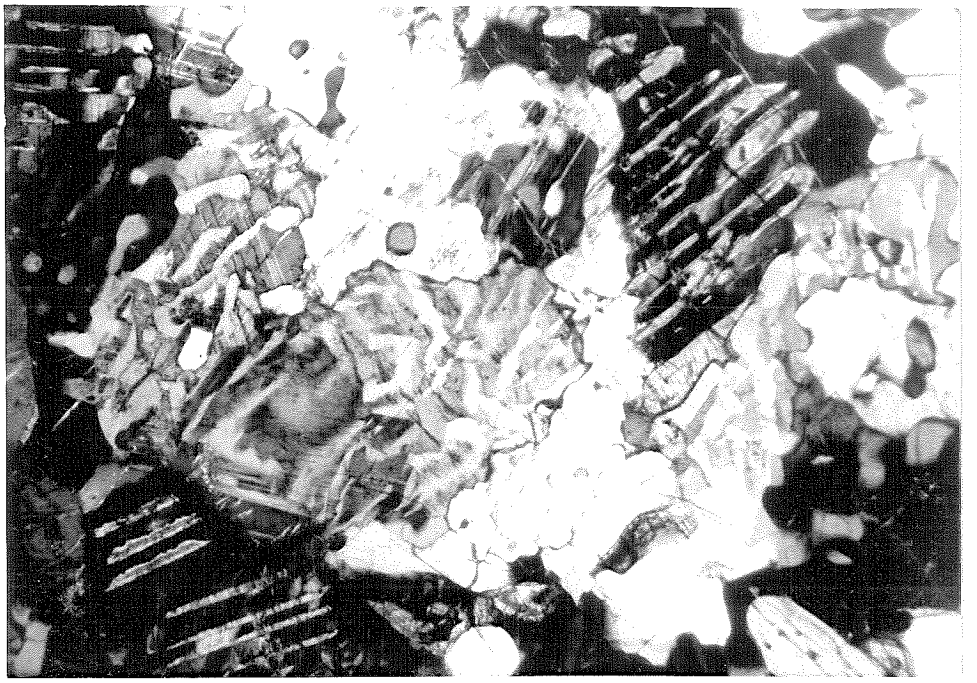

Figure 107 Feldspar exsolution in mangerite. Coarse worm-like lamellae of potassium-feldspar are exsolved from calcic oligoclase. (crossed nicols, 2.06 x 3.19 millimeter field).

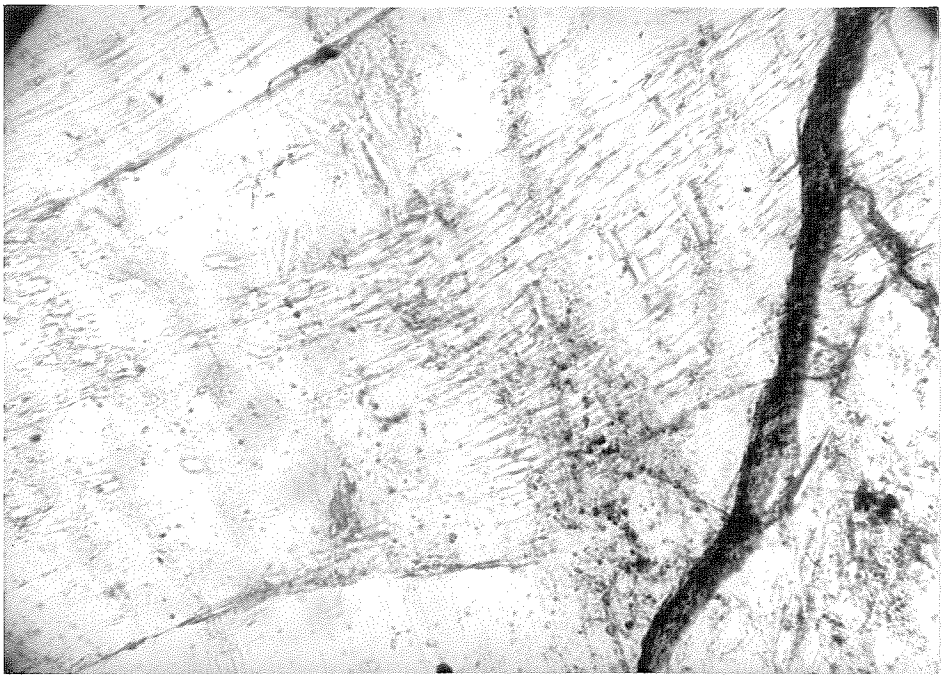

Figure 108 Potassium-feldspar exsolution lamellae concentrated in the bend of a tabular andesine crystal in jotunite. (plane light, 0.50 x 0.76 millimeter field).

Figure 109 Potassium-felspar exsolution lamellae localized along the composition planes of albite twins in a tabular andesine crystal in jotunite. (plane light, 0.50 x 0.76 millimeter field).

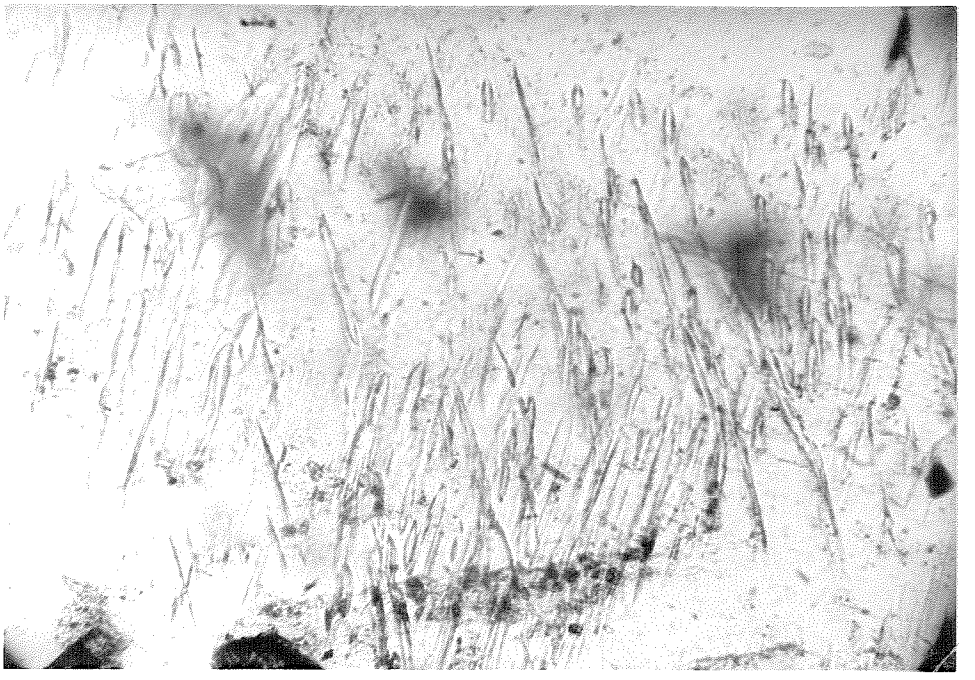

Figure 110 Potassium-feldspar exsolution lamellae of two different orientations in an andesine crystal in jotunite. (plane light, 0.50 x 0.76 millimeter field).

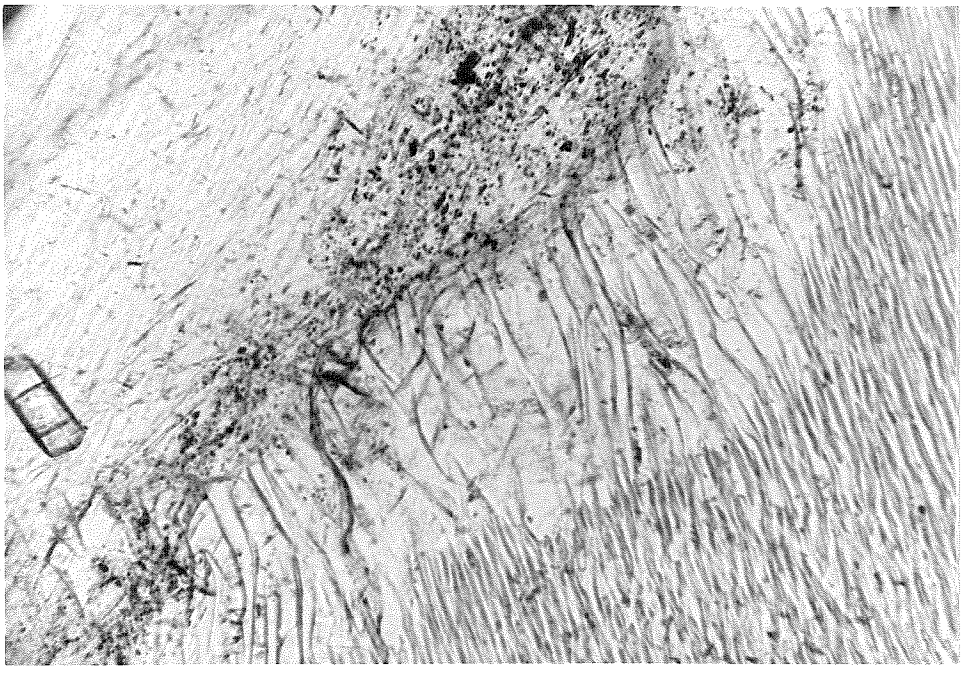

Figure 111 Exsolution lamellae in mesoperthite thickening at the contact with a second mesoperthite crystal in ferrosyenite. Numerous minute inclusions are present in mesoperthite along the contact. (61, plane light, 0.50 x 0.76 millimeter field).

The plagioclase-alkali feldspar intergrowths in these rocks could have origniated by processes of exsolution, parallel growth or by replacement. Although all three processes have been demonstrated in some rocks (Lofgren and Gooley, 1977, Peng, 1970), it seems likely that most of the intergrown feldspars of this body originated by exsolution (except for some feldspars along contacts between primary crystals). Both the mesoperthites and the anti perthites, which are similar to those described by Carstens (1967), originated by an exsolution process.

CHAPTER 6

PETROGENESIS AND STRUCTURAL EVOLUTION

INTRODUCTION

This section summarizes my conclusions, based on the data presented above and interpretation of these data, concerning: (1) the characteristics of the earth's crust in this area prior to intrusion of the body; (2) the nature of the intrusion and characteristics and possible origin of the magama; (3) the crystallization of the body, including the mechanisms and trends of differentiation, the sequence of lithologies produced and the structural development of the body during and immediately following crystallization; and (4) the important petrologic processes of recrystallization and uralitization which occurred immediately following crystallization.

PRE-INTRUSION CONDITIONS

The San Gabriel anorthosite-syenite body was intruded into an area of continental crust which had previously undergone a complex sequence of geologic events. Although presently exposed only in a few relatively limited areas between major strands of the greater San Andreas fault zone, a diverse group of Precambrian crystalline rocks have been identified and geochronologically studied by Silver (1971), who has worked out the following history: (1) A series of volcanic and sedimentary strata probably accumulated in an interval between 1720 and 1650 my ago and were deformed and metamorphosed to amphibolite facies to produce layered quartzofeldspathic geneisses, amphibolites, quartzites and rare calc-silicate beds within the same interval. (2) All of these rocks were intruded by plutons of predominantly porphyritic granodiorite and quartz monzonite in the interval 1625 - 1655 my ago. (3) At about 1410 - 1430

my ago this region was affected by a major regional orogenic event which metamorphosed layered and massive rocks under amphibolite and granulite facies conditions, although relicts of primary structures were locally preserved.

The anorthosite-syenite body was intruded during a short interval about 1200 my ago, primarily if not entirely into rocks which had been metamorphosed under granulite facies conditions. At the time of intrusion, these granulite gneisses were probably sub-horizontal and had been a part of a continental crustal area of relative geological quiescence during the preceding 200 my.

THE PLUTON

Magma which formed the anorthosite-syenite body was intruded into a chamber which eventually reached at least 7 and, more likely, closer to 12 kilometers in maximum thickness and perhaps about 20 kilometers or more in diameter. The evidence indicates that magma must have been injected into the chamber as a series of pulses over some interval of time.

The upper contact was concordant and probably sub-horizontal. The edge increases from a few hundred meters to at least 7 kilometers in thickness and probably reached a minimum of at least 12 kilometers in the center. Thus, the magma chamber probably had the form of a very thick sheet or an inverted cone with an unknown diameter. The chamber must have developed over some interval of time, perhaps starting as a sub-horizontal sheet and developing a conical form as more and more magma was intruded and accommodated in large part by subsidence of the floor

of the chamber. The roof of the chamber was formed by granulite gneisses which were also present beneath a small part of the margin; it is not known what type of rock formed the floor of the chamber elsewhere, but at least part of it is inferred to have been granulite gneiss.

STRUCTURAL EVOLUTION DURING AND IMMEDIATELY FOLLOWING CRYSTALLIZATION

Structural activity which occurred during or soon after crystallization of the body and was important to the evolution of the magma and the sequence and eventual distribution of lithologies include: (1) Possible tilting and large-scale slumping of crystal mush during formation of rocks of the anorthosite-leucogabbro unit, (2) major sags or scarps which developed on the floor of the magma chamber during crystallization of the syenite and jotunite units, (3) pervasive fracturing and cataclasis of rocks of the anorthosite-leucogabbro unit which probably occurred soon after crystallization, and (4) fault displacement of just-crystallized rocks of the anorthosite-syenite body as well as granulite gneisses, which produced mylonitization and recrystallization. The postulated sequence of events leading to the development of these structural features is shown in Figure 112.

SLUMPING

Several lines of evidence suggest that slumping was an important process during accumulation of the crystal mushes which produced the rocks of the anorthosite-leucogabbro unit. Near the southeastern margin of the body several large 1-5 meter structures were probably produced by diapiric emplacement of anorthosite crystal mush into overlying leucogabbro crystal mush (Chapter 3) and may have formed at a time when

Figure 112. Sequence of structural modifications which occurred during crystallization of the San Gabriel anorthosite-syenite body. (This sequence of diagrams is drawn as if the entire body had been formed from a single magma intruded in a single episode. In fact, the body formed by multiple intrusions of magmas, but the same general sequence of structural evolution occurred). (a) Approximate lines of sections; note that Mesozoic and Cenozoic structures have not been removed; the sections are highly interpretive. (b) Magma intruded into a large chamber, ultimately in the form of an inverted cone. (c) Bottom accumulation to fill about 40% of the chamber. (d) Tilting and continued accumulation after about 60% filled. (e) Relative rising of some of the earlier rocks; tectonic forces (in part due to diapiric rising?) squeeze about 30% residual magma into smaller chambers with large marginal scarps of earlier anorthositic rocks. (f) Schematic distribution of lithologies and units at the end of crystallization.

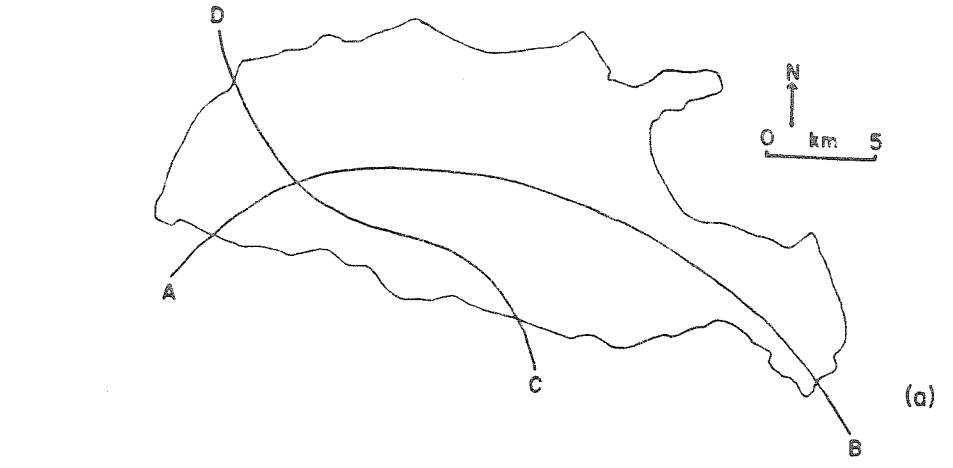

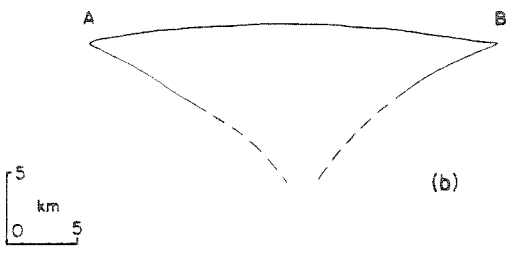

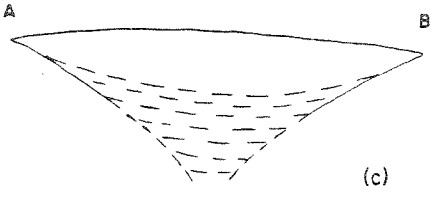

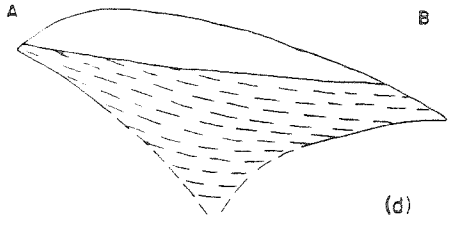

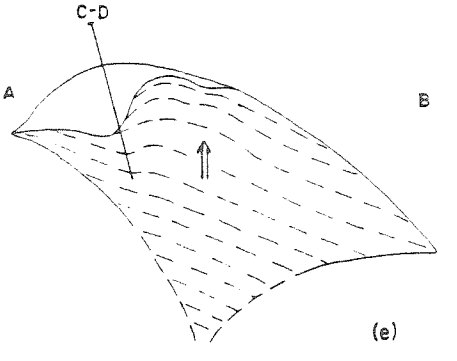

Figure 112.

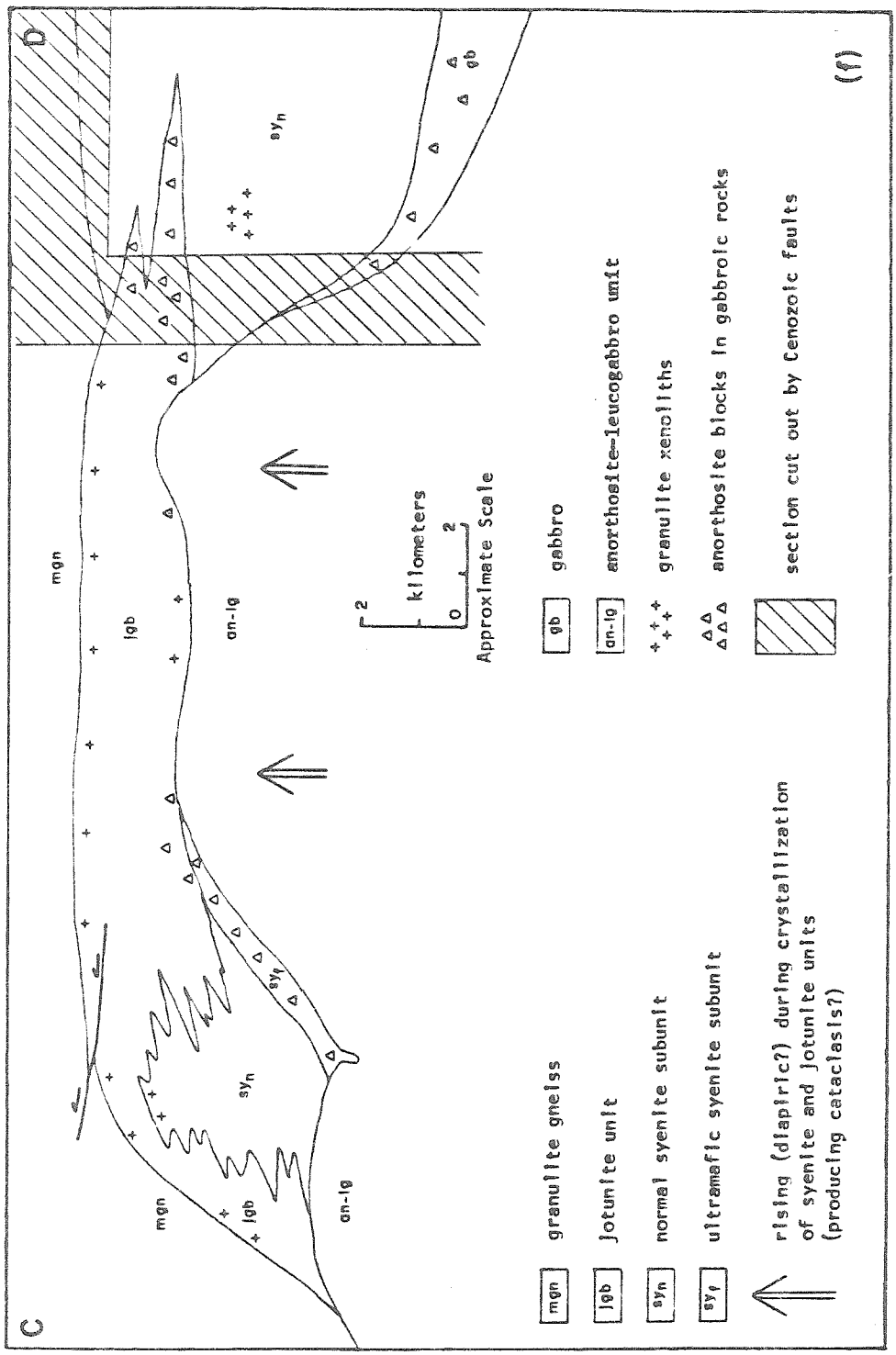
C
D
mgn
lgb
an-lg
sy_n
sy_f
gb
2
0
2
kilometers
Approximate Scale
mgn granulite gneiss
lgb Jotunite unit
sy_n normal syenite subunit
sy_f ultramafic syenite subunit
rising (diapiric?) during crystallization of syenite and Jotunite units (producing cataclasis?)
gb gabbro
an-lg anorthosite-leucogabbro unit
granulite xenoliths
anorthosite blocks in gabbroic rocks
section cut out by Cenozoic faults
(f)

Figure 112.

the accumulating crystal pile was being tilted away from the center of the body. In the same part of the body, irregularities in its roof and the distribution of thick leucogabbro sequences in anorthosite suggest the possibility of large-scale tilting and consequent slumping and sliding of crystal mushes away from the center of the body (Figure 17). Near the southeastern margin of the body, there are occasional abrupt discontinuities in the orientation of cumulate plagioclase tablets ophitically enclosed by large ophitic pyroxene(uralite) crystals (Figure 49). These discontinuities may be the result of slumping of crystal mush prior to completion of intercumulate crystallization. In the central part of the body, the general lack of consistently oriented throughgoing interlayers of leucogabbro in anorthosite may be in part due to widespread slumping of crystal mushes during accumulation.

SCARPS

In the Buck Canyon synform, a large scarp was present in rocks of the anorthosite-leucogabbro unit which formed the floor of the chamber during crystallization of the syenite and jotunite units. This scarp is characterized by the presence of abundant anorthosite blocks and abundant slump structures in adjacent very mafic rocks. More limited scarps are present between lower Pole and Bear Canyons and in uppermost Sand Canyon. It is conceivable that these three scarps were originally all part of a single long structure, but present exposures are insufficient to verify this possibility. Other scarps could have been present on the floor of the chamber during accumulation of rocks of the anorthosite-leucogabbro unit, but the lack of easily-recognized, throughgoing markers in most of this unit would make any such scarps difficult

to recognize.

In upper Pacoima Canyon the base of the Buck Canyon synform is the sharp contact between anorthosite and leucogabbro below and the very mafic rocks of the ultramafic syenite subunit above. Reconstruction of the synform suggests that these rocks accumulated along a south-facing scarp with 2-4 kilometers of vertical relief over a distance of 3-4 kilometers (Figure 38). These rocks were formed by sinking of ferromagnesian minerals and include large angular anorthosite blocks. Abundant slump structures show that these rocks accumulated on the floor of the magma chamber and in a few instances suggest that the floor sloped moderately (perhaps 25-45 degrees) toward the south.

Along this scarp rocks of the anorthosite-leucogabbro unit are cut by numerous dikes, which generally contain at least 50% coarse uralitized ferromagnesians. These dikes were probably produced by downward injection of very mafic magma or of mafic crystal mush. At the base of the scarp a large mass of very mafic rock about 0.5 kilometers wide extends from the main part of the ultramafic syenite subunit about 1.5 kilometers into anorthosite and leucogabbro (Figure 38). This mafic mass may have originated as a crystal mush which accumulated with anorthosite blocks on the floor of the chamber and was subsequently injected downward into underlying anorthosite, similar to the way clastic dikes are formed in some sediments (Young, 1972).

Similar exposures in lower Pole Canyon and upper Sand Canyon are more limited and less well exposed, but may resemble the north side of the Buck Canyon synform. They are also defined by very mafic layered rocks containing numerous anorthosite blocks and abundant slump structures, and could have had 1-2 kilometers of vertical relief.

Following accumulation of the anorthosite-leucogabbro unit, new magma, perhaps mixed with some earlier residual magma, produced the syenite and jotunite units. These units are completely absent above the anorthosite-leucogabbro unit along the northeast margin of the body and are very thick along the southwestern margin, mostly adjacent to the scarps. Part of this magma may have originally been present everywhere above the anorthosite-leucogabbro unit but before crystallization, it was squeezed out of some areas and collected in areas adjacent to the scarps, perhaps marginal to the main part of the body. It seems likely that the same tectonic forces which produced the scarps could have squeezed the magma, and redistributed it into restricted chambers adjacent to the scarps, where rocks of the syenite and jotunite units crystallized.

CATACLASIS

All rocks of the anorthosite-syenite body have undergone extensive cataclasis which is most pronounced in anorthosite and leucogabbro (Figures 8, 46). Anorthosite is commonly cut by fractures of random orientation with spacings of 1-10 millimeters. Higgs (1954) suggested that this cataclastic overprint was the result of autoexplosions due to high fluid pressures in the rock during cooling.

The coarse anorthosite and related rocks were produced by accumulation and bottom crystallization followed by recrystallization. At some time after recrystallization, rocks of the anorthosite-leucogabbro unit may have undergone diapiric rising due to their relatively low density. Martignole and Schrijver (1970) have shown that the Morin anorthosite was emplaced as a solid mass which rose diapirically upward

into quartzofeldspathic gneiss and finally spread laterally. During diapiric rising, the anorthosite was accompanied by largely liquid mangerite moving ahead of it. The evidence of scarps and slumping in the San Gabriel body is compatible with a possible few kilometers of diapiric rising of parts of the anorthosite-leucogabbro unit. Diapiric rising of the central part of the body could have been responsible for development of the marginal scarps, with late magma forced mainly toward the margins and collecting in the areas exterior to the scarps. This could have resulted in extensive fracturing of the large plagioclase crystals in anorthosite. Fracturing of the margins of the rising mass could have provided avenues for emplacement of the numerous dikes near the scarps and disruption of anorthosite along the margin of the diapir could have supplied the large angular blocks present inrocks of the ultramafic syenite subunit and parts of the jotunite unit.

FAULTING

Near the southern margin of the body, a reverse fault which cuts rocks of the jotunite unit and in part separates them from granulite gneiss, was probably active during or very soon after emplacement of the body. Exposed over a distance of about 3 kilometers, offset on this fault was such that the hanging wall was displaced about 300-600 meters upward and outward from the more central part of the body. The fault zone consists of 5-15 meters of strongly sheared gneiss or jotunite which has been partially recrystallized during fault movement and suggests that displacement occurred while the rocks were still hot, probably soon after jotunite crystallization. Restoration of Mesozoic and Cenozoic structures suggests that this may have been a low angle fault.

Rocks adjacent to the northeastern margin of the body have been strongly deformed and partially recrystallized. Deformation occurred along this contact during emplacement of the Mt. Lowe granodiorite in early Mesozoic time (Chapter 3). However, some rocks near the top of the body in upper Big Tujunga Canyon have been very strongly sheared (Figure 18) even though located 1 to 2 kilometers away from the contact of the Mt. Lowe granodiorite and separated from it by apparently normal unsheared gneiss. It is possible that some of the deformation along the northeastern margin of the body occurred prior to emplacement of the Mt. Lowe granodiorite, perhaps soon after crystallization of the anorthosite-leucogabbro unit, since apparently high temperature recrystallization has affected some of the deformed anorthositic rocks. These would have constituted low angle zones of intense shearing generally parallel to the roof of the body. However, the present mapping has not been sufficient to determine if, and to what extent Precambrian deformation might have occurred prior to deformation accompanying emplacement of the Mt. Lowe granodiorite in this area.

ORIGIN OF THE UNITS

THE ANORTHOSITE-LEUCOGABBRO UNIT

Anorthosite, leucogabbro and gabbro of this unit constitute the major part of the San Gabriel anorthosite-syenite body and apparently all formed during the same extended episode of bottom crystal accumulation, as evidenced by their gradational concordant contacts and similar textures and mineral assemblages. Repeated injection of magma occurred, but all of these rocks accumulated more or less continuously and under generally similar conditions. Anorthosite, leucogabbro and gabbro might

be considered as different igneous facies within a thick plutonic unit produced by bottom crystal accumulation. Different igneous facies probably resulted from variation in crystallization conditions, which were different in different parts of the body and at different stratigraphic levels.

Plagioclase was the only liquidus phase producing cumulate crystals during accumulation of most of this unit (anorthosite and most leucogabbro), with pyroxene crystallizing only from intercumulate magma. Pyroxene became a liquidus phase and produced cumulate crystals near the top of this unit, which resulted in formation of gabbroic rocks. Anorthosite and leucogabbro gradually change upward into gabbro, which is abundant near Magic Mountain and forms several discontinuous masses elsewhere. The observed field distribution of the three igneous facies suggests something about the different crystallization conditions which might have produced them.

Although a variety of crystallization conditions must have changed during progressive accumulation of the anorthosite-leucogabbro unit, probably the main factor responsible for the vertical variation of igneous facies was the changing composition of the magma. Gabbro near the top of the unit probably crystallized from a more mafic magma than the magma which produced the underlying anorthosite and leucogabbro. The upward change toward more mafic magma apparently was very gradual, probably from a very feldspathic initial magma, and produced substantially different rock types only near the top, where the transition into more mafic rocks is relatively abrupt and is brought about by the appearance of pyroxene as an abundant cumulate mineral.

Possibly the mafic magma pooled at the roof in some parts of the body, perhaps within sags in the underlying rocks. The thick accumulation of gabbro north and west of Magic Mountain might have been produced by magma collected from an originally widely-distributed but much thinner layer, remnants of which were trapped below the roof elsewhere to produce the gabbro masses along the northeast margin of the body. Direct evidence of sags and pools of gabbroic magma is not so persuasive as the evidence of similar sags and pools of syenitic magma higher in the section, but the overall distribution of gabbro suggests their presence. Just west of the mouth of Bear Canyon mafic gabbro contains large blocks of anorthosite and leucogabbro, suggesting proximity to a steep tectonic scarp. Abrupt thickening of gabbro occurs here from about 300 meters to about 1500 meters over a distance of 2-3 kilometers.

The thick gabbro near Magic Mountain grades into syenite by decrease of color index and increase of potassium-feldspar content. This suggests that differentiation of the magma which produced gabbro might have resulted in a residual magma of syenitic composition. However, the chemical composition of this gabbro is very sodium-rich and is very dissimilar from the composition of syenite (Chapter 5). Uncommon mesoperthite crystals are present in gabbro along the northeast margin of the body. This mesoperthite could be the result of contamination by the adjacent granulite gneiss, or it could be a product of differentiation of the gabbroic magma. If any residual syenitic magma was originally present in this part of the body, then tectonic pressures might have squeezed it out from beneath this part of the roof, causing it to collect elsewhere such as in the Buck Canyon synform.

As described in Chapter 3, in the southeast part of the body, thick leucogabbro subunits constitute as much as 35-40% of the anorthosite-leucogabbro unit. To the northwest, leucogabbro subunits in anorthosite are smaller, less continuous and less abundant. Farther to the northwest, in the more central part of the body, leucogabbro is almost entirely absent except near the top of the unit where anorthosite gradually changes upward to leucogabbro which is overlain by gabbro. These differences probably are evidence of different crystallization conditions between the margin and center of the body.

It is striking that the average overall color index of the anorthosite-leucogabbro unit is probably quite similar, both near the margin, with leucogabbro subunits distributed throughout the section, and near the center, with leucogabbro and gabbro present predominantly near the top of the section. This suggests that the average composition of the stratigraphic section in each area might be representative of the average composition of the original magma. The different distribution of lithologies suggests that crystallization conditions were consistently different in the center as compared to the margin of the intrusion. Near the margin of the intrusion pyroxene was apparently able to crystallize periodically from the intercumulate magma in sufficient quantity to keep the magma at nearly the same composition during accumulation of almost the entire stratigraphic section, leaving only a small amount of more mafic residual magma to form the small gabbro bodies at the top. Nearer the center of the body, apparently very little intercumulate pyroxene crystallized during accumulation of a large part of the stratigraphic section. This resulted in compositions trending toward strong ferromagnesian-enrichment in successively

younger magmas, from which first leucogabbro and finally gabbro crystallized near the top of the unit.

The reason for this difference is not known, but there are several possibilities: (1) More frequent and greater undercooling is likely near the margin of a layered intrusion. Greater undercooling might favor more rapid nucleation and growth of pyroxene in the intercumulate magma, thus producing a rock which might be more nearly representative of the composition of the contemporary magma. (2) The magma chamber was probably thinner near its margin so that convection, which depends in part on the thickness of the convecting fluid, might have been less effective in mixing the magma. Thus near the margin of the chamber the magma might have more often become locally supersaturated in ferromagnesian components and crystallized more pyroxene than did the better-mixed magma in the more central parts of the chamber. (3) Episodic injection of new magma might have produced either the anorthosite or the leucogabbro subunits near the margin of the body, depending on the composition of the new magma. Perhaps more rapid and complete mixing of magma in the central, thicker part of the intrusion allowed uniform crystallization of plagioclase unaffected by injections of new magma. These injections might have locally produced substantial compositional changes in the magma, and therefore in the rocks it crystallized, in the marginal parts of the intrusion where convective mixing was slower and less complete. (4) Slumping within the cumulate pile might have been greater in the center of the body, possibly because of sagging of the bottom of the intrusion as more magma was intruded. This slumping may have forced out more intercumulate magma, and kept the bottom magma more completely mixed so that there was less chance

for pyroxene to crystallize from intercululate magma, resulting in the crystallization of much less leucogabbro. However, there is little evidence of any possible slumping, perhaps because the rock is predominantly pure anorthoiste and because it has been affected by post-cumulous recrystallization.

None of these mechanisms give entirely satisfactory explanations of the lithologic variations observed. The relatively thin cyclic compositional layers and local cresumulate layers may have been produced by periodic undercooling, variations in water pressure, or local superstauration in stagnant magma, but such variations were probably too localized and of insufficient duration to produce the large-scale lithologic variations of alternating relatively homogeneous subunits hundreds of meters in thickness. The larger-scale lithologic changes must have been produced by compositional changes in the magma, probably resulting from periodic injection of new magma separated by intervals of fractional crystallization.

However, the detailed distribution of lithologies raises some difficulties with this interpretation (Plate I). Southeast of Mill Creek a single leucogabbro subunit splits into two thinnner subunits separated by anorthosite, and less than 3 kilometers away the two subunits are separated by at least 1200 meters of anorthoiste. Southeast of the Mill Creek fault, leucogabbro can be traced continuously from near the base of the intrusion southeast to near its margin and then back to the northwest near the roof of the body, stratigraphically about 4000 meters above the starting point and separated from it by a total of about 2500 meters of anorthosite in two thick subunits.

Perhaps the large anorthosite and leucogabbro subunits were produced by surges of newly intruded magma which was incompletely mixed near the margin of the intrusion, but well mixed near its center where few leucogabbro subunits occur. Thick sequences of leucogabbro might have crystallized near the margin of the intrusion wherever convective mixing was poor, while the influx of new magma and/or more complete convective mixing in the center might have favored the crystallization of anorthosite alone. The contact between well-mixed and poorly-mixed magma would thus shift alternately toward and away from the margin of the body and could produce alternating and branching subunits of leucogabbro and anorthosite. This is consistent with the more homogeneous central part of the intrusion, and with the observation that anorthosite subunits almost invariably wedge out as they are traced southeast toward the margin. Toward the center, either convective overturn was more frequent, or the intervals of stagnation between periods of convective mixing became fewer and of shorter duration, and consequently fewer, much smaller and more leucocratic leucogabbro subunits were produced. If this was the controlling factor in the development of the different lithologies, then the detailed distribution and thickness of leucogabbro and anorthosite subunits might aid in understanding the processes which occur in large layered intrusions.

Possibly lateral compositional gradients were present within the magma during crystallization, but the large size of this body, the presence of the contrasting lithologic distributions throughout such a great stratigraphic thickness, and the similar average compositions of the anorthosite-leucogabbro unit in both parts of the body argue against this as a likely possibility.

THE SYENITE UNIT

Formation of the syenite unit began with bottom accumulation of ferromagnesian minerals which formed very mafic gabbros and ultramafites which include large slump blocks of previously formed rocks (especially anorthosite). Olivine and augite were the most abundant ferromagnesians, but large amounts of apatite and ilmenite also accumulated and hypersthene was present in some rocks. Besides the ferromagnesians and the slump blocks, feldspar is present in many of these rocks, commonly making up 20-60% of the rock. Feldspar varies from andesine through antiperthitic oligioclase to mesoperthite, but there is no recognized consistent compositional variation from top to bottom of the ultramafic syenite subunit.

The magma which formed the syenite unit may have been capable of keeping feldspar crystals in suspension because of similar densities and turbulent convection, but allowed the denser ferromagnesian minerals to sink and form the basal ferromagnesian-rich cumulates. The magma collected in at least two major synforms which were forming during its crystallization so that massive slumping along their margins resulted in numerous slump blocks in the ultramafic syenite subunit. The magma was probably very near the density of feldspar so that minor changes in crystallization conditions or even differences in convection or turbulence in the magma might have allowed some feldspar to accumulate along with the ferromagnesian minerals. Some feldspar also must have crystallized from intercumulate liquid trapped in the mafic cumulates. A few intrusions of sill-like bodies of gabbroic rocks into previously accumulated rocks probably also occurred. Some feldspar crystals may be xenocrysts derived from the underlying anorthosite.

As the mafic rocks accumulated at the base, the composition of the overlying magma changed so that it changed from crystallizing calcic andesine (as in the underlying anorthosite-leucogabbro unit) or antiperthitic andesine-oligoclase (in some of the ultramafic syenite subunit) to the mesoperthite characteristic of the bulk of the syenite unit. The different feldspars in the ultramafic syenite subunit, therefore, were incorporated at different stages of differentiation and by different processes: as xenocrysts, as cumulate crystals, from intercumulate magma, or from magmas intruded into previously accumulated rocks. This explains the variable feldspar compositions in the ultramafic syenite subunit and the lack of a consistant cryptic compositional variation. Within the synforms, the mafic slumped rocks were superseded by more homogeneous, leucocratic, mesoperthite-bearing syenite which crystallized under more tranquil conditions. Occasional more mafic layers accumulated only when crystallization conditions varied or some new, less differentiated magma was intruded (such as that which formed the overlying jotunite unit). After crystallization of the syenite unit was nearly complete in the synforms, the jotunite magma was intruded and perhaps was contaminated by syenite.

The syenite unit probably formed the top of the intrusion at the time of its crystallization, as suggested by the presence of gneiss xenoliths near its top in some places. Most of the syenite shows no evidence of formation either by bottom crystal accumulation (density graded layers, slump structures, etc.) or by crystal flotation. The normal syenite subunit may have crystallized slowly from the top downward with nearly continuous reaction so that only very slight differentiation is observed in the lower rocks (mafic-depleted and somewhat

quartz-enriched, perhaps including a small amount of quartz syenite which was observed only in float). The chemical analyses reported in Chapter 5 show that syenite from low in the normal syenite subunit (708) is more fractionated than that from high in the subunit (1030 A and B).

In the Buck Canyon synform, the syenite unit is in contact with overlying jotunite unit rocks which interfinger with syenite and may have been contaminated by limited mixing with syenite. A small part of the contact of the syenite unit may be exposed in lower Sand Canyon, where it is overlain by a thin anorthosite layer which forms the base of a higher gabbroic or jotunitic unit. Numerous small xenoliths of Mendenhall gneiss are present in syenite below this contact, perhaps some as much as 1500 meters stratigraphically below the contact. These xenoliths suggest that the syenite formed the roof of the intrusion prior to intrusion of the overlying gabbroic rocks. Although very poorly exposed, this appears to be a sharp and concordant contact. Syenite is never in contact with Mendenhall gneiss except in these xenoliths. Therefore, it seems unlikely that the syenite could have been produced by partial melting of the granulite country rock at the present level of the pluton.

THE JOTUNITE UNIT

Very common graded layering in rocks of the jotunite unit indicates that they formed by bottom crystal accumulation; some of the uncommon layers in the underlying syenite are also graded, indicating a similar accumulation for at least some syenite. It appears unlikely that gradation from syenite into the overlying more mafic, low-potassium

jotunite could be the result of simple differentiation. Simple intrusion of jotunite magma into previously crystallized syenite might produce interfingering intrusive contacts with numerous sills and tabular xenoliths such as the upper contact of the jotunite unit, but would not explain the complete absence of observed crosscutting relationships and the gradational nature of the contact. The contact relationships might be better explained by intrusion of jotunitic magmas at a time when the syenite unit was only partially crystallized, and mixing of magmas could occur.

Several large gneiss xenoliths in jotunite adjacent to its contact with syenite in the axis of the Buck Canyon synform suggest that syenite formed the roof of the body at one time. The jotunite, which otherwise contains no xenoliths of gneiss near its base in this area, was intruded along the syenite-gneiss contact, with subsequent bottom crystal accumulation on the syenite floor. These geniss xenoliths do not appear to be appreciably assimilated at their margins. The new, more mafic jotunitic magma may have assimilated some syenite and possibly even retained a few partially assimilated syenite xenoliths, especially near its base where rocks intermediate between syenite and jotunite occur near the contact in Pacoima Canyon. Assimilation probably occurred while syenite remained at nearly magmatic temperatures.

In lower Sand Canyon, gabbroic and anorthositic rocks stratigraphically overlie syenite in a small area bounded by the Magic Mountain fault on the north and the Lonetree fault on the south. Although these rocks can not be definitely correlated across these faults with any other parts of the jotunite unit, their position and their ferromagnesian-rich, relatively high-potassium composition suggest they may

be part of the jotunite unit. Xenoliths in underlying syenite suggest that here too, jotunitic magma was intruded along a pre-existing syenite-gneiss roof contact. About a hundred meter interval of anorthosite and leucogabbro lies immediately above the basal contact with syenite and is overlain by altered gabbroic rocks similar to many rocks elsewhere in the jotunite unit. This may be the only example of basal anorthosite in the jotunite unit. Changes in lithologic facies in rocks of the jotunite unit (Plate III) probably reflect differences in the accumulation conditions in different parts of the chamber. Accumulation of much thicker rocks in the Pacoima Canyon area may reflect the presence of a deep sag during crystal accumulation. This sag would explain the abundant slump structures, graded layering and the ultramafic subunit rocks which accumulated only in its deeper parts. On its flanks thinner accumulations produced rocks with less lithologic and structural variability, fewer cyclic layers, and rare slump structures. This younger sag probably developed as a continuation of the earlier Buck Canyon synform.

The lack of cryptic layering within the jotunite unit or within its individual subunits suggests that the jotunitic magma was emplaced as a series of injections. Thus it was not possible for any individual magma to differentiate sufficiently to produce large-scale consistent compositional variations within the accumulating rocks. The marked lateral variations of subunits and numerous dikes of gabbroic composition in the underlying rocks support this interpretation.

Size grading in extremely ferromagnesian-rich layers and abundant slump structures show that these rocks formed on the bottom of the chamber. Very common grading in gabbroic layers suggests that feldspar

sank in the mafic magma, even though its density must have been higher than that of the feldspar, and scattered leucocratic segregations in a few outcrops are best explained by feldspar flotation. Rocks of the jotunite unit formed on the floor by sinking of ferromagnesians and the plagioclase in these rocks may have mainly formed by direct bottom crystallization to produce common apparently density graded layers by a mechanism of cooling and diffussion like that proposed by McBirney and Noyes (1979).

MAGMA

The San Gabriel anorthosite-syenite body was formed by a series of magmas intruded into a large chamber. It may therefore be inappropriate to speak of a single "parent magma" which produced the entire body. However, many successive magma pulses appear to have been very similar in composition, (although the latest magmas were very different from the earliest), and contacts between the three major stratigraphic units are gradational in at least some parts of the body. Thus there exists the possibility that all of the individual magmas were produced as part of a single ongoing episode of magma genesis occurring at greater depth, and that the average composition of the body might give an approximation of at least some fraction of the magma which was generated at depth.

The estimated average composition of the body is given in Chapter 5, Table III. Even though this estimate is subject to large uncertainties, it must serve as the starting point in the discussion of the nature of the magma(s) which produced the body. No chilled rocks have been recognized and all dikes in older rocks above and marginal to the body (mostly with very high color indices) are of different composition than

any likely initial magma.

Most if not all of the rocks of this body originated by some type of cumulate process and so they are not necessarily the same composition as the magma which formed them. Similarly, the average composition of the body as a whole may be different from the bulk composition of the magma which produced it if some of the intruded magma contained a substantial proportion of suspended crystals which accumulated to form rocks which are included in the average composition of the body.

The extremely high content of Al_2O_3 is a striking feature of the average composition and suggests either an anorthositic magma or that plagioclase crystals were abundant in some of the initial intruding magma and contribute to the estimated average composition. If any plagioclase crystals present in the initial magma had been added by partial assimilation of crustal rocks, then the composition of the primary magmas would have been substantially changed by assimilation, and subtraction of the plagioclase crystals from the average composition would leave an initial magma modified from its original composition. If plagioclase crystals had been produced by prior crystallization of a precursor magma, then subtraction of the plagioclase crystals from the average composition might give an initial magma which resembles some generally recognized primary magma type.

The bulk of the plagioclase of the anorthosite-leucogabbro unit lies within a compositional range of An_{40} to An_{55}. Therefore approximations of the composition of possible initial magmas might be calculated by subtracting various proportions of plagioclase of this composition from the estimated average composition. Table V shows the compositions which result from subtraction of 10, 20, 30, 40, and 50 percent

Table V: "Average Composition" Less Various Percentages of Plagioclase (1055 A-1-P-12)

	Average Composition	Plagioclase 1055A-1-P-12	A.C. Less 10%	A.C. Less 20%	A.C. Less 30%	A.C. Less 40%	Less 50%	Trachyandesite*
SiO_2	53.73	58.15	53.24	52.63	51.84	50.78	49.31	51.01
TiO_2	1.17	0	1.30	1.46	1.67	1.95	2.34	1.72
Al_2O_3	22.33	26.09	21.91	21.39	20.72	19.82	18.57	18.18
Fe_2O_3	1.66		1.84	2.08	2.37	2.77	3.32	3.94
FeO	4.54	0.01	5.04	5.67	6.48	7.56	9.07	5.56
MnO	0.08		0.09	0.10	0.11	0.13	0.16	0.10
MgO	1.72	0	1.91	2.15	2.46	2.87	3.44	2.42
CaO	8.08	10.04	7.86	7.59	7.24	6.77	6.12	6.77
Na_2O	5.05	5.55	4.99	4.93	4.84	4.72	4.55	5.56
K_2O	1.18	0.16	1.29	1.44	1.62	1.86	2.20	2.83
P_2O_5	0.42		0.47	0.53	0.60	0.70	0.84	0.90
S	0.04		0.04	0.05	0.06	0.07	0.08	

*Varne (1968)

Table VI: "Average Composition" Less Various Percentages of Andesine Antiperthite*

	Average Composition	Andesine	A.C. less 10%	A.C. less 20%	A.C. less 30%	A.C. less 40%	A.C. less 50%
SiO_2	53.73	58.10	53.24	52.64	51.86	50.82	49.36
TiO_2	1.17		1.30	1.46	1.67	1.95	2.34
Al_2O_3	22.33	26.44	21.87	21.30	20.57	19.59	18.22
Fe_2O_3	1.66	0.04	1.84	2.07	2.35	2.75	3.28
FeO	4.54	0.15	5.03	5.64	6.42	7.47	8.93
MnO	0.08		0.09	0.10	0.11	0.13	0.16
MgO	1.72	0.03	1.91	2.14	2.44	2.85	3.41
CaO	8.08	7.84	8.11	8.14	8.18	8.24	8.32
Na_2O	5.05	6.48	4.89	4.69	4.44	4.10	3.62
K_2O	1.18	1.10	1.19	1.20	1.21	1.23	1.26
P_2O_5	0.42		0.47	0.53	0.60	0.70	0.84
S	0.04		0.04	0.05	0.06	0.07	0.08

*Deer, Howie and Zussman (1966), p. 324, No. 4.

plagioclase ($An_{49}Ab_{50}Or_1$, analysis 1055A-1-P-12) from the average composition and Table VI shows the compositions which result from subtracting these percentages of "andesine antiperthite" ($An_{38}Ab_{56}Or_6$, Deer, Howie and Zussman, 1966, v. 4, p 115, #8) from the average composition. Plagioclase 1055A-1-P-12 has a composition a little more calcic than the average of all those measured from the anorthosite-leucogabbro unit and "andesine antiperthite" is probably similar to the composition of much plagioclase in the gabbroic rocks of the syenite and jotunite units. If the initial magma contained about 40% plagioclase crystals of the composition of 1055A-1-P-12, then its composition (Table V) is similar to that of a trachyandesite (Varne, 1968, p 172). Ryder (1974) cites evidence that the San Gabriel body is andesine-type anorthosite which differentiated from an andesitic magma.

The San Gabriel anorthosite-syenite body was emplaced into continental crust which had previously undergone a long history of deposition, metamorphism, deformation and magmatism covering a period of about 200 my but which had been relatively quiescent over the 200 my immediately preceding generation of the magma which produced it. About 1200 my ago melting again occurred beneath this continental crust to produce a large amount of magma which produced the anorthosite-syenite body.

Magma moved upward into the present level of the crust as a series of separate intrusions, most if not all reaching the chamber prior to complete crystallization of the previous magma. Many successive magmas were probably very similar in composition, but some of the late magmas had very different compositions than earlier magmas. Two of the more likely models for the origin of this series of magmas are: (1) A

single parent magma which evolved by fractional crystallization, assimilation or some other mechanism at depth, and during this evolution, intruded fractions upward to form the anorthosite-syenite body. (2) Some of the different magmas were generated at different levels by melting of different rocks or by differentiation of independent magmas. Each of these possibilities is discussed below.

(1) Perhaps a large amount of continental alkali-olivine basalt was generated beneath this area of previously stable continental crust. Crystallization of this magma began at depth, either in the upper mantle or in the lowest part of the crust. During this initial crystallization, sinking of ferromagnesian minerals and crystallization of plagioclase drove the composition of the residual magma toward that of a trachyandesite relatively enriched in iron and potassium. Some early-formed plagioclase may have accumulated along with the ferromagnesian minerals, but much of the later-formed plagioclase had a lower density than the magma and therefore remained suspended or floated. Thus an extended period of crystallization produced a trachyandesitic magma which contained up to about 50% suspended plagioclase crystals but remained sufficiently fluid to be intruded farther upward into the continental crust. The suspended plagioclase crystals had a longer time to crystallize than if they had sunk, and therefore grew to relatively large sizes of 10 millimeters or more. Yoder (1969) suggested that flotation accumulation in alkalic magma may lead to the formation of some anorthosite.

(2) Partial melting, either in the upper mantle or the lower crust, produced initial magmas of anorthositic composition. Intrusion of a series of these magmas occurred initially. Successively more

gabbroic magmas resulted either from different degrees of partial melting, from melting of different material, or from fractional crystallization at depth. In the later stages of magmatic activity, melting of very different rocks, probably from lower or middle crustal levels, produced a much more potassic magma of syenitic composition. This syenitic magma also intruded upward and in part mixed with some of the more gabbroic magma. Wiebe (1978) concludes that some plutons in the Nain, Labrador area were produced by leuconoritic magmas and that adjacent granitic plutons were generated independently by melting of crustal rocks.

CRYSTALLIZATION AND MAGMATIC TRENDS

Contact relationships, lithologic variations and mineral composition variations indicate that a series of magmas were intruded into the chamber in which the anorthosite-syenite body crystallized. Cumulate textures, crescumulate layers and slump structures (Chapter 3) indicate that most rocks of the anorthosite-leucogabbro and jotunite units were produced by bottom crystal accumulation. Synplutonic tectonism, described above and in Chapter 3, played an important role in producing the final distribution of lithologies in the body. It is evident that plagioclase was the only liquidus mineral during accumulation of most of the body (almost the entire anorthosite-leucogabbro unit). Although erosional discontinuities separate some units from others, gradational contacts are observed in at least some places, between the anorthosite-leucogabbro and syenite units northwest of Magic Mountain, and between the syenite and jotunite units in Pacoima Canyon.

Figure 113. Pseudoternary albite-anorthite-diopside diagram (Lindsley and Emslie, 1967; Emslie, 1970; Muan, 1979) illustrating possible early crystallization history of the magma which produced the anorthosite-syenite body.

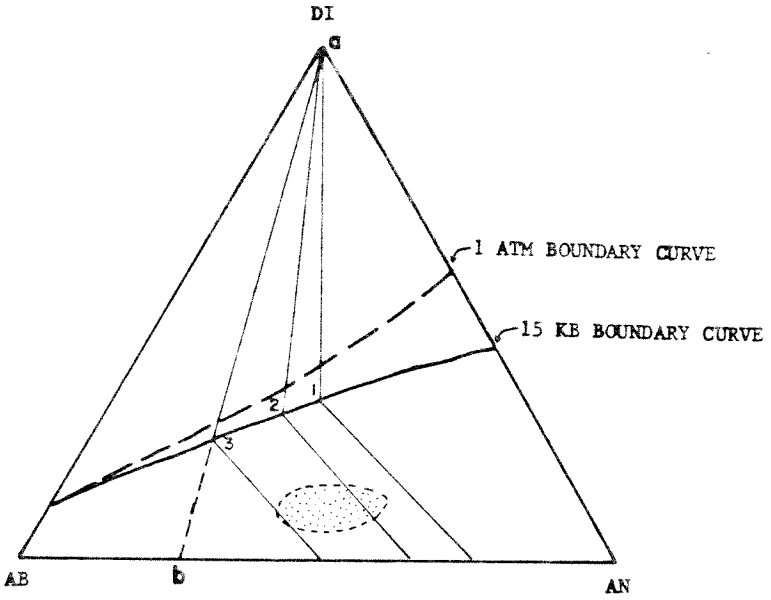
DI
a
1 ATM BOUNDARY CURVE
15 KB BOUNDARY CURVE
1
2
3
AB
b
AN

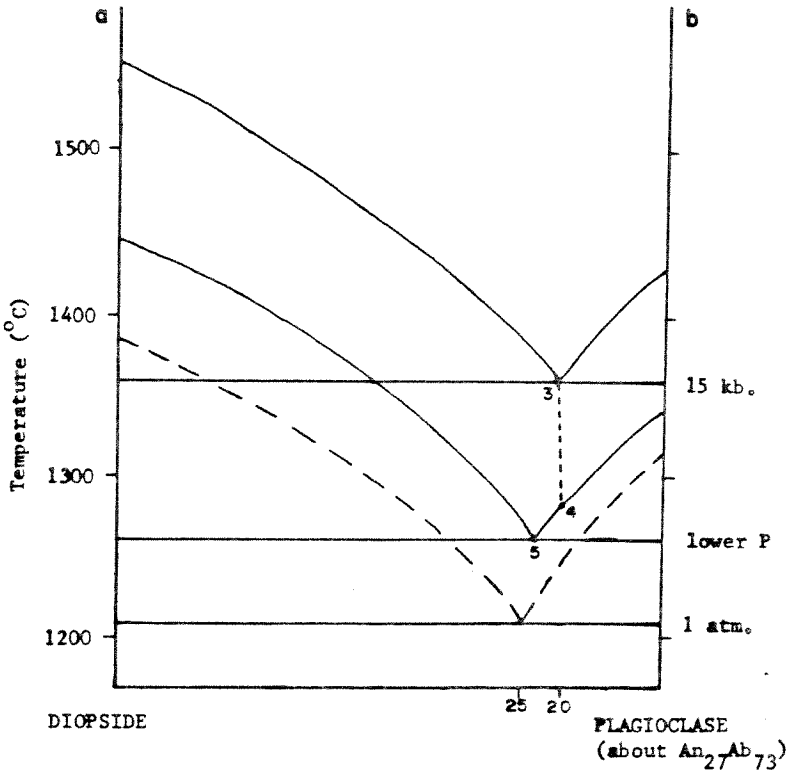
a
b
1500
1400
1300
1200
Temperature (°C)
15 kb.
lower P
1 atm.
3
4
5
25
20
DIOPSIDE
PLAGIOCLASE
(about An27Ab73)

Figure 113.

The two possible models of the origin of the magmas which produced the body are discussed separately below. Each must explain the observations summarized above. Possible trends of magmatic evolution are illustrated on a pseudoternary albite-anorthite-diopside diagram (Lindsley and Emslie, 1967; Emslie, 1970; Muan, 1979) in Figure 113. Although only an approximation, this diagram may be useful in illustrating the early crystallization history of the body since the initial cumulate minerals were predominantly andesine and pyroxene (possibly clinopyroxene); ilmenite and apatite are cumulate minerals only in rocks of the syenite and jotunite units, and olivine is demonstrably an abundant cumulate mineral only in some rocks of the syenite and jotunite units.

THE SINGLE MAGMA HYPOTHESIS

The San Gabriel anorthosite-syenite body might have been produced by a series of consanguineous magmas successively intruded into the present crustal level. Calculations of possible proportions and compositions are included below, but they are included only to test the feasibility of the model, and are not meant to be exact figures required by the model.

(1) Partial melting of sub-continental upper mantle produces a magma of continental alkali-olivine basalt type which collects and begins to crystallize in a chamber at about 50 kilometers depth. The composition of this magma is approximated by point 1 on the Ab-An-Di: diagram ($Di_{30}An_{35}Ab_{35}$).

(2) Crystallization of diopside and plagioclase (An_{75}) and gravitational sinking of both minerals drives the residual magma to the

left along the boundary curve to point 2 (about $Di_{27}An_{31}Ab_{42}$). At this point about 35% of the original magma has crystallized to form layered gabbro with an average color index of 34, and the liquidus plagioclase has reached a composition of An_{65}.

(3) At the composition of about An_{65}, plagioclase crystals begin to float in magma 2 and begin to accumulate in the upper part of the chamber while diopside continues to accumulate on the floor along with some bottom-crystallized plagioclase. Floating plagioclase undergoes continuous reaction with the residual magma which changes composition along the boundary curve to point 3 (about $Di_{20}An_{22}Ab_{58}$). At this point a further 22% of the original magma has crystallized to form layered gabbro with an average color index of 53 and the remaining 43% of the original magma consists of 26% magma and 17% suspended plagioclase crystals of An_{50} composition (60% magma and 40% plagioclase).

(4) Fractions of this magma suspended plagioclase are repeatedly intruded upward into the continental crust to a depth of perhaps about 20 kilometers. This change to lower pressure causes lowering of the liquidus and a shift of the boundary curve away from plagioclase toward the 1 atmosphere curve. These changes can be illustrated on a pseudo-binary section along the line a-b.

As illustrated on the pseudo-binary section (Figure 113b), at the lower pressure the "cotectic" drops about 100 C and shifts from a composition of Di_{20} to Di_{23}. The magma (point 3) is now considerably above the liquidus and is no longer of "cotectic" composition.

(5) Formation of the anorthosite-leucogabbro unit began with the bottom accumulation of the 40% suspended plagioclase. A further 14% of the total intrusion could crystallize plagioclase (very nearly An_{50})

before residual magma reached the boundary curve (point 5) and began to crystallize abundant diopside. Thus under ideal conditions, 53% of the chamber could fill with pure plagioclase before diopside begins to crystallize.

Settling of plagioclase crystals which had previously floated was probably in part the result of the magma's change to a more felsic composition due to slight resorption of plagioclase, and in part due to a slight decrease in density in the lower pressure environment. Two other factors might have also favored the sinking of plagioclase: (a) at least initially the intruded magma was above its liquidus and therefore retained a relatively low viscosity and low yield strength (McBirney and Noyes, 1979) and (b) most suspended crystals had grown to much greater size than plagioclase crystals crystallizing directly from the magma in most layered intrusions and so were much better able to overcome the non-newtonian yield strength of the magma (McBirney and Noyes, 1979, Figure 3) and to sink even with only a minor density contrast. Experiments by Fujii and Kushiro (1977) show that plagioclase of a given composition may float in basaltic magma at high pressure but can sink in the same magma at lower pressure.

(6) More realistically, before the bulk of the magma reaches the boundary curve (point 5), local crystallization of diopside must occur in interstitial magma and stagnant bottom magma. If an additional 14% of the total crystallized in this manner, then 67% of the chamber would fill (64% plagioclase, An_{50} and 3% diopside) before the residual magma reached the boundary curve and began to crystallize abundant diopside.

In the central part of the chamber only small amounts of ferromagnesians crystallized and most of the rock was anorthosite. Near its

margins where cooling was more rapid, more frequent local supersaturation of ferromagnesian constituents occurred so that more ferromagnesians crystallized, and anorthosite alternates with more leucogabbro than in the central area. Throughout the body, rocks near the top of the anorthosite-leucogabbro unit formed when magmas were nearer to the "cotectic" due to mixing with fractionated residua of earlier magmas, and therefore more commonly locally crystallized ferromagnesians. Thus leucogabbro is more abundant everywhere near the top of this unit.

(7) After successive magmas had formed about 65% of the total body, the residual magma, considerably more mafic and with somewhat higher Fe/Fe+Mg ratio, reached the lower pressure "cotectic" and began to continuously crystallize ferromagnesian minerals. Thus the gabbros of the uppermost anorthosite-leucogabbro unit were formed by bottom accumulation of ferromagnesians and concurrent bottom crystallization of feldspar (now An_{35} or less).

(8) At about the same time as abundant ferromagnesians began to accumulate, the increasingly alkali-rich plagioclase began to float in the more mafic magma. This marked the end of crystallization of the anorthosite-leucogabbro unit and produced the very mafic rocks of the ultramafic syenite subunit. In some places the contact is unconformable due to synplutonic tectonism and in other places a gradational contact separates gabbro from overlying rocks of the syenite unit. At this time the liquidus plagioclase was probably about $An_{30}Ab_{65}Or_5$ and the composition of the remaining magma was such that equlibrium crystallization with continuous reaction would have produced a feldspar of about $An_{10}Ab_{50}Or_{40}$ composition.

(9) The syenite unit was formed by bottom accumulation of ferromagnesian minerals accompanied by limited bottom crystallization of feldspar to form the ultramafic syenite subunit. Slow crystallization of the overlying magma by equlibrium continuous reaction with suspended feldspar crystals formed the normal syenite subunit. Because of the slow equlibrium crystallization, the normal syenite subunit is the most uniform of any subunit in the anorthosite-syenite body. The rocks of the normal syenite subunit are slightly more leucocratic, more potassic and more siliceous near its base compared to those near its top, perhaps due to crystallization from the top downward.

(10) The jotunite unit was formed by mafic magmas, some perhaps residua of those which formed the anorthosite-leucogabbro unit, but most probably newly intruded magmas which had differentiated to mafic compositions at depth. Limited mixing of these mafic magmas with syenitic magma occurred, producing gradational contacts and interlayered relationships.

THE INDEPENDENT MAGMAS HYPOTHESIS

The San Gabriel anorthosite-syenite body might have been produced by a series of magmas, at least some of which were generated independently, perhaps in different parts of the crust or mantle, all intruded into the present crustal level. The manner of crystallization of individual magmas (mineral sequence, magmatic trends) would have been very similar to that described in the previous model above, but the individual magmas were not consanguineous.

(1) Partal melting of the lower continental crust produces a leucogabbroic magma. This magma may be heavily charged with plagioclase

crystals, probably either accumulated by flotation, or unmelted residua from the source region. The composition of this magma might lie somewhere in the shaded area in Figure 113.

(2) Successive batches of this magma are intruded upward into the continental crust. For each magma, the lower pressure causes lowering of the liquidus and a shift of the boundary curve away from plagioclase. Some suspended plagioclase, if present, is resorbed and the magma cools to the new liquidus, now on the plagioclase side of the "cotectic". Accumulation of the anorthosite-leucogabbro unit begins with crystallization and bottom accumulation of plagioclase. During this fractional crystallization, the residual magma would shift toward the new "cotectic". Repeated injections of new magma, each mixing with the earlier fractionated liquid, allowed long-continued crystallization of plagioclase as the only liquidus mineral.

(3) The fractionated magma remaining in the chamber finally reached the "cotectic" and began to crystallize ferromagnesian minerals. Crystallization of this magma as well as new magmas, which may now be coming from a similarly fractionated source at depth, produced the gabbroic rocks of the anorthosite-leucogabbro unit, and probably would have finally crystallized jotunitic rocks.

(4) At about the same time that the more mafic rocks began to crystallize, a syenitic magma was generated, possibly by partial melting of crustal rocks from a higher level than those which yielded leucogabbroic melts. These syenitic melts were also intruded upward into the same chamber in which rocks of the anorthosite-leucogabbro unit had previously accumulated and in which the more mafic gabbroic to jotunitic rocks were now accumulating. Limited mixing of the syenitic and the

jotunitic magmas occurred, resulting in gradation between jotunitic and syenitic rocks in some places and interfingering of the two types in other places.

(5) This stage of crystallization was marked by tectonic activity which produced large scarps along the margins of the relatively smaller chambers which contained syenitic and/or jotunitic magmas. Initial crystallization of syenitic magma produced bottom accumulation of ferromagnesian minerals, along with large slump blocks adjacent to the scarps, at the same time that its feldspar largely remained suspended. Eventual completion of crystallization of the bulk of the syenite magma occurred from the top downward.

(6) New injections of mafic magma which had previously fractionated at depth, occurred during and following crystallization of syenite. Crystallization of a series of these magmas produced the jotunite unit. Some of these mafic magmas may have mixed with syenitic magma and thus produced the few ferrosyenitic rocks of the jotunite unit.

POST-CRYSTALLIZATION PROCESSES

Two important widespread processes affected most rocks of the anorthosite-syenite body soon after they had crystallized. Post-cumumulous recrystallization was widespread and produced extremely coarse textures in many rocks, particularly anorthosite. Uralitization occurred soon after crystallization and produced almost universal alteration of ferromagnesian minerals.

POSTCUMULOUS RECRYSTALLIZATION

All anorthosite and leucogabbro was affected by postcumulous recrystallization (Chapter 4, Figure 57) which produced very coarse textures. Recrystallized plagioclase in these rocks commonly reaches 5-20 centimeters and may exceed one meter. Recrystallization must have occurred in rocks in which near-solidus temperatures were maintained over a relatively long time, and may have begun while some interstitial magma remained in the rock. It is unlikely that bulk compositional changes of the whole rock occurred during recrystallization since the composition of recrystallized plagioclase is similar to that of unrecrystallized plagioclase in the same rock (Chapter 5). Compositional variation in recrystallized plagioclase crystals (typically about 4% anorthite content) cannot be related to concentric zonation, and suggests that plagioclase was not homogenized during postcumulous recrystallization.

Widespread recrystallization of syenite produced a finer grained granoblastic texture and also occurred at very high temperatures, apparently mainly above the alkali feldspar solvus.

Recrystallization of jotunite occurred in zones which cut primary layering, but was not so widespread as in the anorthosite-leucogabbro and syenite units. Recrystallization usually produced coarser gabbroic rocks containing pyroxenes and including large biotite crystals in much greater abundance than in unrecrystallized jotunitic rocks. The presence of biotite suggests that recrystallization of jotunitic rocks occurred when fluid pressures were higher than during accumulation of the primary layers.

Widespread recrystallization suggests that most rocks of this body maintained elevated temperatures for an extended period following initial crystallization. The mineralogy and bulk composition of recrystallization rocks suggests that late-stage alkali-enriched hydrous fluids probably facilitated recrystallization, but there is no evidence that major changes of bulk rock composition took place.

URALITIZATION

Complete uralitization of ferromagnesians is characteristic of almost all rocks of this body. The ferromagnesians in recrystallized rocks are pseudomorphs of amphibole after original pyroxene or olivine, so uralitization must have occurred after recrystallization.

Several lines of evidence indicate that uralitization occurred soon after crystallization rather than as a younger unrelated process. (1) Water must have been present in the magma, since red biotite and hornblende are common products of late-stage magmatic crystallization in many mafic rocks of the syenite and jotunite units. (2) Primary ferromagnesians in many rocks were overgrown by small crystals of blue-green hornblende immediately following crystallization, showing that late-stage hydrous fluids must have been present. (3) The degree of uralitization is uniform throughout nearly all rocks of the body, showing no relation to younger intrusive rocks, margins of the body, faults and shear zones, or geographic location. (4) Unuralitized ferromagnesians are found only in rocks of the syenite and jotunite units which crystallized late in the sequence. These late, unuralitized rocks include mafic, iron-rich rocks and leucocratic rocks and crystallized after most rocks

of the body had already undergone uralitic alteration, perhaps after water pressures had decreased from earlier levels.

(5) Magma was emplaced into an extensive terrain which had previously undergone metamorphism under granulite facies conditions so the large amounts of water necessary to produce the uralitization would not have been available from the adjacent country rocks. (6) Taylor (1969) has shown that rocks of the body have O^{18}/O^{16} ratios normal for plagioclase from basalt and gabbro, and are significantly different from ratios characteristic of regional medasedimentary rocks or meteoric waters. These ratios indicate that the water which produced the uralitization probably came from an igneous source.

The above evidence leads to the conclusion that the original magma must have been hydrous and may have approached water saturation in the later part of its crystallization.

CHAPTER 7

MASSIF-TYPE ANORTHOSITE AND THE SAN GABRIEL BODY

INTRODUCTION

The San Gabriel anorthosite-syenite body is an example of massif-type anorthosite which occurs in widespread plutons. The purpose of this chapter is to compare the San Gabriel body to some of the other massif-type anorthosites, to briefly mention some of the possible origins of anorthosite proposed by other authors, and to briefly summarize the contributions of this study to the problem of the origin of anorthosite.

OTHER ANORTHOSITE BODIES

More than 100 massif-type anorthosite bodies are listed by Anderson (1969). They are probably all of Precambrian age and most are between 100 and 10,000 square kilometers in size. Most contain modal orthopyroxene with or without olivine and augite and most have plagioclase compositions which vary little more than 10% - 15% An content, although all massifs encompass the range An_{80} to An_{25} with most between An_{65} and An_{45}. Many anorthosite massifs have been described and a variety of origins have been proposed (DeWaard, 1969); a brief description of a few of these are presented in this section for purposes of comparison with the San Gabriel body.

The Michikamau anorthositic intrusion, which underlies about 2000 square kilometers in west-central Labrador, has been described by Emslie (1965, 1968, 1969). The intrusion had the form of a funnel or lopolith 9 - 10 kilometers thick, which was intruded into quartzo-feldspathic granulite gneisses about 1400 million years ago. The intrusion consists mainly of a layered series of troctolite and leucotroctolite overlain by

a thick anorthosite zone and an upper zone of leucogabbro and gabbro, all of which are cut by late ferrodiorite, ferromonzonite and ferro-adamellite differentiates. Plagioclase ranges from An_{72} to An_{50}. Rhythmic layering and planar plagioclase orientation are widespread and believed to have formed through the action of convection currents. Emslie believes that the intrusion was formed by an aluminous basaltic magma carrying suspended labradorite crystals which rose to accumulate in the upper part of the chamber. Thereafter, solidification took place by bottom crystal accumulation. After about 85% crystallization, collapse of the anorthosite roof caused the remaining iron-enriched differentiates to be displaced upward through fractures to a horizon between the original roof and upper zone gabbros.

Several large anorthosite intrusions are exposed in the Egersund area of southern Norway where they intrude granulite gneisses (Goldschmidt, 1916; Barth, 1933; Michot, 1969). The youngest of these is the Bjerkrem-Sogndal massif, a layered lopolith which underlies about 300 square kilometers and reaches a total thickness of about 5 kilometers in its axis. Although described as synkinematic, this synformal body is relatively undeformed and is made up of cumulates of the anorthosite-mangerite suite. The lower part of the lopolith consists of five rhythmic successions of anorthosite and leuconorite (An_{40-44}) which is followed, without any discontinuity, by a monzonoritic transitional phase and, finally, by a mangeritic phase at the top of the body. These are cumulate rocks, interpreted to have formed by bottom accumulation of plagioclase along with smaller amounts of other minerals, and this lopolithic succession establishes a genetic relationship between anorthosite--the oldest differentiate, and mangeritic rocks--the youngest differentiates

(Michot, 1969; Duchesne, 1972). This lopolith is believed to have formed by gravity differentiation of a series of intermittent pulses of undifferentiated plagioclasic magma (Michot, 1969). Studies of rare-earth elements (Duchesne, et. al, 1974) have shown that the parental magma of this suite is represented by monzonoritic rocks (hypersthene-monzodiorite or jotunite).

The Laramie anorthosite underlies about 100 square kilometers in southeastern Wyoming. It intrudes granulite grade metasediments and has been described by Newhouse and Hagner (1957) and Smith, et al. (1970). This body consists of a central mass of brecciated labradorite anorthosite which appears to thicken toward the center, surrounded by an envelope of gabbroic anorthosite. Syenite and granite (Sherman granite) are described as having gradational contacts with anorthositic rocks (Fowler, 1930), but contain anorthosite and gabbroic anorthosite xenoliths and roof pendants (Klugman, 1960; Smith, et al., 1970). Gneissic layering in anorthosite is believed to be due to flow in the magma (Ramarathnam, 1962). Syenite magma probably differentiated from underlying noritic rocks and was intruded as a highly viscous crystal mush lubricated by a small amount of interstitial magma (Smith, et al., 1970). De Vore (1975) believes that the anorthositic rocks are the residuum of partial melting of metasediments, which produced the liquid which formed the Sherman granite.

Anorthosite and related rocks underlie about 20,000 square kilometers of the Nain, Labrador area. They were intruded into granulitic rocks about 1480 million years ago and have been described by Wheeler (1960), DeWaard and Wheeler (1971) and Wiebe (1978). This is a complex massif made up of a series of intrusions which range from anorthosite

and norite to granite and alaskite which, together, form a large warped and folded body. These rocks consist predominantly of anorthositic to noritic rocks (An_{40-60}) and adamellitic rocks but include a number of bodies constituting a troctolite-syenite suite. Weibe (1979, 1980) believes that at least some of these bodies were produced by crystallization of an anorthositic magma generated near the base of the crust, and that the major granitic plutons represent melts generated from the crust at relatively low temperatures. DeWaard and Wheeler (1971) suggest that fractional crystallization produced a density-stratified magma in which suspended plagioclase crystals accumulated at an intermediate level, underlain by denser troctolitic magma and overlaid by less dense acidic magma. Settling of the plagioclase mass caused local intrusion of the troctolitic magma which differentiated to form the troctolite-syenite suite and caused local intrusive relationships between it and the acidic magma which differentiated to form the adamellite series. Berg (1977) has shown that the Nain complex was emplaced into a non-orogenic environment of low temperature (645-915° C) and moderate depth (12 - 22 kilometers).

Simmons and Hanson (1978) have studied the geochemistry of anorthositic rocks from the Nain area as well as from the Adirondack Mountains and elsewhere. They suggest that massif-type anorthositic plutons are the result of partial melting of tholeiitic compositons at depths shallower than the basalt-eclogite transformation, producing an anorthosite gabbro melt and leaving a pyroxene-dominanted residue.

The Grenville tectonic province of Quebec and Labrador contains several very large and numerous smaller anorthositic plutons, including the Adirondack and Lac St. Jean plutons and the Morin series.

Interpretation of these plutons is more difficult than those described above because they have been metamorphosed and deformed during the Grenville orogeny subsequent to their emplacement. However, several of these bodies have been extensively described in the literature and any discussion of anorthosite and its origin must include the Grenville anorthosites.

The Adirondack anorthosite which underlies about 2000 square kilometers in northeastern New York, was made classic through the work of Buddington (1939), and has been studied by many other authors (Balk, 1930; Berry and Walton, 1961; DeWaard and Romey, 1969: Seifert, et al., (1977). This body is interpreted as a large domed sheet-like body 4 - 5 kilometers in thickness with two roots extending to greater depth (Simmons, 1964). Rocks of this area are an anorthosite and gabbroic anorthosite series (mostly An_{45-55}), and a jotunite-mangerite-quartz mangerite-charnockite series, rocks of which sometimes contain anorthosite xenoliths. The relationship of the two rock series is controversial. Buddington (1972) concludes that the anorthositic rocks were produced by fractional crystallization by plagioclase accumulation of a leucogabbroic magma containing 40% suspended andesine crystals, which was generated at the base of the crust. He believes that the granitic rocks were the result of crystallization of a quartz mangeritic liquid generated independently in a relatively dry deep part of the upper crust. Based on field relationships and rare-earth element studies, Seifert, et al., (1977) and Seifert (1978) conclude that the anorthositic and mangeritic rocks are not related and that the anorthosite massif is a plagioclase crystal cumulate. DeWaard and Romey (1969) favor origin of the entire suite by differentiation of a single magma or else formation of part of

the magma by anatexis of salic gneisses. DeWaard (1970) proposes that a parent magma of dioritic or granodioritic composition (or a basaltic magma altered by assimilation or anatexis) differentiated to form a plagioclase cumulate near the roof, which later settled in large chunks, causing the residual mangeritic magma to intrude in and above the plagioclase cumulate.

The Morin anorthosite complex in southern Quebec underlies about 2500 square kilometers and has been described by Martingnole and Schrijver (1970), Philpotts (1962, 1966), Cote (1960) and Emslie (1975). This complex was intruded into granulite gneisses and metasedimentary rocks and is divided into two lobes which have the form of irregular sheets 2 to 4 kilometers thick, underlain by thin pipes extending to depths of at least 12 kilometers (Kearey, 1978). The anorthositic suite is composed of three principal units which appear to form an intrusive sequence: anorthosite-leucogabbro (An_{42-54}), jotunite and quartz mangerite, all of which have been metamorphosed under upper amphibolite to granulite facies conditions. Philpotts (1966) concludes that the rocks of this suite were formed by a calc-alkaline acid diorite magma from which plagioclase accumulated to form anorthosite at the base of various intrusive sheets. Pyroxene crystallized next and accumulated to form layered norites above anorthosite, and finally, filter pressing separated the acid magma from which the quartz mangerite crystallized.

The Lac St. Jean anorthosite massif in Quebec underlies about 20,000 square kilometers and has been described by Frith and Currie (1976) and Kehlenbeck (1972). The body is considered to be a crustal substratum (Frith and Currie) or a large sheet-like intrusion (Kehlenbeck). The anorthosite and gabbro (An_{40-60}) of this area have been highly

deformed and recrystallixed. Frith and Currie (1976) propose that these rocks formed as the residue remaining after extensive partial melting of tonalite in an orogenic environment at pressures of 5 - 8 kilobars and temperatures of 800 - 1000° C. The same process operating on more potassic rocks would leave monzonitic or quartz syenitic residues.

THE SAN GABRIEL BODY

The San Gabriel anorthosite-syenite body presently underlies about 250 square kilometers in the western San Gabriel Mountains, but scattered outcrops outside of the San Gabriel Mountains (Crowell and Walker, 1962), Powell and Silver, 1980) suggest that the original body was considerably larger. This body was intruded into granulite gneisses about 1220 million years ago to form a large stratiform pluton, probably at least 10 kilometers in thickness which appears to thicken under its center. The body consists predominantly of anorthosite and leucograbbo with smaller amounts of syenite and of jotunitic rocks.

Several aspects of the San Gabriel body contrast markedly with some or all of the anorthosite bodies described above: (1) The San Gabriel body has not been subjected to any high-grade regional metamorphism subsequent to its crystallization, so primary igneous textures and structures are well-preserved in some of the rocks. (2) The San Gabriel body is part of a large allochthonous sheet which has been subjected to severe structural deformation which has resulted in fault displacements and structural relief produced by folding measured in thousands of meters. Although these structural complications hinder reconstruction of the original form of the body, they allow access to different structural

levels of the original body. (3) The San Gabriel body is of limited size, allowing detailed study of the entire body and exposes an intimate association of the anorthositic, gabbroic and syenitic rocks. Possibly no other anorthosite body except perhaps the Bjerkrem-Sogndal exhibits such an intimate and clear-cut association of anorthositic, jotunitic and syenitic rocks.

This study has made several important contributions to the problem of massif-type anorthosite and to Southern California geology. Some of these contributions include:

(1) The geologic map of the anorthosite-syenite terrain of the western San Gabriel Mountains (Plate I) is probably more detailed than that of any other massif-type anorthosite pluton, and is at least as detailed as any other map of a comparable area of crystalline rocks in the Transverse Ranges of Southern California.

(2) Based on geologic mapping, an extended post-plutonic structural history has been recognized, including two episodes of major folding and two major fault sets. This constitutes a significant extension of the pattern of faulting previously recognized in the Soledad Basin. Recognition of the significance of the Mill Canyon structure and the allochthonous nature of the anorthosite-syenite terrain is an important addition to the understanding of thrust faulting in Southern California.

(3) This study has defined and described all of the important lithologies of the anorthosite-syenite suite (anorthosite, leucogabbro, gabbro, ferrogabbro, ultramafite, jotunite, ferrojotunite, mangerite, syenite, ferrosyenite, quartz syenite and various dike rocks) and determined their distributions and contact relationships.

(4) This study describes the mineralogies of each lithology in greater detail than previous studies (Higgs, 1954; Oakeshott, 1958), and the characteristics of individual minerals in the suite, including chemical compositions, exsolution relationships and textural relationships.

(5) Electron microprobe analyses indicate the existence of cryptic compositional variation of plagioclase in rocks of the anorthosite-leucogabbro unit. Alternating more calcic and more sodic plagioclase compositions in rocks of this unit suggest multiple intrusions of more primitive magmas which mixed with previously fractionated magma, and indicate that these rocks formed by crystallization and accumulation in an open system.

(6) The first report of the presence of uninverted pigeonite in anorthosite-related rocks (Carter and Silver, 1972) is another contribution of this study. The presence of uninverted pigeonite is significant in that it may indicate a relatively shallow depth of crystallization of some of the uppermost rocks of the anorthosite-syenite body.

(7) Postcumulous recrystallization has drastically changed the original fabric of most anorthosite and leucogabbro in the San Gabriel body. Description of the resulting rocks and understanding the characteristics of this recrystallization are important to interpreting these rocks. Similar textures of rocks in other massif-type anorthosite bodies may have been produced by similar postcumulous recrystallization.

(8) Pervasive deuteric uralitization has altered primary ferromagnesian minerals in all but a few rocks of the jotunite and syenite units, and also affected ferromagnesian minerals in the adjacent granulite gneiss. This uralitization occurred after crystal accumulation, recrystallization and clinopyroxene-orthopyroxene inversion and exsolution, and suggests that the primary magma(s) probably had a relatively high water content.

(9) The average composition of the San Gabriel body has been estimated (Table III), and is very similar to that suggested by Simmons and Hanson (1978) based on rare-earth element analyses of rocks from other massif-type anorthosite bodies.

(10) This study shows that the San Gabriel body is comprised of a series of rocks formed mainly by bottom crystal accumulation from a series of magmas intruded into approximately the same chamber over a short time interval. It appears likely that each magma was intruded prior to completion of crystallization of the previous magma, although synplutonic tectonism resulted in blocks of earlier rocks being included within later-accumulated rocks. The sequence of lithologies produced by these magmas are anorthosite-leucogabbro (An_{35-55}), followed by ultramafite-ferrosyenite-syenite (mesoperthite), followed by jotunite-ferrojotunite-ferrogabbro-ultramafite (An_{20-45}).

(11) The thickness of the San Gabriel body is at least 7 kilometers and probably exceeds 10-12 kilometers. An unknown thickness of cover originally overlay the body, but its total thickness places some minimum limits on the depth of crystallization of its constituent rocks.

(12) The San Gabriel body is a reasonably typical massif-type andesine anorthosite pluton. This study demonstrates that the San Gabriel body is part of a large deformed stratiform intrusion. Possibly many other "massif-type" anorthosite plutons are stratiform bodies whose rocks formed by bottom crystal accumulation.

An important unresolved question concerns the genetic relationship of the successive magmas which produced the body. The hypothesis that all of these magmas are consanguineous is attractive: the rocks contain similar assemblages and share several common chemical characteristics, they include

a complete range of feldspar and rock compositions, and all of them were emplaced and crystallized in the same part of the crust at very nearly the same time. However, the detailed chemistry, lithologies and field relationships suggest that it is more likely that at least two independently generated magmas combined to form the San Gabriel body. Although complete ranges of mineral compositions and lithologies are present, their detailed sequence does not suggest any simple relationship of later rocks derived by fractional crystallization of earlier rocks. Chemical analyses of rocks from the three units define separate fields with very limited overlap (Figure 83), which cannot be easily related to each other by any simple model of fractional crystallization. Although still uncertain, it seems likely that the anorthosite-leucogabbro unit rocks are consanguineous with most or all of the jotunite unit rocks, and that the syenite unit crystallized from a separate magma with a different origin than that which produced the other rocks (Chapter 6).

Another question raised by this study concerns the postcumulous recrystallization which has affected most anorthosite and leucogabbro. The conditions under which recrystallization occurred, the nature of the driving force and the extent of compositional changes accompanying recrystallization all require further study. Compositional inhomogeneities are present in recrystallized plagioclase. If these are inherited from primary cumulate crystals, then recrystallization must have occurred with surprisingly little compositional homogenization and must be of an unusual nature.

A further question raised by this study concerns the pervasive uralitization which has affected most rocks of the San Gabriel body. The evidence indicates that the fluids which produced the alteration were present during the late stages of magmatic activity and were probably

derived from the magmas which formed the body. The nature of the source which would produce anorthositic or gabbroic magmas with such high water contents is unknown. It is important to ask why the San Gabriel magmas contained so much water, while other primary anorthosite-syenite suites are anhydrous.

These and other unresolved questions might be answered with further study. More detailed mineral composition data could contribute to understanding the San Gabriel body in several ways. Patterns of cryptic layering within units and subunits could be established by analysis of feldspar, pyroxene and olivine. Several mineralogical geothermometers could be applied to these rocks, including those utilizing the alkali-feldspars and ilmenite-pyroxene equilibria. The nature of the uralitization process and the fluids which produced uralitization could be studied with electron microprobe and whole-rock analyses.

A variety of trace element and isotopic studies could contribute to a more complete understanding of the San Gabriel body. Analyses of rare-earth elements in in the different rocks could help answer the question of the relationship of the syenite magma to magmas which crystallized rocks of the anorthosite-leucogabbro and jotunite units. Determination of initial strontium values would also be useful. Oxygen isotope studies of rocks and minerals might give further insight into the nature of the uralitization of these rocks.

The San Gabriel anorthosite-syenite body includes a complete andesine anorthosite-leucogabbro-gabbro-ultramafite-jotunite-mangerite-syenite-quartz syenite suite. Primary mineralogies, textures and structures are preserved in some of these rocks and their field relationships

are well-defined. This study has raised many unresolved questions but it is clear that the geologic nature and relationship of the San Gabriel body can contribute a great deal to the understanding of the origin of massif-type anorthosite pluton.

REFERENCES

REFERENCES

Anderson, A.T., 1969. Massif-type anorthosite: A widespread Precambrian igneous rock. In: Origin of anorthosites and related rocks (Y.W. Isachsen, ed.). N.Y. State Mus. Sci. Serv. Mem. 18, p 47-55.

Anderson, A.T., Morin M., 1969. Two types of massif anorthosites and their implications regarding the thermal history of the crust. In: Origin of anorthosites and related rocks. (Y.W. Isachsen, ed.) N.Y. State Mus. Sci. Serv. Mem. 18, p 57-69.

Balk, R., 1930. Structural geology of the Adirondack anorthosite. J. Geol. v. 38, p 289-302.

Barth, T.F.W., 1933. The large precambrian intrusive bodies in the southern part of Norway. 16th Intern. Geol. Congress Rept., p 297-309.

Berg, J.H., 1977. Regional geobarometry in the contact aureoles of the anorthositic Nain Complex, Labrador. J. Pet., v. 18, p 399-430.

Berry, R.H. and Walton, M.S., 1961. Origin of gneiss with anorthositic and charnockitic affinities, Putnam-Whitehall area, eastern Adirondacks, New York. p 134 in Abstracts for 1961, Geol. Soc. Am., Spec. Pap. 68.

Bridgewater, D., and Harry, W.T. 1968. Anorthosite xenoliths and plagioclase megacrysts in Precambrian intrusions of South Greenland. Medd. Greenland, v. 185, #2, p 1-248.

Buddington, A.F., 1939. Adirondack igeneous rocks and their metamorphism. Geol. Soc. Am., Mem. 7, 354 p.

Buddington, A.F., 1972. Differentiation trends and parental magmas for anorthositic and quartz mangerite series, Adirondacks, New York, Geol. Soc. Am., Mem. 132, p 477-488.

Cameron, E.N., 1969. Postcumulous changes in the eastern Bushveld complex. Am. Min. 54, p 754-779.

Carstens, H., 1967. Exsolution in ternary feldspars. I. On the formation of antiperthites. Contr. Minerals and Petrol., v. 14, p 27-35.

Carter, B., 1970. Structure of the San Gabriel anorthosite massif, California. Trans. Am. Geophys. Union, v. 51, p 446.

Carter, B., and Silver, L.T., 1971. Post-emplacement structural history of the San Gabriel anorthosite complex. Geol. Soc. Am., Cordilleran Sect. 67th annual meeting, Abstr. with Prog., p 92.

Carter, B., and Silver, L.T., 1972. Structure and petrology of the San Gabriel anorthosite-syenite body, California. 24th Int. Geol. Congress, Montreal Rept., Sec. 2., p 303-311.

Cote, P.E., 1960. Chertsey area; Que. Dept. Mines, Geol. Rept. 93, 30 p.

Crowell, J.C., 1962. Displacement along the San Andreas fault, California. Geol. Soc. Am., Spec. Pap. 71, 61 p.

Crowell, J.C., 1973. Problems concerning the San Andreas fault system Southern California. Stanford Univ. Publ. in the Geol. Sci., v. 13, p 125-135.

Crowell, J.C., and Walker, J.W.R., 1962. Anorthosite and related rocks along the San Andreas fault, Southern California. Univ. Calif. Publ. Geol. Sci., v. 40, p 219-288.

Cummings, D., and Regan, R.D., 1976. Aeromagnetic survey of the San Gabriel anorthosite complex, San Gabriel Mountains, Southern California. Geol. Soc. Am., Bull, 87, p 675-680.

Deer, W.A., Howie, R.A., and Zussman, J., 1966. Rock-Forming Minerals, Dongman, London.

Deer, W.A., Howie, R.A., and Zussman, J., 1978. Rock-Forming Minerals, v. 2A, 2nd ed., John Wiley, New York.

Devore, G.W., 1975. The role of partial melting of metasediments in the formation of the anorthosite-norite-syenite complex, Laramie Range, Wyoming. J. Geol., v. 83, p 749-762.

DeWaard, D., 1969. The anorthosite problem: the problem of the anorthosite-charnockite suite of rocks. In: Origin of anorthosite and related rocks (Y.W. Isachsen, ed.). N.Y. State Mus. Sci. Serv. Mem. 18, p 71-91.

DeWaard, D., 1970. The anorthosite-charnockite suite of rocks of Roaring Brook Valley in the eastern Adirondacks (Marcy Massif). Am. Min., v. 55, p 2063-2075.

Dewaard, D., and Romey, W.D., 1969. Chemical and petrologic trends in the anorthosite-charnockite series of the Snowy Mountain Massif, Adirondack highlands. Am. Min., v. 54, p 529-538.

DeWaard, D., Wheeler, E.P., 1971. Chemical and petrogenetic trends in anorthositic and associated rocks of the Nain Massif, Labrador. Lithos, v. 4, p 367-380.

Dickenson, W.R., 1969. Evolution of calc-alkaline rocks in the geosynclinal system of California and Oregon. In: Proceed. of the andesite conference, Int. Upper Mantle Project, Oregon State Dept. Geol. and Mineral Ind., Bull. 65, p 151-156.

Duchesne, J.C., 1972. Iron-titanium oxide minerals in the Bjerkrem-Sogndal Massif, southwestern Norway. J. Pet., v. 13, p 57-81.

Duchesne, J.C., Roelandts, I., Demaiffe, D., Hertogen, J., Gijbels, R., and DeWinter, J., 1974. Rare-earth data on monzonoritic rocks related to anorthosites and their bearing on the nature of the parental magma of the anorthositic series. Earth and Planetary Sci. Letters, v. 24, p 325-335.

Durham, J., Jahns, H., and Savage, 1954. Marine-nonmarine relationships in the Cenozoic section of California. California Div. Mines, Bull. 170, ch. 3, contrib. 7.

Ehlig, P.L., 1958. Geology of the Mount Baldy region of the San Gabriel Mountains, California. Calif. Univ., Los Angeles, Unpublished Ph.D. thesis, 153 p.

Emslie, R.F., 1965. The Michikamau anorthositic intrusion, Labrador. Can. J. Earth Sci., v. 2, p 385-399.

Emslie, R.F., 1968. The geology of the Michikamau intrusion, Labrador. Geol. Surv. Canada, Paper 68-57, 85 p.

Emslie, R.F., 1969. Crystallization and differentiation of the Michikamau intrusion. In: Origin of anorthosite and related rocks (Y.W. Isachsen, ed.). N.Y. State Mus. Sci. Serv. Mem. 18, p 163-173.

Emslie, R.F., 1970. Liquidus relations and subsolidus reactions in some plagioclase-bearing systems. Carnegie Inst. Wash., Geophysical Lab. Yearbook 69, p 148-155.

Emslie, R.F., 1973. Some chemical characteristics of anorthositic suites and their significance. Can. J. Earth Sci., v. 10, p 54-71.

Emslie, R.F., 1975. Major rock units of the Morin Complex, southwestern Quebec. Geol. Surv. Canada, paper 74-48, 37 p.

Fowler, K.S., 1930. The anorthosite area of the Laramie Mountains, Wyoming. Am. J. Sci., v. 19, p 305-315, 373-403.

Frith, R.A., and Currie, K.L., 1976. A model for the origin of the Lac St. Jean anorthosite massif. Can. J. Earth Sci., v. 13, p 389-399.

Fujii, T., and Kushiro, I., 1977. Density, viscosity, and compressibility of basaltic liquid at high pressures. Carnegie Inst. of Wash., Geophysical Lab. Yearbook 76, p 419-424.

Goldschmidt, V.M., 1916. Geologisch-petrographische Studien im Hochgebirge des sudlichen Norwegens, IV, Videnskapsselskapets Skrifter, 1, no. 2.

Grout, F.F., and Schwartz, G.M., 1939. The geology of the anorthosites of the Minnesota coast of Lake Superior. Minn. Geol. Surv., Bull. 28.

Hershey, O.H., 1902. Some crystalline rocks of Southern California: Am. Geologist, v. 29, p 273-290.

Higgs, D.F., 1954. Anorthosite and related rocks of the western San Gabriel Mountains, Southern California. Univ. Calif., Publ. Geol. Sci., v. 30, p 171-222.

Hodal, J., 1945. Rocks of the anorthosite kindred in Vossestrand, Norway. Norsk. Geol. Tidsskr. 24, p 129-243.

Irvine, T.N., 1965. Sedimentary structures in igneous intrusions with particular reference to the Duke Island ultramafic complex. In Primary sedimentary structures and their hydrodynamic interpretation, G.V. Middleton (ed.), p. 220-232.

Irvine, T.N., and Barager, W.R.A., 1971. A guide to the chemical classification of the common volcanic rocks. Can. J. Earth Sci., v. 8, p 523-548.

Isachsen, Y.W., ed., 1969. Origin of anorthosite and related rocks. N.Y. State Mus. and Sci. Service, Mem. 18, 406 p.

Jahns, R.H., 1954. Pegmatites of Southern California: California Div. Mines, Bull. 170, ch. 7, contrib. 5.

Jahns, R.H., and Muehlberger, R., 1954. Geology of the Soledad basin, Los Angeles County: California Div. Mines, Bull. 170, ch. 1, map sheet 6.

Jennings, C.W., and Strand, R.G. (compilers), 1969. Geologic map of California, Los Angeles Sheet. Calif. Div. Mines and Geology, Sacramento, California.

Kearey, P., 1978. An interpretation of the gravity field of the Morin anorthosite complex, southwest Quebec. Geol. Soc. Am., Bull. 89, p 467-475.

Kehlenbeck, M.M., 1972. Deformation textures in the Lac Rouvray anorthosite mass. Can. J. Earth Sci., v. 9, p 1087-1098.

Klugman, M.A., 1960. Laramie anorthosite (abs.) Geol. Soc. Am., Bull. 71, p. 1906.

Kolderup, C.F., 1904. Die labradorfelse des westlichen Norwegens, II. Die labradorfelse und die mit denselben verwandten Gesteine im dem Bergensgebiete: Bergens Mus. Aarbog 12, 129 p.

Lindsley, D.H., and Emslie, R.F., 1967. Effect of pressure on the boundary curve in the system diopside-albite-anorthite. Carnegie Inst. Wash., Geophysical Lab. Yearbook 66, p 479-480.

Lofgren, G.E., and Gooley, R., 1977. Simultaneous crystallization of feldspar intergrowths from the melt. Am. Min., v. 62, p 217-228.

Martignole, J., and Schrijver, K., 1970. Tectonic setting and evolution of the Morin anorthosite, Greenville Province, Quebec. Geol. Soc. Finl. Bull. 42, p 165-209.

McBirney, A.R., and Noyes, R.M., 1979. Crystallization and layering of the Skaergaard Intrusion. J. Pet. v. 20, p 487-554.

Michot, P., 1969. Geological environments of the anorthosites of South Rogaland, Norway. In: Origin of anorthosite and related rocks (Y.W. Isachsen, ed). N.Y. State Mus. Sci. Serv. Mem. 18, p 411-423.

Miller, W.J., 1928. Anorthosite in Los Angeles County, California: Geol. Soc. Am., Bull. 39, p 164-165.

Miller, W.J., 1929. Rocks of the southwestern San Gabriel Mountains (summary statement). Pan. Am. Geologist, v. 41, p 369-370.

Miller, W.J., 1930. Rocks of the southwestern San Gabriel Mountians, California (abst.): Geol. Soc. Am., Bull., v. 41, p 149.

Miller, W.J., 1931. Anorthosite in Los Angeles County, California. J. Geol., v. 39, p 331-344.

Miller, W.J., 1934. Geology of the western San Gabriel Mountains of California. Univ. Calif., Los Angeles, Publ. in Math. and Phys. Sci., v. 1, p 1-114.

Morton, D.M., and Streitz, R., 1969. Reconnaissance map of major landslides, San Gabriel Mountains, California. Calif. Div. Mines and Geol., Map Sheet 15.

Muan, A., 1979. Crystallization in silicate systems, p 77-132 in: The evolution of the igneous rocks (H.S. Yoder, ed.), Princeton Univ. Press.

Muehlberger, W.R., 1958. Geology of the northern Soledad basin, Los Angeles County, California. Am. Assoc. Petroleum Geologists, Bull. 42, p 1812-1844.

Mueller, R.F., 1970. Two-step mechanism for order-disorder kinetics in silicates. Am. Min., v. 55, p 1210-1218.

Neuerburg, G.J., 1954. Allanite pegmatite, San Gabriel Mountains, Los Angeles County, California. Am. Min., v. 39, p 831-834.

Newhouse, W.H., and Hagner, A.F., 1957. Geologic map of the anorthosite areas, southern part of the Laramie Range, Wyoming. U.S. Geol. Survey, Mineral Invest. Field Studies Map MF 119.

Oakeshott, G.B., 1936. A detailed geologic section across the western San Gabriel Mountains of California. Univ. Southern Calif., Ph.D. thesis.

Oakeshott, G.B., 1937. Geology and mineral deposits of the western San Gabriel Mountains, Los Angeles County. California Jour. Mines and Geology, v. 33, p 215-249.

Oakeshott, G.B., 1938. Geomorphology from detailed geologic mapping, western San Gabriel Mountains. Assoc. Pacific Coast Geographers Yearbook, v. 4, p 30-31.

Oakeshott, G.B., 1948. Titaniferous iron-ore deposits of the western San Gabriel Mountains, Los Angeles County, California. California Div. Mines, Bull. 129, p 245-266.

Oakeshott, G.B., 1949. Titanomagnetite rocks of the western San Gabriel Mountains, California (abst.). Geol. Soc. Am., Bull. 60, p 1942-1943.

Oakeshott, G.B., 1952. Geology of the northern margin of San Fernando Valley. Petroleum World, p 20-24.

Oakeshott, G.B., 1954. Geology of the western San Gabriel Mountains, Los Angeles County. Calif. Div. Mines, Bull. 170, ch. 1, map sheet 9.

Oakeshott, G.B., 1958. Geology and mineral deposits of the San Fernando Quadrangle, Los Angeles County, California. Calif. Div. Mines, Bull. 172, p 1-147.

Peng, C.C.J., 1970. Intergranular albite in some granites and syenites of Hong Kong. Am. Min., v. 55, p 270-282.

Philpotts, A.R., 1962. Belleau-Desaulniers area, Counties of St. Maurice, Maskinonge and Laviolette. Quebec Dept. Nat. Res., Prelim, Rept. 480.

Philpotts, A.R., 1966. Origin of the anorthosite-mangerite rocks in southern Quebec. J. Pet., v. 7, p 1-64.

Philpotts, A.R., 1967. Origin of certain iron-titanium oxide and apatite rocks. Econ. Geol., v. 62, p 303-315.

Phipps, R.T., 1951. Geology of the Monte Cristo mining area. Calif. Inst. of Technology, M.S. thesis.

Powell, R.E., and Silver, L.T., 1980. Tectonic superposition of crystalline terrains in the Chuckawalla to Pinto Mountians region, eastern Transverse Ranges, Southern California. Geol. Soc. Am., Abstracts with Programs, v. 12, p 498.

Ramberg H., 1962. Intergranular precipitation of albite formed by unmixing of alkali feldspar. Neues Jahrb. Mineral., Abh. 98, p 14-34.

Ramarathnam, S., 1962. Geology and petrology of the southern part of the Laramie anorthosite, Albany County, Wyoming (abs.) Geol. Soc. Am., Spec. Paper 68, p 97.

Ryder, G., 1974. A rationale for the origins of massif anorthosites. Lithos v. 7, p 139-146.

Ryder, G., Malcuit, R.J., and Vogel, T.A., 1975. Differentiation of an andesine-type anorthosite: The San Gabriel Suite. Lithos, v. 8, p 311-316.

Seifert, K.E., Voigt, A.F., Smith, M.F., and Stensland, W.A., 1977. Rare earths in the Marcy and Morin anorthosite complexes. Can. J. Earth Sci., v. 14, p 1033-1045.

Silver, L.T., 1971. Problems of crystalline rocks of the Transverse Ranges. Geol. Soc. Am., Abstracts with Programs, v. 3, p 193-194.

Silver, L.T., and Carter, B.A., 1965. Precambrian syenites of northern Los Angeles County, California. Geol. Soc. Am., Spec. Paper 87, p 228-229.

Silver, L.T., McKinney, C.R., Deutsch, S., and Bolinger, J., 1963. Precambrian age determinations in the western San Gabriel Mountains, California. J. Geol., v. 71, p 196-214.

Simmons, G., 1964. Gravity survey and geological interpretation, northern New York. Geol. Soc. Am., Bull. 75, p 81-98.

Simmons, C.E., and Hanson, G.N., 1978. Geochemistry and origin of massif-type anorthosites. Contr. Min. Petr., v. 66, p 119-135.

Sinclair, J.D., 1954. Erosion in the San Gabriel Mountains of California. Am. Geophysical Union, Trans., p 264-268.

Smith, B.C., Hodge, D.S., and Smithson, S.B., 1970. Geology and geophysics of syenites associated with Laramie anorthosite, Wyoming. Contr. to Geol., Univ. of Wyoming, v. 9, p 27-39.

Spittler, T.E., Arthur, M.A., 1973. Post-early Miocene displacement along the San Andreas fault in Southern California. Stanford Univ. Publ. in Geol. Sci, v. 13., p 374-382.

Taylor, R.B., 1956. The Duluth gabbro complex, Duluth, Minnesota, p 43-66 in Schwartz, G.M., Editor, Guidebook for field trips, Minneapolis meeting, Geol. Soc. Am.

Taylor, H.P., 1969. Oxygen isotope studies of anorthosites, with particular reference to the origin of bodies in the Adirondack Mountains, New York. In: The origin of anorthosite and related rocks (Y.W. Isachsen, ed.). N.Y. State Mus. Sci. Serv. Mem. 18, p 111-134.

Varne, R., 1968. The petrology of Maroto Mountain, Eastern Uganda, and the origin of nephelinites. J. Pet., v. 9, p 169-190.

Wager, L.R., Brown, G.M., and Wadsworth, W.J., 1960. Types of igneous cumulates. J. Pet., v. 1, p 73-85.

Wheeler, E.P., 1960. Anorthosite-adamellite complex of Nain, Labrador. Geol. Soc. Am., Bull. 71, p 1755-1762.

Weibe, R.A., 1978. Anorthosite and associated plutons, southern Nain complex, Labrador. Can. J. Earth Sci., v. 15, p 1326-1340.

Weibe, R.A., 1979. Anorthositic dikes, southern Nain complex, Labrador. Am. Jour. Sci., v. 279, p 394-410.

Weibe, R.A., 1980. Comingling of contrasted magmas in the plutonic environment: examples from the Nain anorthositic complex. J. Geol., v. 88, p 197-210.

Yoder, H.D., 1969. Experimental studies bearing on the origin of anorthosite. In: Origin of anorthosite and related rocks (Y.W. Isachsen, ed.) N.Y. State Mus. Sci. Serv. Mem. 18, p 13-22.

Young, G.M., 1972. Downward intrusive breccias in the Huronian Espanola formation, Ontario, Canada. Can. J. Earth Sci., v. 9, p 756-762.

APPENDIX A

MINERAL MODES OF ROCKS OF THE SAN GABRIEL ANORTHOSITE-SYENITE BODY

MODES OF ROCKS OF THE SAN GABRIEL ANORTHOSITE-SYENITE BODY

These present approximate volume percentages of minerals based on thin section point counts. Unless otherwise indicated, all modes represent 1200 points counted on a single thin section. Modes of all analyzed specimens (*) represent 4000 points counted on four thin sections.

Anorthosite-Leucogabbro Unit Rocks

	Anorthosite				Leucogabbro					
Specimen	16	18*	42	103	276*	1055A*,[1]	1055B*,[2]	1202[3]	1204[4]	Road-cut[5]
Plagioclase	92	96	94	87	65	81	73	67	69	70
Quartz				Tr.						
Opaque	Tr.	Tr.	Tr.	Tr.	1	1	2	4		2
Apatite	Tr.	Tr.	Tr.	Tr.						
Hornblende-Uralite					34	18	25	29	37	28
Biotite				Tr.						
Epidote	3	1	2	4	Tr.					
W. Mica-Sericite	2	3	3	8						
Chlorite	3	Tr.	1		Tr.					

* = analyzed specimen

1 = 5 mm grid on cut slab (31 x 30 cm area)

2 = 5 mm grid on cut slab (23 x 26 cm area)

3 = 5 mm grid on cut slab (11 x 25 cm area)

4 = 2 mm grid on cut slab (7 x 10 cm area)

5 = 30 cm grid on roadcut on Angeles Forest Hwy. (1200 points)

Mafic to Very Mafic Rocks

	Ultramafic Syenite Subunit					Ultramafic Jotunite Subunit			
Specimen	335*	387*	388 B	388C	202	61C*	61A	102A	102B*
Plagioclase		Tr.			46			19	20
Anti-perthite			35	20		3			
Mesoperthite	50					40			
Olivine	15	49	25	32			42	33	36
Hypersthene					9	2			
Augite	15	5	17	21	21	30	22	10	8
Kaersutite	Tr.	10			15		2	8	8
Opaque	14	20	11	17	9	18	18	21	18
Apatite	5	12	11	9	Tr.	7	16	9	9
Spinel			Tr.	Tr.	Tr.		Tr.	Tr.	1
Biotite	1		1	1			Tr.		
"Alteration"		4							

*Analyzed specimen

Syenite Unit Rocks

Specimen	5B	45	50	111*	626	1030B*
Plagioclase		4				2
Antiperthite	6			34		
Mesoperthite	56	64	44	44	75	61
Microcline-Perthite			18	3		
Quartz	31	2	2			
Olivine					5	3
Augite					8	17
Pigeonite					Tr.	1
Opaque	1	2	3	9	3	5
Apatite	Tr.	3	3	1	3	2
Biotite		12	19			
Hornblende-Uralite	7	8	8	10	4	8
W. Mica-Sericite	Tr.				1	
Chlorite			3			
Epidote	Tr.	4		Tr.		
Zircon	Tr.	1		Tr.	1	1

*Analyzed specimen

Jotunite Unit Rocks

Specimen	70	11*	32*	100*	142	250
Plagioclase	40	33	45	55	55	
Antiperthite	20	25	1	15		74
Mesoperthite					1	
Olivine		Tr.		4		11
Hypersthene	10	12		4	21	
Augite	15	17		15	7	5
Pigeonite	Tr.	1		2	2	
Opaque	6	4	5	3	10	4
Apatite	3	3	6	2	4	5
Biotite	Tr.	3	7			1
Hornblende-Uralite	5	1	21	Tr.		
W. Mica-Sericite	1		5	Tr.		
Chlorite		1	10	Tr.		
Epidote	Tr.					

*Analyzed specimen